Influencing the homing and differentiation of MNCs in hereditary hemorrhagic telangiectasia

Dingenouts, C.K.E.

Citation

Dingenouts, C. K. E. (2019, February 27). *Influencing the homing and differentiation of MNCs in hereditary hemorrhagic telangiectasia*. Retrieved from https://hdl.handle.net/1887/69046

Version: Not Applicable (or Unknown)

License: Licence agreement concerning inclusion of doctoral thesis in the Institutional Repository of the University of Leiden

Downloaded from: https://hdl.handle.net/1887/69046

Note: To cite this publication please use the final published version (if applicable).

Cover Page

Universiteit Leiden

Leiden University
Repository

The handle http://hdl.handle.net/1887/69046 holds various files of this Leiden University dissertation.

Author: Dingenouts, C.K.E.
Title: Influencing the homing and differentiation of MNCs in hereditary hemorrhagic telangiectasia
Issue Date: 2019-02-27

Influencing the homing and differentiation of MNCs in hereditary hemorrhagic telangiectasia

Calinda Kiana Estel Dingenouts

Promotor:
Prof. Dr. M.J. Goumans

Co-promotor:
Dr. W. Bakker

Promotiecommissie:

Prof. Dr. H.H. Versteeg	
Prof. Dr. A.J. van Zonneveld	
Prof. Dr. A. Zwijsen	Catholic University of Leuven
Dr. I.E. Hoefer	University Medical Center Utrecht

Printed by: Gildeprint, Enschede
Cover: Artwork by Aboriginal artist Caroline Numina, ‘Bush Medicine Leaves’, Darwin, Australia

ISBN 978-94-6323-485-6

Copyright © 2019, Calinda K.E. Dingenouts
All rights reserved. No part of this book may be reproduced or transmitted, in any form or by any means, without prior written permission of the author.

The studies were performed at the Department of Cell and Chemical Biology of the Leiden University Medical Centre and were supported by the Netherlands Institute of Regenerative Medicine (NIRM, grant No. FES0908) and the Dutch Heart Foundation (grant No. NHS2009B063)

This publication of this dissertation was made possible by the Dutch Heart Foundation.

Influencing the homing and differentiation of MNCs in hereditary hemorrhagic telangiectasia

Proefschrift

ter verkrijging van
de graad van Doctor aan de Universiteit Leiden,
op gezag van Rector Magnificus prof.mr. C.J.J.M. Stolker,
volgens besluit van het College voor Promoties
te verdedigen op woensdag 27 februari 2019
klokke 16:15 uur

door

Calinda Dingenouts

geboren te Vlaardingen
in 1986

Table of contents

Chapter 1: General introduction 7

Chapter 2: Mononuclear cells and vascular repair in HHT 19

Chapter 3: Inhibiting DPP4 in a mouse model of HHT1 results in a shift towards regenerative macrophages and reduces fibrosis after myocardial infarction 39

Chapter 4: BMP receptor inhibition enhances tissue repair in endoglin deficient mice 69

Chapter 5: DPP4 inhibition enhances wound healing in endoglin heterozygous mice through modulation of macrophage signaling and differentiation 93

Chapter 6: Endoglin deficiency alters the epicardial response following myocardial infarction 117

Chapter 7: General discussion 141

Summary 157

Nederlandse Samenvatting 159

Acknowledgements 161

Curriculum Vitae 163

List of Publications 165

1

General introduction

Background

Hereditary hemorrhagic telangiectasia (HHT) or Rendu-Osler-Weber disease is a rare genetic autosomal dominant disorder, known for its endothelial dysplasia causing arteriovenous malformations, severe nose bleeds and internal bleedings1. HHT has an estimated prevalence affecting 1 in 5000 people[1,2]. HHT severity and disease onset are highly variable between patients, and symptoms progressively worsen with age[3]. HHT is officially diagnosed if a patient has 3 out of the 4 criteria, namely epistaxis, telangiectasias, arteriovenous malformations (AVMs) and/or a first degree relative with HHT. As establishing the diagnosis for HHT was often difficult, clinicians treating HHT patients gathered on Curaçao, where they decided on guidelines to improve diagnosis, the Curaçao criteria. The Curaçao criteria are now a standardized set of symptoms and characteristics. When patients are diagnosed, genetic testing is performed to identify the mutation[4,5].

The clinical symptoms remain important in the diagnosis of HHT, as the mutations underlying the disease are sometimes still unknown. So far, several HHT mutations with known target genes have been identified. Although not in every patient a mutation is found, in the majority of patients mutations are found in genes belonging to the TGFβ superfamily, causing a disbalance in the TGFβ signaling pathway by haploinsufficiency of the remaining functional protein[6,7]. HHT type 1 (HHT1) is the most prevalent HHT variant, and its mutation lies in the endoglin gene[8], encoding a protein which functions as co-receptor of TGFβ, and is crucial to neo-angiogenesis and vascular repair[9]. Mutations in the second most prevalent variant is the activin receptor-like kinase 1 (ALK1) and is referred to as HHT2[10]. ALK1 is a TGFβ type I receptor involved in the angiogenic switch; the promotion and inhibition of angiogenesis[11]. HHT3 and HHT4 are caused by mutations in chromosome 5 and 7 respectively, but the genes or proteins affected are not yet identified[12,13]. Mutations in the third gene are in SMAD4, a downstream signaling protein of TGFβ/BMP, causing the combined syndrome of juvenile polyposis, known as JP-HHT[14]. Recently BMP9 (a ligand for ALK1) was identified as a fourth gene responsible for HHT5[15]. The various mouse models available that represent the HHT variants are discussed in more detail in Chapter 2 of this thesis.

TGFβ signaling and endothelial cells

The vascular defects and impaired angiogenesis in HHT1 are primarily caused by malfunctioning of the activation of ECs. Endoglin is highly expressed on activated endothelial cells (ECs) and it is crucial for angiogenesis, providing signaling involving proliferation, migration and remodeling of the extracellular matrix[9,16]. The effects of endoglin haploinsufficiency are therefore extensively researched in this cell type. Endoglin is a co-receptor for TGFβ, a multifunctional cytokine involved in many cellular processes ranging from proliferation, migration and fibrosis to apoptosis. Upon tissue damage, TGFβ is released by the extracellular matrix, apoptotic cells or platelets, and secreted by fibroblasts, macrophages and T lymphocytes[17,18].

The TGFβ signaling pathway encompasses the TGFβ superfamily of ligands, all binding to a specific type I/II receptor combination (Fig. 1). The TGFβ superfamily of ligands can be divided in two groups, the TGFβ ligands and BMP ligands. Upon binding of the ligand to the type II receptor, a receptor type I is recruited and a tetrameric complex is formed, after which the type II receptor kinase activates the type I receptor. The type I receptor kinase in turn phosphorylates intracellular receptor-regulated SMADs (R-SMADs) proteins. ALK1 can form a complex with the TGFβ or BMP receptor type II in the presence of ALK5 and the presence of endoglin as co-receptor[19-22]. The TGFβ receptor type I consists of two subtypes, ALK1 signaling via SMADs 1, 5 and 8, and ALK5 signaling via SMAD 2 and 3. In ECs, TGFβ-ALK1 signaling leads to proliferation and migration, whereas TGFβ-ALK5 signaling leads to a quiescent state of the EC. Endoglin mainly stimulates the TGFβ-ALK1 pathway, and suppresses the TGFβ-ALK5 pathway[23]. After forming a complex with the common mediator SMAD or co-SMAD: SMAD4, the R-SMAD and co-SMAD complex translocates to the nucleus where it acts as a transcription factor and modifies target gene expression.

The TGFβ signaling pathway is tightly controlled and involves many activators and inhibitors. Although endothelial cells[24] and pericytes[25] have been the main research focus for HHT, mononuclear cells (MNCs) also play an important role in vascular homeostasis, integrity and repair. We have previously shown that endoglin heterozygosity impairs homing of HHT1-MNCs[26]. Studies in HHT1 patients reported increased occurrences of severe bacterial infections in, such as cerebral, hepatic, muscular and other infections[27,28], possibly due to the impaired MNC response.

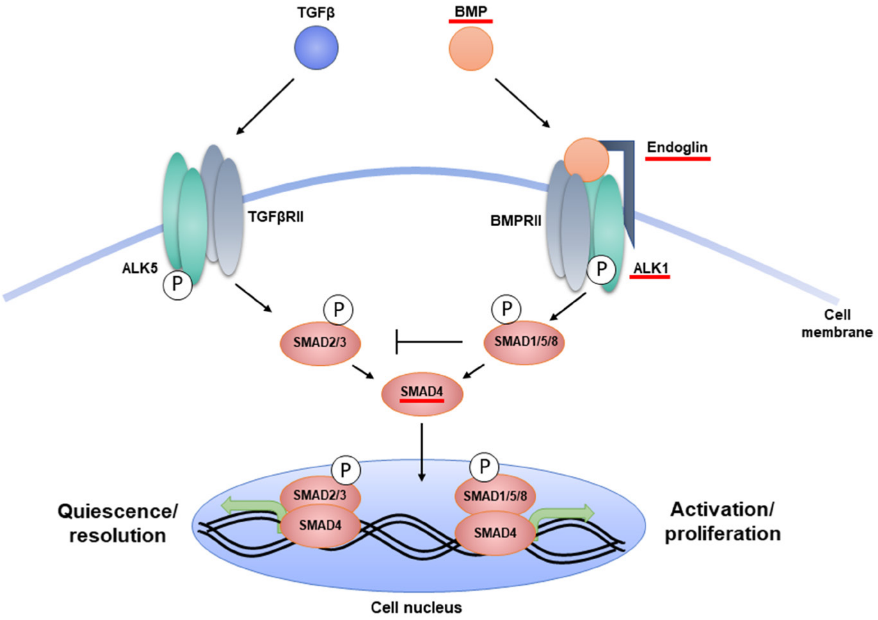
TGFβ
BMP
Endoglin
TGFβRII
BMPRII
ALK5
P
ALK1
P
P
SMAD2/3
SMAD1/5/8
SMAD4
Cell membrane
P
P
SMAD2/3
SMAD4
SMAD1/5/8
SMAD4
Quiescence/ resolution
Activation/ proliferation
Cell nucleus

Fig. 1 Schematic representation of TGFβ signaling. Underlined in red are the proteins affected in various HHT subtypes.

MNC trafficking and homing towards tissue damage

The process by which MNCs are attracted to ischemic, damaged or inflamed tissue is tightly regulated. The first step in the homing process is regulated via the stromal cell derived factor- 1 (SDF1) – CXCR4 axis. MNCs are recruited from the bone marrow and spleen via the circulation to the site of injury. The MNCs are retained within the tissue by high SDF1 levels[29]. Upon ischemia, hypoxia inducible factor 1 alpha (HIF1α) induces expression of SDF1 in the ischemic cells, which is then released into the bloodstream. This increases systemic SDF1 levels and causes MNCs to be released from the bone marrow and spleen, traffic through the circulation and home to the site of injury –the source of SDF1 production– responding to SDF1 upon its binding to the receptor CXCR4[29,30].

There is a delicate balance between SDF1 and CXCR4, and skewing of either one of the proteins or regulators involved in their activation or inhibition will result in impaired homing, a defective inflammatory response and hamper wound healing and tissue repair.

DPP4 and its inhibition

Because the MNCs cannot be allowed to migrate indefinitely, there is suppression of the homing signal; dipeptidyl peptidase-4 (DPP4/CD26). By cleaving the first 2 aminoacids, SDF1 is unable to bind to its receptor or reduce the levels of CXCR4[31,32]. DPP4 is a potent proteolytic enzyme[33,34]. It is a 110kd transmembrane protein and is expressed by various cell types, such as endothelial cells, epithelial cells, melanocytes, monocytes and lymphocytes[35,36]. DPP4 is able to enzymatically cleave aminoterminal dipeptides after a proline or an alanine amino acid from specific target proteins. DPP4 inhibition is a well-known therapy currently in use for type 2 diabetes mellitus (T2DM). In T2DM, DPP4 cleaves glucagon-like peptide-1 (GLP1), an incretin hormone which is released upon food intake, stimulating insulin release. DPP4 inhibitors function via the decrease of incretin degradation, thereby preventing low insulin levels.

To summarize, SDF1 is produced in tissues shortly after an ischemic event, and mobilizes MNCs from the bone marrow to the circulation. Subsequent homing of CXCR4+ cells from the blood to the site of injury is mediated by the SDF1 gradient and its receptor CXCR4. DPP4 was also found to co-localize with CXCR4, and both were internalized upon SDF1 binding[37]. DPP4 enzymatically inactivates SDF1, therefore playing a critical role in limiting MNC recruitment to ischemic areas.

Outline of the thesis

The aim of my thesis is to understand the effect of endoglin heterozygosity on macrophage-mediated wound healing and tissue repair (Overview in Fig. 2). Regulating the levels of DPP4 is essential for MNCs to home towards damaged tissue, and thereby contributes to efficient repair. We have also previously reported that in HHT1, MNC-DPP4 levels are elevated and homing of HHT1-MNCs towards injured tissue is impaired[26]. When we pre-treated the MNCs from HHT1 patients with a DPP4 inhibitor, and injected these into mice with induced myocardial infarction (MI), these cells were now able to home to the site of injury[26]. In previous studies TGFβ has been reported to modulate DPP4 levels on MNCs[38-40]. However, the impact and role of TGFβ signaling and the systemic application of DPP4 inhibition were not yet fully investigated. Therefore we studied the effect of DPP4 inhibition on tissue repair after dermal injury and myocardial infarction in endoglin

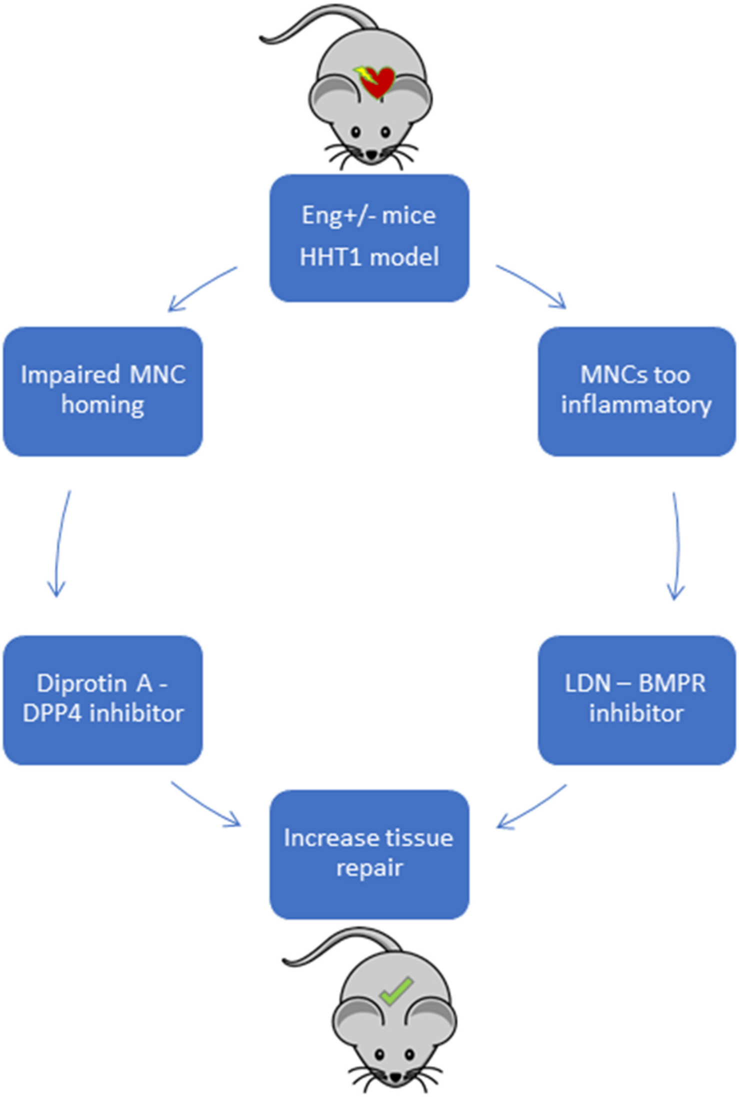
Eng+/- mice
HHT1 model
Impaired MNC homing
MNCs too inflammatory
Diprotin A - DPP4 inhibitor
LDN – BMPR inhibitor
Increase tissue repair

Fig. 2 Schematic representation of the different aims and approaches to influence HHT1-MNC homing and differentiation to restore tissue repair. Endoglin heterozygous mice were used to model HHT1. In various experimental methods inducing ischemic and/or tissue damage, we aimed to improve tissue repair in the mice via two approaches. First, using DPP4 inhibition, we intended to increase the SDF1-CXCR4 homing mechanism, to restore the impaired homing capacity of the HHT1-MNCs. The second approach was focused on correcting the M1/M2 differentiation in Eng+/- mice. Via use of the BMPR inhibitor LDN we aimed to restore the skewed BMP/TGFβ signaling; stimulating the TGFβ pathway signaling thereby resulting in improved M2 differentiation.

heterozygous mice, a mouse model of HHT1. We hypothesize that one explanation for the symptoms observed in HHT1 is that the MNCs required for tissue repair and an optimal inflammation response are also affected in their proper functioning. We therefore studied the impaired reparative capacity of macrophages in HHT1 and the deficiency of TGFβ signaling affecting the inflammatory characteristics of macrophages.

Outline per chapter

HHT1 is caused by mutations in the TGFβ co-receptor endoglin. It was therefore long considered a disorder affecting angiogenesis only. In recent years it has become clear that endoglin heterozygosity disturbs the function of many more cell types and processes. In the following chapters, I will describe several aspects of tissue repair using the mouse model for HHT1, the endoglin heterozygous mouse.

In Chapter 2, a general overview is given on HHT genetics, etiology and signaling, in particular focusing on the role of circulating mononuclear cells, both their impaired homing and contribution to repair in HHT.

In Chapter 3, we show that inhibiting DPP4 in vivo by treating Eng+/- mice after experimentally induced MI, restored homing of MNCs and benefits short term cardiac recovery by reducing fibrosis. Surprisingly, the number of reparative M2 macrophages increased, suggesting that DPP4 inhibition reduces the pro-inflammatory immune response after MI. Furthermore, in Eng+/- mice treated with the DPP4 inhibitor, the number of capillaries present in the infarct border zone increased, whereas number of arteries decreased. This suggests that angiogenesis is stimulated while arteriogenesis is inhibited by DPP4 inhibitor treatment in Eng+/- mice.

In Chapter 4, we explore the use of the small molecule BMPR inhibitor LDN-193189. Endoglin heterozygosity disturbs the BMP/TGFβ signaling balance. In vitro analysis of macrophage differentiation revealed that LDN treatment increased the number of reparative macrophages. By inhibiting BMP signaling using LDN, we aimed to stimulate TGFβ signaling in the Eng+/- animals. Treatment of Eng+/- mice with LDN restored cardiac function and reduced fibrosis after experimentally induced MI. In a second ischemia model, experimentally induced hind limb ischemia, LDN improved blood flow recovery of Eng+/- mice. We found that macrophage signaling via canonical and non-canonical pathways is severely impaired by endoglin heterozygosity.

As macrophage differentiation and tissue repair is impaired in HHT1, in Chapter 5 we studied the effect of DPP4 inhibition in a dermal wounding model in Eng+/- animals, assessing the healing of the lesion. Compared to untreated animals, dermal application of a DPP4 inhibitor increased wound closure speed and increased M2 macrophage numbers in the lesion area. Levels of fibrosis were decreased, signifying a reduction in scarring of the wound site. Furthermore, investigation of intracellular signaling in macrophages showed that in cultured Eng+/- macrophages, non-canonical signaling was severely deregulated.

In Chapter 6 we describe another defect in HHT1 mice: an abnormal epicardial response after myocardial damage. In this study, we analyzed the composition and the behavior of the epicardial layer at different time-points post-MI and found that epicardial thickening is delayed. Furthermore, the epicardium was hyperactive in its response to cardiac ischemic injury when assessed at 14 days post-MI. Systemically treating Eng+/- mice with a DPP4 inhibitor reduced epicardial thickening 14 days post-MI and increased the percentage of macrophages present in the epicardial infarct border zone.

Finally, in Chapter 7 the results and conclusions of the previous chapters are summarized and discussed in light of future research to understanding HHT.

References

1. Rozenberg, D., Leek, E. & Faughnan, M.E. Prevalence and nature of dyspnea in patients with hereditary hemorrhagic telangiectasia (HHT). Respir Med 109, 768-777 (2015).

2. Begbie, M.E., Wallace, G.M. & Shovlin, C.L. Hereditary haemorrhagic telangiectasia (Osler-Weber-Rendu syndrome): a view from the 21st century. Postgrad Med J 79, 18-24 (2003).

3. Plauchu, H., de Chadarévian, J.P., Bideau, a. & Robert, J.M. Age-related clinical profile of hereditary hemorrhagic telangiectasia in an epidemiologically recruited population. American journal of medical genetics 32, 291-297 (1989).

4. Shovlin, C.L. Hereditary haemorrhagic telangiectasia: pathophysiology, diagnosis and treatment. Blood reviews 24, 203-219 (2010).

5. Shovlin, C.L., et al. Diagnostic criteria for hereditary hemorrhagic telangiectasia (Rendu-Osler-Weber syndrome). American journal of medical genetics 91, 66-67 (2000).

6. Bourdeau, a., et al. Endoglin expression is reduced in normal vessels but still detectable in arteriovenous malformations of patients with hereditary hemorrhagic telangiectasia type 1. The American journal of pathology 156, 911-923 (2000).

7. Bourdeau, A., et al. Potential Role of Modifier Genes Influencing Transforming Growth Factor-β1 Levels in the Development of Vascular Defects in Endoglin Heterozygous Mice with Hereditary Hemorrhagic Telangiectasia. The American Journal of Pathology 158, 2011-2020 (2001).

8. McAllister, K.A., et al. Endoglin, a TGF-beta binding protein of endothelial cells, is the gene for hereditary haemorrhagic telangiectasia type 1. Nat Genet 8, 345-351 (1994).

9. van Laake, L.W., et al. Endoglin Has a Crucial Role in Blood Cell-Mediated Vascular Repair. Circulation 114, 2288-2297 (2006).

10. Johnson, D.W., et al. Mutations in the activin receptor-like kinase 1 gene in hereditary haemorrhagic telangiectasia type 2. Nat Genet 13, 189-195 (1996).

11. Larrivée, B., et al. ALK1 Signaling Inhibits Angiogenesis by Cooperating with the Notch Pathway. Developmental Cell 22, 489-500 (2012).

12. Cole, S.G., Begbie, M.E., Wallace, G.M.F. & Shovlin, C.L. A new locus for hereditary haemorrhagic telangiectasia (HHT3) maps to chromosome 5. Journal of medical genetics 42, 577-582 (2005).

13. Bayrak-toydemir, P., et al. Rapid Publication A Fourth Locus for Hereditary Hemorrhagic Telangiectasia Maps to Chromosome 7. American Journal of Medical Genetics 2162, 2155-2162 (2006).

14. Gallione, C.J., et al. SMAD4 mutations found in unselected HHT patients. Journal of medical genetics 43, 793-797 (2006).

15. Wooderchak-Donahue, W.L., et al. BMP9 Mutations Cause a Vascular-Anomaly Syndrome with Phenotypic Overlap with Hereditary Hemorrhagic Telangiectasia. The American Journal of Human Genetics 93, 530-537 (2013).

16. Lebrin, F. & Mummery, C.L. Endoglin-mediated vascular remodeling: mechanisms

underlying hereditary hemorrhagic telangiectasia. Trends in cardiovascular medicine 18, 25-32 (2008).

17. Grainger, D.J., Mosedale, D.E. & Metcalfe, J.C. TGF-β in blood: a complex problem. Cytokine & Growth Factor Reviews 11, 133-145 (2000).

18. Wan, M., et al. Injury-activated transforming growth factor β controls mobilization of mesenchymal stem cells for tissue remodeling. Stem cells 30, 2498-2511 (2012).

19. Lebrin, F., et al. Endoglin promotes endothelial cell proliferation and TGF-beta/ALK1 signal transduction. EMBO J 23, 4018-4028 (2004).

20. Goumans, M.J. & Ten Dijke, P. TGF-beta Signaling in Control of Cardiovascular Function. Cold Spring Harb Perspect Biol (2017).

21. Goumans, M.J., Lebrin, F. & Valdimarsdottir, G. Controlling the angiogenic switch: a balance between two distinct TGF-b receptor signaling pathways. Trends Cardiovasc Med 13, 301-307 (2003).

22. Goumans, M.J., Zwijsen, A., Ten Dijke, P. & Bailly, S. Bone Morphogenetic Proteins in Vascular Homeostasis and Disease. Cold Spring Harb Perspect Biol (2017).

23. Goumans, M.J., Liu, Z. & ten Dijke, P. TGF-β signaling in vascular biology and dysfunction. Cell Research 19, 116-127 (2009).

24. Sugden, W.W. & Siekmann, A.F. Endothelial cell biology of Endoglin in hereditary hemorrhagic telangiectasia. Curr Opin Hematol 25, 237-244 (2018).

25. Thalgott, J., Dos-Santos-Luis, D. & Lebrin, F. Pericytes as targets in hereditary hemorrhagic telangiectasia. Frontiers in Genetics 5, 1-16 (2015).

26. Post, S., et al. Impaired recruitment of HHT-1 mononuclear cells to the ischaemic heart is due to an altered CXCR4/CD26 balance. Cardiovascular Research 85, 494-502 (2010).

27. Guilhem, A., Malcus, C., Clarivet, B. & Plauchu, H. Immunological abnormalities associated with hereditary haemorrhagic telangiectasia. 351-362 (2013).

28. Dupuis-Girod, S., et al. Hemorrhagic hereditary telangiectasia (Rendu-Osler disease) and infectious diseases: an underestimated association. Clinical infectious diseases: an official publication of the Infectious Diseases Society of America 44, 841-845 (2007).

29. Ceradini, D.J., et al. Progenitor cell trafficking is regulated by hypoxic gradients through HIF-1 induction of SDF-1. Nature medicine 10, 858-864 (2004).

30. Cencioni, C., Capogrossi, M.C. & Napolitano, M. The SDF-1/CXCR4 axis in stem cell preconditioning. Cardiovascular research 94, 400-407 (2012).

31. Christopherson, K.W., Hangoc, G. & Broxmeyer, H.E. Cell surface peptidase CD26/dipeptidylpeptidase IV regulates CXCL12/stromal cell-derived factor-1α-mediated chemotaxis of human cord blood CD34+ progenitor cells. The Journal of Immunology 169, 7000 (2002).

32. Yoo, E., et al. Loss of CD26 protease activity in recipient mice during hematopoietic stem cell transplantation results in improved transplant efficiency. Transfusion 53, 878-887 (2013).

33. Lambeir, A.M., et al. Kinetic investigation of chemokine truncation by CD26/dipeptidyl peptidase IV reveals a striking selectivity within the chemokine family. Journal of Biological Chemistry 276, 29839-29845 (2001).

34. Lambeir, A.-M., Durinx, C., Scharpé, S. & De Meester, I. Dipeptidyl-peptidase IV from bench to bedside: an update on structural properties, functions, and clinical aspects of the enzyme DPP IV. Critical reviews in clinical laboratory sciences 40, 209-294 (2003).

35. Yamada, K., et al. Localization of CD26/DPPIV in nucleus and its nuclear translocation enhanced by anti-CD26 monoclonal antibody with anti-tumor effect. Cancer cell international 9, 17 (2009).

36. Zhong, J., et al. A potential role for dendritic cell/macrophage-expressing DPP4 in obesity-induced visceral inflammation. Diabetes 62, 149-157 (2013).

37. Herrera, C., et al. Comodulation of CXCR4 and CD26 in human lymphocytes. J Biol Chem 276, 19532-19539 (2001).

38. Reinhold, D., et al. Inhibitors of dipeptidyl peptidase IV induce secretion of transforming growth factor beta 1 in PWM-stimulated PBMC and T cells. Immunology 91, 354-360 (1997).

39. Steinbrecher, a., et al. Targeting dipeptidyl peptidase IV (CD26) suppresses autoimmune encephalomyelitis and up-regulates TGF-beta 1 secretion in vivo. Journal of immunology (Baltimore, Md. : 1950) 166, 2041-2048 (2001).

40. Arndt, M., et al. Dipeptidyl peptidase IV (DP IV/CD26) mRNA expression in PWM-stimulated T-cells is suppressed by specific DP IV inhibition, an effect mediated by TGF-beta(1). Biochemical and biophysical research communications 274, 410-414 (2000).

2

Mononuclear Cells and Vascular Repair in HHT

Dingenouts C.K.E., Goumans M.J. and Bakker W.

Frontiers in Genetics. 2015 Mar 23;6:114.

Abstract

Hereditary hemorrhagic telangiectasia (HHT) or Rendu-Osler-Weber disease is a rare genetic vascular disorder known for its endothelial dysplasia causing arteriovenous malformations and severe bleedings. HHT-1 and HHT-2 are the most prevalent variants and are caused by heterozygous mutations in endoglin and ALK1, respectively. An undervalued aspect of the disease is that HHT patients experience persistent inflammation. Although endothelial and mural cells have been the main research focus trying to unravel the mechanism behind the disease, wound healing is a process with a delicate balance between inflammatory and vascular cells. Inflammatory cells are part of the mononuclear cells (MNCs) fraction, and can, next to eliciting an immune response, also have angiogenic potential. This biphasic effect of MNCs can hold a promising mechanism to further elucidate treatment strategies for HHT patients. Before MNCs are able to contribute to repair, they need to home to and retain in ischemic and damaged tissue. Directed migration (homing) of mononuclear cells following tissue damage is regulated by the stromal cell derived factor 1 (SDF1). MNCs that express the C-X-C chemokine receptor 4 (CXCR4) migrate towards the tightly regulated gradient of SDF1. This directed migration of monocytes and lymphocytes can be inhibited by dipeptidyl peptidase 4 (DPP4). Interestingly, MNCs of HHT patients express elevated levels of DPP4 and show impaired homing towards damaged tissue. Impaired homing capacity of the MNCs might therefore contribute to the impaired angiogenesis and tissue repair observed in HHT patients. This review summarizes recent studies regarding the role of MNCs in the etiology of HHT and vascular repair, and evaluates the efficacy of DPP4 inhibition in tissue integrity and repair.

Keywords: Homing, Myocardial Ischemia and Infarction, TGF-beta, Dipeptidyl peptidase 4, Mononuclear Cells, Regenerative Medicine, Tissue Therapy, Cardiovascular Disease

HHT and the underlying genetic causes

Hereditary hemorrhagic telangiectasia (HHT) or Rendu-Osler-Weber disease is a genetic vascular disorder. The onset of the disease and severity is variable for each individual patient and will intensify as the disease progresses with age (Plauchu et al. 1989). To be diagnosed with HHT, a patient has to have 3 of the 4 Curaçao criteria, namely epistaxis, telangiectasias, arteriovenous malformations (AVMs), or a first degree relative with HHT. After diagnosis, patients are genetic screened to identify the underlying mutation (Shovlin et al. 2000). Since the underlying mutation cannot always be identified in every patient, the clinical symptoms are still important for the diagnosis of HHT. To date, 4 genes were found to be mutated, resulting in 4 different HHT subtypes. All genes identified are components of the Transforming Growth Factor beta (TGFβ) signaling pathway. The identified mutations will not generate aberrant proteins, but will rather result in haploinsufficiency, a reduction of the functional protein levels by 50%, causing a disbalance in the TGFβ signaling pathway (Bourdeau et al. 2000; Abdalla & Letarte 2006). HHT-1 is the most prevalent HHT subtype, comprising 53% of Dutch HHT patients (Letteboer et al. 2008). The HHT-1 mutation lies in the endoglin gene (McAllister et al. 1994), a TGFβ co-receptor modulating TGFβ and BMP signaling and crucial for angiogenesis and vascular repair (Pardali et al. 2010). The second most prevalent gene found to be mutated is the activin receptor-like kinase 1 (ALK1) and causes HHT-2 (Johnson et al. 1996). Approximately 40% of the Dutch HHT patients have this HHT-2 variant (Letteboer et al. 2008). ALK1 is a type I receptor able to signal downstream of either BMP or TGFβ, depending on the ligand availability and receptor context (Goumans et al. 2009). Hundreds of variants have been described for both HHT-1 and HHT-2, amounting to approx. 87% of HHT cases globally, leaving about 15-20% of HHT families without a characterized mutation (Garg et al. 2014). HHT-3 and HHT-4 are linked to loci on chromosome 5 and 7 respectively, but the exact genes affected are not yet identified (Cole et al. 2005; Bayrak-toydemir et al. 2006). The third and fourth gene in which mutations are found causing HHT are BMP9 and SMAD4. Interestingly, BMP9 is a ligand for ALK1 (Wooderchak-Donahue et al. 2013) and SMAD4 is a transcription factor involved in transducing BMP and TGFβ signals from the cell membrane into the nucleus. Mutations in SMAD4 cause a combined syndrome of HHT and juvenile polyposis (Gallione et al. 2006).

In this review the consequences of a disturbed TGFβ signaling cascade caused by the different mutations found in HHT will be described, especially how this affects mononuclear cell (MNC) functioning and their capacity to repair.

Impaired angiogenesis in HHT is caused by disrupted TGFβ signaling

As mentioned above, all genes that have been found mutated in HHT are linked to TGFβ signaling. Upon tissue damage, TGFβ is released by the extracellular matrix, apoptotic cells or secreted by platelets, macrophages and T lymphocytes (Grainger et al. 2000; Wan et al. 2012). TGFβ is the prototypic member of a large superfamily to which also activin and BMPs belong. To be able to signal, TGFβ ligands bind to the TGFβ receptor type II, and BMP ligands can to bind to both the BMP receptor type I and II (Goumans et al. 2009). Upon binding of the ligand, a TGFβ type I receptor is recruited and a heterotetrameric complex is formed, which in turn phosphorylates intracellular receptor regulated SMAD proteins. In endothelial cells, TGFβ can signal using two type I receptors, namely via ALK5 resulting in the phosphorylation of SMAD 2 and 3, or by the BMP type I receptor, ALK1 followed by activation of SMAD 1, and 5. ALK1 can only form a complex with the TGFβ receptor type II in the presence of ALK5 in the tetrameric complex and the presence of endoglin as co-receptor (Lebrin et al. 2004; Goumans et al. 2009).

The presence of these two pathways might explain the biphasic effect TGFβ has on angiogenesis, since TGFβ-ALK1 signaling induces endothelial cell proliferation and migration, whereas TGFβ-ALK5 signaling leads to a quiescent endothelium. Endoglin mainly stimulates the TGFβ-ALK1 pathway, and is thought to suppress TGFβ-ALK5 signaling (Goumans et al. 2008). After phosphorylation, the receptor regulated SMADs form a complex with SMAD4, and translocate into the nucleus where they act as a transcription factor to ensure target gene expression.

Since endoglin is involved in endothelial cell proliferation, migration and remodeling of the extracellular matrix (Abdalla & Letarte 2006; Lebrin et al. 2004), the vascular defects and impaired angiogenesis observed in HHT-1 are largely explained by malfunctioning of the endothelial cells (Liu et al. 2014; Jerkic et al. 2006; Düwel et al. 2007). However, although highly expressed on activated endothelial cells, endoglin is also present on stromal cells, smooth muscle cells, mesenchymal and hematopoietic stem cells, and mononuclear cells (MNC) (Kapur et al. 2013). The importance of endoglin for endothelial cell homeostasis became evident when endothelial cells that lack one allele of endoglin were studied. Endoglin heterozygous endothelial cells exhibit reduced ALK1-Smad1/5 signaling. Unexpectedly, these cells adapted their ALK5 expression with a decrease of 80% and therefore also have reduced ALK5-Smad2/3 signaling (Lebrin et al. 2004; Lebrin & Mummery 2008). In contrast, endoglin deficient endothelial cells show an increased ALK1 and ALK5 signaling (Pece-Barbara et al. 2005). This demonstrates that endoglin haploinsufficiency affects downstream TGFβ signaling and gene adaptation. When comparing different studies, we could conclude that the mutations underlying the various HHT subtypes converge in the ALK1 arm of the TGFβ pathway; affecting endoglin, ALK1, BMP9 and SMAD4 proteins. The imbalance caused by the haploinsufficiency of these proteins skews TGFβ signaling towards endothelial cell quiescent state, leading to impaired angiogenesis after tissue injury.

Another manifestation in HHT is the formation of weak blood vessels, as a result of impaired maturation. Lebrin and co-workers found that the anti-angiogenic drug thalidomide induces the recruitment of mural cells such as pericytes and vascular smooth muscle cells. The recruitment of these cells to vessel branching points enhanced the maturation of HHT vessels and reduced the occurrence of epistaxis (Lebrin et al. 2010). Unfortunately thalidomide treatment is prone to side effects such as peripheral neuropathy and fatigue (Ghobrial & Rajkumar 2003; Morawska & Grzasko 2014). Current research is focused on finding a compound with similar mode of action, restoring the maturation of the diseased blood vessels.

Unravelling the etiology and mechanism behind HHT: lessons from mouse models

Murine models have given valuable insights into the mechanism behind the mutations found in HHT patients. The different heterozygous mouse models confirmed that the defect in TGFβ signaling due to the haploinsufficiency resembled HHT, as they developed similar vascular abnormalities like telangiectasias, arteriovenous malformations and endothelial dysplasia (Lowery & de Caestecker 2010). While endoglin deficient mice are embryonically lethal around embryonic day (E)10.5 and show defects in cardiac development and impaired maturation of blood vessels in the yolk sac (Arthur et al. 2000; Bourdeau et al. 1999), endoglin heterozygous mice are vital. However, adult endoglin heterozygous mice show impaired angiogenesis, arteriovenous malformations and display cerebral vascular abnormalities (Satomi et al. 2003; Van Laake et al. 2006). Choi et al. specifically deleted endoglin in endothelial and smooth muscle cells using the SM22α-Cre mouse model. Combined with local VEGF stimulation in the brain, this endoglin deletion causes cerebral AVMs (Choi et al. 2014). However, VEGF stimulation together with deletion of endoglin in the endothelium alone is already enough to cause vascular dysplasia (Choi et al. 2012).

ALK1 deficient mice are also embryonically lethal on E10.5 due to severe hematopoietic defects, arteriovenous malformations and impaired angiogenesis in the embryo as well as in the yolk sac (Sorensen et al. 2003; Urness et al. 2000; Oh et al. 2000). ALK1 heterozygous mice are viable and display HHT-2 like symptoms, such as vascular malformations, lesions and hemorrhages (Srinivasan 2003). Interestingly, endothelial cell specific ALK1 deletion leads to the formation of retinal AVMs and pulmonary hemorrhages, but also causes a reduced expression of endoglin (Tual-Chalot et al. 2014).

Since SMAD4 null mice are embryonically lethal at day 7, and SMAD4 heterozygous mice show no abnormalities, developing a mouse model for this subtype of HHT is not possible (Takaku et al. 1998). Even an endothelium specific SMAD4 deletion is embryonically lethal, as it shows angiogenic as well as cardiac defects (Lan et al. 2007; Qi et al. 2007).

The most recent HHT mutation identified lies within the gene for BMP9. Surprisingly, BMP9 knock-out mice develop normally and do not show any vascular defects (Chen et al. 2013). This lack of phenotype is most likely due to rescue by the closely related BMP10. Interestingly, injection of BMP10 neutralizing antibody into the BMP9 knock-out mice reduced the expansion of the retinal vasculature (Ricard et al. 2012; Chen et al. 2013). This shows that removal of both BMP9 and BMP10 ligands is necessary to induce vascular abnormalities.

In conclusion, mice heterozygous for endoglin or endothelium specific deletion of endoglin resembling HHT-1 (Arthur et al. 2000; Choi et al. 2012; Choi et al. 2014) and animals heterozygous for ALK1 mice resembling HHT-2 (Srinivasan 2003), are suitable mouse models to unravel the etiology and mechanism behind HHT. Whether or not the double knock-out for BMP9/BMP10 will resemble a HHT subtype still needs to be established.

Endoglin expression on MNC and its implications for inflammatory and regenerative properties

As mentioned, endoglin and ALK1 are not only expressed on endothelial cells, but also on some subsets of the mononuclear cell (MNC) fraction. The MNC fraction is an essential cell population during the inflammatory response and the repair process of damaged tissue. The MNC fraction consists of numerous different cell types with highly adaptive responses and cell plasticity. The most predominant cell types within the MNC fraction are T lymphocytes, monocytes and macrophages. Furthermore, there are several smaller cell populations present, such as natural killer cells, dendritic cells and endothelial progenitor cells (EPCs) (Isner et al. 2001).

In healthy subjects, endoglin is upregulated in activated monocytes, but this is impaired in HHT-1 patients (Sanz-Rodriguez et al. 2004). Interestingly, the increased expression of endoglin on activated monocytes was also impaired in HHT-2 patients (Sanz-Rodriguez et al. 2004). We propose that impaired signaling via endoglin and subsequent ALK1 signaling in MNC, and especially monocytes, might be causing immunological problems such as increased infection rate and leukopenia as reported (Guilhem et al. 2013; Peter et al. 2014).

Two phases of MNC recruitment during tissue repair

During tissue repair, two phases are essential, the inflammation and the regeneration phase. The MNCs, and especially the monocytes and macrophages, play important and distinct roles in these two phases (figure 1).

The first inflammatory phase is known as the acute phase, characterized by the infiltration of neutrophils, T lymphocytes and activated monocytes differentiating into inflammatory macrophages (Figure 1). T lymphocytes and inflammatory macrophages are necessary for the clearance of any infectious organisms and the removal of dead tissue and cell debris after an ischemic event and/or injury. The second regenerative phase is initiated when the initial influx of inflammatory cells is (partly) cleared from the site of injury. Secreted cytokines and growth factors stimulate a secondary phase of MNC and resident cells towards the regeneration area. Locally, TGFβ levels are elevated which will activate local endothelial cells and stimulate proliferation and repair/replace damaged vessels. Furthermore, the remaining MNCs, including a second type of monocytes that differentiate towards regenerative macrophages, are recruited which will shift the microenvironment towards tissue repair. The regenerative macrophages are able to induce cell proliferation, angiogenesis and tissue remodeling. For an optimal resolution and recovery of damage tissues, both the inflammatory as well as regenerative macrophages are essential players. To note, macrophages have a high plasticity and are able to change between phenotypes, depending on their microenvironment (Kim & Hematti 2010; Sindrilaru et al. 2011; Mantovani et al. 2013). Furthermore, macrophages have the capacity to interact with lymphocytes, as well as interact with and influence the viability and growth of mesenchymal stem cells and progenitor cells (Freytes et al. 2012). In addition, recent studies demonstrated that TGFβ stimulates the proliferation of regenerative macrophages, inducing a pro-fibrotic phenotype (Murray et al. 2011).

MNC and inflammation in HHT

The composition of the MNC fraction is different in HHT patients compared to healthy subjects. The amount of peripheral blood NK and T lymphocytes was found to be reduced in HHT-1, HHT-2, but also in the unidentified subtypes of HHT patients, while the B lymphocyte and monocyte populations were unaffected, including the phagocytic activity of the monocytes (Guilhem et al. 2013). Furthermore, TGFβ and endoglin have been shown to be essential factors during inflammation and tissue repair, (Shull et al. 1992; Kulkarni et al. 1993; Larsson & Goumans 2001; Ishida et al. 2004; Doetschman et al. 2012). As a consequence of these observations, HHT-1 and HHT-2 patients show an increased infection rate and leukopenia (Mathis et al. 2012; Guilhem et al. 2013), revealing an important role for disturbed inflammatory responses in HHT.

Since a role for ALK1 signaling in MNCs is less profound, we will focus on the function of endoglin in inflammatory responses. A role for endoglin in inflammatory disease became evident when Torsney and co-workers studied the expression of endoglin in human tissue samples and during wound healing. First, tissue sections taken from various affected organs (bowel, liver and skin) in diseases such as inflammatory bowel disease, liver cirrhosis and granuloma showed that endothelial endoglin expression was highly upregulated, and correlated with inflammatory cell infiltrate, including lymphocytes and macrophages, in the immediate surrounding tissue (Torsney et al. 2002). Second, tissue sections from e.g. skin lesions showed that there was a strong increase of endoglin 1-2 days after wounding, and a high level of endoglin persisted for up to one month. Interestingly, the peak of endothelial endoglin gene expression was reached at day 4, with the subsequent peak of protein expression

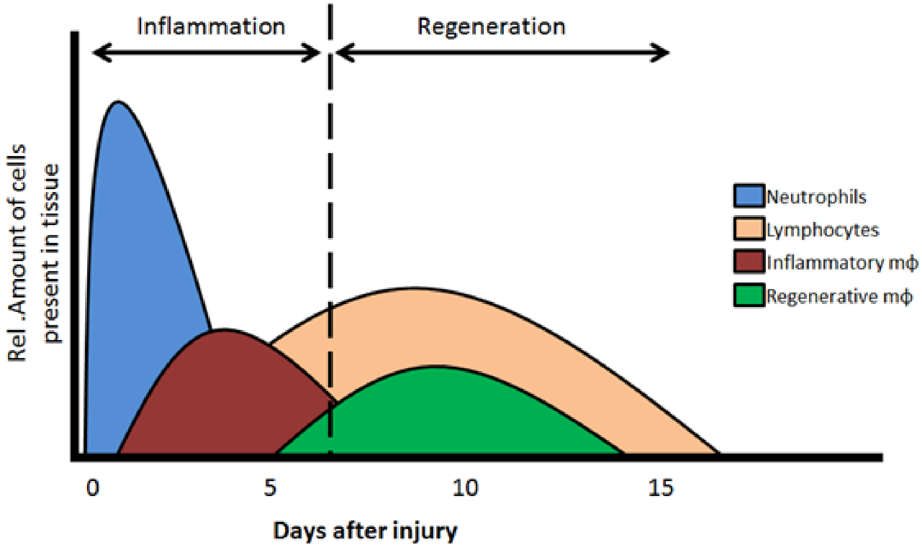

Figure 1. Two phases of MNC recruitment. In the acute phase (day1-4) of tissue injury acute inflammation is initiated by the recruitment of neutrophils, monocytes and inflammatory type macrophages. Resolution of the inflammatory response in regeneration phase is elicited by the recruitment/dedifferentiation of regenerative monocytes/macrophages and lymphocytes. Macrophages = mφ. Adapted from Nahrendorf et al. 2007 and Loebbermann et al. 2012.

at day 7, which coincides with the highest influx of inflammatory cells during the first week after tissue injury, also known as the acute inflammatory phase (Nahrendorf et al. 2007 and Figure 1).

In endoglin heterozygous mice, the restoration of a myocardial infarction was disturbed compared to wild type mice. This was characterized by a reduced cardiac function and by impaired vascularization of the damaged tissue. Interestingly, injection of human MNCs isolated from healthy volunteers into the circulation of the mice after myocardial infarction improved cardiac output and restored angiogenesis, while MNCs from HHT-1 patients did not have this effect (Van Laake et al. 2006). Further analysis revealed that there were significant lower numbers of MNCs of HHT-1 patients at the site of injury after myocardial infarction when compared to control MNC (Post et al. 2010; Van Laake et al. 2006). In a similar study analyzing the kidneys, a reduced number of migrated MNC and macrophages was observed in endoglin heterozygous mice (Docherty et al. 2006). In conclusion, HHT patients have altered subsets of MNCs and the differential expression of endoglin can explain the disturbance in their inflammatory response.

Recruitment of MNC: homing

MNC can either be recruited from different sites, such as the spleen, bone marrow or they are already resident in tissue or blood. The process by which MNCs, and also stem cells, are attracted to sites of ischemia or inflammation is tightly regulated. The main cellular homing mechanism is the SDF1-CXCR4 axis (figure 2). MNCs are retained in the bone marrow and spleen due to the high SDF1 levels (Ceradini et al. 2004). During ischemic disease, such as coronary artery, cerebrovascular or peripheral artery disease, levels of SDF1 are increased. The occlusion of an artery results in hypoxia and an increase in hypoxia inducible factor 1 alpha (HIF1α) levels. HIF1α induces the expression of SDF1, which is then released into the bloodstream creating a gradient of SDF1, causing HSCs and MNCs to be recruited from the bone marrow and spleen, and migrate towards the highest SDF1 concentration present in the damaged tissue (Cencioni et al. 2012). A disturbed homing balance may result in increased fibrosis and adverse remodeling. For example, sustained activation of the SDF1-CXCR4 axis is observed in lung vessels of idiopathic pulmonary fibrosis patients (Smadja et al. 2014) and it was suggested that circulating fibrocytes contribute to intense remodeling of the pulmonary vasculature. Furthermore, infiltration of leukocytes can be mediated by integrins interacting and binding to endoglin, which could well be diminished in HHT-1 patients (Rossi et al. 2013). Besides hypoxia, BMP9 is also a potent inducer of SDF1. The effects of BMP9 on SDF1 have been extensively studied in endothelial cells. Surprisingly, knockdown of either endoglin or ALK1 were shown to impair the upregulation of SDF1 by BMP9 (Young et al. 2012). Mutations in BMP9 are thus likely to decrease SDF1 levels, resulting in an impaired MNC homing capacity. In conclusion, impaired homing of MNC and impaired SDF1 regulation are a common feature of HHT. In contrast, in other vascular diseases like atherosclerosis it has been described that enhanced homing of MNCs is part of the pathology. In atherosclerosis, low density lipoproteins (LDL) increase endothelial SDF1 levels at the distal ends of the atherosclerotic plaques. In addition, LDL-induced SDF1 expression increase monocyte homing *in vitro* and monocyte adhesion via ICAM-1 interaction to the endothelium was enhanced and accelerated the progression of atherosclerotic plaque formation (Wei et al. 2012).

Regulation of MNC recruitment by DPP4

The recruitment of MNCs to sites of tissue damage is tightly regulated. In homeostasis, a negative regulator dipeptidyl peptidase 4 (DPP4) is able to prevent an uncontrollable infiltration of MNCs. DPP4, also known as CD26, is a 110kd transmembrane protein expressed by many different cell types, including endothelial cells, epithelial cells, melanocytes, monocytes and lymphocytes (Yamada et al. 2009; Zhong et al. 2013). DPP4 is a peptidase that will enzymatically remove aminoterminal dipeptides after a proline or an alanine from specific proteins such as SDF1, neuropeptide Y or glucagon-like-protein 1. DPP4 also has non-enzymatic functions. It can influence T lymphocyte function by binding to adenosine deaminase, and acts as a stimulatory factor in T lymphocyte activation pathways (Yamada et al. 2009). Furthermore, DPP4 can interact and co-internalize with CXCR4 (Christopherson et al. 2002), again inhibiting the SDF1-CXCR4 axis. The presence of DPP4 on the MNC membrane and target tissue, as well as the presence of the soluble form in plasma will influence the migration and recruitment of MNCs. How soluble DPP4 is produced is not completely understood. One study suggests that soluble DPP4 is formed by shedding DPP4 from the cell membrane, while another study suggest that DPP4 is secreted by either liver epithelium or lymphocytes (Cordero et al. 2009; Z. Wang et al. 2014). The soluble form of DPP4 only lacks the intracellular and transmembrane parts, but keeps its enzymatic function (Lambeir et al. 2003). Enhanced DPP4 activity will result in enhanced cleavage of SDF1, resulting in loss of its chemotaxic function. The cleavage of SDF1 therefore effectively puts a brake on the homing signal (Christopherson et al. 2002). SDF1 has three isoforms, SDF1α, β and γ. While the functions of SDF1α and β are similar (Shioda et al. 1998), SDF1γ has a higher affinity for the binding protein for chemokines, heparan sulfate (Rueda et al. 2012). Heparan sulfate protects

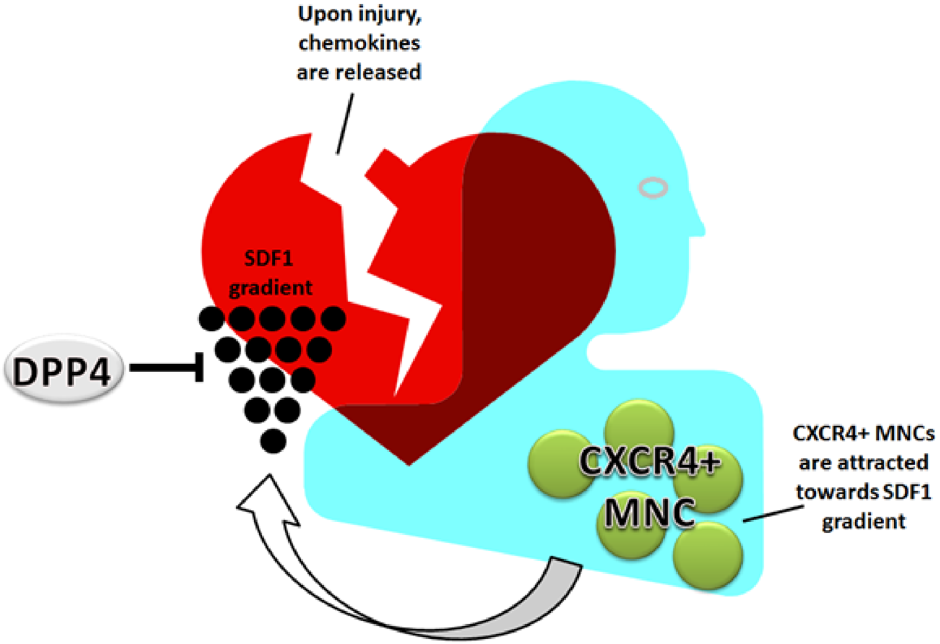
Upon injury, chemokines are released
SDF1 gradient
DPP4
CXCR4+ MNC
CXCR4+ MNCs are attracted towards SDF1 gradient

Figure 2. Homing of MNC: the SDF1-CXCR4 axis. MNCs circulate through the vasculature or are retained by high SDF1 in bone marrow and spleen. Upon ischemia or tissue damage, SDF1 is released into the bloodstream creating an attracting gradient for MNCs. The MNCs home towards the damaged tissue via this gradient. This process is negatively regulated by DPP4.

SDF1 against proteolysis induced by DPP4, keeping the homing signal intact. SDF1γ was found primarily expressed in the adult mouse heart and to a lesser extent in the brain (Torres & Ramirez 2009). However, this restriction of organ expression in mice might not be similar in humans or during disease as SDF1γ was found upregulated in synovial dendritic cells and endothelial cells in patients with rheumatoid arthritis (Santiago et al. 2012). The role of SDF1γ in other diseases and the effects of decreased sensitivity to DPP4 are still unknown. However, increasing the expression of SDF1γ may be an option to stimulate the homing process in HHT-1 patients, making it a very interesting topic for future research.

Alternative homing pathways and mechanisms

Although the SDF1-CXCR4 axis is the main pathway, there are other mechanisms that influence the homing and the mobilization of MNCs. For example, SDF1 is capable of binding to an alternative chemokine receptor, CXCR7. CXCR7 functions as a SDF1 receptor and increases MNC survival and adhesion (Döring et al. 2014). Furthermore, CXCR4 is able to bind to macrophage migration inhibitory factor (MIF). MIF is upregulated after MI, and specifically increases monocyte homing by competing with SDF1 for binding to CXCR4. One other factor that influences homing is interferon-inducible protein 10 (IP10 or CXCL10). This peptide is secreted by a wide variety of cells, including MNCs, fibroblasts and endothelial cells. IP10 functions as a lymphocyte chemotaxic cytokine after binding to its receptor CXCR3. Besides stimulating homing, IP10 can also induce migration and proliferation of endothelial cells and vascular smooth muscle cells (van den Borne et al. 2014). The decreased numbers of lymphocytes found in HHT patients (Guilhem et al. 2013) together with the impaired resolution of inflammation (Peter et al. 2014), suggest upregulation of IP10 might be another strategy to increase homing of MNC in HHT patients and restricting the inflammatory response. The sympathetic nervous system is another pathway involved in the stimulation of homing and modulation of inflammatory responses. Wang et al. showed that after stroke, β3-adrenergic receptor activity reduces the expression of SDF1 in the bone marrow, while the expression of CXCR4 was increased in bone marrow cells. The activated β3-adrenergic receptor also increased the levels of prostaglandin E2 in the bone marrow, which in turn mediates T lymphocyte activation via RANKL (J. Wang et al. 2014). Moreover, cationic lipids such as C3a, anaphylatoxin and cathelicidin increase cell responsiveness to low SDF1 gradients, so-called 'priming'(Ratajczak et al. 2012). In summary, the body has several mechanisms to respond to stress signals, resulting in a rapid and increased mobilization of MNC into the bloodstream followed by homing to the site of injury. The SDF1-CXCR4 axis is the most prominent and is malfunctioning in HHT-1 patients. Stimulating one of the other pathways may correct the homing deficiency present in HHT patients.

DPP4 inhibition in Type II Diabetes Mellitus and cardiovascular disease

DPP4 inhibitors like Sitagliptin, Vildagliptin and Saxagliptin are currently in use to treat patients with type 2 diabetes mellitus (T2DM). Already at baseline, serum DPP4 levels are higher in T2DM patients compared to controls. DPP4 inhibition reduces the cleavage of glucagon-like-peptide 1, an incretin protein that is released upon food intake to decrease insulin levels (Deacon et al. 1998; Mentlein et al. 1993). Interestingly, T2DM patients show a decrease in progenitor cell mobilization (including EPC) from the bone marrow to the circulation – comparable to the impaired homing defect found in HHT. That DPP4 inhibition is a feasible treatment modality for the improvement of MNC homing is strengthened by the observation that in DPP4 deficient mice the mobilization capacity of the progenitor cell population was restored after myocardial infarction, and angiogenesis improved (Zaruba et al. 2009). Interestingly, high serum DPP4 levels were found to be associated with the occurrence of left ventricular dysfunction in T2DM patients (Ravassa et al. 2013). Furthermore, DPP4 inhibition can affect cardiomyocyte metabolism by restoring their ability to switch back to fatty acid metabolism during stress (Witteles et al. 2012). There are many more actions of DPP4 where inhibition is capable of having protective effects in cardiac ischemia-reperfusion injury (Matheeussen et al. 2012). First, DPP4 is able to cleave the vasoconstrictor neuropeptide Y, stimulating angiogenesis via the eNOS pathway. Second, brain natriuretic peptide (BNP) is associated with congestive heart failure and is upregulated after ischemia (Mishra et al. 2014; Santaguida et al. 2014). BNP is cleaved by DPP4, providing protective effects through decreased natriuresis and vasodilation (Vanderheyden et al. 2009). Furthermore, DPP4 has a collagen binding domain – and consequently decreases collagen and fibronectin production, and thereby has the potential to decrease fibrosis (Thielitz et al. 2007). Thus, inhibiting DPP4 has a beneficial effect on tissue repair in more ways than only stimulating the SDF1-CXCR4 axis. DPP4 inhibition using Sitagliptin has no effect on MNC subsets in healthy individuals (Price et al. 2013), while in disease the effects of DPP4 inhibition on MNC migration are profound. In both wild type mice and mice with (induced) continuously proliferating cardiomyocytes, combining DPP4 inhibition with granulocyte colony-stimulating factor (G-CSF) increased stem cell mobilization and stimulated myocardial repair (Zaruba et al. 2009; Theiss et al. 2011; Zaruba et al. 2012; Theiss et al. 2013), not only via increased retention in the ventricular wall, but also via reduction of the adverse remodeling and enhanced angiogenesis. Patients who recover from a myocardial infarction express high DPP4 levels on their MNCs, which is associated with a decreased heart function (Post et al. 2012). DPP4 inhibition is therefore also an interesting treatment option for improving cardiac recovery. The first meta analyses using DPP4 inhibition in clinical trials show no adverse reactions and even a reduction of cardiovascular risks in T2DM patients treated with DPP4 inhibitors (such as Alogliptin, Vildagliptin, Sitagliptin, Saxagliptin or Linagliptin) (Monami et al. 2013; Avogaro et al. 2014). In contrast, DPP4 inhibition causes an increased prothrombogenic status of endothelial cells and correlates with upregulated tissue factor, the initiator of the coagulation cascade (Krijnen et al. 2012). This implicates that care should be taken i.e., treatment may not always be beneficial to patients with increased coagulation status. Nonetheless, the overall data implicate that DPP4 inhibition has positive effects on tissue repair and subsequent cardiovascular function.

DPP4 inhibition in HHT

Interestingly, the expression of DPP4 is increased on MNCs from HHT-1 patients and might explain the disturbed homing of MNC and impaired tissue repair (Van Laake et al. 2006; Post et al. 2010). In a follow up study the MNCs of HHT-1 patients were pretreated with a DPP4 inhibitor, which restored the amount of cells present at the site of infarct (Post et al. 2010). This study again suggests that not only the endothelial cells are affected in HHT-1, but also that the immune cells are involved. How MNCs are specifically affected by the disrupted TGFβ signaling in HHT patients is still not clear. However, several studies point toward a direct link between endoglin and the migratory capacity and function of MNC (Post et al. 2010; Torsney et al. 2002). In-vitro studies also demonstrated a possible direct link between TGFβ and DPP4. For example, the inhibition of DPP4 increases the expression of TGFβ in MNC (Reinhold et al. 1997; Arndt et al. 2000), but induces a reduction of TGFβ expression in skin fibroblasts (Thielitz et al. 2007). In contrast, TGFβ is able to downregulate DPP4 expression in MNC and to reduce the numbers of DPP4+ cells. In HHT-1 patients this effect was less profound, but the DPP4 concentration on the cells is greatly reduced (Post et al. 2010; Post et al. 2012). How DPP4 might interfere with TGFβ signaling and vice versa is not clear. It was suggested that DPP4 has a co-receptor function with CD2 and CD3 on T lymphocytes, providing a possible direct way of interacting with TGFβ/endoglin signaling on the cell membrane (Morimoto & Schlossman 1998; Gorrell et al. 2001).

Clinical perspectives and conclusion

HHT is not only a disease that affects the endothelial cells, the MNCs are also affected. The recruitment of MNCs is impaired, due to increased levels of DPP4 and reduced levels of endothelial membrane endoglin. The inhibition of DPP4 in other vascular diseases shows beneficial results not only on the homing towards damaged tissues, but also on the recovery of functioning of the targeted tissue. For HHT, we know that DPP4 inhibition improves the homing of MNCs. Its impact on actual tissue repair is unknown, and intriguing for future research. DPP4 inhibition will potentially restore homing and stimulate angiogenesis and tissue repair in HHT. However, this only holds true when the function of MNC are not impaired, e.g. improved homing of inflammatory macrophages will hamper the regenerative process. More knowledge on the homing and functioning of MNC can therefore contribute to develop and improve new therapeutic strategies for HHT.

Acknowledgements

This work is funded by the Netherlands Institute for Regenerative Medicine (NIRM) and the Dutch Heart Foundation.

References

Abdalla, S. a & Letarte, M., 2006. Hereditary haemorrhagic telangiectasia: current views on genetics and mechanisms of disease. *Journal of medical genetics*, 43(2), pp.97–110.

Arndt, M. et al., 2000. Dipeptidyl peptidase IV (DP IV/CD26) mRNA expression in PWM-stimulated T-cells is suppressed by specific DP IV inhibition, an effect mediated by TGF-beta(1). *Biochemical and biophysical research communications*, 274(2), pp.410–414.

Arthur, H.M. et al., 2000. Endoglin, an ancillary TGFbeta receptor, is required for extraembryonic angiogenesis and plays a key role in heart development. *Developmental biology*, 217(1), pp.42–53.

Avogaro, A., Vigili de Kreutzenberg, S. & Fadini, G.P., 2014. Cardiovascular actions of GLP-1 and incretin-based pharmacotherapy. *Current diabetes reports*, 14(5), p.483.

Bayrak-toydemir, P. et al., 2006. Rapid Publication A Fourth Locus for Hereditary Hemorrhagic Telangiectasia Maps to Chromosome 7. *American Journal of Medical Genetics*, 2162, pp.2155–2162.

Van den Borne, P. et al., 2014. The multifaceted functions of CXCL10 in cardiovascular disease. *BioMed research international*, 2014.

Bourdeau, a et al., 2000. Endoglin expression is reduced in normal vessels but still detectable in arteriovenous malformations of patients with hereditary hemorrhagic telangiectasia type 1. *The American journal of pathology*, 156(3), pp.911–23.

Bourdeau, A. et al., 1999. A murine model of hereditary hemorrhagic telangiectasia. *Journal of Clinical Investigation*, 104(10), pp.1343–1351.

Cencioni, C., Capogrossi, M.C. & Napolitano, M., 2012. The SDF-1/CXCR4 axis in stem cell preconditioning. *Cardiovascular research*, 94(3), pp.400–7.

Ceradini, D.J. et al., 2004. Progenitor cell trafficking is regulated by hypoxic gradients through HIF-1 induction of SDF-1. *Nature medicine*, 10(8), pp.858–864.

Chen, H. et al., 2013. Context-dependent signaling defines roles of BMP9 and BMP10 in embryonic and postnatal development. *Proceedings of the National Academy of Sciences of the United States of America*, 110(29), pp.11887–92.

Choi, E.-J. et al., 2012. Minimal homozygous endothelial deletion of Eng with VEGF stimulation is sufficient to cause cerebrovascular dysplasia in the adult mouse. *Cerebrovascular diseases (Basel, Switzerland)*, 33(6), pp.540–7.

Choi, E.-J. et al., 2014. Novel brain arteriovenous malformation mouse models for type 1 hereditary hemorrhagic telangiectasia. *PloS one*, 9(2), p.e88511.

Christopherson, K.W., Hangoc, G. & Broxmeyer, H.E., 2002. Cell surface peptidase CD26/dipeptidylpeptidase IV regulates CXCL12/stromal cell-derived factor-1α-mediated chemotaxis of human cord blood CD34+ progenitor cells. *The Journal of Immunology*, 169(12), p.7000.

Cole, S.G. et al., 2005. A new locus for hereditary haemorrhagic telangiectasia (HHT3) maps to chromosome 5. *Journal of medical genetics*, 42(7), pp.577–82.

Cordero, O.J., Salgado, F.J. & Nogueira, M., 2009. On the origin of serum CD26 and its altered concentration in cancer patients. *Cancer Immunology, Immunotherapy*, 58(11), pp.1723–1747.

Deacon, C.F., Hughes, T.E. & Holst, J.J., 1998. Dipeptidyl peptidase IV inhibition potentiates the insulinotropic effect of glucagon-like peptide 1 in the anesthetized pig. *Diabetes*, 47(5), pp.764–9.

Docherty, N.G. et al., 2006. Endoglin regulates renal ischaemia-reperfusion injury. *Nephrology, dialysis, transplantation : official publication of the European Dialysis and Transplant Association - European Renal Association*, 21(8), pp.2106–19.

Doetschman, T. et al., 2012. Transforming growth factor beta signaling in adult cardiovascular diseases and repair. *Cell and tissue research*, 347(1), pp.203–23.

Döring, Y. et al., 2014. The CXCL12/CXCR4 chemokine ligand/receptor axis in cardiovascular disease. *Frontiers in physiology*, 5(June), p.212.

Düwel, A. et al., 2007. Reduced tumor growth and angiogenesis in endoglin-haploinsufficient mice. *Tumour biology : the journal of the International Society for Oncodevelopmental Biology and Medicine*, 28(1), pp.1–8.

Freytes, D.O. et al., 2012. Macrophages Modulate the Viability and Growth of Human Mesenchymal Stem. *Journal of Cellular Biochemistry*.

Gallione, C.J. et al., 2006. SMAD4 mutations found in unselected HHT patients. *Journal of medical genetics*, 43(10), pp.793–7.

Garg, N. et al., 2014. Optimal management of hereditary hemorrhagic telangiectasia. *Journal of blood medicine*, pp.191–206.

Ghobrial, I. & Rajkumar, S., 2003. Management of thalidomide toxicity. *The journal of supportive oncology*, 1(3), pp.194–205.

Gorrell, M.D., Gysbers, V. & McCaughan, G.W., 2001. CD26: a multifunctional integral membrane and secreted protein of activated lymphocytes. *Scandinavian journal of immunology*, 54(3), pp.249–264.

Goumans, M.J., Liu, Z. & ten Dijke, P., 2009. TGF-β signaling in vascular biology and dysfunction. *Cell Research*, 19(1), pp.116–127.

Goumans, M.J., Zonneveld, A.J. Van & ten Dijke, P., 2008. Transforming Growth Factor β – Induced Endothelial-to- Mesenchymal Transition : A Switch to Cardiac Fibrosis? *Trends in Cardiovascular Medicine*, 18(8), pp.293–298.

Grainger, D.J., Mosedale, D.E. & Metcalfe, J.C., 2000. TGF-β in blood: a complex problem. *Cytokine & Growth Factor Reviews*, 11(1-2), pp.133–145.

Guilhem, A. et al., 2013. Immunological abnormalities associated with hereditary haemorrhagic telangiectasia. *Journal of internal medicine*, (274), pp.351–362.

Ishida, Y. et al., 2004. The Essential Involvement of Cross-Talk between IFN-gamma and TGF-beta in the Skin Wound-Healing Process. *The Journal of Immunology*, 172(3), pp.1848–1855.

Isner, J.M. et al., 2001. Bone Marrow as a Source of Endothelial Cells for Natural and Iatrogenic Vascular Repair. *Annals of the New York Academy of Sciences*, 953a, pp.75–84.

Jerkic, M. et al., 2006. Reduced angiogenic responses in adult Endoglin heterozygous mice. *Cardiovascular research*, 69(4), pp.845–54.

Johnson, D.W. et al., 1996. Mutations in the activin receptor-like kinase 1 gene in hereditary haemorrhagic telangiectasia type 2. *Nat Genet*, 13(2), pp.189–195.

Kapur, N.K., Morine, K.J. & Letarte, M., 2013. Endoglin: a critical mediator of cardiovascular health. *Vascular Health and Risk Management*, 9, pp.195–206.

Kim, J. & Hematti, P., 2010. Mesenchymal stem cell-educated macrophages: a novel type of alternatively activated macrophages. *Experimental Hematology*, 37(12), pp.1445–1453.

Krijnen, P.A.J. et al., 2012. Loss of DPP4 activity is related to a prothrombogenic status of endothelial cells: implications for the coronary microvasculature of myocardial infarction patients. *Basic research in cardiology*, 107(1), pp.1–13.

Kulkarni, A.B. et al., 1993. Transforming growth factor beta null mutation in mice causes excessive inflammatory response and early death. *Proc. Nati. Acad. Sci.*, 90, pp.770–774.

Van Laake, L.W. et al., 2006. Endoglin has a crucial role in blood cell-mediated vascular repair. *Circulation*, 114(21), pp.2288–2297.

Lambeir, A.-M. et al., 2003. Dipeptidyl-peptidase IV from bench to bedside: an update on structural properties, functions, and clinical aspects of the enzyme DPP IV. *Critical reviews in clinical laboratory sciences*, 40(3), pp.209–94.

Lan, Y. et al., 2007. Essential role of endothelial Smad4 in vascular remodeling and integrity. *Molecular and cellular biology*, 27(21), pp.7683–92.

Larsson, J. & Goumans, M., 2001. Abnormal angiogenesis but intact hematopoietic potential in TGFβ type I receptor deficient mice. *The EMBO Journal*, 20(7), pp.1663–1673.

Lebrin, F. et al., 2004. Endoglin promotes endothelial cell proliferation and TGF-beta/ALK1 signal transduction. *The EMBO journal*, 23(20), pp.4018–28.

Lebrin, F. et al., 2010. Thalidomide stimulates vessel maturation and reduces epistaxis in individuals with hereditary hemorrhagic telangiectasia. *Nature medicine*, 16(4), pp.420–428.

Lebrin, F. & Mummery, C.L., 2008. Endoglin-mediated vascular remodeling: mechanisms underlying hereditary hemorrhagic telangiectasia. *Trends in cardiovascular medicine*, 18(1), pp.25–32.

Letteboer, T.G.W. et al., 2008. Genotype-phenotype relationship for localization and age distribution of telangiectases in hereditary hemorrhagic telangiectasia. *American journal of medical genetics.*, 146A(21), pp.2733–9.

Liu, Z. et al., 2014. ENDOGLIN Is Dispensable for Vasculogenesis , but Required for Vascular Endothelial Growth Factor-Induced Angiogenesis. *PLOS ONE*, 9(1), pp.1–12.

Loebbermann, J. et al., 2012. Regulatory T cells expressing granzyme B play a critical role in controlling lung inflammation during acute viral infection. *Mucosal Immunology*, 5(2), pp.161–172.

Lowery, J.W. & de Caestecker, M.P., 2010. BMP signaling in vascular development and disease. *Cytokine & growth factor reviews*, 21(4), pp.287–298.

Mantovani, A. et al., 2013. Macrophage plasticity and polarization in tissue repair and remodelling. *The Journal of pathology*, 229(2), pp.176–85.

Matheeussen, V., Jungraithmayr, W. & De Meester, I., 2012. Dipeptidyl peptidase 4 as a therapeutic target in ischemia/reperfusion injury. *Pharmacology & Therapeutics*, 136(3), pp.267–82.

Mathis, S. et al., 2012. Cerebral abscesses in hereditary haemorrhagic telangiectasia: a clinical and microbiological evaluation. *Clinical neurology and neurosurgery*, 114(3), pp.235–40.

McAllister, K.A. et al., 1994. Endoglin, a TGF-beta binding protein of endothelial cells, is the gene for hereditary haemorrhagic telangiectasia type 1. *Nat Genet*, 8(4), pp.345–351.

Mentlein, R., Gallwitz, B. & Schmidt, W.E., 1993. Dipeptidyl-peptidase IV hydrolyses gastric inhibitory polypeptide, glucagon-like peptide-l(7-36)amide, peptide histidine methionine and is responsible for their degradation in human serum. *Eur. J. Biochem*, 214, pp.829–835.

Mishra, R.K. et al., 2014. B-type Natriuretic Peptides for the Prediction of Cardiovascular Events in Patients With Stable Coronary Heart Disease: The Heart and Soul Study. *Journal of the American Heart Association*, 3(4).

Monami, M. et al., 2013. Dipeptidyl peptidase-4 inhibitors and cardiovascular risk: a meta-analysis of randomized clinical trials. *Diabetes, Obesity and Metabolism*, 15(2), pp.112–120.

Morawska, M. & Grzasko, N., 2014. Therapy-related peripheral neuropathy in multiple myeloma patients. *Hematological oncology*.

Morimoto, C. & Schlossman, S.F., 1998. The structure and function of CD26 in the T-cell immune response. *Immunological Reviews*, 161(1), pp.55–70.

Murray, L. et al., 2011. TGF-beta driven lung fibrosis is macrophage dependent and blocked by Serum amyloid P. *The international journal of biochemistry & cell biology*, 43(1), pp.154–62.

Nahrendorf, M. et al., 2007. The healing myocardium sequentially mobilizes two monocyte subsets with divergent and complementary functions. *The Journal of experimental medicine*, 204(12), pp.3037–47.

Oh, S.P. et al., 2000. Activin receptor-like kinase 1 modulates transforming growth factor-beta 1 signaling in the regulation of angiogenesis. *Proceedings of the National Academy of Sciences*, 97(6), pp.2626–2631.

Pardali, E., Goumans, M.J. & ten Dijke, P., 2010. Signaling by members of the TGF-beta family in vascular morphogenesis and disease. *Trends in cell biology*, 20(9), pp.556–567.

Pece-Barbara, N. et al., 2005. Endoglin null endothelial cells proliferate faster and are more responsive to transforming growth factor beta1 with higher affinity receptors and an activated Alk1 pathway. *The Journal of biological chemistry*, 280(30), pp.27800–8.

Peter, M. et al., 2014. Impaired resolution of inflammation in the Endoglin heterozygous mouse model of chronic colitis. *Mediators of Inflammation*, 2014.

Plauchu, H. et al., 1989. Age-related clinical profile of hereditary hemorrhagic telangiectasia in an epidemiologically recruited population. *American journal of medical genetics*, 32(3), pp.291–7.

Post, S. et al., 2010. Impaired recruitment of HHT-1 mononuclear cells to the ischaemic heart is due to an altered CXCR4/CD26 balance. *Cardiovascular research*, 85(3), pp.494–502.

Post, S. et al., 2012. Reduced CD26 expression is associated with improved cardiac function after acute myocardial infarction: insights from the REPERATOR study. *Journal of molecular and cellular cardiology*, 53(6), pp.899–905.

Price, J.D. et al., 2013. Effects of short-term sitagliptin treatment on immune parameters in healthy individuals, a randomized placebo-controlled study. *Clinical and experimental immunology*, 174(1), pp.120–8.

Qi, X. et al., 2007. Essential role of Smad4 in maintaining cardiomyocyte proliferation during murine embryonic heart development. *Developmental Biology*, 311(1), pp.136–146.

Ratajczak, M.Z. et al., 2012. A novel perspective on stem cell homing and mobilization: review on bioactive lipids as potent chemoattractants and cationic peptides as underappreciated modulators of responsiveness to SDF-1 gradients. *Leukemia*, 26(1), pp.63–72.

Ravassa, S. et al., 2013. The activity of circulating dipeptidyl peptidase-4 is associated with subclinical left ventricular dysfunction in patients with type 2 diabetes mellitus. *Cardiovascular diabetology*, 12, p.143.

Reinhold, D. et al., 1997. Inhibitors of dipeptidyl peptidase IV induce secretion of transforming growth factor beta 1 in PWM-stimulated PBMC and T cells. *Immunology*, 91, pp.354–360.

Ricard, N. et al., 2012. BMP9 and BMP10 are critical for postnatal retinal vascular remodeling. *Blood*, 119(25), pp.6162–71.

Rossi, E. et al., 2013. Endothelial endoglin is involved in inflammation: Role in leukocyte adhesion and transmigration. *Blood*, 121(2), pp.403–415.

Rueda, P. et al., 2012. Homeostatic and tissue reparation defaults in mice carrying selective genetic invalidation of CXCL12/proteoglycan interactions. *Circulation*, 126(15), pp.1882–95.

Santaguida, P.L. et al., 2014. BNP and NT-proBNP as prognostic markers in persons with acute decompensated heart failure: a systematic review. *Heart failure reviews*.

Santiago, B. et al., 2012. CXCL12γ isoform is expressed on endothelial and dendritic cells in rheumatoid arthritis synovium and regulates T cell activation. *Arthritis and rheumatism*, 64(2), pp.409–17.

Sanz-Rodriguez, F. et al., 2004. Mutation analysis in Spanish patients with hereditary hemorrhagic telangiectasia: deficient endoglin up-regulation in activated monocytes. *Clinical chemistry*, 50(11), pp.2003–11.

Satomi, J. et al., 2003. Cerebral vascular abnormalities in a murine model of hereditary hemorrhagic telangiectasia. *Stroke; a journal of cerebral circulation*, 34(3), pp.783–9.

Shioda, T. et al., 1998. Anti-HIV-1 and chemotactic activities of human stromal cell-derived factor 1α (SDF-1α) and SDF-1β are abolished by CD26/dipeptidyl peptidase IV-mediated cleavage. *Proceedings of the National Academy of Sciences* , 95 (11), pp.6331–6336.

Shovlin, C.L. et al., 2000. Diagnostic criteria for hereditary hemorrhagic telangiectasia (Rendu-Osler-Weber syndrome). *American journal of medical genetics*, 91(1), pp.66–7.

Shull, M.M. et al., 1992. Targeted disruption of the mouse transforming growth factor-beta 1 gene results in multifocal inflammatory disease. *Nature*, 359(6397), pp.693–699.

Sindrilaru, A. et al., 2011. An unrestrained proinflammatory M1 macrophage population induced by iron impairs wound healing in humans and mice. *The Journal of clinical investigation*, 121(3), p.985.

Smadja, D.M. et al., 2014. Cooperation between human fibrocytes and endothelial colony-forming cells increases angiogenesis via the CXCR4 pathway. *Thrombosis and haemostasis*, 112(5), pp.1–12.

Sorensen, L.K. et al., 2003. Loss of distinct arterial and venous boundaries in mice lacking endoglin, a vascular-specific TGFbeta coreceptor. *Developmental biology*, 261(1), pp.235–250.

Srinivasan, S., 2003. A mouse model for hereditary hemorrhagic telangiectasia (HHT) type 2. *Human Molecular Genetics*, 12(5), pp.473–482.

Takaku, K. et al., 1998. Intestinal Tumorigenesis in Compound Mutant Mice of both Dpc4(Smad4) and

Apc Genes. *Cell*, 92(5), pp.645–656.

Theiss, H.D. et al., 2013. Antidiabetic gliptins in combination with G-CSF enhances myocardial function and survival after acute myocardial infarction. *International journal of cardiology*, 168, pp.3359–3369.

Theiss, H.D. et al., 2011. Dual stem cell therapy after myocardial infarction acts specifically by enhanced homing via the SDF-1/CXCR4 axis. *Stem cell research*, 7, pp.244–255.

Thielitz, A. et al., 2007. Inhibitors of dipeptidyl peptidase IV-like activity mediate antifibrotic effects in normal and keloid-derived skin fibroblasts. *Journal of Investigative Dermatology*, 128(4), pp.855–866.

Torres, R. & Ramirez, J.C., 2009. A chemokine targets the nucleus: Cxcl12-gamma isoform localizes to the nucleolus in adult mouse heart. *PloS one*, 4(10), p.e7570.

Torsney, E. et al., 2002. Inducible expression of human endoglin during inflammation and wound healing in vivo. *Inflammation Research*, 51(9), pp.464–470.

Tual-Chalot, S. et al., 2014. Endothelial depletion of Acvrl1 in mice leads to arteriovenous malformations associated with reduced endoglin expression. *PloS one*, 9(6).

Urness, L.D., Sorensen, L.K. & Li, D.Y., 2000. Arteriovenous malformations in mice lacking activin receptor-like kinase-1. *Nature genetics*, 26(3), pp.328–31.

Vanderheyden, M. et al., 2009. Dipeptidyl-peptidase IV and B-type natriuretic peptide. From bench to bedside. *Clinical chemistry and laboratory medicine : CCLM / FESCC*, 47(3), pp.248–52.

Wan, M. et al., 2012. Injury-activated transforming growth factor β controls mobilization of mesenchymal stem cells for tissue remodeling. *Stem cells*, 30(11), pp.2498–511.

Wang, J. et al., 2014. Cerebral ischemia increases bone marrow CD4(+)CD25(+)FoxP3(+) regulatory T cells in mice via signals from sympathetic nervous system. *Brain, behavior, and immunity*, (August).

Wang, Z. et al., 2014. Soluble DPP4 originates in part from bone marrow cells and not from the kidney. *Peptides*, 57, pp.109–17.

Wei, D. et al., 2012. Upregulation of SDF-1 is associated with atherosclerosis lesions induced by LDL concentration polarization. *Annals of biomedical engineering*, 40(5), pp.1018–27.

Witteles, R.M. et al., 2012. Dipeptidyl peptidase 4 inhibition increases myocardial glucose uptake in nonischemic cardiomyopathy. *Journal of cardiac failure*, 18(10), pp.804–9.

Wooderchak-Donahue, W.L. et al., 2013. BMP9 Mutations Cause a Vascular-Anomaly Syndrome with Phenotypic Overlap with Hereditary Hemorrhagic Telangiectasia. *The American Journal of Human Genetics*, 93(3), pp.530–537.

Yamada, K. et al., 2009. Localization of CD26/DPPIV in nucleus and its nuclear translocation enhanced by anti-CD26 monoclonal antibody with anti-tumor effect. *Cancer cell international*, 9, p.17.

Young, K. et al., 2012. BMP9 regulates endoglin-dependent chemokine responses in endothelial cells., 120(20), pp.4263–4273.

Zaruba, M.M. et al., 2012. Granulocyte colony-stimulating factor treatment plus dipeptidylpeptidase-IV inhibition augments myocardial regeneration in mice expressing cyclin D2 in adult cardiomyocytes. *European heart journal*, 33(1), pp.129–137.

Zaruba, M.M. et al., 2009. Synergy between CD26/DPP-IV inhibition and G-CSF improves cardiac function after acute myocardial infarction. *Cell Stem Cell*, 4(4), pp.313–323.

Zhong, J. et al., 2013. A potential role for dendritic cell/macrophage-expressing DPP4 in obesity-induced visceral inflammation. *Diabetes*, 62(1), pp.149–57.

3

Inhibiting DPP4 in a mouse model of HHT1 results in a shift towards regenerative macrophages and reduces fibrosis after myocardial infarction

Dingenouts C.K.E., Bakker W., Lodder K., Wiesmeijer K.C., Moerkamp A.T., Maring J.A., Arthur H.M., Smits A.M., Goumans M.J.

PLoS One. 2017 Dec 18;12(12):e0189805.

Abstract

Aims: Hereditary Hemorrhagic Telangiectasia type-1 (HHT1) is a genetic vascular disorder caused by haploinsufficiency of the TGFβ co-receptor endoglin. Dysfunctional homing of HHT1 mononuclear cells (MNCs) towards the infarcted myocardium hampers cardiac recovery. HHT1-MNCs have elevated expression of dipeptidyl peptidase-4 (DPP4/CD26), which inhibits recruitment of CXCR4-expressing MNCs by inactivation of stromal cell-derived factor 1 (SDF1). We hypothesize that inhibiting DPP4 will restore homing of HHT1-MNCs to the infarcted heart and improve cardiac recovery.

Methods and Results: After inducing MI, wild type (WT) and endoglin heterozygous (*Eng*$^{+/-}$) mice were treated for 5 days with the DPP4 inhibitor Diprotin A (DipA). DipA increased the number of CXCR4^{+} MNCs residing in the infarcted *Eng*$^{+/-}$ hearts (*Eng*$^{+/-}$ 73.17±12.67 vs. *Eng*$^{+/-}$ treated 157.00±11.61, P=0.0003) and significantly reduced infarct size (*Eng*$^{+/-}$ 46.60±9.33% vs. *Eng*$^{+/-}$ treated 27.02±3.04%, P=0.03). Echocardiography demonstrated that DipA treatment slightly deteriorated heart function in *Eng*$^{+/-}$ mice. An increased number of capillaries (*Eng*$^{+/-}$ 61.63±1.43 vs. *Eng*$^{+/-}$ treated 74.30±1.74, P=0.001) were detected in the infarct border zone whereas the number of arteries was reduced (*Eng*$^{+/-}$ 11.88±0.63 vs. *Eng*$^{+/-}$ treated 6.38±0.97, P=0.003). Interestingly, while less M2 regenerative macrophages were present in *Eng*$^{+/-}$ hearts prior to DipA treatment, (WT 29.88±1.52% vs. *Eng*$^{+/-}$ 12.34±1.64%, P<0.0001), DPP4 inhibition restored the number of M2 macrophages to wild type levels.

Conclusions: In this study, we demonstrate that systemic DPP4 inhibition restores the impaired MNC homing in *Eng*$^{+/-}$ animals post-MI, and enhances cardiac repair, which might be explained by restoring the balance between the inflammatory and regenerative macrophages present in the heart.

Introduction

Hereditary Hemorrhagic Telangiectasia type 1 (HHT1) is a haploinsufficient genetic vascular disorder caused by mutations in the transforming growth factor beta (TGFβ) co-receptor endoglin (CD105). HHT1 is characterized by 'leaky' vessel formation due to impaired TGFβ signaling, demonstrated by internal organ bleeding, endothelial hyperplasia, arteriovenous malformations (AVMs) and recurrent epistaxis, up to 8 times a day[1,2]. Interestingly, endoglin heterozygous mice (*Eng*$^{+/-}$) can develop the same clinical features as HHT1 patients[3,4]. In time, depending on the genetic background[5], *Eng*$^{+/-}$ mice develop AVMs clearly visible in the ear, and even suffer from nosebleeds, making the *Eng*$^{+/-}$ mouse a good experimental model to gain more insight in the etiology of HHT1.

The partial loss of endoglin results in reduced angiogenesis[6], and defective collateral artery formation after hind limb ischemia in *Eng*$^{+/-}$ mice[7], emphasizing the necessity of sufficient endoglin expression for proper revascularization after tissue damage[8,9]. Although endoglin is mainly expressed by endothelial cells (ECs), several other cell types including smooth muscle cells (SMCs) and mononuclear cells (MNCs) have endoglin on their cell surface[10]. Due to the prominent role of endoglin in endothelial cell signaling and behavior, HHT1 is generally considered a result of endothelial dysfunction. However, it has become clear that the other cell types expressing endoglin, e.g. immune cells, may have a severe impact on angiogenesis and tissue repair as well[11-13].

Previously we showed that *Eng*$^{+/-}$ mice display a diminished cardiac recovery after experimentally induced myocardial infarction (MI) compared to wild type littermates[14]. The reduced cardiac function is partially rescued when human control MNCs were injected into the tail vein of *Eng*$^{+/-}$ mice. Interestingly, delivery of MNCs isolated from peripheral blood of HHT1 patients did not increase heart function post-MI. Furthermore, endoglin heterozygosity reduced the homing capacity of MNCs to the injured myocardium due to enhanced dipeptidyl peptidase-4 (DPP4, also known as CD26) expression levels[14,15]. This suggests that a defect in MNCs, and not only endothelial cells, may play a role in the pathology of HHT1.

During the cardiac post-injury response, homing of MNCs to the site of injury is regulated by the stromal cell-derived factor 1 (SDF1)-CXC chemokine receptor type 4 (CXCR4) axis. SDF1 levels are increased within the first 24 hours after MI[16]. MNCs expressing the SDF1 receptor CXCR4 respond to this gradient by homing to the site of injury. The SDF1-CXCR4 axis is tightly controlled by the negative regulator DPP4. The catalytic enzyme DPP4 inactivates SDF1 by cleaving off the first two of its amino-terminal peptides, thereby decreasing the ability to recruit CXCR4-expressing MNCs towards the SDF1 gradient[17].

Another important target of DPP4 is the glucagon-like peptide-1 (GLP1). Preserving GLP1 via DPP4 inhibition stimulates insulin secretion and has therefore been the recent focus for treatment of type 2 diabetes mellitus (T2DM). Interestingly, DPP4 inhibition was shown to have multiple off-target effects that are potentially beneficial in the treatment of cardiovascular disease[18,19]. These DPP4 inhibitory actions are GLP1 independent and can range from having an anti-inflammatory effect[20,21] to having a stimulating effect on MNC migration[15] and differentiation[22,23]. Pre-treating MNCs of HHT1 patients with the DPP4 inhibitor Diprotin A (DipA) before injection into the circulation restored their homing to the ischemic myocardium[15]. Unfortunately, this is not a suitable protocol for clinical practice to pre-treat MNCs of HHT1 patients, as cells have to be isolated in sufficient numbers from the patients' peripheral blood, treated with a DPP4 inhibitor and re-injected. Therefore, the aim of this study is to determine whether systemic application of a DPP4 inhibitor is as effective in restoring homing of *Eng*$^{+/-}$ MNCs to the site of ischemic injury.

Materials & Methods

Animals and study design

Experiments and analyses were conducted on male endoglin wild type (*Eng*$^{+/+}$, or referred to as WT) and heterozygous (*Eng*$^{+/-}$) transgenic mice and LysM-Cre-*Eng*$^{fl/+}$ / LysM-Cre-*Eng*$^{fl/fl}$ (endoglin targeted recombination under regulation of the Lysosome M promoter) transgenic mice. All mouse strains were kept on a C57BL/6Jico background (Charles River). To obtain the *Eng*-conditional knockout mouse lines, endoglin floxed mice (*Eng*$^{fl/fl}$) were cross-bred with LysM-Cre[24,25] animals to create the LysM-Cre-*Eng*$^{fl/+}$ and LysM-Cre-*Eng*$^{fl/fl}$ mice. All mouse experiments were approved by the regulatory authorities of Leiden University (the Netherlands) and were in compliance with the guidelines from Directive 2010/63/EU of the European Parliament on the protection of animals used for scientific purposes.

Humane endpoints were observed 5 days post-MI and onwards, as the following criteria and symptoms: when mice displayed reduced mobility, decreased grooming, and/or impaired reaction to external stimuli. In addition, for 3 days post-MI and onwards: when the wound area displayed bleeding, swelling, redness and/or discharge, the mice would be euthanized by carbon dioxide. The mice were weighed at the day of surgery and at the cardiac ultrasound time points and euthanized when more than 15% loss of weight occurred. All mice that died before meeting the criteria for euthanasia –just after myocardial infarction or within 10 days post-MI- died because of cardiac rupture due to the deterioration of cardiac tissue after ligation of the left anterior descending coronary artery. Animal health and behavior were monitored on a daily basis by the research and/or animal care staff, all trained in animal care and handling. Once animals reached endpoint criteria, the euthanasia was performed immediately or at the least the same day when reported.

Myocardial infarction in mice

Myocardial infarction (MI) was experimentally induced as described before[15]. The mice (n=5-18 per group) were anesthetized with isoflurane (1.5-2.5%), intubated and ventilated, after which the left anterior descending (LAD) coronary artery was permanently ligated by placement of a suture. The mice were treated with the analgesic drug Temgesic, both pre-operative and 24 hrs post-operative to relieve pain. The mice were randomly allocated and treated i.p. with either 100 µl distilled water daily (Milli-Q ultrapure, sterile water = MQ treated or control group) or 100 µl DPP4 inhibitor (5 nMol, 55 µg/kg/day, Diprotin A, Sigma-Aldrich) for the first 5 or 14 days post-MI.

Cardiac function measurements

Mice were anesthetized with isoflurane (1.5-2.5%), after which cardiac ultrasound was performed and recorded with the Vevo 770 (VisualSonics, Inc., Toronto, CA) system, using a 30 MHz transducer (RMV707B). Imaging was performed on the longitudinal axis of the left ventricle using the EKV (Electrocardiography-based Kilohertz Visualization) in long axis view imaging mode. The percentage ejection fraction was determined by tracing of the volume of the left ventricle during the systolic and diastolic phase using the imaging software Vevo770 V3.0 (VisualSonics, Inc., Toronto, CA).

Cultured macrophages from mouse bone marrow

Monocytes were isolated from the mice femur and tibia and subsequently cultured in RPMI 1640 culture media (#11875093, Gibco, ThermoFisher Scientific), supplemented with 10% FBS (#10270, Fetal Bovine Serum, Gibco, ThermoFisher Scientific) and 1 ng/ml granulocyte-macrophage colony stimulating factor (GM-CSF, #315-03, Peprotech) to induce differentiation into macrophages. Macrophage cultures from 3 mice of each genotype were pooled to obtain sufficient protein to perform Western blot analysis.

Western blotting

Cultured macrophages were lysed on ice with cold radio immunoprecipitation assay (RIPA) lysis buffer (in house) supplemented with protease inhibitors (Complete protease inhibitor cocktail tablets, Roche Diagnostics, #11697498001) and protein concentration was measured using BCA protein assay (Pierce BCA Protein Assay Kit, #23225, ThermoFisher Scientific). Equal amounts of protein were loaded onto 10% SDS-polyacrylamide gel and transferred to an Immobilon-P transfer membrane (# IPVH00010, PVDF membrane, Millipore). The blots were blocked for 1 h using 10% milk in Tris-Buffered Saline and 0.1% Tween-20 solution and incubated O/N with goat anti-mouse endoglin (1:1000 dilution, BAF1097, R&D Systems) or mouse anti-β-Actin (1:10.000 dilution, A5441, Sigma-Aldrich). Blots were incubated for 1 h with horse radish peroxidase anti-goat (goat anti-mouse IgG Poly-HRP Secondary Antibody HRP conjugate, #32230, ThermoFisher Scientific) or anti-mouse (ECL mouse IgG, HRP-linked whole Ab #NA931, Sigma-Aldrich, GE Healthcare, UK). Blots were developed in a Kodak X-omat 1000 processor with Thermo Scientific SuperSignal West Dura (Extended Duration Substrate) or SuperSignal West Pico and exposed to Fuji SuperRX medical X-ray film. Analysis was performed using Image J (National Institute of Mental Health, Bethesda, Maryland, USA).

Immunofluorescence and immunohistochemistry

Hearts were dissected from carbon dioxide-euthanized mice, 4, 14 or 28 days post-MI, fixated overnight at 4^{o}C in 4% paraformaldehyde in PBS, and then washed with PBS, 50% EtOH and 70% EtOH for 1 h each, followed by embedding in paraffin wax. Sections of 6 µm thickness were mounted onto coated glass slides (VWR SuperFrost Plus microscope slides). The paraffin sections were stained as previously described[26] using antigen retrieval. Primary antibodies were incubated overnight at 4^{o}C and directed against rat anti-mouse CXCR4 (clone 2B11, dilution 1:100, # 551852, BD Pharmingen), rat anti-mouse MAC3 (CD107b, dilution 1:200, #550292, BD Biosciences), rabbit anti-mouse Mannose Receptor (CD206, dilution 1:300, ab64693, Abcam), rabbit anti-mouse alpha smooth muscle actin (αSMA, dilution 1:500, ab5694, Abcam), rat anti-mouse PECAM-1 (CD31, dilution 1:800, #TLD-4E8, BD Pharmingen) and goat anti-mouse cardiac troponin I (cTnI, 1:1000 dilution, #4T21, HyTest). Appropiate fluorescent-labelled secondary antibodies (ThermoFisher Scientific) were incubated for 1.5 h, at 1:250 dilutions. The slides were mounted with Prolong Gold-DAPI Antifade (# P36931, ThermoFisher Scientific) reagent.

Staining of fibrotic tissue was performed using Picrosirius Red (PSR) collagen staining which includes deparaffinization, 1 h incubation with PSR solution (Sirius red F3B, CI 35780, Sigma Aldrich, in Picrine acid solution, # 690550, Klinipath), washing in acidified water and mounting with Entellan (#107960, Merck) reagent. Staining of macrophages present in the infarct border zone using rat anti-mouse MAC3 (CD107b, dilution 1:200, BD Biosciences) was performed using avidin/biotin-based DAB peroxidase staining with the Vectastain ABC system (Vector Laboratories) and hematoxylin counterstain to visualize cell nuclei.

Flow cytometry

After isolation of the hearts (n=3-6), the left ventricle was excised and washed with PBS. Heart tissue was digested in collagenase I (450 U/ml), collagenase XI (125 U/ml), DNase I (60 U/ml) and hyaluronidase (60 U/ml) (Sigma-Aldrich #H3506) at 37^{0}C for 1 h. Hearts were subsequently homogenized through a 100-µm cell strainer (VWR-Corning #10054-458). MNCs were isolated using Ficoll gradient (Histopaque-1083, Sigma, # 10831). Mouse MNCs from either 50 µL of whole blood (treated 5min with erythrocyte lysis buffer, #930725, Alrijne hospital Leiden), or cells isolated from heart, bone marrow and spleen were labeled 1 h at room temperature with anti-mouse CD11b (1:1600, BD Biosciences, #561114) and Ly6C (1:800, BD Biosciences, #561085) for macrophages. Macrophages were identified as inflammatory M1: Ly6G^{-}/CD11b^{+}/Ly6C^{high} and regenerative M2 macrophages: Ly6G^{-}/CD11b^{+}/Ly6C^{low} as previously described[27]. Lymphocytes subsets were labeled with CD3e (1:800, BD Biosciences, #558214), CD4 (1:800, Invitrogen, #MCD0422), CD8a (1:1600, BD Biosciences, #553032) and Ly6G (1:1600, BD Biosciences, #560602) in buffer (2mM EDTA/ 0.5% BSA in PBS).

All acquisitions were performed on a LSRII flow cytometer (BD Biosciences) and analyzed by FACS Diva software (BD Biosciences) and Flowing software 2.5.1 (Cell Imaging Core, Turku Centre for Biotechnology, Finland). Gating strategies are provided in S7 Figure.

Morphometry

Infarct size was determined in Picrosirius Red staining images by calculating the percentage infarct area of the total left ventricular area. Cell infiltration was determined by quantification of 2 to 4 digital images per heart, at the border zone inside the infarcted area, taken at 40x magnification (CaseViewer 3D Histech). The same method was used for quantification of capillary and artery presence, except analysis was now at the outside border zone of the infarct, where cardiomyocytes were still viable. Data were blinded to the investigator and quantified by using ImageJ v1.46r (NIH, USA).

Statistics

All results are expressed as mean ± standard error of the mean (SEM). Statistical significance was accepted at $p<0.05$. Statistical significance was evaluated using one-way ANOVA testing for difference between multiple groups. Adjustment for multiple comparisons with either Tukey’s or Dunnett’s testing and unpaired students T-testing for testing between two groups, using Graphpad Prism v6 for Windows. For data with groups where n=3, non-parametric testing was performed with Kruskal-Wallis ANOVA and Dunn’s multiple comparisons test. Significant differences between survival curves were tested with a log-rank Mantel-Cox test.

Results

Involvement of macrophage-expressed endoglin during cardiac regeneration

We have previously shown that HHT1 MNCs are impaired in their homing capacity towards ischemic tissue[14]. To establish the endogenous contribution of MNCs to the *Eng*$^{+/-}$ phenotype, an LysM-specific mouse model for targeting myeloid cells (monocytes, macrophages and granulocytes) was generated. Mice with either a heterozygous or homozygous deletion for LysM-specific endoglin were analyzed. To validate recombination, MNCs were allowed to differentiate towards macrophages in the presence of GM-CSF and western blot analysis showed reduced endoglin expression in the LysM-Cre-*Eng*$^{fl/+}$, and a near absence of endoglin in the LysM-Cre-*Eng*$^{fl/fl}$ macrophages (Fig. 1A and B).

The deletion of endoglin in monocytes did not affect survival post-MI (Fig. 1C). Analysis of cardiac function showed a trend towards reduced EF in the LysM-Cre-*Eng*$^{fl/fl}$ mice (Fig. 1D, WT 34.07±3.65% vs LysM-Cre-*Eng*$^{fl/fl}$ 22.73±4.30%, P=0.09), suggesting an involvement of endoglin in macrophage function during cardiac repair. However, since cardiac dysfunction of the LysM-Cre-*Eng*$^{fl/fl}$ phenotype post-MI is not as pronounced as the reduction in EF seen in the *Eng*$^{+/-}$ mouse after MI (Fig. 1D, WT 32.45±4.06% vs. *Eng*$^{+/-}$ 17.98±2.06%, $P<0.05$), we concluded that the injury response in HHT1 is likely to be an interplay between a multitude of cell types, only partially represented by the LysM population. We therefore continued by analyzing the effect of DPP4 inhibitor treatment in the *Eng*$^{+/-}$ animals.

DPP4 inhibition restores the *in vivo* MNC homing capacity in *Eng*$^{+/-}$ mice

Macrophage infiltration is important for proper repair of damaged tissue [12,28,29]. Pre-treatment of the HHT1-MNCs, expressing enhanced levels of DPP4, with a DPP4 inhibitor prior to intravenous injection after experimentally induced MI in the mouse restored homing of these cells to the infarct site. Therefore, we asked the question whether systemic administration of a DPP4 inhibitor would have the same effect, and treated mice with the DPP4 inhibitor Diprotin A (DipA) systemically via intraperitoneal (i.p.) injection from day 0 till day 5 post-MI. Flow cytometric analysis of blood samples at baseline revealed that the mice did not display any leukopenia because of endoglin heterozygosity (S1 Figure; gating strategy provided in S7 Figure A and B). At day 4 post-MI, during the peak of inflammatory cell influx [12], MNC homing to the infarcted border zone is diminished in *Eng*$^{+/-}$ mice (Fig. 2A) as shown by a decrease in the number of CXCR4 positive MNCs in the infarct border zone (Fig. 2A, quantification in B).

Systemic DipA treatment of *Eng*$^{+/-}$ mice did not affect survival up to 14 days post-MI (S2 Figure), nor did it hematopoietic cell release from the bone marrow (data not shown), or granulocyte presence in the blood or infarcted cardiac tissue (S3 Figure and gating strategy provided in S7 Figure C). DipA treatment did increase the homing of CXCR4 expressing cells to the infarct border zone of *Eng*$^{+/-}$ heart to similar levels as observed in MQ treated WT mice (Fig. 2B, WT control 154.50±17.21 and *Eng*$^{+/-}$ control 73.17±12.67 vs. *Eng*$^{+/-}$ DipA treated 157.00±11.61, P=0.0003). DipA treatment of control mice did not result in a significant increase in MNC influx post-MI, suggesting that a maximal homing capacity is already achieved in these animals (Fig. 2B, WT control 154.50±17.21vs. WT DipA treated 178.00±6.50). The same restorative effect on homing was observed for MAC3 positive macrophages. Quantification of MAC3^{+} cells in the infarct border zone showed a decreased number of macrophages in infarcted hearts of *Eng*$^{+/-}$ mice, but their homing is enhanced upon

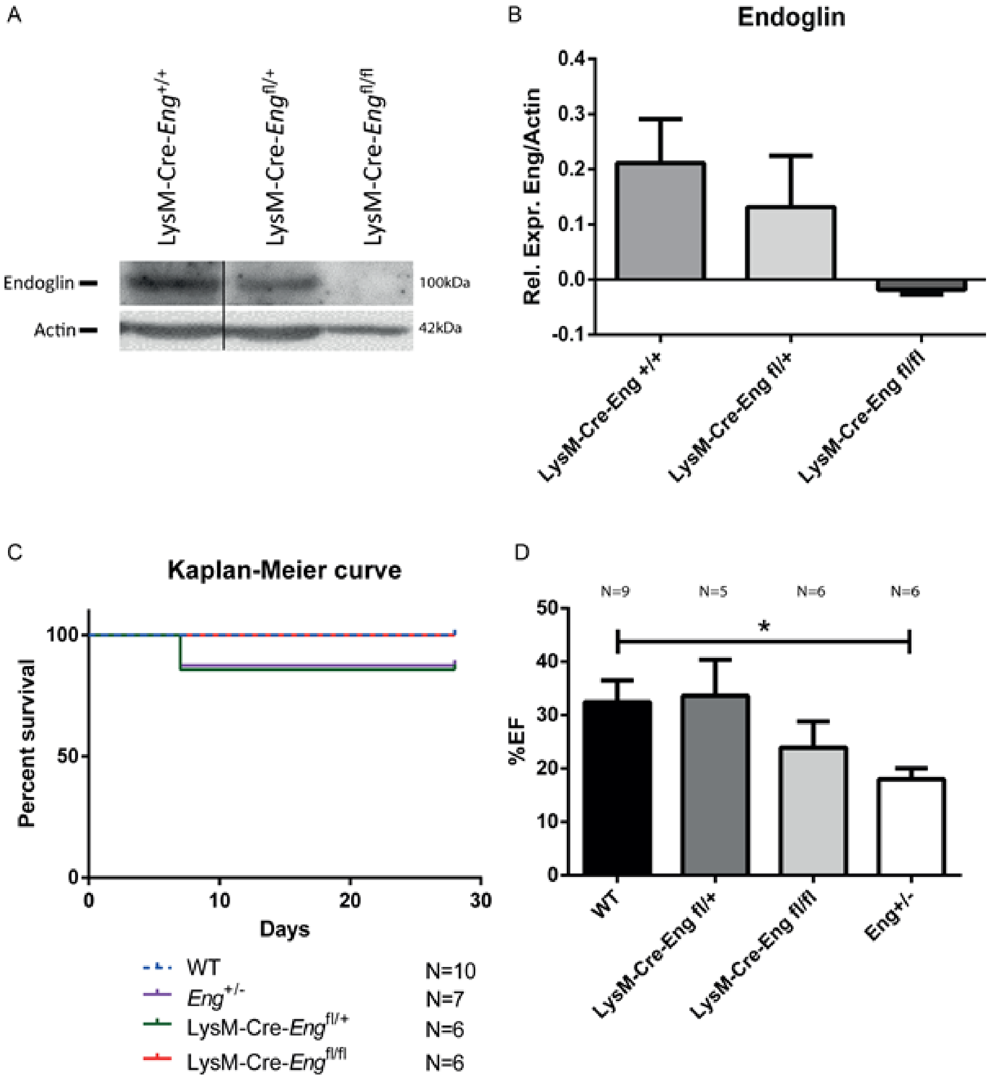

Fig. 1. Monocyte specific knock-out of endoglin does not recapitulate the Eng+/- phenotype. **(A) Western blot analysis of endoglin protein expression in LysM-Cre-Eng+/+, LysM-Cre-Engfl/+ and LysM-Cre-Engfl/fl cultured macrophages. A representative experiment is shown. (B) Quantification of the Western blots for endoglin protein in LysM-Cre-Eng+/+, LysM-Cre-Engfl/+ and LysM-Cre-Engfl/fl cultured macrophages in two independent experiments(macrophage cultures from 3 individual mice of each genotype were pooled per western blot). (C) Kaplan-Meier survival curve of wild type (WT), LysM-Cre-Engfl/+ and LysM-Cre-Engfl/fl mice 28 days post-MI (n=6-10). (D) Cardiac function in percentage ejection fraction (%EF) 14 days post-MI. Cardiac function was measured by ultrasound in long axis view (n=5-9). Data are shown as mean ± SEM, *P<0.05.**

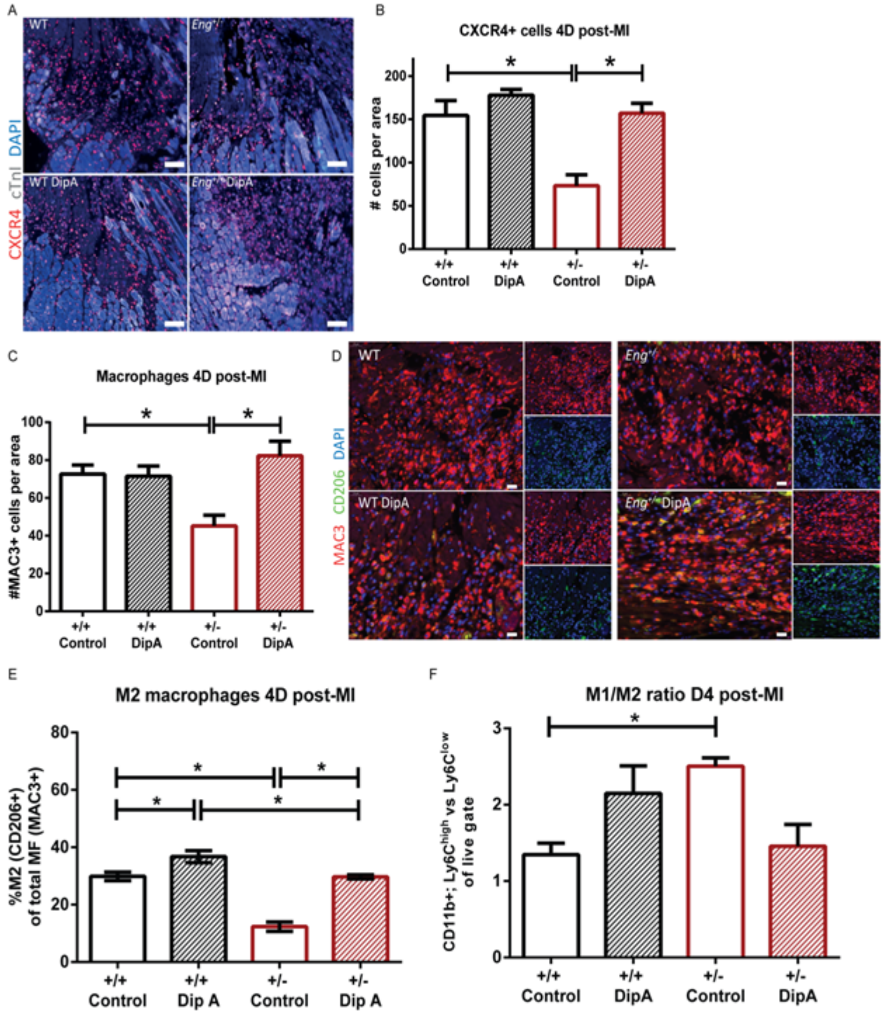

Fig. 2. DPP4 inhibitor treatment of Eng+/- mice restores homing of MNCs to injured myocardium at 4 days post-MI.

(A) Representative microscopy images of CXCR4 expression in the infarct border zone. White = surviving myocardium, black/grey area = infarcted myocardium. Photos taken at 30x magnification. Scale bar: 50µm. CXCR4 = red, cTnI = white, DAPI nuclear staining= blue. (B) Quantification of CXCR4 expressing cells in the infarct border zone (n=6-8). Data shown are mean ± SEM, *P<0.05. (C) Quantification of MAC3 positive cells in the infarct border zone (n=6-7). Data shown are mean ± SEM, *P<0.05. (D) Representative microscopy images of MAC3+/CD206- (%M1) and MAC3+/CD206+ (%M2) expressing cells in the infarct border zone. Smaller panels: Top panel is the MAC3 signal, lower panel is the CD206 signal. Photos taken at 50x magnification. Scale bar: 20µm MAC3 = red, CD206 = green, DAPI = blue. (E) Quantification of the ratio of MAC3+/CD206- (%M1) and MAC3+/CD206+ (%M2) expressing cells in the infarct border zone (n=6-7). (F) Flow cytometric analysis of the macrophage population in the infarct area, ratio of inflammatory M1(Ly6G-/CD11b+/Ly6Chigh) versus regenerative M2 macrophages (Ly6G-/CD11b+/Ly6Clow) (n=3-6, non-parametric ANOVA testing). Control = MQ treated, DipA = Diprotin A treated group. Data shown are mean ± SEM, *P<0.05.

systemic treatment with DipA (Fig. 2C, *Eng*$^{+/-}$ 45.17±5.73 vs. *Eng*$^{+/-}$ DipA treated 82.27±7.68, P=0.002 and representative photos of DAB staining in S4 Figure).

As observed for the CXCR4 expressing cells, DipA treatment did not affect the number of macrophages present in the infarcted hearts of wild type mice. Since there are two main populations of macrophages involved in tissue repair [12], we analyzed the effect of DPP4 inhibition on the inflammatory-like (M1) and regenerative-like (M2) macrophage subtypes in the infarct border zone (Fig. 2D). Analysis of the percentage of M2 in the total macrophage population (represented by the percentage MAC3/CD206 positive cells) revealed a decrease in M2 in *Eng*$^{+/-}$ mice compared to wild types (Fig. 2E, WT 29.88 ±1.52% vs. *Eng*$^{+/-}$ 12.34±1.64%, P<0.0001). After DipA treatment, there was a significant increase in the percentage of M2 macrophages within the total population of macrophages in both wild type and *Eng*$^{+/-}$ mice, and consequently a decrease in M1 macrophages. Importantly, DipA was able to restore the M1/M2 ratio in *Eng*$^{+/-}$ mice to WT levels. We further corroborated our findings by flow cytometric analysis of the macrophage population in the infarct area. Inflammatory M1 (Ly6G^{-}/CD11b^{+}/Ly6C^{high}) were increased in the *Eng*$^{+/-}$ at baseline compared to regenerative M2 macrophages (Ly6G^{-}/CD11b^{+}/Ly6C^{low}). DPP4 inhibition showed a trend towards a decrease in M1 macrophages (Fig. 2F and gating strategy provided in S7 Figure D). Thus, systemic DipA treatment of *Eng*$^{+/-}$ mice restores homing of MNCs to, as well as the macrophage M1/M2 balance in the injured heart 4 days post-MI.

DPP4 inhibition reduces infarct size

By treating the mice with DipA from day 0 to 5 post-MI, homing was stimulated during the peak of inflammatory cell influx (Fig. 3A). To assess the effect of DipA treatment on infarct size we quantified the fibrotic area using Picrosirius red staining at day 14 post-MI (Fig. 3B and C). As expected, control *Eng*$^{+/-}$ mice showed an increase in infarct size compared to WT controls (Fig. 3C, WT control 24.30±2.12% vs. *Eng*$^{+/-}$ control 46.60±9.33%, P=0.009). Upon DipA treatment, no effect on infarct size was detected in wild type animals (Fig. 3C, WT DipA 27.41±3.74%), however in *Eng*$^{+/-}$ mice a significant decrease in infarct size was observed (Fig. 3C, *Eng*$^{+/-}$ control 46.60±9.33% vs. *Eng*$^{+/-}$ DipA 27.02±3.04%, P=0.02), which resulted in similar infarct sizes as observed in the wild type mice.

Effect of DPP4 inhibition on cardiac function

Since DPP4 inhibition enhanced homing of circulating MNCs to the injured heart, reduced infarct size and increased the number of regenerative macrophages present in the heart, we investigated the effect of DipA treatment on cardiac function after MI using ultrasound at baseline, and day 7 and day 14 after MI. Baseline analysis showed that cardiac function at baseline was similar between wild type and *Eng*$^{+/-}$ mice is similar (S5 Figure). At 7 and 14 days post-MI, control treated *Eng*$^{+/-}$ animals showed a significantly lower cardiac EF compared to control treated wild type mice (Fig. 4A, WT control day 7; 31.01±4.32% vs. *Eng*$^{+/-}$ control day 7;18.68±1.84% and WT control day 14; 32.45±4.06% vs. *Eng*$^{+/-}$ control day 14; 17.98±2.06%). Treating wild type animals with DipA did not result in significant changes in the EF (Fig. 4B, also compare to 4A, WT DipA treated day 7; 27.53±3.24% vs. WT DipA treated day 14; 34.15±2.69%). Interestingly, DipA treatment in *Eng*$^{+/-}$ did result in normalization of the EF to the same values as WT animals at day 7 (Fig. 4B, *Eng*$^{+/-}$ DipA treated day 7; 26.94±5.65%), although at day 14, it was less pronounced (Fig. 4B, *Eng*$^{+/-}$ DipA treated day 14; 22.02±3.65%). Nevertheless, these functional data coincide with the

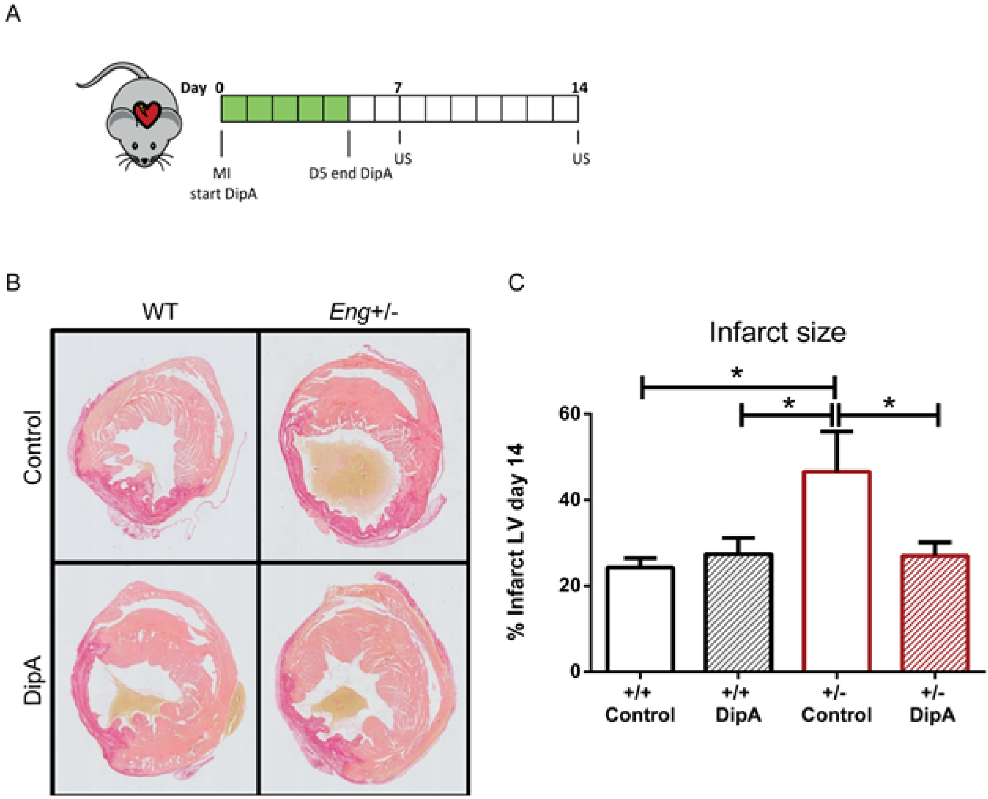

Fig. 3. DPP4 inhibitor treatment reduces infarct size.
(A) Experimental protocol and treatment overview. At day 0, MI is induced and DPP4 inhibition is started (shown in green) till day 5 post-MI by intraperitoneal (i.p.) injection of DipA (treatment group) or distilled water (control group). Cardiac echography was performed at day 7 and 14 post-MI. (B) Histological analysis of the infarct size by Picrosirius red staining for collagen (n=5-9). Transverse sections of left ventricle, photos taken at 1.0x magnification. Infarct area = dark pink, healthy myocardium = light pink, blood cells = yellow. (C) Quantification of Picrosirius red staining in left ventricle (LV). Mice were subjected to MI and treated with either distilled water or DipA from day 0 till day 5 by daily i.p. injection (n=5-9). Control = MQ treated, DipA = Diprotin A treated group. Data shown are mean ± SEM, *P<0.05.

reduced infarct size observed in Fig. 3.

As we observed that endoglin heterozygosity skews the M1/M2 ratio towards a more inflammatory profile, both homing and/or differentiation of *Eng*$^{+/-}$ MNCs might be delayed. Therefore, we prolonged the daily DipA treatment from 5 till 14 days post-MI. Extended DPP4 inhibition resulted in a similar decrease in cardiac function in wild type mice compared to short term (5 days post-MI) treated mice (Fig. 4C). While initially DPP4 inhibition in the *Eng*$^{+/-}$ animals improves cardiac function, *Eng*$^{+/-}$ mice showed a gradual reduction of cardiac function in the 6 month follow-up (ΔEF in Fig. 4C and %EF is provided in S6 Figure). Thus, neither short term nor prolonged DipA treatment resulted in a long term beneficial effect on heart function in *Eng*$^{+/-}$ mice.

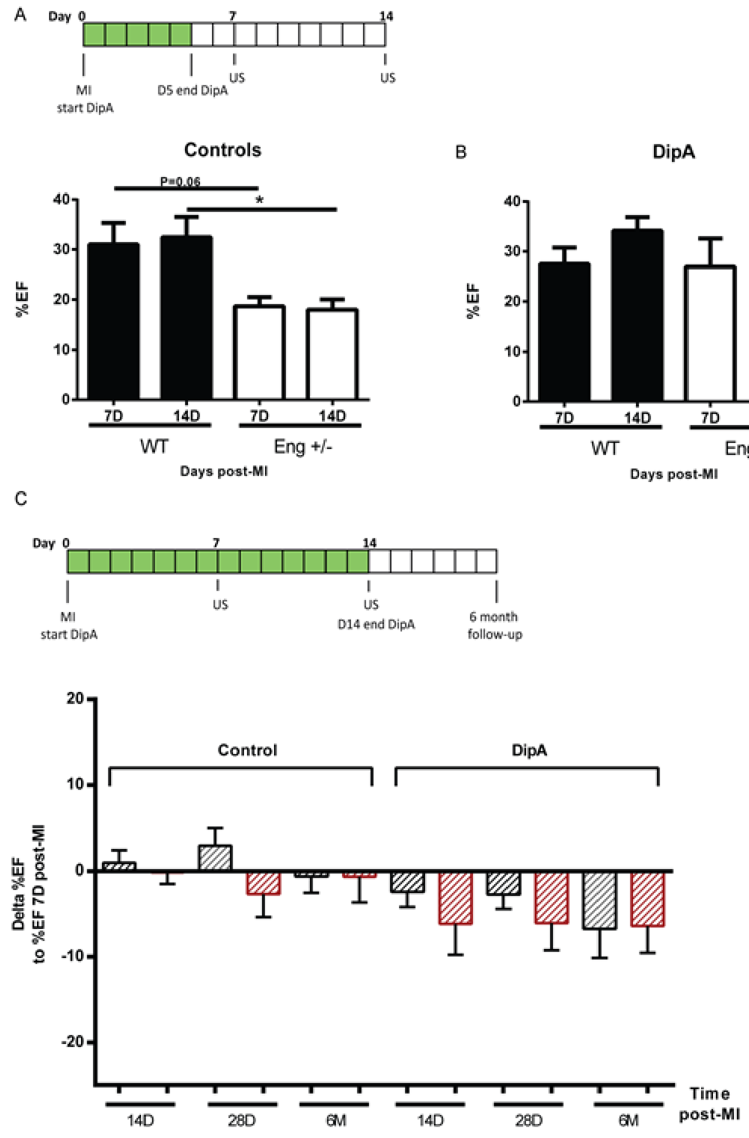

Fig. 4. DipA treatment does not maintain improved cardiac function of Eng+/- mice after MI. (A) Experimental overview and percentage EF at 7 and 14 days post-MI of control treated mice, measured by ultrasound via left ventricle tracing (n=5-9). Data shown are mean ± SEM, *P<0.05. (B) Percentage EF 7 and 14 days post-MI of DipA treated mice, measured by ultrasound via left ventricle tracing. Note that the control WT and Eng+/- groups are the repeat of measurements used for Fig. 1D (n=9-11). Data shown are mean ± SEM, *P<0.05. (C) Long term treatment overview and Δ%EF. DipA treatment (shown in green) up to 14 days post-MI and cardiac function with extended follow-up of 6 months (n=5-11). Data depicted as ΔEF are the EF at the time point indicated on the x-axis compared to EF measured at day 7 post-MI. Cardiac function was measured by ultrasound via left ventricle tracing. DipA= DPP4 inhibitor Diprotin A, US = Ultrasound measurement. Control = MQ treated, DipA = Diprotin A treated group. Data shown are mean ± SEM, *P<0.05.

DPP4 inhibition increases angiogenesis but decreases vessel maturation in *Eng*$^{+/-}$ animals

Since neoangiogenesis is important for cardiac repair post-MI, we investigated the effect of DipA treatment on vascularization by staining the hearts for PECAM-1 and αSMA and analyzed the presence of capillaries and arteries in the infarct border zone. The number of capillaries in the *Eng*$^{+/-}$ mice was increased compared to wild type animals (Fig. 5A). In both wild type as well as *Eng*$^{+/-}$ mice, DipA treatment further increased the number of capillaries present in the border zone (Fig. 5A, *Eng*$^{+/-}$ 61.63±1.43 vs. *Eng*$^{+/-}$ treated 74.30±1.74, P=0.001). Surprisingly, the number of arteries in the infarct border zone was significantly lower in the DPP4 inhibitor treated *Eng*$^{+/-}$ mice (*Eng*$^{+/-}$ 11.88±0.63 vs. *Eng*$^{+/-}$ treated 6.38±0.97, P=0.003), which may suggest that vessel maturation or arteriogenesis is impaired (Fig. 5B).

Macrophage presence in the ventricular wall is prolonged in *Eng*$^{+/-}$ mice

Tissue repair is a tightly controlled process, with a delicate balance between the influx of inflammatory cells needed to remove cell debris after ischemia, and their resolution thereafter when damaged tissue is repaired. A prolongation of the inflammatory phase is detrimental for tissue repair. Interestingly, a significantly higher number of macrophages was observed in the infarct border zone of the *Eng*$^{+/-}$ mice compared to the wild type mice 14 days post-MI (Fig. 5C, WT 7.06±0.97 vs. *Eng*$^{+/-}$ 25.13±2.76, P<0.0001). DipA treatment of *Eng*$^{+/-}$ did not reduce the total number of macrophages to wild type levels.

Analyzing the macrophage phenotypes, we observed a disbalance in the M1/M2 ratio in the hearts of *Eng*$^{+/-}$ mice 4 days post-MI. Therefore, macrophage quantity and subtype in the heart was also analyzed 14 days post-MI. Interestingly, *Eng*$^{+/-}$ DipA treated mice showed an increase in M2 levels reaching wild type levels (Fig. 5D WT 51.7% vs. *Eng*$^{+/-}$ treated 52.7%), while in wild type mice DipA treatment resulted in a significant drop in the percentage of M2 cells (Fig. 5D WT 51.7% vs. WT treated 22.0%, P=0.04). These results suggest that there is a prolonged inflammatory response and possibly an impaired resolution of inflammation in *Eng*$^{+/-}$ mice, and the macrophage balance can be skewed towards the M2 subtype by DPP4 inhibition.

Discussion

In this study we demonstrate that after MI, the decrease in myocardial function observed in our HHT1 animal model is not solely caused by a disturbed endothelium response, but also in part by impaired MNC function. MNC homing and differentiation into inflammatory and regenerative macrophages is important for proper tissue repair. In our previous research, we found that MNC homing towards the ischemic myocardium is severely affected by endoglin heterozygosity, together with enhanced DPP4 levels[15]. Here, we demonstrate that homing of MNCs to the ischemic myocardium could be restored by systemic DPP4 inhibition. Although DipA treatment did reduce the infarct size in *Eng*$^{+/-}$ mice to similar levels as in wild type animals, it did not result in long term improvement of EF. Detailed analysis of the infarcted ventricle demonstrated that neovascularization was increased in the *Eng*$^{+/-}$ infarct border zone upon DPP4 inhibition, while arteriogenesis or vessel maturation was dramatically decreased. Furthermore, analyzing the macrophage subsets, a prolonged presence of inflammatory-like macrophages (M1) was observed. We therefore conclude that the inflammatory and regenerative function of *Eng*$^{+/-}$ macrophages is affected. Interestingly, DPP4 inhibition could restore this M1/M2 imbalance to WT levels.

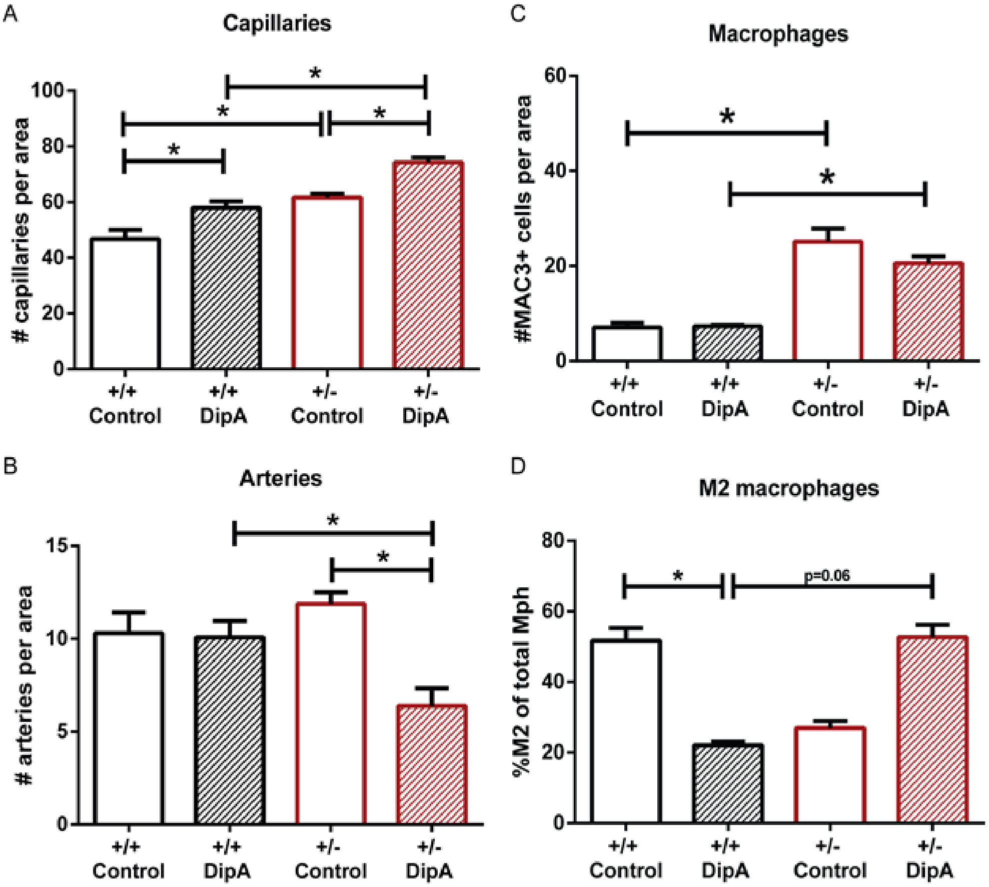

Fig. 5. DPP4 inhibition affects angiogenesis in the infarct border zone post-MI.
(A) Capillaries in infarct border zone, day 14 post-MI. Quantification of PECAM-1 positive vessels per area (n=4-6). Data shown are mean ± SEM, *P<0.05. (B) Arteries in infarct border zone, day 14 post-MI. Quantification of PECAM-1/αSMA positive vessels per area (n=4-6). Data shown are mean ± SEM, *P<0.05. (C) Quantification of total macrophage (MAC3) number in day 14 post-MI hearts (n=4-6). Data shown are mean ± SEM, *P<0.05. (D) Quantification of MAC3+/CD206+ (%M2) expressing cells in the infarct border zone 14 days post-MI (n=3-6). Control = MQ treated, DipA = Diprotin A treated group. Data shown are mean ± SEM, *P<0.05.

Complete endoglin deficiency in mice results in embryonic lethality around mid-gestation due to cardiovascular defects and the formation of enlarged fragile vessels[4]. *Eng*$^{+/-}$ mice or endothelial deletion of endoglin in adult mice results in a relatively mild phenotype. Only after a secondary hit like induction of tissue damage or inflammation, the impairments of endoglin deficiency become apparent in the form of reduced angiogenesis and the development of AVMs[30-32]. In the current study, we observed that the macrophage specific deletion of *Eng* did not result in similar levels of cardiac deterioration as found in *Eng*$^{+/-}$ animals, implying a multifactorial nature of HHT1. This emphasizes the need for endoglin heterozygosity to be present in all cell types of the heart to recapitulate the HHT1 disease phenotype.

Furthermore, we show that the homing capacity of MNCs in the *Eng*$^{+/-}$ mice could be restored by systemic DPP4 inhibitor treatment. In cardiovascular patients an association was found between increased DPP4 presence on MNCs and poor recovery after coronary intervention[33]. Together with our observation of decreased homing capacity of the MNCs, HHT1 now proves to affect other cell types and functions as well, in particular the lymphocytes and monocytes[31,32,34,35]. Macrophages are an important subfraction of the MNC population, as macrophages have both inflammatory and angiogenic capacity and are essential in tissue regeneration and remodeling[28]. The shift of the inflammatory-like macrophages (M1) to the regenerative-like macrophages (M2) is essential for optimal resolution of inflammation[36]. Immune function and the angiogenic capacity of macrophages are most likely impaired in $Eng^{+/-}$ mice[37,38]. Recent studies suggested that there is an intrinsic inflammatory defect in HHT1 patients as well. Investigators report leukopenia, increased risk of infection[34] and impaired endoglin upregulation in activated monocytes of HHT1 patients[35]. We now observed an increased ratio of M1/M2 macrophages in $Eng^{+/-}$ mice hearts post-MI, which may indicate that the increase in M1 macrophages is due to either impaired differentiation of the M1 towards M2 macrophages, or decreased homing capacity of M2 macrophages. In renal ischemia-reperfusion injury, the same disbalance in M1/M2 was also reported in $Eng^{+/-}$ mice[39]. DPP4 inhibition has been shown to shift the M1/M2 balance towards more reparative macrophages[22,23]. We show that in $Eng^{+/-}$ mice DipA treatment restored both the total number of macrophages as well as the M1/M2 ratio. This effect was maintained up to 10 days after cessation of DPP4 inhibitor treatment. The shift of the macrophage population towards M2 induced by DPP4 inhibition was also observed by Brenner et al.[22], when analyzing macrophage presence in the aortic walls of $ApoE^{-/-}$ mice in a model for atherosclerosis. Likewise, a reduction of atherosclerotic lesions[20] and total macrophage presence was reported in $ApoE^{-/-}$ mice treated with DPP4 inhibitor, together with a reduction in smooth muscle cell proliferation[40]. DPP4-null mice had an increased expression of M2 genes[41] and furthermore, DPP4 inhibition had anti-inflammatory effects on macrophages in general by decreasing pro-inflammatory NFκB signaling[42]. An increase in M2 macrophages was also observed upon DPP4 inhibitor treatment in another atherosclerosis model using $LDLR^{-/-}$ mice[43], moreover, a recent meta-analysis showed a decreased infection rate in T2DM patients treated with a DPP4 inhibitor[44]. Here we show for the first time, to our knowledge, that DPP4 inhibition polarizes the M1/M2 ratio towards a more regenerative phenotype in a mouse model for HHT1. Furthermore, our data suggests that endoglin heterozygosity not only impairs homing of the MNCs, but affects proper differentiation and/or function of the macrophages, as we find more M1 at the infarct site and a decrease in resolution of immune cells 14 days post-MI in $Eng^{+/-}$ animals.

In addition to improved homing of circulating (stem) cells, we and others show that DPP4 inhibition significantly stimulated vascularization and cardiac repair[45-47]. In conjunction an increase in capillary number was observed at the infarct border zone, confirming an increase in endothelial regeneration, possibly by enhanced presence of regenerative M2 macrophages. Interestingly, the number of arteries present was found to be significantly lowered in the DPP4 inhibitor treated $Eng^{+/-}$ mice. Vessel maturation is known to be affected in $Eng^{+/-}$ mice, due to dysfunctional mural cells and pericytes[48,49]. Our results therefore suggest that DPP4 inhibitor treatment most likely further impairs vessel maturation in $Eng^{+/-}$ mice, due to its involvement in vascular smooth muscle cell recruitment[50,51].

DPP4 inhibitors have been reported to increase cardiomyocyte survival, however the exact mechanism is not yet fully understood. DPP4 has many targets beside SDF1, like atrial natriuretic peptide (ANP)- a protein associated with cardiomyocyte survival[52]. DPP4 inhibition might therefore decrease the inactivation of ANP by DPP4, and contribute to cardiomyocyte survival/protection. Furthermore, when MI was performed in $DPP4^{-/-}$ mice, these mice show an increased survival compared to DPP4$^{+/+}$ mice[52]. DPP4 inhibitor treatment in previous reports already showed a modest, albeit not significant gain of cardiac function in wild type mice after MI[53]. Interestingly, at day 14 post-MI the infarct size in *Eng*$^{+/-}$ mice treated with DipA was significantly smaller and similar in size compared to wild type control levels. Concordantly, we observed an initial increase in EF upon DipA treatment. However, improved cardiac function in *Eng*$^{+/-}$ mice was not preserved at day 14 post-MI. These results suggest that DPP4 inhibition conveys a decrease of the fibrotic response in *Eng*$^{+/-}$ animals, resulting in a reduced infarct size, though this is not reflected in a sustained improvement of heart function. This could be in part explained by the fact that although capillary presence is increased, in HHT1 endothelial functionality is impaired, forming leaky vessels. Secondly, the misbalanced MNC population present in HHT1 might result in an exaggerated and prolonged immune response, which is likely to disturb tissue repair.

We hypothesized that when homing of *Eng*$^{+/-}$ MNCs to the infarct site was restored, cardiac function would improve, as was observed in wild type animals[46,53]. Although increased homing and a decrease in infarct size were observed, this did not correlate with a long term positive effect on cardiac function. The *Eng*$^{+/-}$ mice showed either a reduced differentiation towards, or presence of the regenerative macrophage subtype and interestingly this level could be corrected by DPP4 inhibition. However, although the fibrotic response was restored to wild type levels and MNC recruitment was re-established, the *Eng*$^{+/-}$ mice still show a decrease in cardiac function. This suggests that the impaired function of the *Eng*$^{+/-}$ MNCs that homed to the infarct site still exists. Combining DPP4 inhibition with G-CSF treatment for enhanced MNC recruitment, Zaruba et al. showed that ameliorated MNC homing resulted in a significant increase in cardiac function in mice. However, testing this treatment in patients suffering from MI, the combination failed to show any beneficial effect on cardiac function[54,55].

How DPP4 inhibition affects MNC function is still unclear. DPP4 inhibition is already being tested in several clinical trials in cardiovascular disease (CVD), and meta-analyses of the risks involved have proven to be varied in outcome. Several meta-analyses have been performed in the field of T2DM. Upon DPP4 inhibition, no increase in CVD was observed in T2DM patients, but risk of infection was reduced[44]. In addition, although no effect was seen on cardiovascular mortality, short term DPP4 inhibition reduced chances of MI events, while long term treatment showed a possible increase in heart failure cases[56,57]. Other meta-analyses showed either no effect or a reduction of cardiovascular events, also with long term treatment[58-61].

As described in this study, DPP4 inhibition positively affects cardiac fibrosis and initially, also cardiac function. We showed by using a PSR staining that fibrosis is enhanced in *Eng*$^{+/-}$ mice and decreases upon DPP4 inhibition. A relation between DPP4 inhibition and reduction in fibrosis was also demonstrated in a kidney model[62]. Furthermore, inhibition of DPP4-positive fibroblasts reduced scarring of murine dermal wounds[63] and DPP4 inhibition also mediated antifibrotic effects in dermal fibroblasts[64]. DPP4 inhibition is shown to be cardioprotective in several studies (reviewed in Grilo et al.[65]). A study overexpressing DPP4 resulted in promoted mammary tumorigenesis and transformation of epithelial cells[66], indicating DPP4 inhibition is the way forward.

DPP4 and its inhibition has a multitude of functions and effects, many of which are still poorly understood. This is exemplified by the study from Zhu et al.[67], where they show that DPP4 is able to target neuropeptide Y and peptide YY in the cardiac nerves, proteins that can result in activation of cardiac fibroblasts. To the contrary, many anti-fibrotic aspects have been described, and by various mechanisms; DPP4 inhibitors were reported to lower active TGFβ (via reduction of DPP4 -CIM6PR membrane receptor interaction) and also decrease fibronectin expression[68-70]. Together, the beneficial effects of DPP4 inhibition on MNC homing, reduction in fibrosis and restoration of regenerative macrophage differentiation could provide a suitable treatment for general tissue repair in HHT1 patients. However, this study suggests that treating HHT1 patients with a DPP4 inhibitor post-MI should not be considered as monotherapy, but ought to be combined with additional MNC stimulating agents and/or arteriogenic stimulation. Although DPP4 inhibition is an accepted treatment in T2DM patients, a better understanding of its mode of action should first be gained before further conducting clinical trials for applying this treatment on any other disease or disorder like HHT1.

Acknowledgements

We would like to thank Prof. Dr. P ten Dijke, Dr. M.R. De Vries and Prof. Dr. P. Quax for providing cytokines/antibodies and Dr. I. Hoefer for valuable discussions.

References

1. Lebrin, F., *et al.* Endoglin promotes endothelial cell proliferation and TGF-β/ALK1 signal transduction. *The EMBO Journal* **23**, 4018-4028 (2004).

2. Goumans, M.-J., Lebrin, F. & Valdimarsdottir, G. Controlling the Angiogenic SwitchA Balance between Two Distinct TGF-b Receptor Signaling Pathways. *Trends in Cardiovascular Medicine* **13**, 301-307 (2003).

3. Bourdeau, A., Dumont, D.J. & Letarte, M. A murine model of hereditary hemorrhagic telangiectasia. *Journal of Clinical Investigation* **104**, 1343-1351 (1999).

4. Arthur, H.M., *et al.* Endoglin, an Ancillary TGFβ Receptor, Is Required for Extraembryonic Angiogenesis and Plays a Key Role in Heart Development. *Developmental Biology* **217**, 42-53 (2000).

5. Bourdeau, A., *et al.* Potential Role of Modifier Genes Influencing Transforming Growth Factor-β1 Levels in the Development of Vascular Defects in Endoglin Heterozygous Mice with Hereditary Hemorrhagic Telangiectasia. *The American Journal of Pathology* **158**, 2011-2020 (2001).

6. Jerkic, M., *et al.* Reduced angiogenic responses in adult Endoglin heterozygous mice. *Cardiovascular research* **69**, 845-854 (2006).

7. Seghers, L., *et al.* Shear induced collateral artery growth modulated by endoglin but not by ALK1. *Journal of Cellular and Molecular Medicine* **16**, 2440-2450 (2012).

8. López-novoa, J.M., *et al.* The physiological role of endoglin in the cardiovascular system. *American Journal of Physiology-Heart and Circulatory Physiology* **299**, 959-974 (2010).

9. Liu, Z., *et al.* ENDOGLIN Is Dispensable for Vasculogenesis, but Required for Vascular Endothelial Growth Factor-Induced Angiogenesis. *PLoS ONE* **9**, e86273 (2014).

10. Kapur, N., Morine, K. & Letarte, M. Endoglin: a critical mediator of cardiovascular health. *Vascular Health and Risk Management* **9**, 195 (2013).

11. Ben-Mordechai, T., *et al.* Macrophage subpopulations are essential for infarct repair with and without stem cell therapy. *Journal of the American College of Cardiology* **62**, 1890-1901 (2013).

12. Nahrendorf, M., *et al.* The healing myocardium sequentially mobilizes two monocyte subsets with divergent and complementary functions. *The Journal of experimental medicine* **204**, 3037-3047 (2007).

13. van Amerongen, M.J., Harmsen, M.C., van Rooijen, N., Petersen, A.H. & van Luyn, M.J.A. Macrophage depletion impairs wound healing and increases left ventricular remodeling after myocardial injury in mice. *The American journal of pathology* **170**, 818-829 (2007).

14. van Laake, L.W., *et al.* Endoglin Has a Crucial Role in Blood Cell-Mediated Vascular Repair. *Circulation* **114**, 2288-2297 (2006).

15. Post, S., *et al.* Impaired recruitment of HHT-1 mononuclear cells to the ischaemic heart is due to an altered CXCR4/CD26 balance. *Cardiovascular Research* **85**, 494-502 (2010).

16. Askari, A.T., *et al.* Effect of stromal-cell-derived factor 1 on stem-cell homing and tissue regeneration in ischaemic cardiomyopathy. *Lancet* **362**, 697-703 (2003).

17. Ceradini, D.J., *et al.* Progenitor cell trafficking is regulated by hypoxic gradients through HIF-1 induction of SDF-1. *Nature medicine* **10**, 858-864 (2004).

18. Read, P.A., Khan, F.Z., Heck, P.M., Hoole, S.P. & Dutka, D.P. DPP-4 Inhibition by Sitagliptin Improves the Myocardial Response to Dobutamine Stress and Mitigates Stunning in a Pilot Study of Patients With Coronary Artery Disease. *Circulation: Cardiovascular Imaging* **3**, 195-201 (2010).

19. Best, J.H., *et al.* Risk of cardiovascular disease events in patients with type 2 diabetes prescribed the glucagon-like peptide 1 (GLP-1) receptor agonist exenatide twice daily or other glucose-lowering therapies: a retrospective analysis of the LifeLink database. *Diabetes care* **34**, 90-95 (2011).

20. Ta, N.N., Schuyler, C.A., Li, Y., Lopes-Virella, M.F. & Huang, Y. DPP-4 (CD26) Inhibitor Alogliptin Inhibits Atherosclerosis in Diabetic Apolipoprotein E–Deficient Mice. *Journal of Cardiovascular Pharmacology* **58**, 157-166 (2011).

21. Fadini, G.P., *et al.* The Oral Dipeptidyl Peptidase-4 Inhibitor Sitagliptin Increases Circulating Endothelial Progenitor Cells in Patients With Type 2 Diabetes: Possible role of stromal-derived factor-1. *Diabetes Care* **33**, 1607-1609 (2010).

22. Brenner, C., *et al.* DPP-4 inhibition ameliorates atherosclerosis by priming monocytes into M2 macrophages. *International Journal of Cardiology* **199**, 163-169 (2015).

23. Waumans, Y., *et al.* The Dipeptidyl Peptidases 4, 8, and 9 in Mouse Monocytes and Macrophages: DPP8/9 Inhibition Attenuates M1 Macrophage Activation in Mice. *Inflammation* **39**, 413-424 (2016).

24. Choi, E.-J., *et al.* Novel brain arteriovenous malformation mouse models for type 1 hereditary hemorrhagic telangiectasia. *PloS one* **9**, e88511 (2014).

25. Clausen, B.E., Burkhardt, C., Reith, W., Renkawitz, R. & Förster, I. Conditional gene targeting in macrophages and granulocytes using LysMcre mice. *Transgenic Research* **8**, 265-277 (1999).

26. Duim, S.N., Kurakula, K., Goumans, M.J. & Kruithof, B.P.T. Cardiac endothelial cells express Wilms' tumor-1. Wt1 expression in the developing, adult and infarcted heart. *Journal of Molecular and Cellular Cardiology* **81**, 127-135 (2015).

27. Sager, H.B., *et al.* Proliferation and Recruitment Contribute to Myocardial Macrophage Expansion in Chronic Heart Failure. *Circulation Research* **119**, 853-864 (2016).

28. Mantovani, A., Biswas, S.K., Galdiero, M.R., Sica, A. & Locati, M. Macrophage plasticity and polarization in tissue repair and remodelling. *The Journal of pathology* **229**, 176-185 (2013).

29. Frantz, S. & Nahrendorf, M. Cardiac macrophages and their role in ischemic heart disease. *Cardiovascular research* **102**, 1-9 (2014).

30. Garrido-Martin, E.M., *et al.* Common and distinctive pathogenetic features of arteriovenous malformations in hereditary hemorrhagic telangiectasia 1 and hereditary hemorrhagic telangiectasia 2 animal models--brief report. *Arteriosclerosis, thrombosis, and vascular biology* **34**, 2232-2236 (2014).

31. Rossi, E., *et al.* Endothelial endoglin is involved in inflammation: Role in leukocyte adhesion and transmigration. *Blood* **121**, 403-415 (2013).

32. Peter, M.R., *et al.* Impaired Resolution of Inflammation in the Endoglin Heterozygous Mouse Model of Chronic Colitis. *Mediators of Inflammation* **2014**, 1-13 (2014).

33. Post, S., *et al.* Reduced CD26 expression is associated with improved cardiac function after acute myocardial infarction. *Journal of Molecular and Cellular Cardiology* **53**, 899-905 (2012).

34. Guilhem, A., Malcus, C., Clarivet, B. & Plauchu, H. Immunological abnormalities associated with hereditary haemorrhagic telangiectasia. 351-362 (2013).

35. Sanz-Rodriguez, F., *et al.* Mutation analysis in Spanish patients with hereditary hemorrhagic telangiectasia: deficient endoglin up-regulation in activated monocytes. *Clinical chemistry* **50**, 2003-2011 (2004).

36. Sindrilaru, A., *et al.* An unrestrained proinflammatory M1 macrophage population induced by iron impairs wound healing in humans and mice. *Journal of Clinical Investigation* **121**, 985-997 (2011).

37. Aristorena, M., *et al.* Expression of endoglin isoforms in the myeloid lineage and their role during aging and macrophage polarization. *Journal of cell science* **127**, 2723-2735 (2014).

38. Ojeda-Fernández, L., *et al.* Mice Lacking Endoglin in Macrophages Show an Impaired Immune Response. *PLOS Genetics* **12**, e1005935 (2016).

39. Docherty, N.G., *et al.* Endoglin regulates renal ischaemia-reperfusion injury. *Nephrology, dialysis, transplantation : official publication of the European Dialysis and Transplant Association - European Renal Association* **21**, 2106-2119 (2006).

40. Ervinna, N., *et al.* Anagliptin, a DPP-4 Inhibitor, Suppresses Proliferation of Vascular Smooth Muscles and Monocyte Inflammatory Reaction and Attenuates Atherosclerosis in Male apo E-Deficient Mice. *Endocrinology* **154**, 1260-1270 (2013).

41. Röhrborn, D., Wronkowitz, N. & Eckel, J. DPP4 in diabetes. *Frontiers in Immunology* **6**, 1-20 (2015).

42. Shinjo, T., *et al.* DPP-IV inhibitor anagliptin exerts anti-inflammatory effects on macrophages, adipocytes, and mouse livers by suppressing NF-kappaB activation. *Am J Physiol Endocrinol Metab* **309**, E214-223 (2015).

43. Shah, Z., *et al.* Long-term dipeptidyl-peptidase 4 inhibition reduces atherosclerosis and inflammation via effects on monocyte recruitment and chemotaxis. *Circulation* **124**, 2338-2349 (2011).

44. Tricco, A.C., *et al.* Safety and effectiveness of dipeptidyl peptidase-4 inhibitors versus intermediate-acting insulin or placebo for patients with type 2 diabetes failing two oral antihyperglycaemic agents: a systematic review and network meta-analysis. *BMJ Open* **4**, e005752 (2014).

45. Brenner, C., *et al.* Short-term inhibition of DPP-4 enhances endothelial regeneration after acute arterial injury via enhanced recruitment of circulating progenitor cells. *International journal of cardiology* **177**, 266-275 (2014).

46. Zaruba, M.-M., *et al.* Granulocyte colony-stimulating factor treatment plus dipeptidylpeptidase-IV inhibition augments myocardial regeneration in mice expressing cyclin D2 in adult cardiomyocytes. *European Heart Journal* **33**, 129-137 (2012).

47. Theiss, H.D., *et al.* Dual stem cell therapy after myocardial infarction acts specifically by enhanced homing via the SDF-1/CXCR4 axis. *Stem Cell Research* **7**, 244-255 (2011).

48. Rossi, E., *et al.* Endoglin regulates mural cell adhesion in the circulatory system. *Cellular and Molecular Life Sciences* **73**, 1715-1739 (2016).

49. Lebrin, F., *et al.* Thalidomide stimulates vessel maturation and reduces epistaxis in individuals with hereditary hemorrhagic telangiectasia. *Nature Medicine* **16**, 420-428 (2010).

50. Mancini, M.L., *et al.* Endoglin plays distinct roles in vascular smooth muscle cell recruitment and regulation of arteriovenous identity during angiogenesis. *Developmental Dynamics* **238**, 2479-2493 (2009).

51. Choi, S.H., *et al.* Dipeptidyl peptidase-4 inhibition by gemigliptin prevents abnormal vascular remodeling via NF-E2-related factor 2 activation. *Vascular Pharmacology* **73**, 11-19 (2015).

52. Sauve, M., *et al.* Genetic Deletion or Pharmacological Inhibition of Dipeptidyl Peptidase-4 Improves Cardiovascular Outcomes After Myocardial Infarction in Mice. **59**(2010).

53. Zaruba, M.-M., *et al.* Synergy between CD26/DPP-IV Inhibition and G-CSF Improves Cardiac Function after Acute Myocardial Infarction. *Cell Stem Cell* **4**, 313-323 (2009).

54. Brenner, C., *et al.* Sitagliptin plus granulocyte colony-stimulating factor in patients suffering from acute myocardial infarction: A double-blind, randomized placebo-controlled trial of efficacy and safety (SITAGRAMI trial). *International Journal of Cardiology* **205**, 23-30 (2016).

55. Gross, L., *et al.* Combined therapy with sitagliptin plus granulocyte-colony stimulating factor in patients with acute myocardial infarction — Long-term results of the SITAGRAMI trial. *International Journal of Cardiology* **215**, 441-445 (2016).

56. Savarese, G., *et al.* Cardiovascular effects of dipeptidyl peptidase-4 inhibitors in diabetic patients: A meta-analysis. *International Journal of Cardiology* **181**, 239-244 (2015).

57. Zhong, J., Maiseyeu, A., Davis, S.N. & Rajagopalan, S. DPP4 in Cardiometabolic Disease: Recent Insights From the Laboratory and Clinical Trials of DPP4 Inhibition. *Circulation Research* **116**, 1491-1504 (2015).

58. Frederich, R., *et al.* A systematic assessment of cardiovascular outcomes in the saxagliptin drug development program for type 2 diabetes. *Postgraduate medicine* **122**, 16-27 (2010).

59. Patil, H.R., *et al.* Meta-analysis of effect of dipeptidyl peptidase-4 inhibitors on cardiovascular risk in type 2 diabetes mellitus. *The American journal of cardiology* **110**, 826-833 (2012).

60. Cobble, M.E. & Frederich, R. Saxagliptin for the treatment of type 2 diabetes mellitus:

assessing cardiovascular data. *Cardiovascular Diabetology* **11**, 6 (2012).

61. Koska, J., Sands, M., Burciu, C. & Reaven, P. Cardiovascular effects of dipeptidyl peptidase-4 inhibitors in patients with type 2 diabetes. *Diab Vasc Dis Res* **12**, 154-163 (2015).

62. Shi, S.*, et al.* Interactions of DPP-4 and integrin β1 influences endothelial-to-mesenchymal transition. *Kidney International* **88**, 479-489 (2015).

63. Rinkevich, Y.*, et al.* Skin fibrosis. Identification and isolation of a dermal lineage with intrinsic fibrogenic potential. *Science* **348**, aaa2151 (2015).

64. Thielitz, A.*, et al.* Inhibitors of dipeptidyl peptidase IV-like activity mediate antifibrotic effects in normal and keloid-derived skin fibroblasts. *Journal of Investigative Dermatology* **128**, 855-866 (2007).

65. Grilo, G.A., Shaver, P.R. & de Castro Bras, L.E. The Prospective Cardioprotective Effects of DPP-4 inhibition in the ischemic myocardium. *J Mol Cell Cardiol* **93**, 44-46 (2016).

66. Choi, H.J.*, et al.* Dipeptidyl peptidase 4 promotes epithelial cell transformation and breast tumourigenesis via induction of PIN1 gene expression. *Br J Pharmacol* **172**, 5096-5109 (2015).

67. Zhu, X., Gillespie, D.G. & Jackson, E.K. NPY 1–36 and PYY 1–36 activate cardiac fibroblasts: an effect enhanced by genetic hypertension and inhibition of dipeptidyl peptidase 4. *American Journal of Physiology - Heart and Circulatory Physiology* **309**, H1528-H1542 (2015).

68. Gangadharan Komala, M., Gross, S., Zaky, A., Pollock, C. & Panchapakesan, U. Linagliptin Limits High Glucose Induced Conversion of Latent to Active TGFß through Interaction with CIM6PR and Limits Renal Tubulointerstitial Fibronectin. *Plos One* **10**, e0141143 (2015).

69. Kanasaki, K.*, et al.* Linagliptin-Mediated DPP-4 Inhibition Ameliorates Kidney Fibrosis in Streptozotocin-Induced Diabetic Mice by Inhibiting Endothelial-to-Mesenchymal Transition in a Therapeutic Regimen. *Diabetes* **63**, 2120-2131 (2014).

70. Panchapakesan, U. DPP4 Inhibition in Human Kidney Proximal Tubular Cells - Renoprotection in Diabetic Nephropathy? *Journal of Diabetes & Metabolism* **S9**, 1-8 (2013).

Supplementary Figures

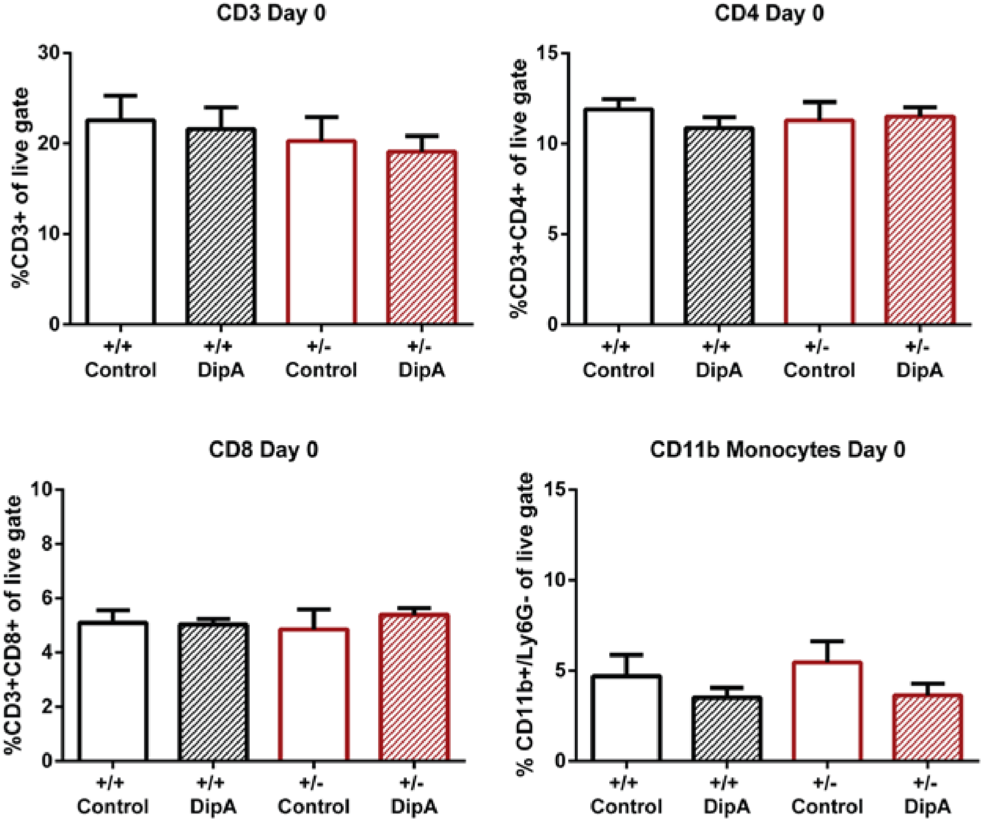

S1 Figure. Eng+/- mice do not display leukopenia.
Flow cytometric analysis of the major leukocyte subsets in the circulation of the mice groups at day 0 (pre-MI and pre-DipA treatment). Leukocytes labeled for anti-mouse CD3, CD3+/CD4+, CD3+/CD8+ and CD11b+/Ly6G- (n=3-6, non-parametric ANOVA testing). Control = MQ treated, DipA = Diprotin A treated group. Data shown are mean ± SEM, *P<0.05.

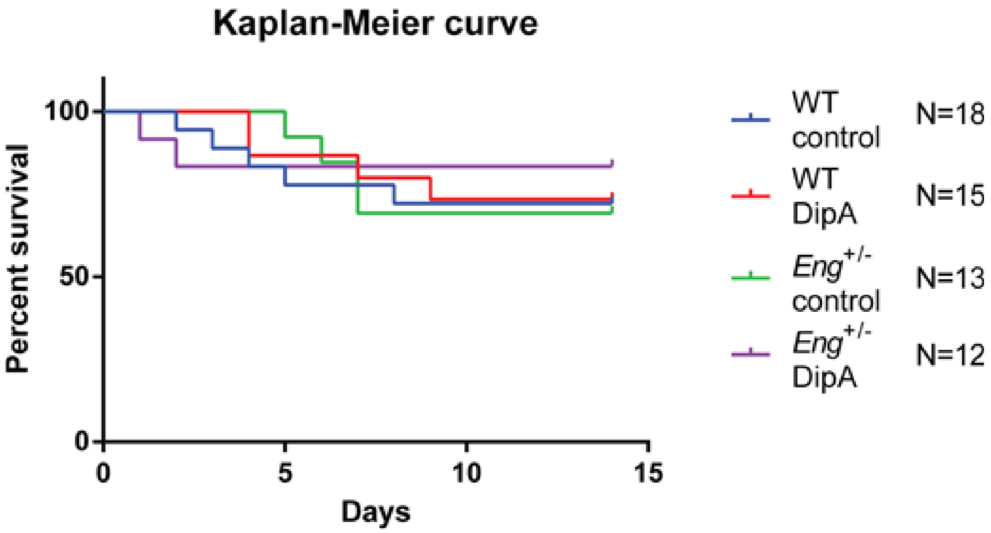

S2 Figure. DPP4 inhibition does not affect survival of WT and Eng+/- mice.
Kaplan-Meier curve of WT and Eng+/- mice 14 days post-MI. Graph depicts percentage of surviving WT and Eng+/- mice, control and DipA treated animals (n=12-18). Control = MQ treated, DipA = Diprotin A treated group.

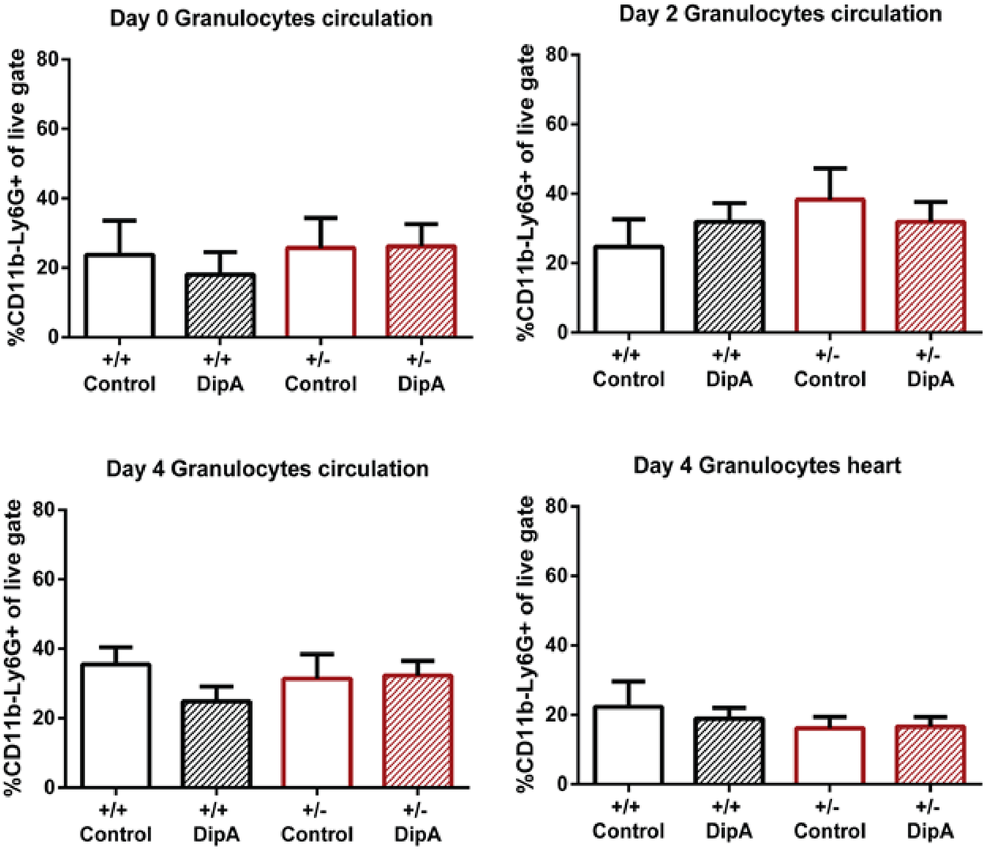

S3 Figure. The granulocyte subset is not affected in Eng+/- mice at baseline or by DipA treatment 4 days post-MI.

Flow cytometric analysis of the granulocyte subset in the circulation of the mice at (A) day 0 (pre-MI and pre-DipA treatment) and (B) day 2 and (C) 4 post-MI in the circulation. (D) Granulocytes isolated form the infarcted part of the LV 4 days post-MI. Leukocytes labeled with anti-mouse CD11b, Ly6G. Granulocytes were identified as the CD11b-/Ly6G+ population of the live gate (n=3-6, non-parametric ANOVA testing). Control = MQ treated, DipA = Diprotin A treated group. Data shown are mean ± SEM, *P<0.05.

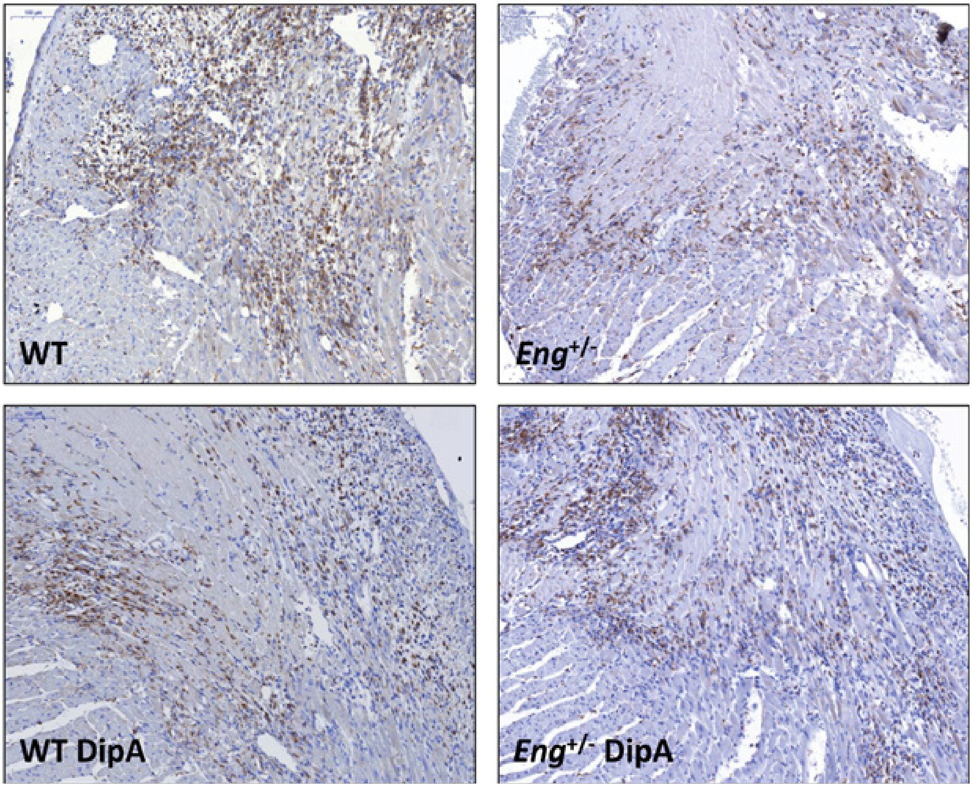

S4 Figure. MAC3 expressing cells in the infarct border zone 4 days post-MI.
Transversal sections of mouse hearts were stained for macrophage marker MAC3 using immunohistochemistry (n=6-7). Photos taken at 15x magnification. MAC3 = brown, nuclei = blue.

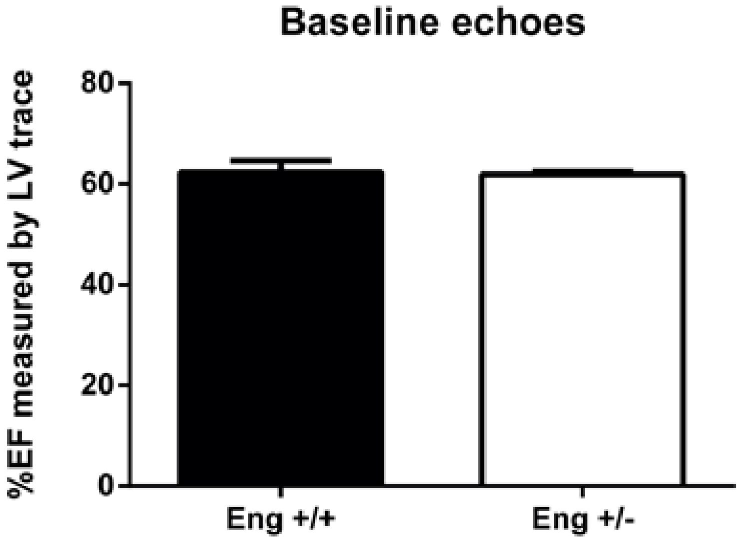

S5 Figure. Eng+/- mice show no difference in baseline ejection fraction.
Baseline cardiac function in percent ejection fraction (%EF) between WT and Eng+/- mice (n=4).. Cardiac function was measured by ultrasound. Data shown are mean ± SEM, *P<0.05.

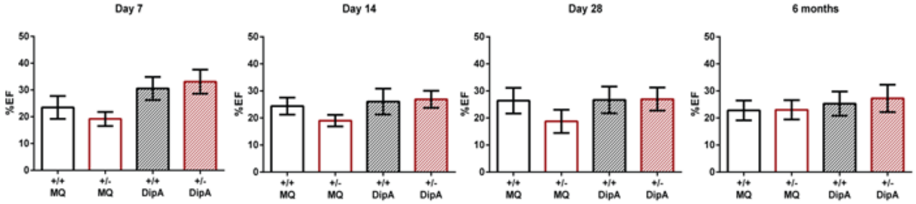

S6 Figure. DPP4 inhibition does not improve cardiac function long term.
Percentage EF 7, 14, 28 days and 6 months post-MI of WT(+/+) and Eng+/- (+/-) mice, control (Milli-Q ultrapure sterile water, MQ) and DipA treated animals. EF was measured by ultrasound and analyzed by left ventricle tracing (n=5-11). Data shown are mean ± SEM, *P<0.05.

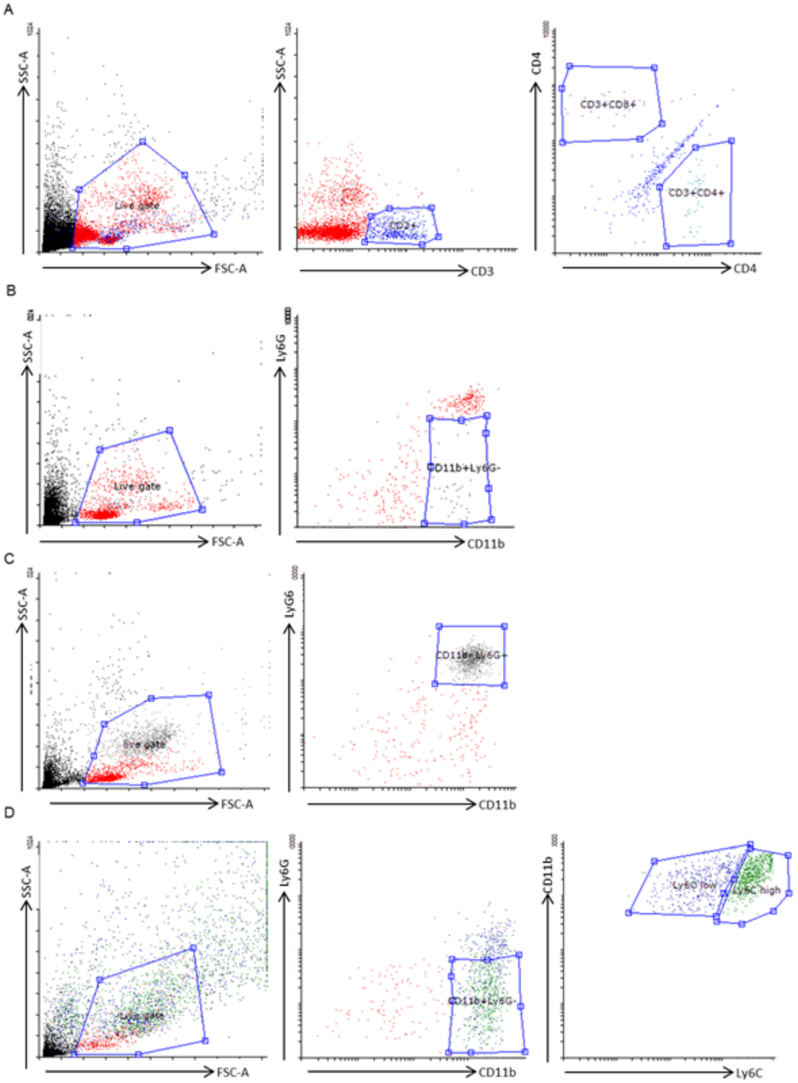

S7 Figure. Flow cytometry gating strategy T-cells, monocytes and macrophages.
(A) Gating strategy for CD3, 4 and 8 T-cells in the blood. The first gating step is a gate for live cells using FSC and SSC. T-cells are subsequently identified using CD3. T-cells subsets are then identified with CD4 and CD8.
(B) Monocytes gating strategy in the blood. The first gating step is a gate for live cells using FSC and SSC. The second gating step is for monocytes, identified by CD11b positive and Ly6G negative labeling.
(C) Granulocyte gating strategy in the blood. The first gating step is a gate for live cells using FSC and SSC, the granulocytes are subsequently identified by Ly6G.
(D) Macrophage subsets gating strategy from MNCs isolated from the left ventricle. The first gating step is a gate for live cells using FSC and SSC, the monocytes are identified by CD11b positive and Ly6G negative labeling. The inflammatory-like M1 macrophages are then subsequently identified by Ly6Chigh and regenerative-like M2 macrophages identified by Ly6Clow labeling.

4

BMP receptor inhibition enhances tissue repair in endoglin heterozygous mice

Calinda K.E. Dingenouts[1#&], Wineke Bakker[1&], Kirsten Lodder[1], Karien C. Wiesmeijer[1], Asja T. Moerkamp[1], Hans-Jurgen J. Mager[2], Repke J. Snijder[2], Cornelius J.J. Westermann[2], Margreet R. de Vries[3], Paul H.A. Quax[3], Marie-José Goumans*[1]

1. Department of Cell and Chemical Biology, Leiden University Medical Center, Leiden, The Netherlands
2. St. Antonius Hospital, Nieuwegein, the Netherlands,
3. Department of Surgery, Leiden University Medical Center, Leiden, The Netherlands

# Current Address: Department of Infectious Diseases, Leiden University Medical Center, Leiden, The Netherlands

&/* Authors contributed equally

Manuscript rebuttal under revision

Abstract

Hereditary hemorrhagic telangiectasia type 1 (HHT1) is a severe vascular disorder caused by mutations in the TGFβ/BMP co-receptor endoglin. Endoglin haploinsufficiency results in impaired neovascularization and tissue repair after ischemic injury like myocardial infarction (MI) or hind limb ischemia. Furthermore, HHT1 patients display an impaired immune response, demonstrated by increased infection rates. To date it is still not understood to what extend immune cells are affected by the HHT1 pathology. Therefore we investigated the immune response during wound repair in $Eng^{+/-}$ mice, a model for HHT1. We observed that these mice had a prolonged period of monocyte-derived macrophage infiltration after experimentally induced MI. Moreover, there was an increased number of inflammatory $Ly6C^{high}/CD206^{-}$-macrophages (M1-like) at the expense of reparative $Ly6C^{low}/CD206^{+}$-macrophages (M2-like). Interestingly, HHT1 patients showed increased numbers of inflammatory macrophages. In vitro analysis revealed that TGFβ-induced differentiation of $Eng^{+/-}$ monocytes into M2 macrophages was blunted. Inhibiting BMP signaling by treating monocytes with BMP receptor inhibitor LDN-193189 normalized their differentiation. Systemic LDN treatment after MI improved heart function and enhanced vascularization in both wild type and $Eng^{+/-}$ mice. The beneficial effects of LDN were also observed in the hind limb ischemia model. While blood flow recovery was hampered in vehicle treated animals, LDN treatment improved tissue perfusion recovery in $Eng^{+/-}$ mice. In conclusion, BMPR inhibition restores HHT1 macrophage imbalance in vitro and improves tissue repair after ischemic injury in $Eng^{+/-}$ mice.

Introduction

Endoglin (also known as CD105) is a transmembrane protein that functions as a co-receptor for Transforming Growth Factor-β (TGFβ)1 and TGFβ3. Mutations in endoglin resulting in haploinsufficiency are the cause of the autosomal dominant vascular disorder *Hereditary Hemorrhagic Telangiectasia type 1 (*HHT1). HHT1 is rare life-threatening disorder characterized by local angiodysplasia like arterial venous malformations, telangiectasia and recurrent epistaxis. Besides vascular dysplasia, an impaired immune response was also observed in HHT1 patients, evident by e.g. increased infection rates in the brain, joints and liver[1]. To gain more insight into the etiology of HHT1, the murine model for HHT1, the endoglin heterozygous (*Eng*$^{+/-}$) mouse, has been extensively studied. Similar to HHT1 patients, *Eng*$^{+/-}$ mice display decreased wound healing[2] and impaired resolution of inflammation[3]. We have previously shown that *Eng*$^{+/-}$ mice also have a delay in blood flow recovery and a reduction of collateral artery and capillary formation after hind limb ischemia (HLI)[4]. Furthermore, *Eng*$^{+/-}$ have reduced myocardial repair after experimentally induced myocardial infarction (MI)[5], and systemic application of wild type mononuclear cells (MNCs) stimulated revascularization of the injured myocardium and restored cardiac recovery of *Eng*$^{+/-}$ mice, an effect not seen when MNCs of HHT1 patients were used[5]. The exact role of endoglin in inflammation and tissue repair is not yet completely understood, but a rapid increase in expression levels of endoglin during the inflammatory phase of wound healing suggests endoglin is involved in these processes[6-8]. Furthermore, while in healthy individuals the expression of endoglin is upregulated in activated monocytes[9], this response is impaired both in HHT1 patients[10] and *Eng*$^{+/-}$ mice[11], resulting in e.g. an increased infection rate and leukopenia[1,3,11,12].

Endoglin exerts its effect by modulating TGFβ and bone morphogenetic protein (BMP) signaling, two pathways proven to be essential during cardiovascular development and disease[13,14], inflammation and tissue repair[15-20]. TGFβ is the prototypic member of a large family of growth factors to which also the activins and BMPs belong[13]. Upon tissue damage, TGFβ is released from the extracellular matrix, and/or secreted by activated fibroblasts, endothelial cells, platelets, macrophages and T-cells[21-23]. TGFβ signaling is initiated by binding of the ligand to a complex of type I and type II (TβRII) transmembrane receptors. In endothelial cells and macrophages, TGFβ can propagate the signal by forming a complex between the TβRII and a type I receptor known as activin receptor-like kinase (ALK). Signaling via the type I receptor ALK5 results in phosphorylation of the transcription factors Small mothers against decapentaplegic (Smad)2 and Smad3. Complex formation of TβRII and the type I receptor ALK1 is followed by activation of Smad1 and Smad5. ALK1 can only signal via TGFβ by forming a heterotetrameric complex consisting of two TGFβ type II receptors, ALK1 and ALK5, in the presence of endoglin as co-receptor[24-26]. In the absence of endoglin, major vascular defects and impaired angiogenesis are observed, which can only partly be explained by malfunctioning of the endothelial cells by enhanced TGFβ/ALK5 signaling. It is however not known what the role of endoglin deficiency in monocytes entails and how this contributes to vascular repair after an ischemic event.

Cardiac repair after MI can be divided in 3 phases: the ischemic phase, the inflammatory phase and the regenerative phase[27]. During the ischemic phase, cells within the obstructed area are devoid of oxygen and nutrients and go into apoptosis or necrosis. In the inflammatory phase, cellular debris within the injured myocardium are resolved by recruitment of immune cells, inflammatory-like macrophages (M1-like, from here onwards referred to as 'M1'), secretion of cytokines and degradation of extracellular matrix[27]. Approximately 5 days post-MI, the regenerative phase starts and is hallmarked by the release of cytokines stimulating vascularization, recruitment of endothelial progenitor cells and differentiation of regenerative-like macrophages (M2-like, from here onwards referred to as ‘M2’)[27,28]. The immune cells resolve after 2-3 weeks and a fibrous scar is formed[27]. Although we have shown impaired vascular recovery after ischemic injury in *Eng*$^{+/-}$ mice using two different models[4,5,29], as well as a disbalance in M1/M2 macrophages[29], the relation between these two observations and endoglin heterozygosity is still poorly understood. Therefore, the aim of this study is to elucidate the effect of endoglin heterozygosity on M1 and M2 macrophages during the different phases of cardiac recovery. We show that hampered differentiation of *Eng*$^{+/-}$ monocytes into M2 macrophages contributed to the impaired tissue repair. Moreover, the impaired macrophage differentiation was confirmed in monocytes of HHT1 patients, which could be restored by inhibiting BMP signaling. Finally, BMP receptor inhibition improved tissue repair of both the *Eng*$^{+/-}$ ischemic myocardium as well as the *Eng*$^{+/-}$ ischemic hind limb.

Methods

Clinical studies

The procedures performed were approved by the medical ethics committee of the St. Antonius Hospital Nieuwegein, the Netherlands. The study conforms to the principles outlined in the 1964 Declaration of Helsinki and its later amendments. All persons gave their informed consent prior to their inclusion in this study. Venous blood samples from 7 HHT1 patients and 5 age- and gender-matched healthy human volunteers were collected. Peripheral blood MNCs were isolated by density gradient centrifugation using Ficoll Paque Plus (GE Life sciences, #17-1440-02), according to the manufacturer’s protocol.

Animals

All mouse experiments were approved by the regulatory authorities of Leiden University (the Netherlands) and were in compliance with the guidelines from Directive 2010/63/EU of the European Parliament on the protection of animals used for scientific purposes. Experiments were conducted in 10-12 weeks old *Eng*$^{+/+}$ and *Eng*$^{+/-}$ male or female C57BL/6Jico mice (Charles River).

Myocardial infarction

Myocardial infarction (MI) was induced in male mice, as described before [35]. Briefly, mice were anesthetized with isoflurane (1.5-2.5%), intubated and ventilated, after which the left anterior descending coronary artery was permanently ligated. The mice were given the analgesic drug Temgesic, both pre-operative and 24hrs post-operative to relieve pain. Mice were randomly allocated to the treatment or placebo control groups. Placebo or LDN-193189 (2.0 mg/kg, Axon Medchem, #Axon1509) was administered twice daily via intraperitoneal injection from 2 days after MI till day 14. Heart function was measured by echocardiography 14 days post-MI after which the hearts were isolated and fixated in 4% paraformaldehyde (in PBS) and embedded in paraffin.

Animal health and behavior were monitored on a daily basis by the research and/or animal care staff, all trained in animal care and handling. Humane endpoints were observed as the following criteria and symptoms: when mice displayed reduced mobility, decreased grooming, and/or impaired reaction to external stimuli. In addition, for 3 days post-MI and onwards: when the incision area displayed bleeding, swelling, redness and/or discharge, the mice would be euthanized by carbon dioxide. The mice were weighed at the day of surgery and at the echocardiography time points and euthanized when more than 15% loss of weight occurred. Mice that died before meeting the criteria for euthanasia –just after myocardial infarction or within 10 days post-MI- died because of cardiac rupture due to the deterioration of cardiac tissue.

Cardiac function measurements

Mice were anesthesized with isoflurane (1.5-2.5%), after which echocardiography was performed and recorded using the Vevo 770 (VisualSonics, Inc., Toronto, CA) system, using a 30 MHz transducer (RMV707B). Imaging was performed on the longitudinal axis of the left ventricle using the EKV (Electrocardiography-based Kilohertz Visualization) imaging mode. The percentage ejection fraction was determined by tracing of the volume of the left ventricle during the systolic and diastolic phase using the imaging software Vevo770 V3.0 (VisualSonics, Inc., Toronto, CA).

Hind limb ischemia and perfusion imaging

Hind limb ischemia (HLI) was induced as described before[30]. In brief, male and female mice were anesthetized by intraperitoneal injection of midazolam (8.0 mg/kg, Roche Diagnostics), medetomidine (0.4 mg/kg, Orion), and fentanyl (0.08 mg/kg, Janssen Pharmaceuticals). Ischemia of the left hind limb was induced by electrocoagulation of the left femoral artery, the right hindlimb served as control. After surgery, anesthesia was antagonized with flumazenil (0.7 mg/kg, Fresenius Kabi), atipamezole (3.3 mg/kg, Orion), and buprenorphine (0.2 mg/kg, MSD Animal Health). Blood flow recovery to the hind limb was measured using laser Doppler perfusion imaging (LDPI, Moore Instruments). During LDPI measurements, mice were anesthetized by intraperitoneal injection of midazolam (8.0 mg/kg, Roche Diagnostics) and medetomidine (0.4 mg/kg, Orion). After LDPI, anesthesia was antagonized by subcutaneous injection of flumazenil (0.7 mg/kg, Fresenius Kabi) and atipamezole (3.3 mg/kg, Orion). Humane endpoints after induction of HLI were observed as the following criteria and symptoms: when mice displayed reduced mobility, decreased grooming, and/or impaired reaction to external stimuli. Furthermore, when the incision wound area displayed bleeding, swelling, redness and/or discharge, the mice would be euthanized by carbon dioxide.

Immunohistochemistry

Hearts were dissected from carbon dioxide-euthanized mice, fixated overnight at 4^{0}C in 4% paraformaldehyde (in PBS), dehydrated and embedded in paraffin wax. Hearts were cut in 6 µm sections, mounted onto coated glass slides (VWR SuperFrost Plus), and stained for the presence of macrophages in the infarct border zone using rat anti-mouse MAC3 (CD107b, dilution 1:200, BD Biosciences, #550292) and goat anti-rat biotinylated secondary antibody (1:300, Vector Laboratories, #BA-9400). An avidin/biotin-based DAB peroxidase staining was used (Vectastain ABC system, Vector Laboratories, #PK-4000) to detect antibody binding, next to a hematoxylin counterstain for cell nuclei.

Infarct size was determined by Picrosirius Red (PSR) collagen staining; slides were deparaffinized and hydrated, followed by 1 h incubation with PSR solution; 0.1gram Sirius Red F3B (Merck) dissolved in 100 ml saturated picric acid solution (pH=2.0) (Sigma, #P6744). Slides were washed in acidified water, dehydrated in ethanol and mounted with Entellan (Merck) mountant.

Immunofluorescent stainings were performed using standard protocol as previously described[31] for visualization of capillaries by PECAM (CD31, dilution 1:800, Santa Cruz , #sc-1506), arteries by both PECAM (CD31, dilution 1:800, Santa Cruz Biotechnology Inc.) and αSMA (alpha smooth muscle actin, dilution 1:500, Abcam) and macrophages were stained with CD11b (MAC-1, dilution 1:200, Biolegend, #1012505, clone M1/70), MAC-3 (CD107b, dilution 1:200, BD Biosciences, #550292) and CD206 (dilution 1:300, Abcam, #ab64693). Simultaneously detection of p-Smad1/5/8 (dilution 1:100, Cell signaling, #9511) was performed by 30 min antigen retrieval and subsequently p-Smad2 (dilution 1:200, Cell signaling, #3101) was amplified using a TSA™-Biotin System (Tyramide Signal Amplification) Kit (Perkin Elmer Life Science, #NEL700A). Fluorescent-labelled secondary antibodies (ThermoFisher Scientific) were incubated for 1.5 h, at 1:250 dilutions. Sections were mounted with Prolong® Gold Antifade mountant with DAPI (ThermoFisher Scientific, # P36931).

Isolation of immune cells from murine hearts

Hearts were harvested from the mice 4 days post- MI and put in PBS buffer on ice. After excision of the left ventricle, the tissue was put into 1ml digestion buffer (450U Collagenase A, Sigma Aldrich, # 10103578001, 60U hyaluronidase, Sigma Aldrich, #H3506, 60U DNAse-1, Roche, #10104159001) at 37°C for 1 h. The tissue homogenate was filtered through an 80μm cell strainer (Falcon # 352350) and MNCs were isolated using Ficoll density gradient specific for small mammalians (Histopaque-1083, Sigma Aldrich # 10831). Flow cytometry and staining was performed as described below.

Flow cytometry

Mouse monocytes from either 50 μL of whole blood, bone marrow mononuclear cells, or from heart lysates were stained for CD11b (with anti-mouse CD11b, BD Biosciences, #561114), Ly6C (Bio-rad Laboratories, # MCA2389A647T or BD Biosciences, #561085) and CD206 (Bio-rad Laboratories, #MCA2235A488T), to identify M1 and M2 macrophages respectively.

Human monocytes were isolated from peripheral blood, by ficoll gradient separation. Total MNCs (3×10^5 cells per sample) were stained with anti-CD14-ECD (Beckman Coulter, IM2707U) and anti-CD16-APC (Beckman Coulter, # A66330). Fluorescence was measured with LSRII flow cytometer (BD Biosciences) and analyzed by FACS Diva (BD Biosciences) and FlowJo software (FlowJo LLC).

Cultured macrophages from mouse bone marrow

Monocytes were isolated from the bone marrow using CD11b+ magnetic beads (Miltenyi

Biotec MACS #130-049-601) and subsequently cultured in RPMI medium (Gibco RPMI 1640 Medium, #11875-093), supplemented with 10% FBS (Fetal Bovine Serum, Gibco, ThermoFisher Scientific, #10270) and 1ng/ml GM-CSF (Peprotech, #315-03) to induce differentiation into macrophages. After 3 days, the attached cells were stimulated with TGFβ3 (1 ng/ml, kind gift of Dr. K. Iwata), ALK5 kinase was inhibited using SB-431542 (10μM, Tocris, #1614), BMPR type I (ALK1/2/3) were inhibited using LDN-193189 (100nM, Axon Medchem, #Axon1509) addition for 4 days.

Western blot analysis

For intracellular protein analysis, at day 6 of culture the macrophages were serum starved overnight after which they were either stimulated or not for 1 h with TGFβ and/or inhibitors at the indicated concentrations, after which cells were lysed with RIPA lysis buffer (5 M NaCl, 0.5 M EDTA, pH 8.0, 1 M Tris, pH 8.0, NP-40 (IGEPAL CA-630), 10% sodium deoxycholate, 10% SDS, in dH_2O) supplemented with phosphatase inhibitors (1M NaF Sigma Aldrich # S7920, 10% NaPi Avantor #3850-01, 0.1M NaVan Sigma Aldrich # S6508) and protease inhibitors (Complete protease inhibitor cocktail tablets, Roche Diagnostics, #11697498001). Protein concentration was measured using Pierce BCA protein assay (ThermoFisher Scientific, #23225). Equal amounts of protein were loaded onto 10% SDS-polyacrylamide gel and transferred to an Immobilon-P transfer membrane (PVDF membrane, Millipore, # IPVH00010). The blots were blocked for 1 h using 5% milk in TBST (Tris-buffered saline, 0.1% Tween20) solution and incubated O/N with rabbit anti-mouse phosphorylated Smad2 (Cell signaling, #3101), total Smad2/3 (BD Biosciences, BD610842), mouse anti-mouse phosphorylated ERK1/2 (Sigma-Aldrich, #M8159), rabbit anti-mouse total ERK1/2 (p44/42 MAPK, Cell Signaling, #4695, clone 137F5), rabbit anti-mouse phosphorylated p38 (Cell Signaling Technology, #9211) and mouse anti-rabbit total p38 (Santa Cruz Biotechnology Inc. #535). Blots were incubated for 60 minutes with horse radish peroxidase anti-rabbit (ECL rabbit IgG, HRP-linked whole Ab, GE Healthcare, #NA934V) or anti-mouse (ECL mouse IgG, HRP-linked whole Ab, GE Healthcare, #NA931V) antibodies. Blots were developed in an X-omat 1000 processor (Kodak) with SuperSignal West Dura Extended Duration Substrate (ThermoFisher Scientific, #37071) or SuperSignal West Pico Chemiluminescent Substrate (ThermoFisher Scientific, # 34080AB) and exposed to SuperRX medical X-ray film (Fujifilm Corporation). Analysis was performed using Image J (Version 1.51, National Institutes of Health, USA). Full-length blots are included in the Supplementary Information file.

Statistical analysis

Statistical significance was evaluated by unpaired Student's t-test between 2 groups or ANOVA with Bonferroni correction to test between multiple groups with GraphPad Prism 6 software. Values are represented as meanSD or SEM when otherwise indicated. Values of $P<0.05$ are denoted as statistically significant.

Data availability

No datasets were generated or analyzed during the current study. The results generated during and/or analyzed during the current study are available from the corresponding author on reasonable request.

Results

Endoglin deficiency results in prolonged inflammation and reduced M2 macrophage presence after MI

Recruitment of inflammatory cells and timely resolution is essential for cardiac tissue repair. An inadequate or excessive inflammatory response is detrimental in the injured myocardium and can lead to adverse remodeling. We therefore investigated the effects of endoglin heterozygosity on the influx of monocytes during the inflammation phase after experimentally induced MI. We first determined if endoglin heterozygosity influences MNC composition at baseline. Before induction of MI, we observed no differences in MNC subtypes, like macrophages, lymphocytes, NK-cells, neutrophils and granulocytes in blood and bone marrow between wild type (WT, *Eng*$^{+/+}$) and endoglin heterozygous (*Eng*$^{+/-}$) mice (data not shown). Subsequently we induced MI and assessed the number of macrophages present in the heart using immunohistochemical analysis. Four days post-MI, MAC-3 expressing macrophages were present in large numbers in the border zone of the infarcted hearts of both WT and *Eng*$^{+/-}$ mice (Fig. 1a and b). Macrophage infiltration in the WT hearts was cleared 14 days post MI (Fig. 1a and b), confirming previous studies reporting that the inflammatory response is most pronounced at day 3-5 and cleared after approximately two weeks[27]. Interestingly, at 14 days post-MI MAC-3 expressing cells were still easily detectable in the infarct border zone of *Eng*$^{+/-}$ mice (Fig. 1b), suggesting a delay in macrophage resolution.

To further characterize the phenotype of these macrophages, we determined the expression of CD11b, a general monocyte/macrophage marker, and CD206, a specific marker for M2 (regenerative) macrophages facilitating the healing process. Immunofluorescent analysis of the spleen, used as control tissue, showed the presence of CD11b positive resident monocytes, while no CD206 staining was observed (Fig. 1c). Four days post-MI, hearts of WT mice harbor similar numbers of CD11b and CD206 expressing cells, suggesting that the macrophages present in the heart are M2 macrophages. In contrast, in the hearts of *Eng*$^{+/-}$ mice CD11b^{+} cells were easily detectable, while only limited expression of CD206 was present. We quantified these observations using flow cytometry on single cell suspensions of mouse hearts (Fig. 1d). At day 4 post-MI the *Eng*$^{+/-}$ hearts contained significantly less M2 macrophages while the number of pro-inflammatory M1 macrophages was significantly increased (Fig. 1d, $p<0.0001$ and $p=0.0011$ respectively). This suggests a macrophage polarization in the injured *Eng*$^{+/-}$ heart towards a less regenerative macrophage phenotype.

Endoglin deficiency reduces in vitro differentiation of regenerative macrophages in both HHT1 mice and patients

To gain more insight in how endoglin heterozygosity may influence macrophage differentiation we isolated bone marrow derived CD11b+ monocytes and used immunofluorescence to analyze their differentiation towards macrophages in vitro. Endoglin is expressed on murine macrophages and co-staining of endoglin together with the inflammatory macrophage marker Ly6C, revealed that endoglin is specifically present on murine macrophages with a low expression level of Ly6C (Fig. 2a). Macrophages with high expression levels of Ly6C, known as the inflammatory-like (M1-like) subtype, show low expression levels of endoglin (Fig. 2a). More detailed analysis of the different macrophage subtypes in Eng+/- mice and HHT1 patients was performed using flow cytometry. Inflammatory (M1) macrophages were identified by the expression of CD11b, high levels of Ly6C and low CD206 expression for mouse macrophages, and the expression of CD14 and absence of CD16 expression for human cells (Fig. 2b). Regenerative (M2) macrophages were identified by the expression of CD11b,

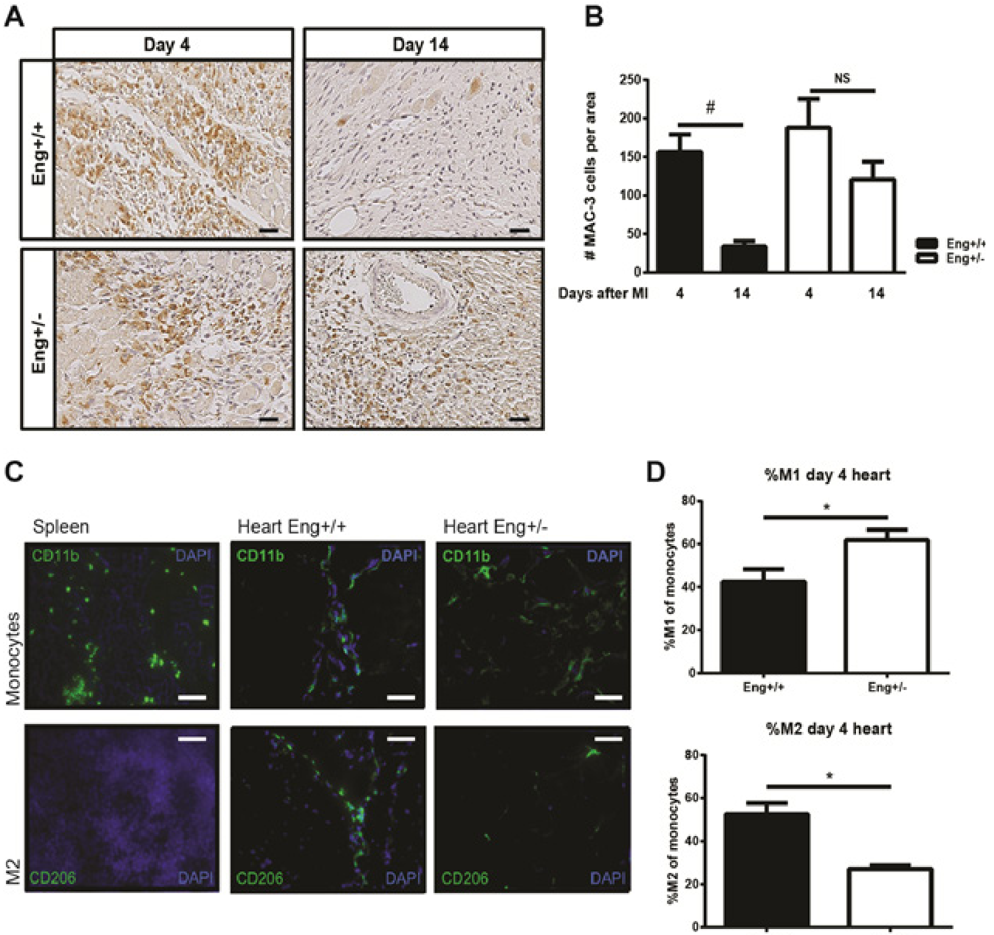
A
Day 4
Day 14
Eng+/+
Eng+/-
B
# MAC-3 cells per area
250
200
150
100
50
0
#
NS
Days after MI
4
14
4
14
Eng+/+
Eng+/-
C
Spleen
Heart Eng+/+
Heart Eng+/-
Monocytes
CD11b
DAPI
M2
CD206
DAPI
D
%M1 day 4 heart
%M1 of monocytes
80
60
40
20
0
*
Eng+/+
Eng+/-
%M2 day 4 heart
%M2 of monocytes
80
60
40
20
0
*
Eng+/+
Eng+/-

Fig. 1 Prolonged macrophage infiltration and decreased M2 after myocardial infarction in Eng+/- mice. a Cardiac sections of Eng+/+ and Eng+/- mice were stained for macrophages. Representative pictures of MAC-3 expressing macrophage (MAC-3= brown; nuclei= blue) at day 4 and 14 after MI. Scale bar: 50µm. b Quantification of the MAC3 positive cells at day 4 and 14 after MI in cardiac section of Eng+/+ and Eng+/- mice. N=5-16 mice per group. c To determine the number of M1 vs M2 monocytes splenic tissue and infarcted cardiac muscle tissue were stained with CD11b as a general monocyte marker and CD206 as M2 macrophage marker 4 days after MI. Scale bar: 50µm. d To quantify the two macrophage subtypes, the ratio M1/M2 macrophages was determined by flow cytometry using a single cell suspension of Eng+/+ and Eng+/- mice hearts 4 days post MI. The inflammatory M1 macrophage was identified by CD11b+/Ly6Chigh/CD206- selection and the regenerative M2 by CD11b+/Ly6Clow/CD206+ selection. N=5-16 mice per group. * $p<0.05$, # $p<0.001$

low levels of Ly6C and high expression of CD206 for mice, and the expression of both CD14 and CD16 for human cells (Fig. 2b). Monocytes isolated from Eng+/- mice as well as HHT1 patients show an increased percentage of inflammatory macrophages ($p=0.006$ and $p=0.008$) and a reduction of regenerative macrophages, compared to macrophages from WT mice and healthy volunteers (Fig. 2c, $p=0.02$ and $p=0.008$ respectively).

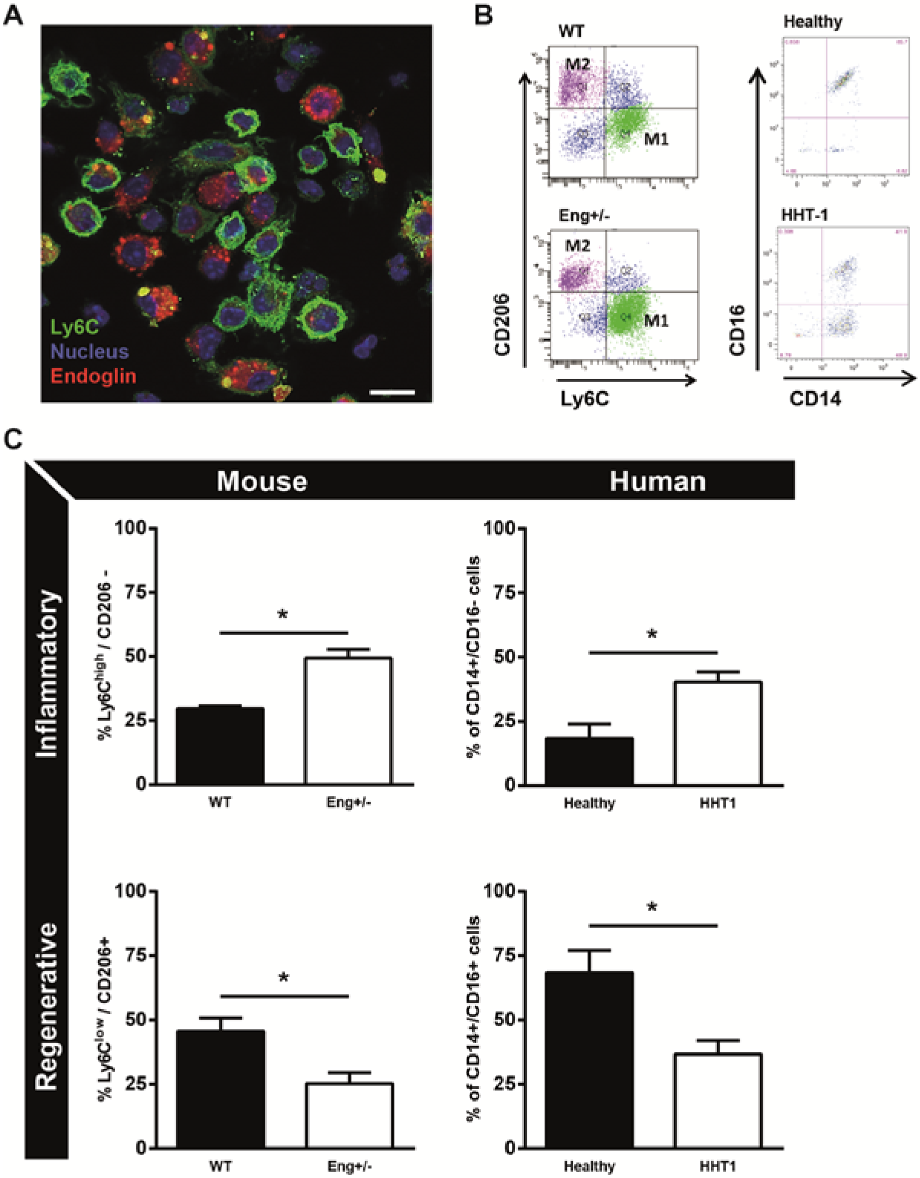

Fig. 2 Macrophage phenotype is dependent on endoglin expression.

a Macrophages isolated from WT mice were stained with endoglin (red), Ly6C (green) and dapi (nuclei, blue). Scale bar: 10µm. b Representative flow charts of mouse and human isolated monocytes of Eng+/- mice and HHT1 patients and their healthy controls. For mouse inflammatory monocytes were distinguished by CD11b+/Ly6Chigh/CD206- and regenerative monocytes by CD11b+/Ly6Clow/CD206+ expression. For human, inflammatory monocytes were distinguished by CD14+CD16- and regenerative monocytes by CD14+/CD16+ expression. c quantification of the flow cytometry data as represented in B, divided in inflammatory and regenerative monocytes of mouse and human. Mouse samples: N=5-16 mice per group. Human samples: 7 HHT1 patients and 5 age- and gender-matched healthy human volunteers. * $p<0.05$; ** $p<0.01$

In vitro switch of macrophage differentiation by adaptation of the TGFβ signaling response

As endoglin is a co-receptor of TGFβ, we next investigated the effect of stimulation and inhibition of the TGFβ-signaling pathway on macrophage differentiation. Monocytes isolated from bone marrow of WT mice were cultured for 3 days in the presence of GM-CSF to stimulate their differentiation into macrophages after which 1ng/ml of TGF ligand was added for either 24 or 96 hours. While 24 hours of TGFβ stimulation had little effect on the percentage of M1 and M2 macrophages compared to non-stimulated cells, 96 hours of TGFβ stimulation skewed macrophage differentiation towards a M2 phenotype (Fig. 3a, p=0.001). This TGFβ increase in M2 macrophages was blocked by adding SB-431542 (SB), a potent ALK5 kinase inhibitor, to WT monocyte cultures, but not by adding the BMPRI inhibitor LDN-193189 (LDN) (Fig. 3b). The M1/M2 macrophage numbers did not change when monocytes isolated from *Eng*$^{+/-}$ mice were stimulated with TGFβ nor did inhibition of the ALK5 kinase by stimulating the cells with SB. Interestingly, when LDN was added to TGFβ stimulated macrophage cultures, the differentiation towards M1 macrophages was reduced, resulting in a normalization of the ratio of *Eng*$^{+/-}$ M1-M2 macrophages to WT levels (Fig. 3c).

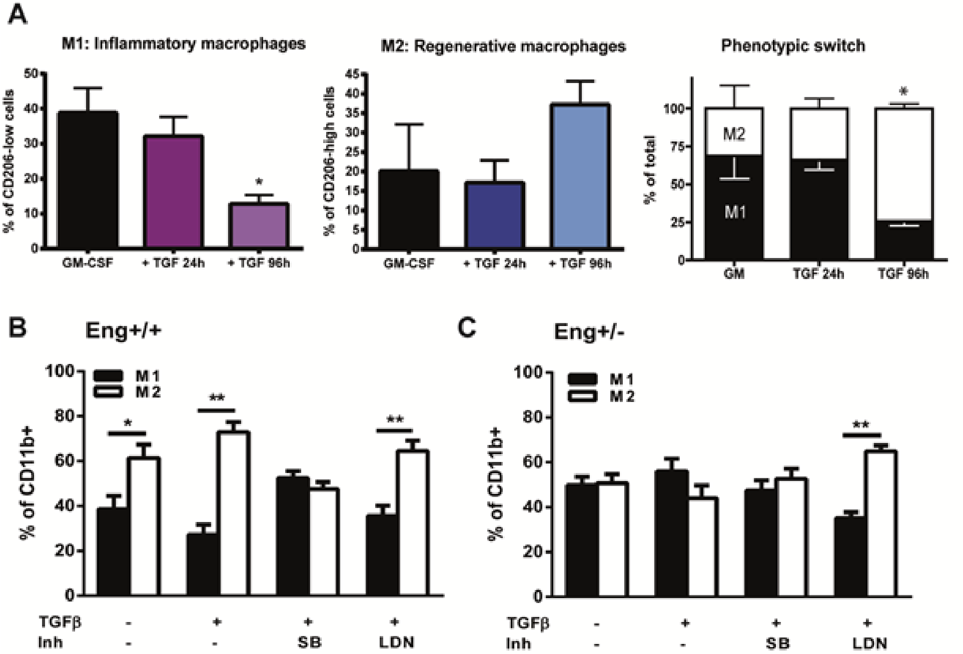

Fig. 3 TGFβ signaling influences macrophage subtype differentiation. a Macrophages from Eng+/+ mice cultured with either GM-CSF for 7 days only or in combination of TGFβ (2.5 ng/ul) for 24h and 96h. The macrophage phenotype was determined based on the expression of Ly6C high (M1) and low (M2) of the CD11b expressing macrophages. * p=0.001 difference in the number of M1 and M2 between GM-CSF vs TGFβ stimulation for 96h. b-c BM isolated monocytes from Eng+/+ (b) and Eng+/- (c) mice were cultured in the presence of GM-CSF in the presence or absence of TGFβ (2.5ng/ul), SB (10μM), or LDN (100nM). The macrophage subtype was determined based on the expression of Ly6C high (M1) and low (M2) of the CD11b expressing macrophages. *p=0.007; **p<0.0001

TGFβ/BMP and non-Smad signaling in *Eng*$^{+/-}$ macrophages is impaired

TGFβ transduces its signal from the membrane to the nucleus by phosphorylation of downstream effectors: canonical Smads and non-canonical signaling proteins ERK and p38. To explore which pathway was used, monocytes from WT and *Eng*$^{+/-}$ mice were differentiated into macrophages, serum starved and stimulated for 60 min with TGFβ and/or indicated inhibitors; SB or LDN. TGFβ was not able to detectably phosphorylate Smad1/5 after serum starvation in neither WT nor *Eng*$^{+/-}$ macrophages (data not shown). For Smad2 however, both WT and *Eng*$^{+/-}$ macrophages showed an induction of Smad2 phosphorylation upon stimulation with TGFβ, which was blocked when SB was added, but not by LDN (Fig. 4a and b). Phosphorylation of Smad2 was not different between WT and *Eng*$^{+/-}$ macrophages. Interestingly, while LDN did not influence TGFβ-induced p-Smad2 in WT macrophages, a significant increase was observed in the *Eng*$^{+/-}$ macrophages (Fig. 4b).

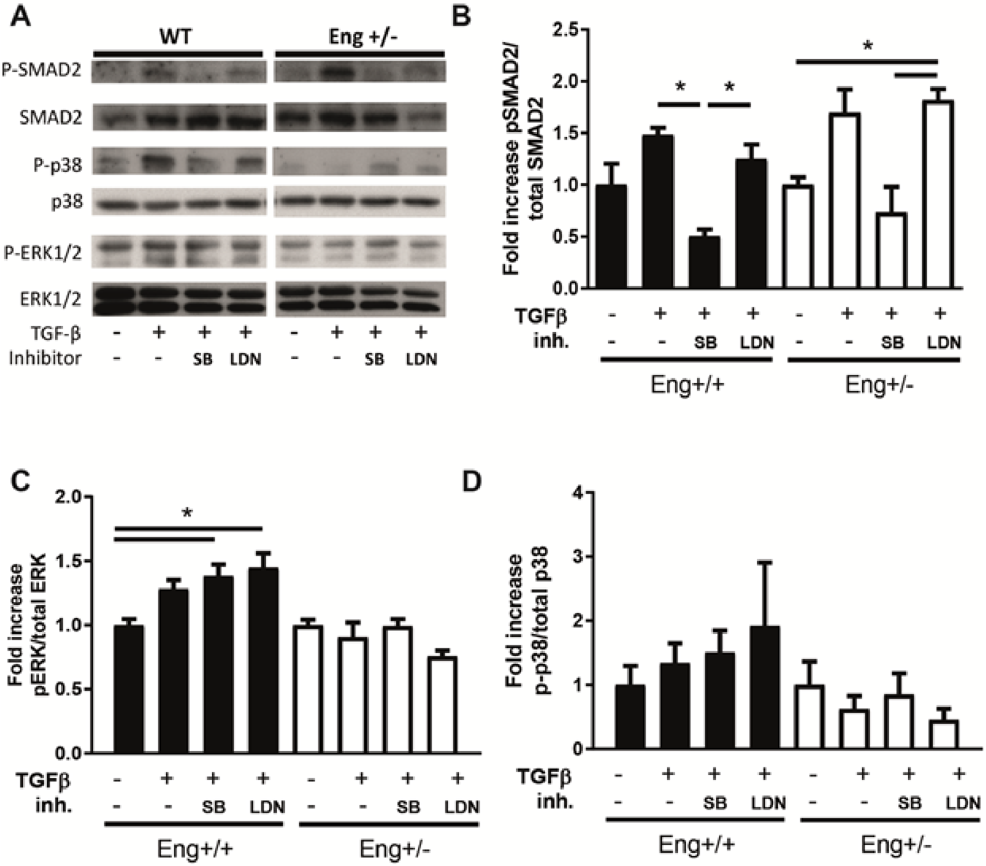

Fig. 4 Eng+/- macrophages show blunted TGFβ and BMP signaling responses in vitro.
a Western blot analysis of Eng+/+ and Eng+/- cultured murine macrophages with GM-CSF, stimulated 60 min with TGFβ (2.5ng/ul), SB (10µM), LDN (100nM). Representative blots of n=3 are shown. Full-length blots are included in the Supplementary Information file. b Densitometric analysis of the blots shown in a has been performed, expressed as the percentage of phosphorylated Smad2 relative to total amount of Smad2 protein. N=3. c Quantification of the blots as shown in a, expressed as the percentage of phosphorylated ERK relative to total amount of ERK protein. N=3. d Quantification of the blots as shown in a, expressed as the percentage of phosphorylated p38 relative to total amount of p38 protein, N=3-4. Error bars are SEM. * $p<0.05$

Since TGFβ can also signal via Smad independent pathways[32-34], we next analyzed the non-canonical pathways known to be involved in stress, inflammation and differentiation responses: the MAPK and p38 pathways. ERK1/2 phosphorylation was increased in WT macrophages upon stimulation with TGFβ, and was further enhanced when SB or LDN were added to TGFβ-stimulated WT macrophages (Fig. 4a and c). Macrophages derived from *Eng*$^{+/-}$ mice did not show an effect on ERK1/2 phosphorylation when stimulated with TGFβ, neither in the presence nor absence of SB or LDN (Fig. 4c). Phosphorylation of p38 showed the same trend as ERK; an increase in p-p38 in WT cells upon TGFβ stimulation and further enhancement in the presence of SB or LDN, while there was no response or even a trend towards reduced p-p38 in *Eng*$^{+/-}$ macrophages (Fig. 4a and d). In summary, *Eng*$^{+/-}$ macrophages show increased Smad2 phosphorylation when BMP signaling is inhibited, while the non-canonical pathways show decreased responsiveness.

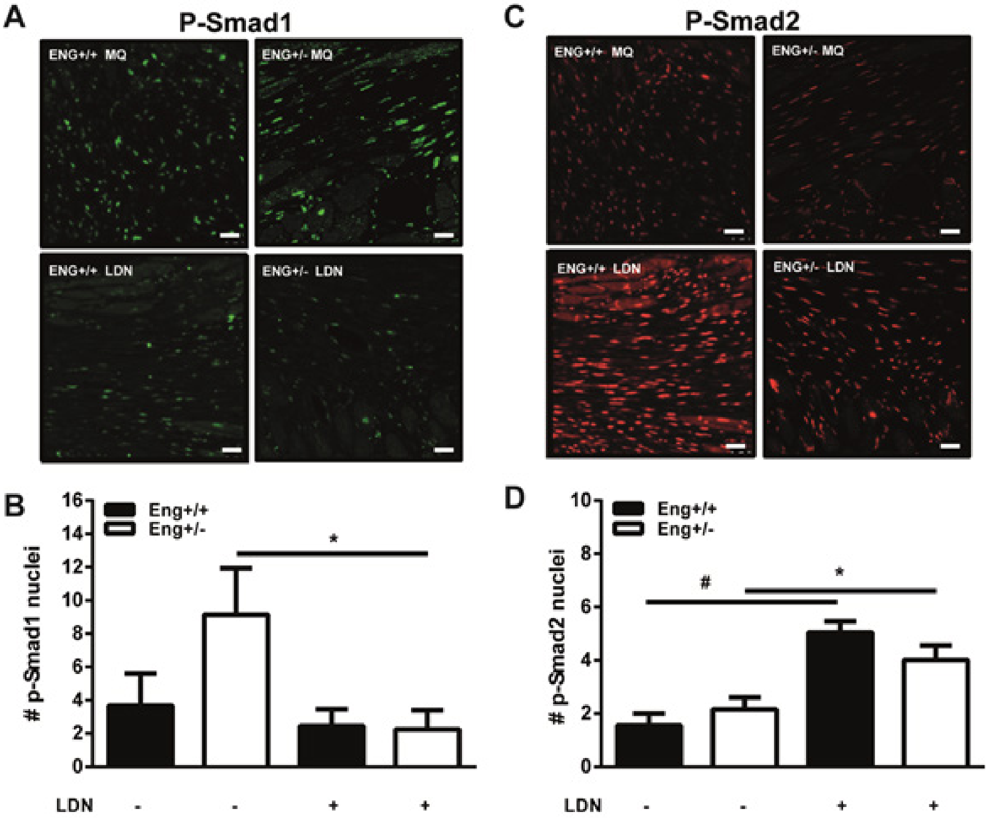

Fig. 5 LDN decreases p-Smad1 and induces p-Smad2 in the infarct border zone.
a Paraffin heart sections were stained for p-Smad1 and quantified for positive stained nuclei. Eng+/+ and Eng+/- mice treated with LDN or placebo. Representative images of heart sections 14 days post-MI are shown. N=5-16 mice per group. b Paraffin heart sections were stained for p-Smad2 staining and quantified for positive stained nuclei. Eng+/+ and Eng+/- mice treated with LDN or placebo. Representative images of heart sections 14 days post-MI are shown. N=5-16 mice per group. Scale bars: 30µm. *p<0.05; #p<0.001

LDN treatment improves cardiac function

Since LDN influences the TGFβ response in $Eng^{+/-}$ *in vitro*, we next investigated whether LDN may influence the impaired cardiac recovery of $Eng^{+/-}$ mice after MI. LDN was systemically administered 2-14 days after the induction of MI. The efficacy of the LDN treatment was confirmed by a reduction in the number of cells positive for phosphorylated Smad1 (Fig. 5a) and an increased number of cells expressing phosphorylated Smad2 (Fig. 5b) 14 days post-MI. In both WT and $Eng^{+/-}$ mice, LDN treatment significantly improved cardiac function (Fig. 6a, $p=0.02$ and $p=0.03$ respectively) and reduced infarct size (Fig. 6b, $p=0.02$ and $p<0.001$ respectively). Investigating the infarct border zone of these mice in more detail revealed that LDN treatment increased capillary density in WT hearts, but had no effect on the number of capillaries in $Eng^{+/-}$ mice. Interestingly, LDN treatment did not change the number of arteries in WT hearts, whereas in $Eng^{+/-}$ animals the number of arteries significantly increased (Fig. 6c, quantification in 6d, 6e, $p<0.05$).

LDN treatment improves perfusion recovery after Hind Limb Ischemia

$Eng^{+/-}$ mice have a delayed perfusion recovery after induction of ischemia in the mouse hind limb (Fig. 7)[4]. Therefore, to determine whether the effect of LDN was specific for the heart or a more general response of endoglin heterozygosity to an ischemic insult, we chose the hind limb ischemia model in addition to the experimentally induced MI. After ligation of the femoral artery, $Eng^{+/-}$ or WT mice were treated with LDN or vehicle and perfusion recovery was measured by Laser Doppler Perfusion Imaging (LDPI) at day 7 post ligation. Interestingly, while blood flow in the hind limb of WT mice was not different between LDN or vehicle treated animal, LDN treatment significantly improved the hampered paw perfusion in $Eng^{+/-}$ mice (Fig. 7, $p=0.002$). Overall, we conclude that tissue repair in $Eng^{+/-}$ mice after ischemic damage in both experimentally induced myocardial and hind limb ischemia was improved by LDN treatment, suggesting that LDN treatment has a general beneficial effect on ischemic tissue repair.

Discussion

The natural response of the body to ischemic injury is to stimulate neovascularization. The influx of circulating monocytes is important for cardiac repair post MI and contributes to the revascularization of ischemic tissue[35,36]. The pro-angiogenic role of endoglin, a TGFβ co-receptor, in vascular development is well established[26,37,38]. We have previously reported that the enhanced deterioration of cardiac function after experimentally induced MI in $Eng^{+/-}$ mice results from impaired capacity of HHT1 MNCs to home to the site of injury and accumulate in the infarct zone to stimulate vessel formation[5,39]. In this study, we show that monocytes are depending on the expression of endoglin to be able to differentiate from an inflammatory M1 macrophage towards a regenerative M2 macrophage and endoglin heterozygosity prolongs the inflammatory response after myocardial infarction. This observation may explain why patients[1,40,41] and mice[3,11] haplo-insufficient for endoglin show prolonged inflammation and delayed wound healing and tissue repair after injury.

We demonstrated that TGFβ differently influenced the differentiation of wild type versus $Eng^{+/-}$ or HHT1 macrophages. Wild type monocytes differentiate to M2 macrophages in an ALK5 dependent manner while inhibition of the BMP type I receptors did not influence their differentiation. Macrophages heterozygous for endoglin did not differentiate towards

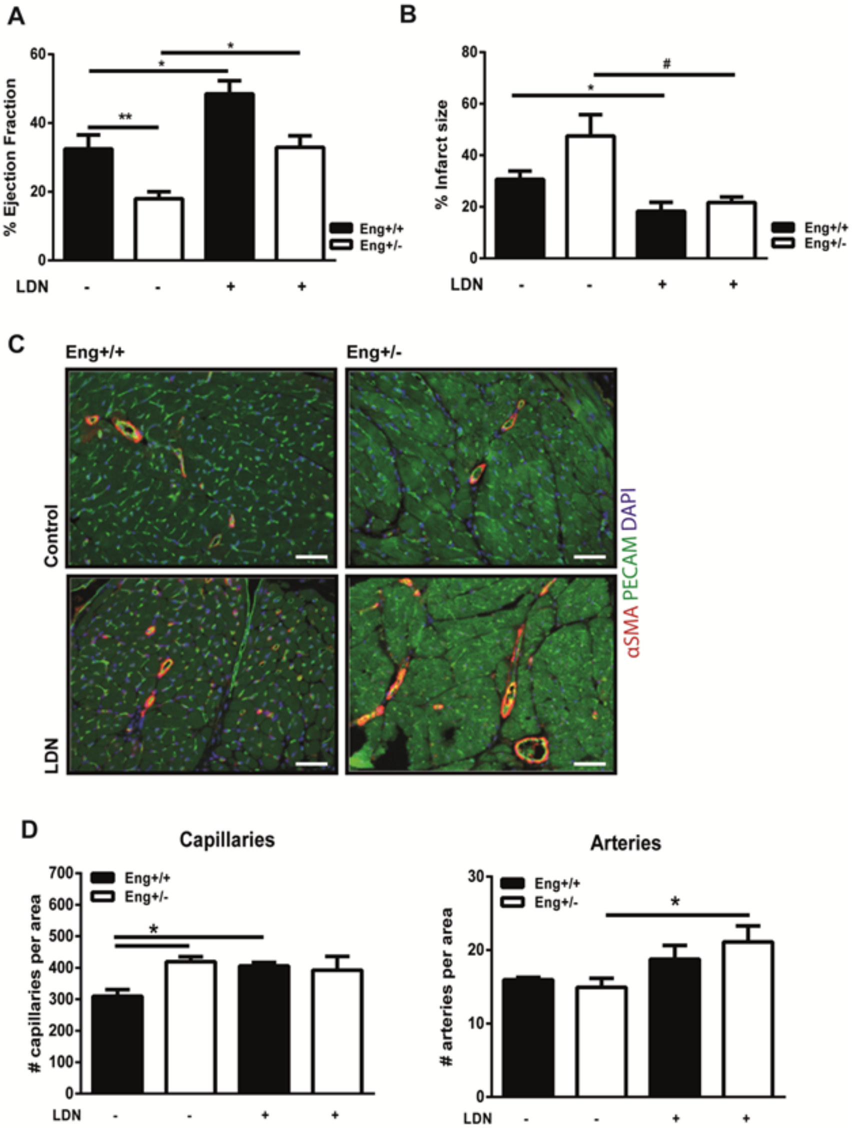

Fig. 6 LDN restores cardiac function in Eng+/- to normal levels 14 days after MI.
a Cardiac ejection fraction percentage of Eng+/+ and Eng+/- mice 14 days post-MI, treated with LDN or placebo. N=5-16 mice per group. b Infarct size was determined in both Eng+/+ and Eng+/- mice using Picrosirius Red staining. Top row: representative pictures of murine transversal heart sections with infarct size (purple) determined by Picrosirius Red staining. 1.0x magnification. Bottom, quantification of infarcted area as percentage of total LV area. N=5-16 mice per group. c-d LDN treatment influences cardiac neo-vascularization post-MI. c Paraffin sections of mouse heart tissue were analyzed for the number of capillaries by staining for PECAM (green) and arteries by analyzing the expression of αSMA (red) and PECAM (green). N=5-16 mice per group. d Quantification of the number of capillaries (left) and arteries (right) in Eng+/+ and Eng+/- mice treated with or without LDN. N=5-16 mice per group. Scale bar: 50µm. * $p<0.05$; ** $p<0.01$; # $p<0.001$

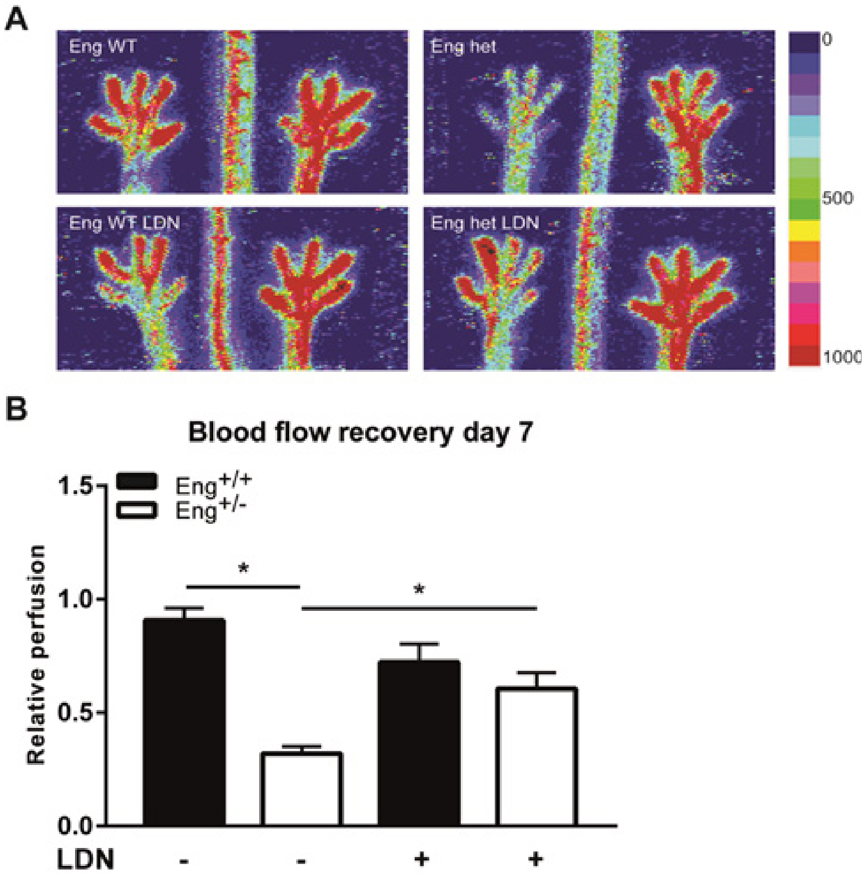

Fig. 7 Hind limb blood flow recovery in female mice increases with LDN treatment.
a Representative images of blood flow recovery in the paws as measured by laser Doppler perfusion imaging (LDPI), 7 days after HLI and subsequent treatment with LDN. Colors indicate the level of flow as indicated on the right panel of the figure. The left side limb has HLI, the right side limb was used as control. b Quantification of LDPI measurements, N=5-7 female mice per group. Black bars= WT, white bars= Eng+/-.* p<0.05.

M2 upon TGFβ stimulation, while inhibition of BMP-signaling resulted in a shift towards M2 macrophages. TGFβ is well known as an anti-inflammatory/pro-fibrotic cytokine and is mainly secreted by M2 macrophages[42,43]. We have previously shown that there was no difference in TGFβ, TβRII, ALK1 and ALK5 expression in WT vs HHT1 mononuclear cells[5], and endothelial cells deprived of endoglin expression are unable to process and secrete active TGFβ[44]. We hypothesized that the defect in TGFβ/BMP ligand processing due to deficiency in the co-receptor endoglin could play a role in the impaired TGFβ-directed differentiation of *Eng*$^{+/-}$ macrophages and explain why inhibition of BMP signaling can restore defective endoglin/TGFβ signaling. The absence of endoglin may skew the tight balance that often exists between TGFβ and BMP signaling, and inhibition of the BMP type I receptor kinases may push this balance towards enhanced TGFβ signaling, thereby restoring M2 macrophage differentiation.

The main defect observed in TGFβ signaling in *Eng*$^{+/-}$ monocytes was related to the non-Smad signaling pathway. *Eng*$^{+/-}$ macrophages were still able to signal via the canonical TGFβ/Smad pathway and phosphorylation of Smad2 was significantly increased in combination with LDN treatment. We did observe reduced activation of the non-canonical MAPK/ERK pathway. An overall misbalance in ERK and p38 signaling has a pronounced effect on inflammation status and in reaction to stress[45]. Previous studies have reported the involvement of endoglin in the MAPK/ERK pathway. In dermal fibroblasts, endoglin haploinsufficiency did not affect basal or TGFβ induced pERK1/2 while the basal levels of Akt show a higher degree of phosphorylation[46]. In endothelial cells the activation levels of Akt were not different between WT and *Eng*$^{+/-}$ cells, while ERK and p38 were more active in *Eng*$^{+/-}$ endothelial cells[47]. We show that in macrophages heterozygous for endoglin, ERK1/2 phosphorylation is impaired and neither stimulation nor inhibition of TGFβ signaling resulted in the phosphorylation of ERK1/2. ERK signaling is involved in cell growth and differentiation[48], and may affect apoptosis[49]. Defects in these aforementioned processes could explain the prolonged inflammatory status we observed in *Eng*$^{+/-}$ mice. In addition to impaired ERK activation, *Eng*$^{+/-}$ macrophages showed decreased phosphorylation of p38 in response to TGFβ stimulation and BMP inhibition. P38 is involved in TGFβ-directed monocyte migration and inhibits monocyte proliferation[50], also has anti-angiogenic properties and is reported to be involved in maintaining proper balance in the angiogenic response[51]. Phosphorylated p38 was reported to inhibit VEGF signaling[52], and *Eng*$^{+/-}$ cells exhibit increased VEGF expression[47]. We hypothesize that reduced levels of p-p38 could therefore be involved in the endothelial hyperplasia and impaired angiogenesis found in HHT1 patients[53,54].

In summary, the present data shows that the inability of MNCs from HHT1 patients to induce neoangiogenesis post-MI is not solely due to impaired recruitment of the MNCs to the site of injury[39], but impaired macrophage differentiation, mainly towards an inflammatory phenotype, will also disturb myocardial repair. The impaired differentiation towards the regenerative M2 macrophage subtype due to endoglin heterozygosity could be restored by LDN stimulation, inhibiting BMP type I receptors, confirming both BMP-dependent and non-canonical modulation of macrophage function in HHT1. Furthermore, cardiac ejection fraction after MI and reperfusion recovery after HLI were improved with LDN treatment. Cumulatively, our results imply that treating HHT1 patients with a BMP type I receptor inhibitor would improve tissue repair. Interestingly, more target specific BMP inhibition methods are already being tested in clinical trials as anti-angiogenesis therapy in cancer patients[55]. Overall, inhibition of the BMP signaling pathway can direct regenerative macrophage differentiation and could be considered as a novel therapeutic target in patients with ischemic tissue damage.

Acknowledgements

This work was financially supported by the Netherlands Institute for Regenerative Medicine (NIRM, FES0908), the Dutch Heart Foundation (NHS2009B063), and by the Netherlands Cardiovascular Research Initiative: the Dutch Heart Foundation, Dutch Federation of University Medical Centres, the Netherlands Organization for Health Research and Development, and the Royal Netherlands Academy of Sciences (CVON-PHAEDRA consortium).

Author Contributions

C.D and M.J.G wrote the main manuscript text. C.D, W.B, K.L, M.d.V and K.W performed experiments. C.D, W.B and M.d.V prepared the figures. All authors reviewed the manuscript.

Competing financial interests

The authors declare no competing financial interests.

References

1. Guilhem, A., Malcus, C., Clarivet, B. & Plauchu, H. Immunological abnormalities associated with hereditary haemorrhagic telangiectasia. 351-362 (2013).

2. Pérez-Gómez, E.*, et al.* Impaired wound repair in adult endoglin heterozygous mice associated with lower NO bioavailability. *The Journal of investigative dermatology* **134**, 247-255 (2014).

3. Peter, M.R.*, et al.* Impaired Resolution of Inflammation in the Endoglin Heterozygous Mouse Model of Chronic Colitis. *Mediators of Inflammation* **2014**, 1-13 (2014).

4. Seghers, L.*, et al.* Shear induced collateral artery growth modulated by endoglin but not by ALK1. *Journal of Cellular and Molecular Medicine* **16**, 2440-2450 (2012).

5. van Laake, L.W.*, et al.* Endoglin Has a Crucial Role in Blood Cell-Mediated Vascular Repair. *Circulation* **114**, 2288-2297 (2006).

6. Torsney, E., Charlton, R., Parums, D., Collis, M. & Arthur, H.M. Inducible expression of human endoglin during inflammation and wound healing in vivo. *Inflammation research : official journal of the European Histamine Research Society ... [et al.]* **51**, 464-470 (2002).

7. Rossi, E.*, et al.* Endothelial endoglin is involved in inflammation: role in leukocyte adhesion and transmigration. *Blood* **121**, 403-415 (2013).

8. Rossi, E., Lopez-Novoa, J.M. & Bernabeu, C. Endoglin involvement in integrin-mediated cell adhesion as a putative pathogenic mechanism in hereditary hemorrhagic telangiectasia type 1 (HHT1). *Frontiers in genetics* **5**, 457 (2014).

9. Aristorena, M.*, et al.* Expression of endoglin isoforms in the myeloid lineage and their role during aging and macrophage polarization. *Journal of cell science* **127**, 2723-2735 (2014).

10. Sanz-Rodriguez, F.*, et al.* Mutation analysis in Spanish patients with hereditary hemorrhagic telangiectasia: deficient endoglin up-regulation in activated monocytes. *Clinical chemistry* **50**, 2003-2011 (2004).

11. Ojeda-Fernández, L.*, et al.* Mice Lacking Endoglin in Macrophages Show an Impaired Immune Response. *PLOS Genetics* **12**, e1005935 (2016).

12. Zhang, R.*, et al.* Persistent infiltration and pro-inflammatory differentiation of monocytes cause unresolved inflammation in brain arteriovenous malformation. *Angiogenesis* **19**, 1-11 (2016).

13. Goumans, M.J. & Ten Dijke, P. TGF-beta Signaling in Control of Cardiovascular Function. *Cold Spring Harb Perspect Biol* (2017).

14. Goumans, M.J., Zwijsen, A., Ten Dijke, P. & Bailly, S. Bone Morphogenetic Proteins in Vascular Homeostasis and Disease. *Cold Spring Harb Perspect Biol* (2017).

15. Doetschman, T.*, et al.* Transforming growth factor beta signaling in adult cardiovascular diseases and repair. *Cell and tissue research* **347**, 203-223 (2012).

16. Ishida, Y., Kondo, T., Takayasu, T., Iwakura, Y. & Mukaida, N. The Essential Involvement of Cross-Talk between IFN-gamma and TGF-beta in the Skin Wound-Healing Process. *The Journal of Immunology* **172**, 1848-1855 (2004).

17. Kulkarni, A.B.*, et al.* Transforming growth factor beta 1 null mutation in mice causes excessive inflammatory response and early death. *Proceedings of the National Academy of Sciences of the United States of America* **90**, 770-774 (1993).

18. Larsson, J. Abnormal angiogenesis but intact hematopoietic potential in TGF-beta type I receptor-deficient mice. *The EMBO Journal* **20**, 1663-1673 (2001).

19. Russell, N.S.*, et al.* Blood and lymphatic microvessel damage in irradiated human skin: The role of TGF-β, endoglin and macrophages. *Radiotherapy and Oncology* **116**, 455-461 (2015).

20. Shull, M.M.*, et al.* Targeted disruption of the mouse transforming growth factor-β1 gene results in multifocal inflammatory disease. *Nature* **359**, 693-699 (1992).

21. Grainger, D.J., Mosedale, D.E. & Metcalfe, J.C. TGF-β in blood: a complex problem. *Cytokine & Growth Factor Reviews* **11**, 133-145 (2000).

22. Wan, M.*, et al.* Injury-activated transforming growth factor β controls mobilization of mesenchymal stem cells for tissue remodeling. *Stem cells* **30**, 2498-2511 (2012).

23. Chuva de Sousa Lopes, S.M.*, et al.* Connective tissue growth factor expression and Smad signaling during mouse heart development and myocardial infarction. *Dev Dyn* **231**, 542-550 (2004).

24. Goumans, M.-j., van Zonneveld, A.J. & ten Dijke, P. Transforming Growth Factor β–Induced Endothelial-to-Mesenchymal Transition: A Switch to Cardiac Fibrosis? *Trends in Cardiovascular Medicine* **18**, 293-298 (2008).

25. Goumans, M.J., Liu, Z. & Ten Dijke, P. TGF-beta signaling in vascular biology and dysfunction. *Cell research* **19**, 116-127 (2008).

26. Lebrin, F.*, et al.* Endoglin promotes endothelial cell proliferation and TGF-β/ALK1 signal transduction. *The EMBO journal* **23**, 4018-4028 (2004).

27. Nahrendorf, M.*, et al.* The healing myocardium sequentially mobilizes two monocyte subsets with divergent and complementary functions. *The Journal of experimental medicine* **204**, 3037-3047 (2007).

28. Mills, C.D., Harris, R.A. & Ley, K. Macrophage Polarization: Decisions That Affect Health. *Journal of clinical & cellular immunology* **6**(2015).

29. Dingenouts, C.K.E.*, et al.* Inhibiting DPP4 in a mouse model of HHT1 results in a shift towards regenerative macrophages and reduces fibrosis after myocardial infarction. *PLoS One* **12**, e0189805 (2017).

30. Welten, S.M.J.*, et al.* Inhibition of 14q32 MicroRNAs miR-329, miR-487b, miR-494, and miR-495 increases neovascularization and blood flow recovery after ischemia. *Circulation Research* **115**, 696-708 (2014).

31. Duim, S.N., Kurakula, K., Goumans, M.J. & Kruithof, B.P.T. Cardiac endothelial cells express Wilms' tumor-1. Wt1 expression in the developing, adult and infarcted heart. *Journal of Molecular and Cellular Cardiology* **81**, 127-135 (2015).

32. Massagué, J. How cells read TGF-beta signals. *Nature reviews. Molecular cell biology* **1**, 169-178 (2000).

33. Nakagawa, T., *et al.* Role of ERK1/2 and p38 mitogen-activated protein kinases in the regulation of thrombospondin-1 by TGF-beta1 in rat proximal tubular cells and mouse fibroblasts. *Journal of the American Society of Nephrology : JASN* **16**, 899-904 (2005).

34. Zhang, Y.E. Non-Smad Signaling Pathways of the TGF-beta Family. *Cold Spring Harb Perspect Biol* **9**(2017).

35. Frangogiannis, N.G. The inflammatory response in myocardial injury, repair, and remodelling. *Nature Reviews Cardiology* **11**, 255-265 (2014).

36. Gombozhapova, A., *et al.* Macrophage activation and polarization in post-infarction cardiac remodeling. *J Biomed Sci* **24**, 13 (2017).

37. ten Dijke, P., Goumans, M.-J. & Pardali, E. Endoglin in angiogenesis and vascular diseases. *Angiogenesis* **11**, 79-89 (2008).

38. Tual-Chalot, S., *et al.* Endothelial depletion of Acvrl1 in mice leads to arteriovenous malformations associated with reduced endoglin expression. *PloS one* **9**(2014).

39. Post, S., *et al.* Impaired recruitment of HHT-1 mononuclear cells to the ischaemic heart is due to an altered CXCR4/CD26 balance. *Cardiovascular Research* **85**, 494-502 (2010).

40. Dupuis-Girod, S., *et al.* Hemorrhagic hereditary telangiectasia (Rendu-Osler disease) and infectious diseases: an underestimated association. *Clinical infectious diseases: an official publication of the Infectious Diseases Society of America* **44**, 841-845 (2007).

41. Mathis, S., *et al.* Cerebral abscesses in hereditary haemorrhagic telangiectasia: a clinical and microbiological evaluation. *Clinical neurology and neurosurgery* **114**, 235-240 (2012).

42. Braga, T.T., Agudelo, J.S.H. & Camara, N.O.S. Macrophages during the fibrotic process: M2 as friend and foe. *Frontiers in Immunology* **6**, 1-8 (2015).

43. Vernon, M.A. & Mylonas, K.J. Macrophages and Renal Fibrosis. *Seminars in Nephrology* **30**, 302-317 (2010).

44. Carvalho, R.L., *et al.* Defective paracrine signalling by TGFbeta in yolk sac vasculature of endoglin mutant mice: a paradigm for hereditary haemorrhagic telangiectasia. *Development* **131**, 6237-6247 (2004).

45. Kebir, D.E. & Filep, J.G. Modulation of neutrophil apoptosis and the resolution of inflammation through β2 integrins. *Frontiers in Immunology* **4**, 1-15 (2013).

46. Pericacho, M., *et al.* Endoglin Haploinsufficiency Promotes Fibroblast Accumulation during Wound Healing through Akt Activation. *PLoS ONE* **8**, e54687 (2013).

47. Park, S., *et al.* Endoglin regulates the activation and quiescence of endothelium by participating in canonical and non-canonical TGF- signaling pathways. *Journal of Cell Science* **126**, 1392-1405 (2013).

48. Monick, M.M., *et al.* Constitutive ERK MAPK activity regulates macrophage ATP production and mitochondrial integrity. *Journal of immunology (Baltimore, Md. : 1950)* **180**, 7485-7496 (2008).

49. Sawatzky, D.A., Willoughby, D.A., Colville-Nash, P.R. & Rossi, A.G. The Involvement of the Apoptosis-Modulating Proteins ERK 1/2, Bcl-xL and Bax in the Resolution of Acute Inflammation in Vivo. *The American Journal of Pathology* **168**, 33-41 (2006).

50. Olieslagers, S., Pardali, E., Tchaikovski, V., Ten Dijke, P. & Waltenberger, J. TGF-β1/ALK5-induced monocyte migration involves PI3K and p38 pathways and is not negatively affected by diabetes mellitus. *Cardiovascular Research* **91**, 510-518 (2011).

51. Aguirre-Ghiso, J.A. Models, mechanisms and clinical evidence for cancer dormancy. *Nature Reviews Cancer* **7**, 834-846 (2007).

52. Gomes, E. & Rockwell, P. p38 MAPK as a negative regulator of VEGF/VEGFR2 signaling pathway in serum deprived human SK-N-SH neuroblastoma cells. *Neurosci Lett* **431**, 95-100 (2008).

53. Abdalla, S.A. Hereditary haemorrhagic telangiectasia: current views on genetics and mechanisms of disease. *Journal of Medical Genetics* **43**, 97-110 (2005).

54. Thalgott, J., Dos-Santos-Luis, D. & Lebrin, F. Pericytes as targets in hereditary hemorrhagic telangiectasia. *Frontiers in Genetics* **5**, 1-16 (2015).

55. de Vinuesa, A.G., Bocci, M., Pietras, K. & ten Dijke, P. Targeting tumour vasculature by inhibiting activin receptor-like kinase (ALK)1 function. *Biochemical Society Transactions* **44**, 1142-1149 (2016).

5

DPP4 inhibition enhances wound healing in endoglin heterozygous mice through modulation of macrophage signaling and differentiation

C.K.E. Dingenouts[1#], K. Lodder[1], A.T. Moerkamp[1], K.B. Kurakula[1], W. Bakker[1], I.E. Hoefer[2], H.M. Arthur[3], M.J. Goumans[1]*

1. Department of Cell and Chemical Biology, Leiden University Medical Center, Leiden, the Netherlands.
2. Department of Experimental Cardiology, Division Heart and Lungs, University Medical Center Utrecht, the Netherlands.
3. Institute of Genetic Medicine, Newcastle University, International Centre for Life, Newcastle upon Tyne, United Kingdom.

#Current address: Department of Infectious Diseases, Leiden University Medical Center, Leiden, the Netherlands.

Manuscript in preparation

Introduction

In non-pathological wound healing, inflammation and subsequent repair is tightly regulated through complex processes and signaling pathways[1-3]. After infiltrating immune cells (e.g. neutrophils, M1 macrophages, T cells) clear the cell debris and foreign bodies, they are gradually replaced by a population of cells with regenerative capacities (e.g. M2 macrophages, epithelial progenitor cells, fibroblasts)[4,5]. During wound inflammation and repair, the transmembrane protein endoglin (*ENG,* CD105) is highly expressed in endothelial cells and expression coincides with the infiltration of the immune cells[6].

Endoglin is a transforming growth factor beta (TGFβ) co-receptor, facilitating the TGFβ-receptor (TGFβR) complex binding several TGFβ family growth and differentiation factors including for example TGFβ isoforms, activins, NODAL, and bone morphogenetic proteins (BMPs) and many others[7,8]. TGFβ transduces its signal via a canonical and a non-canonical pathway. The canonical signaling pathway of TGFβ starts with binding of TGFβ/BMP cytokines to a heterotetrameric complex consisting of two type I and two type II receptors. While binding of TGFβ to a complex containing ALK5 induces Smad2 and/or Smad3 phosphorylation, BMP binds to a complex harboring ALK1/2/3/6, phosphorylating Smad1/5/8[8-10]. Phosphorylation of the SMADs propagate the signal intracellularly, and co-SMAD4 binding together with the phosphorylated SMADs causes the formation of a SMAD complex. The SMAD complex translocates to the nucleus where transcription of multiple genes is affected. The TGFβ/BMP pathway has been studied most extensively in endothelial cells (ECs). In ECs, TGFβ signaling via the ALK1-SMAD1/5/8 pathway results in proliferation and migratory signals, whereas signaling via ALK5-SMAD2/3 results in a decrease in proliferation and migration.

Endoglin has an important function in initiation and regulation of angiogenesis by stimulating ECs[10-12]. In ECs, endoglin mainly stimulates the ALK1-SMAD1/5/8 pathway resulting in angiogenesis and limits activation of the ALK5-SMAD2/3 pathway, which promotes a quiescent vascular state[10]. However endoglin can still promote/activate the SMAD2/3 signaling via the formation of a heteromeric complex of ALK1 combined with ALK5, underlining the complexity of endoglin-TGFβ signaling[9,13].

The prominent role of endoglin in vessel formation is most apparent in the vascular disorder hereditary hemorrhagic telangiectasia type 1 (HHT1), where endoglin haploinsufficiency causes endothelial hyperplasia and impaired angiogenesis[14-17]. The mouse model for HHT1, the endoglin heterozygous ($Eng^{+/-}$) mouse displayed impaired mononuclear cell (MNC) homing towards sites of ischemic damage[18]. Furthermore, MNCs expressed increased levels of dipeptidyl peptidase 4 (DPP4)[19]. Homing of MNCs is primarily regulated by the stromal cell-derived factor 1(SDF1)- CXC chemokine receptor type 4 (CXCR4) axis. MNCs express the CXCR4 receptor, specific for the chemokine SDF1[20]. SDF1 is upregulated and released into the bloodstream upon cell damage and stress, creating a chemokine gradient leading the MNCs expressing CXCR4 towards the site of tissue damage[21]. The SDF1-CXCR4 axis is negatively regulated by enzymatic activity of DPP4. DPP4 cleaves the di-amino-terminal peptides of SDF1, thereby inactivating the homing signal[22]. DPP4 is membrane-bound, but its extra-cellular domain can be cleaved resulting in an soluble form with its enzymatic function still intact[23]. The generation of a soluble form of DPP4 occurs under hypoxic conditions and is mediated by matrix metalloproteases[24]. In HHT1, both CXCR4 and DPP4 were found in elevated surface expression levels on MNCs[19] suggesting that the SDF1-CXCR4 axis is dysregulated in these patients.

Besides impaired homing of MNCs towards SDF1, HHT1 patients and endoglin heterozygous mice harbor an impaired immune response[25-28], suggesting that endoglin not only affects angiogenesis, but also plays an important role in the inflammation phase during the wound healing process[6,18,29,30]. In *Eng*$^{+/-}$ mice, wound healing was reported to be delayed due to reduced keratinocyte proliferation and nitric oxide (NO) avaliability[30]. Furthermore, while fibroblast activation is a necessary action for wound repair, *Eng*$^{+/-}$ wound fibroblasts were found to be hyperactive and aggravated fibrosis through increased AKT signaling[31].

We previously reported that in *Eng*$^{+/-}$ animals the inflammatory (M1-like) and regenerative (M2-like) macrophage content are imbalanced in the infarcted heart. Others also found wound healing in *Eng*$^{+/-}$ to be disrupted[30]. MNCs are essential during the inflammatory response and wound healing[4,32,33] and in previous research we were able to restore immune cell homing and increase cardiac repair in *Eng*$^{+/-}$ mice by the use of DPP4 inhibition[19,34]. Furthermore, DPP4 inhibitor treatment increased the number of M2-like macrophages[34]. We hypothesized that macrophage function and/or differentiation in the *Eng*$^{+/-}$ mice in dermal wound healing is impaired as well, and could potentially be restored by DPP4 inhibition. Therefore in this study, we aimed to use DPP4 inhibition to improve *Eng*$^{+/-}$ MNC function in dermal wound repair.

Material and methods

Mice and dorsal skin wounding experiments

Experiments and analyses were conducted on male endoglin wild type (*Eng*$^{+/+}$, referred to as WT) and heterozygous (*Eng*$^{+/-}$) transgenic mice. All mouse strains were kept on a C57BL/6Jico background (Charles River).

Wild type and *Eng*$^{+/-}$ mice were anesthesized with subdermal Ketamin (100 mg/kg) and Xylazin (10 mg/kg) injection. The dorsal area was depilated using razor followed by application of depilating crème. After sterilization of the skin with 70% ethanol, 4 x 6 mm punches were made through the dorsal skin fold as described previously[35]. The wound area was measured horizontally and vertically with digital caliper, and photographed.

DPP4 inhibitor Sitagliptin (Merck) was dissolved in demineralized water to 1mg/ml, of which 10 ul was topically applied to the wound areas, in total 10 ug Sitagliptin per applied dosis. Demineralized water was used as control treatment. Wound size was measured at day 0, 2, 4, 6, 8 and 10 post-wounding. During measurements, the mice were anesthesized with 2% isoflurane. Mice were divided in a 5-day and 10-day follow-up period post-wounding. Mice were carbon dioxide-euthanized after which skin biopsies were dissected. Mice were randomally allocated into groups of n=6-7 for each treatment. Animal health and behavior were monitored on a daily basis by the research and/or animal care staff, all trained in animal care and handling. All mouse experiments were approved by the regulatory authorities of Leiden University (the Netherlands) and were in compliance with the guidelines from Directive 2010/63/EU of the European Parliament on the protection of animals used for scientific purposes.

Immunofluorescent analysis

Skin was dissected from carbon dioxide-euthanized mice and placed into a container with PBS. The tissue was fixated overnight (O/N) at 4°C in 4% paraformaldehyde in PBS, and then washed with PBS, 50% EtOH and 70% EtOH for 1 h each, followed by embedding in paraffin wax. Paraffin tissue sections of 6 µm thickness were mounted onto coated glass slides (VWR SuperFrost Plus microscope slides). The tissue were stained as previously described using antigen retrieval (Duim 2015). Primary antibodies were incubated O/N at 4°C and directed against: rat anti-mouse MAC3 (CD107b, dilution 1:200, BD Biosciences), rabbit anti-mouse Mannose Receptor (CD206, dilution 1:300, NFκB-p-p65 (1:1000 #11260, Signaling Antibodies) and goat anti-mouse p-IKKα/β (1:1000, #SC21661, Santa Cruz). Appropiate fluorescent-labelled secondary antibodies (ThermoFisher Scientific) were incubated for 1.5 h, at 1:250 dilutions. The slides were mounted with Prolong Gold-DAPI Antifade (# P36931, ThermoFisher Scientific) reagent. Photos were taken with fluorescent digital slide scanner (Pannoramic scanner, Sysmex) and analyzed with CaseViewer software (3DHistech).

Macrophage differentiation and cell culture

Femur and tibia were isolated from WT and *Eng*$^{+/-}$ mice. Bone marrow was flushed using syringes filled with PBS. Cells were seeded onto culture dishes in RPMI 1640 culture media (#11875093, Gibco, ThermoFisher Scientific), supplemented with 10% FBS (#10270, Fetal Bovine Serum, Gibco, ThermoFisher Scientific), 0.2% Penicillin-Streptomycin and 1 ng/ml granulocyte-macrophage colony stimulating factor (GM-CSF, #315-03, Peprotech). Media was refreshed at day 3, with added DPP4 inhibition, either 100µM Sitagliptin (Merck) or 100µM Diprotin A (Sigma-Aldrich) to the culture medium. On day 6 of culture, cells were placed onto serum-free RPMI media, and LPS was added for 24 hrs to stimulate an inflammatory response. Cells were stimulated with TGFβ 5ng/ml and/or freshly added DPP4 inhibitor for 60 minutes before washing with cold PBS, and lysis of the cells for western blotting, see description below.

Western blotting

Cultured macrophages were lysed on ice with cold radio immunoprecipitation assay (RIPA) lysis buffer (in house) supplemented with phosphatase inhibitors((1M NaF Sigma Aldrich #S7920, 10% NaPi Avantor #3850-01, 0.1M NaVan Sigma Aldrich # S6508), protease inhibitors (Complete protease inhibitor cocktail tablets, Roche Diagnostics, #11697498001) and protein concentration was measured using BCA protein assay (Pierce BCA Protein Assay Kit, #23225, ThermoFisher Scientific). Equal amounts of protein were loaded onto 10% SDS-polyacrylamide gel and transferred to an Immobilon-P transfer membrane (# IPVH00010, PVDF membrane, Millipore). The blots were blocked for 60 minutes using 10% milk in Tris-Buffered Saline and 0.1% Tween-20 solution and incubated O/N at 4°C with mouse anti-mouse anti-β-Actin (1:10.000 dilution, A5441, Sigma-Aldrich), rabbit anti-mouse phosphorylated Smad2 (Cell signaling, #3101), total Smad2/3 (BD Biosciences, BD610842), mouse anti-mouse phosphorylated ERK1/2 (Sigma-Aldrich, #M8159), rabbit anti-mouse total ERK1/2 (a.k.a. p44/42 MAPK, Cell Signaling, #4695, clone 137F5), rabbit anti-mouse phosphorylated p38 (Cell Signaling Technology, #9211), rabbit anti-mouse phosphorylated AKT (Cell Signaling Technology, #9271), rabbit anti-mouse total-AKT (pan) (Cell Signaling Technology, #4691), Vinculin (Sigma #V9131). and rabbit anti-mouse total p38 (Santa Cruz Biotechnology Inc. #535). Blots were incubated for 1 h with horse radish peroxidase anti-goat (ThermoFisher Scientific, #32230), anti-rabbit (ECL rabbit IgG, HRP-linked whole Ab, GE Healthcare, #NA934V) or anti-mouse (ECL mouse IgG, HRP-linked whole Ab, GE Healthcare, #NA931V). Blots were developed in a Kodak X-omat 1000 processor with Thermo Scientific SuperSignal West Dura (Extended Duration Substrate) or SuperSignal West Pico and exposed to Fuji SuperRX medical X-ray film. Analysis was performed using Image J (National Institute of Mental Health, Bethesda, Maryland, USA).

ELISA assay

MNC media samples were used for ELISA detection of MCP-1 (MCP-1 ELISA construction kit, Antigenix America Inc. #RRF423CKC) and IL-6 (IL-6 ELISA construction kit, Antigenix America Inc. #RRF600CKC) according to the manufacturer's protocol. Plates were read at 450nm using a microplate reader.

HEK293T cell culture and luciferase reporter assay

HEK293T cells were seeded at density of 1.0×10^5 cells/ml in 48-well plates in DMEM media (Gibco, ThermoFisher Scientific) supplemented with 10% FBS (Fetal Bovine Serum, Gibco, ThermoFisher Scientific, #10270), and transfected with a NFκB subunit p65 reporter plasmid using PEI (Fermentas) transfection reagent, as described previously[36]. Twenty-four hours after transfection, cells were serum-starved for 8 h followed by O/N treatment with Sitagliptin (Merck) at the indicated concentrations. Next, cells were stimulated with TNF-α (50 ng/ml) for 8 h and cell lysates were prepared for measuring luciferase activity with a Perkin Elmer luminometer. The internal control, β-Galactosidase Reporter plasmid, was used in the same samples to normalize transfection efficiency.

Statistics

All results are expressed as mean ± standard error of the mean (SEM). Statistical significance was evaluated using one-way ANOVA for difference between multiple groups and statistical significance was accepted at $p<0.05$. In case the p value was significantly different between groups, T-testing was performed. Adjustment for multiple comparisons was made with either Tukey's or Dunnett's testing and unpaired students T-testing for testing between two groups. Survival curves were tested with a log-rank Mantel-Cox test. Analysis was performed using Graphpad Prism v6 software.

Results

DPP4 inhibition using Sitagliptin enhances wound closure in *Eng*$^{+/-}$ mice

Wild type (WT) and *Eng*$^{+/-}$ mice were first assessed in their capacity for wound healing over time. We confirmed that *Eng*$^{+/-}$ indeed display reduced wound healing compared to wild type litter mates (Fig. 1A and B). Next we analyzed the effect of treatment with the DPP4 inhibitor Sitagliptin on dermal wound closure. Interestingly, applying Sitagliptin to the wound of wild type mice only delayed closure of the epidermis (Fig. 1A and C). In the *Eng*$^{+/-}$ mice treatment with the DPP4 inhibitor Sitagliptin normalized wound repair to wild type levels (Fig. 1A and D).

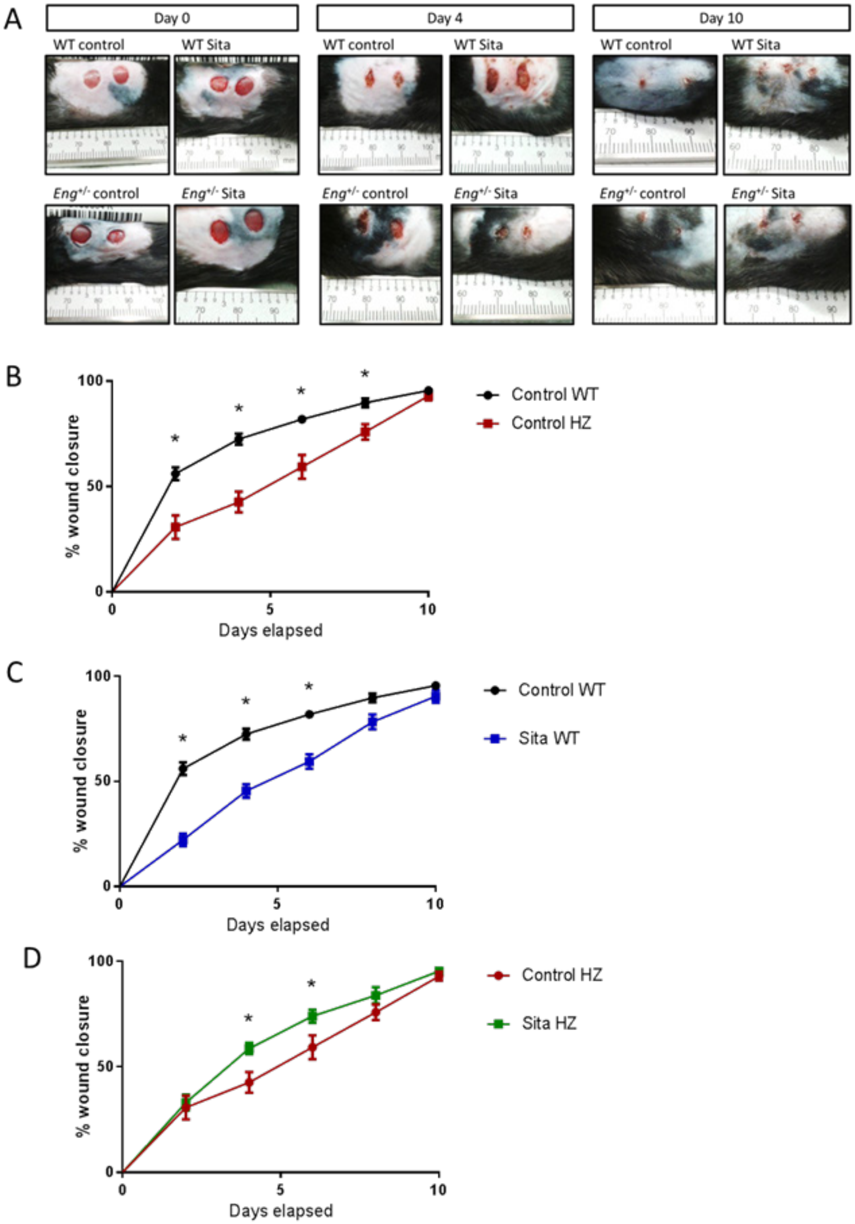

Fig. 1 Sitagliptin enhances tissue repair in Eng+/- mice. A) WT and Eng+/- wound closure over time, day 0, 4 and 10. Wounds from WT and Eng+/- mice treated with DPP4 inhibitor Sitagliptin (Sita) or placebo control. Wound closure in Eng+/- mice is delayed compared to wild type mice. Sitagliptin enhances tissue repair in Eng+/- mice. B) Quantification of average wound closure over time. Treatment with DPP4 inhibitor Sitagliptin. WT control vs. Eng+/- (in graph: HZ-heterozygous) control treated animals. C) WT control vs. WT Sitagliptin treated animals. Sitagliptin delays tissue repair in wild type mice. D) Eng+/- control vs. Eng+/- Sitagliptin treated animals. Sitagliptin enhances tissue repair in Eng+/- mice.

DPP4 inhibition decreases fibrosis in the *Eng*$^{+/-}$ wound area

Since Sitagliptin had a different effect on wound closure in WT versus *Eng*$^{+/-}$ mice, we performed further tissue analyses to gain more insight in this observation. Although DPP4 inhibitors are mainly used in T2DM to prevent cleaving of incretins – DPP4 has a lot more known and unknown targets. One of the events in wound healing is the activation of fibroblasts, cells that are necessary to create new extracellular matrix ECM and collagen for wound contraction and scar formation[37]. Since DPP4 inhibition is reported to have an anti-fibrotic effect[38-41], we analyzed the effect of Sitagliptin on the expression of αSMA, a marker for myofibroblasts formation. αSMA was quantified in sections 5 days post-wounding. In control treated *Eng*$^{+/-}$ mice, αSMA content was significantly increased in the wound area compared to WT animals (Fig. 2). Upon Sitagliptin treatment the αSMA levels in the wounding area of WT mice were not affected. However, the αSMA levels in the wounding area of *Eng*$^{+/-}$ mice were decreased significantly, suggesting myofibroblast presence and/or activity was inhibited by DPP4 inhibition.

DPP4 inhibition increases the number of M2 macrophages in the wound area

We previously reported that in *Eng*$^{+/-}$ animals the inflammatory (M1-like) macrophages were increased compare to reparative (M2-like) macrophage numbers and these mice show a disrupted cardiac repair. Therefore we next investigated whether or not macrophage function and/or differentiation in the *Eng*$^{+/-}$ mice in dermal wound healing is impaired as well. To further determine the impact of DPP4 inhibition, we analyzed the presence of the MAC3^{+}/CD206^{+} M2-like (referred to as 'M2') macrophages near the wound area (Fig. 3A). Topical Sitagliptin treatment on dermal wounds significantly increased the numbers of M2 in both WT and *Eng*$^{+/-}$ mice (Fig. 3B).

DPP4 inhibition blunts macrophage stress responses to LPS stimulation

Because of the change in macrophage population (towards the reparative type) observed when we applied topical Sitagliptin treatment, we next questioned whether or not there is an effect of DPP4 inhibition on the intracellular signaling of both the WT and *Eng*$^{+/-}$ macrophages. And moreover, whether there is a change response to signals present in the tissue and/or disrupted signaling in the *Eng*$^{+/-}$ macrophages. To investigate whether DPP4 inhibitor specific effects would vary we also added a second competitive DPP4 inhibitor– Diprotin A- in addition to Sitagliptin. The main difference between the two inhibitors is that Diprotin A has reversible DPP4 inhibition, whereas Sitagliptin inhibits DPP4 irreversibly. We then investigated activation of TGFβ and stress related intracellular signaling pathways. Murine monocytes were isolated from bone marrow aspirates, and stimulated with GM-CSF for 7 days to induce differentiation into macrophages. DPP4 inhibition was added to the culture at day 3 to pre-sensitize the cells and ensure optimal DPP4 inhibition.

Activation of the canonical TGFβ pathway via ALK5 - SMAD2/3 phosphorylation was determined via pSMAD2 (pSMAD1/5/8 was not detectable in our cells). In both the WT and *Eng*$^{+/-}$ cells pSMAD2 activation was increased when TGFβ was added to the culture (similar to findings by Letarte et al. 2005 in HHT1-HUVECs[42]) (Fig. 4A and B). Surprisingly, upon addition of Sitagliptin pSMAD2 decreased in *Eng*$^{+/-}$ and WT, and also the total SMAD levels went down, even when stimulated with TGFβ.

To understand the effect of Sitagliptin on inflammation, we stimulated the macrophages with

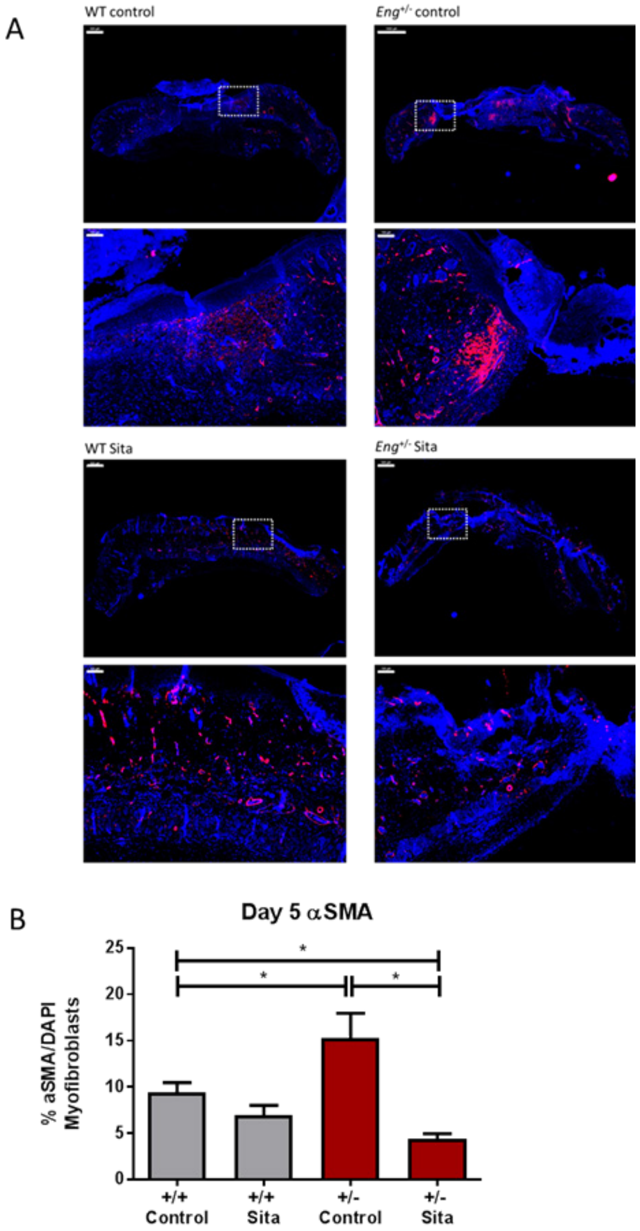
A
WT control
Eng+/- control
WT Sita
Eng+/- Sita
B
Day 5 αSMA
% aSMA/DAPI Myofibroblasts
0
5
10
15
20
25
*
*
*
+/+ Control
+/+ Sita
+/- Control
+/- Sita

Fig. 2 Sitagliptin treatment decreases activated fibroblast presence in the skin surrounding wounded area. A) Histological analysis of activated myofibroblast presence during Eng+/- wound healing. Immunofluorescence staining of αSMA on PFA-fixed Paraffin-embedded wounds from WT and Eng+/- mice at day 5 post-wounding. Upper panels: skin section overview. Lower panels: magnification of inset depicted in upper panels. Scale bars WT control, WT sita and Eng+/- = 500µm, Eng+/- control=1000µm. All scale bars of the insets/magnifications=100µm B) Quantification of activated fibroblasts of immunofluorescence staining of aSMA on PFA-fixed Paraffin-embedded wounds from WT and Eng+/- mice at day 5 post-wounding.

LPS, 24hrs before harvesting. Induction of pSMAD2 increased markedly, and this effect was even more pronounced in the *Eng*$^{+/-}$ cells. When TGFβ was added, pSMAD2 increased in both WT and *Eng*$^{+/-}$ cells. With Sitagliptin inhibition a decrease was observed in the *Eng*$^{+/-}$ macrophages, whereas we did not observe a difference in the WT cells. PSMAD2 is strongly induced in the LPS-treated cells, and co-treatment with TGFβ induces pSMAD2 to an even greater extend. LPS with Sitagliptin added does not show any pSMAD2 difference compared to the LPS only signal (Fig. 4). Co-treatment of both TGFβ and Sitagliptin does not show any additional increase. Sitagliptin's inhibitory effect was not detectable in the

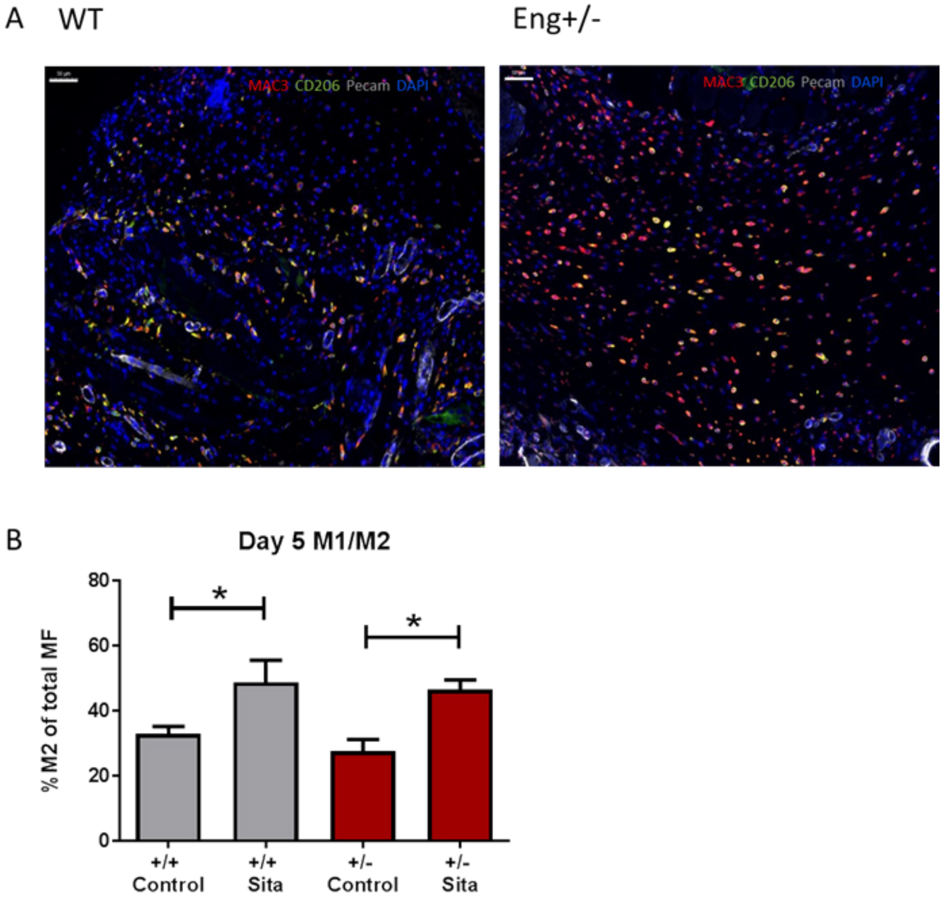

Fig. 3 DPP4 inhibition results in an increased reparative macrophage presence. A) Histological analysis of macrophage presence during Eng+/- wound healing. Representative immunofluorescence staining image of MAC3 and CD206 on PFA-fixed paraffin-embedded wounds from WT and Eng+/- mice at day 5 post-wounding. MAC3=red, CD206=green, Pecam=white, DAPI=blue. Scale bar = 50µm B) Sitagliptin treatment increases M2 presence in the skin surrounding wounded area. Percentage CD206+ cells (M2 macrophages) of total MAC3+ macrophages present in the wound border zone.

LPS treated macrophages. Overall, while pSMAD2 signaling is affected by DPP4 inhibition, it does not vary significantly between WT and *Eng*$^{+/-}$ (Fig. 4B). These results suggest the macrophage signaling affected by DPP4 inhibition are probably not SMAD–mediated and involve other TGFβ-related pathways. Therefore, we next investigated the effects of DPP4 inhibition on non-SMAD TGFβ signaling. Activation of the non-canonical/SMAD TGFβ pathway and AKT is part of a survival pathway, and also involved in cell proliferation and M2 differentiation. pAKT was found increased in *Eng*$^{+/-}$ at endogenous levels. In both WT and *Eng*$^{+/-}$ cells pAKT decreases upon Sitagliptin addition, though in WT macrophages the inhibition of pAKT is more pronounced. This could indicate that the response via AKT signaling is blunted in *Eng*$^{+/-}$ macrophages.

The combination of TGFβ and Sitagliptin inhibits AKT phosphorylation (Fig. 4A). The total amounts of AKT were also decreased by Sitagliptin addition. LPS stimulation of the macrophages caused an increase of pAKT; this induction was even more pronounced in the *Eng*$^{+/-}$ (Fig. 4A).The increase in pAKT to additional TGFβ stimulation was similar in both WT and *Eng*$^{+/-}$ macrophages. With the addition of Sitagliptin we observed either no effect or a slight increase in the WT macrophages, whereas the signal steadily decreased in the *Eng*$^{+/-}$ cells. The combination of TGFβ with Sitagliptin gave varying results in the WT cells, but

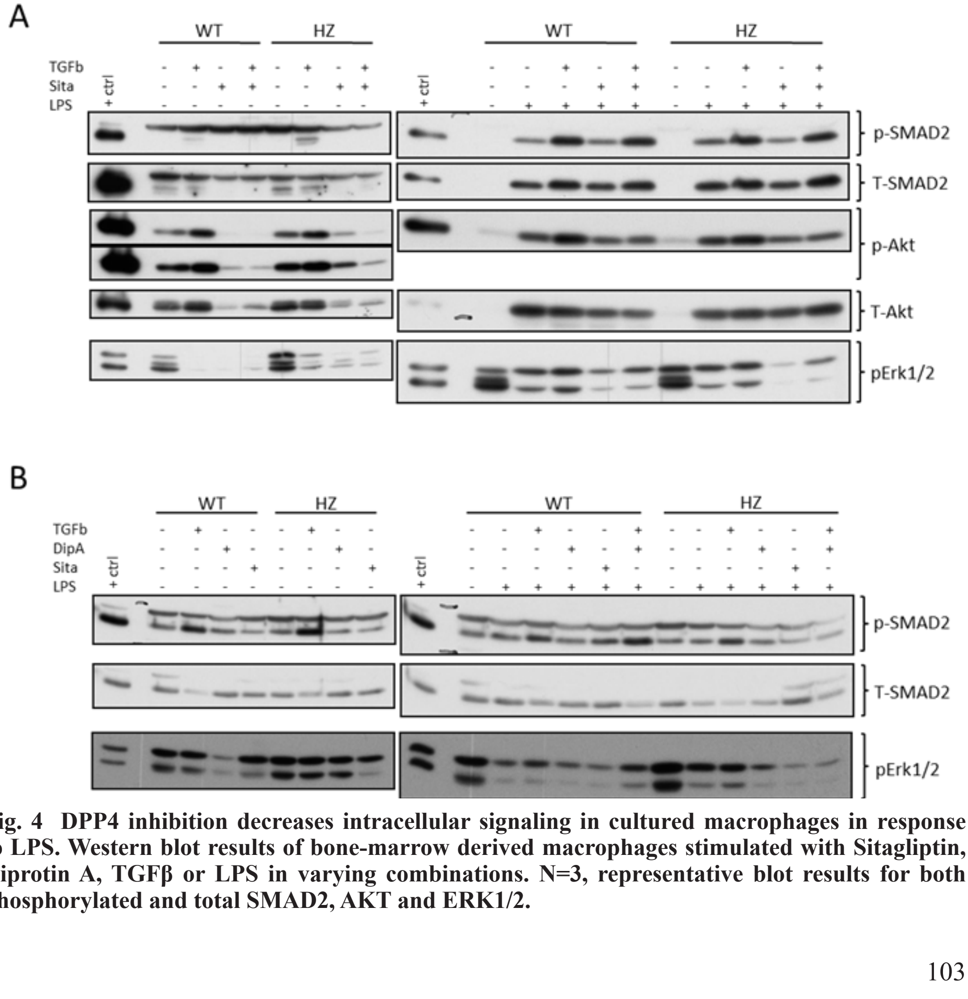

Fig. 4 DPP4 inhibition decreases intracellular signaling in cultured macrophages in response to LPS. Western blot results of bone-marrow derived macrophages stimulated with Sitagliptin, Diprotin A, TGFβ or LPS in varying combinations. N=3, representative blot results for both phosphorylated and total SMAD2, AKT and ERK1/2.

showed a reproducible decrease in the *Eng*$^{+/-}$ macrophages, returning the amount of pAKT to Sitagliptin-only levels. We conclude that both in physiological/non-inflammatory and in inflammatory conditions TGFβ-induced pAKT is negated by DPP4 inhibition.

ERK signaling is known to be involved in cell proliferation[43], survival[44], and pro-inflammatory cell responses[45,46]. Therefore we analyzed the effect of Sitagliptin on pERK1/2 in both WT and *Eng*$^{+/-}$ macrophages. Interestingly, the endogenous level of pERK1/2 was already increased in the *Eng*$^{+/-}$ macrophages. Treatment with either Sitagliptin or DipA led in both WT and *Eng*$^{+/-}$ cells to a decrease in phosphorylation, although more pronounced in the *Eng*$^{+/-}$ macrophages. TGFβ did not change the pERK1/2 levels in either WT or *Eng*$^{+/-}$ cells. Sitagliptin also inhibited the TGFβ-induced ERK1/2 phosphorylation. Co-treatment with TGFβ and Sitagliptin decreased pERK1/2 in equal amount for both wild type and *Eng*$^{+/-}$ cells. Total levels of ERK1/2 were not affected.

LPS stimulation increased pERK1/2 in both WT and *Eng*$^{+/-}$ macrophages. Treatment with Sitagliptin or co-treatment with TGFβ to the LPS pre-treated cultures consistently decreased the pERK1/2 response in both WT and *Eng*$^{+/-}$ macrophages. This indicates that LPS and/or TGFβ -induced pERK1/2 is repressed by DPP4 inhibition, indicating an anti-inflammatory response by the DPP4 inhibitor. We confirmed the anti-inflammatory effect of Sitagliptin via a luciferase reporter assay for NFκB expression in HEK293T cells. Addition of the DPP4 inhibitor resulted in a significant decrease in NFκB expression (Fig. 5).

We conclude that Sitagliptin is able to reduce macrophage stress signaling responses after LPS stimulation, most likely influencing the polarization of these cells towards a more reparative phenotype, the M2 cells. As we now prove that DPP4 inhibition is able to influence TGFβ-related signaling and cell stress responses, this might explain the difference in wound repair in the wild type and *Eng*$^{+/-}$ mice, and we speculate that endoglin heterozygosity most likely impairs the correct functioning of these macrophages.

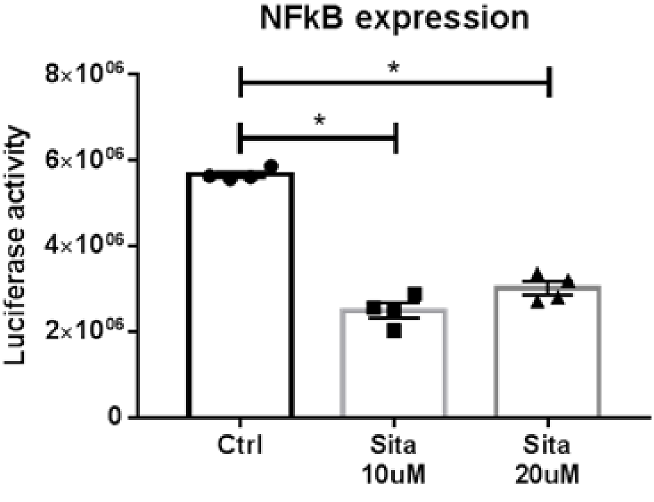

Figure 5. NFκB expression decreases with DPP4 inhibition. Luciferase reporter assay on lysates of HEK293T cells. Sitagliptin was added to the culture at 10µM and 20µM. *=p<0.05

The inflammatory response of *Eng*$^{+/-}$ macrophages is modulated by DPP4 inhibition

The major increase of M2 macrophages present in the wound area raised the question how DPP4 inhibition is able to alter the inflammatory response. We therefore determined the *in vitro* expression of one of the key inflammatory cytokines involved in the macrophage chemotaxic response, Monocyte Chemoattractant Protein-1 (MCP-1, CCL2)[47]. ELISA analysis of the supernatants showed that MCP-1 levels are higher in the *Eng*$^{+/-}$ macrophages compared to the wild type cells (Fig. 6A), indicating a possible hyper-inflammatory status in *Eng*$^{+/-}$ animals.

When Sitagliptin was added to the culture, no changes were detectable in extracellular MCP-1 levels from WT cells (Fig. 6C), while in the *Eng*$^{+/-}$ macrophages the MCP-1 level decreased significantly (Fig. 6D), restoring MCP-1 expression to WT levels (Fig. 6B). When pretreating the macrophages with LPS, we observed a similar trend, MCP-1 level was higher in the *Eng*$^{+/-}$ macrophages. However there was no significant difference in MCP-1 expression level after Sitagliptin addition (Fig. 7 A and B). LPS treatment may therefore abolish the effects of Sitagliptin we observed without LPS addition to the culture.

Another important cytokine in dermal wound healing is interleukin-6 (IL-6). IL-6 was found to be involved in keratinocyte proliferation[48,49] and macrophage differentiation[50,51]. When the macrophages were stimulated with LPS to induce IL-6 production, the IL-6 level was decreased in the *Eng*$^{+/-}$ cells (Fig. 7C) (As previously reported by Scharpfenecker et al.[52]). Sitagliptin treatment however did not affect IL-6 cytokine levels (Fig. 7D). These results

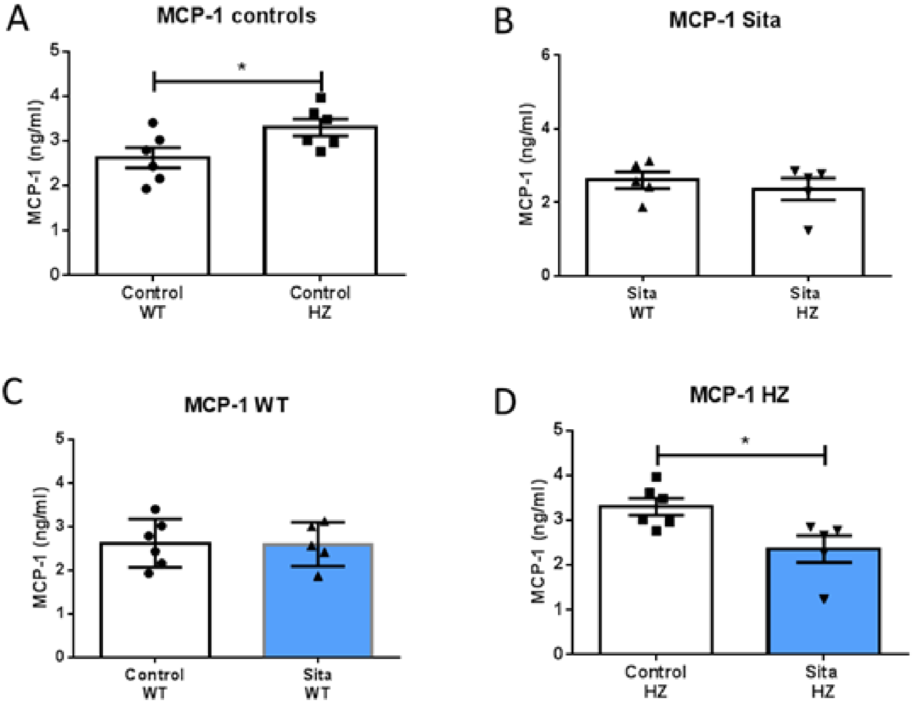

Figure 6. MCP-1 levels and the effect of DPP4 inhibition in cultured murine macrophages. Macrophage culture media samples were used for ELISA detection of MCP-1. Measurements were performed with media samples from n=5-6 mice per group. SEM, *=p<0.05

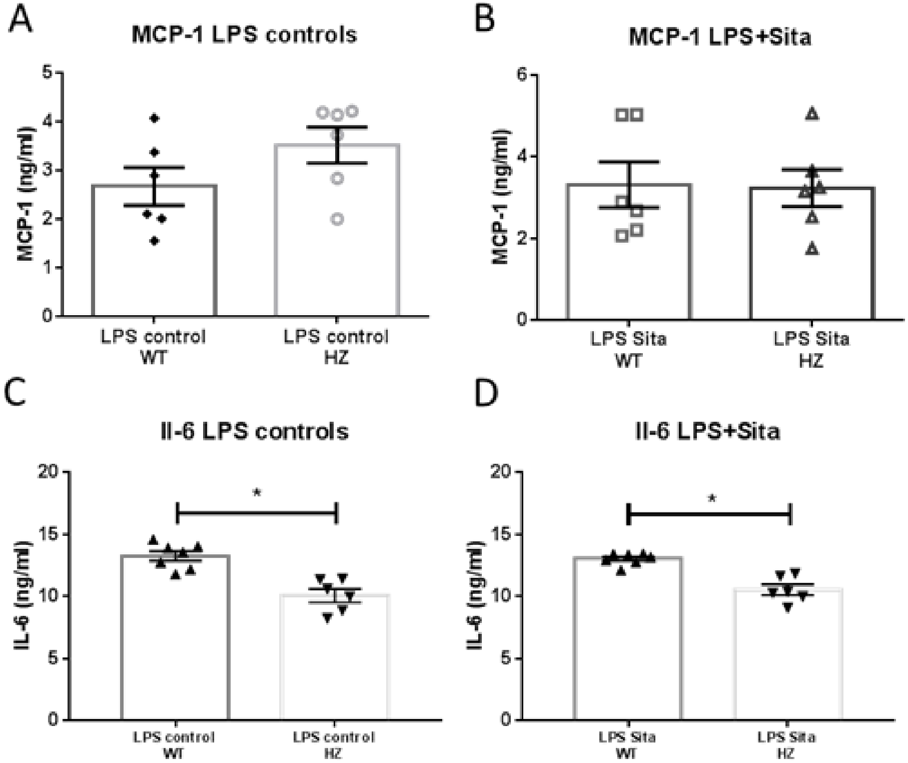

Figure 7. Effect of DPP4 inhibition on expression of inflammatory-related cytokines IL-6 and MCP-1 in macrophage culture after LPS stimulation. Macrophage culture media samples were used for ELISA detection of MCP-1 and IL-6. LPS was added for 24 hrs. A) MCP-1 control treated macrophages B) MCP-1 Sitagliptin treated macrophages C) IL-6 control treated macrophages D) IL-6 Sitagliptin treated macrophages. Measurements were performed with media samples from n=5-6 mice per group. SEM, *=p<0.05

suggest that low IL-6 levels at baseline might reduce keratinocyte proliferation, and could affect macrophage function as well.

To further unravel the mechanism explaining the localized wound tissue responses, we next examined tissue samples from the *in vivo* wounding study. We analyzed the expression of inflammatory markers localized directly next to the wounding site. Tissue sections were stained for inflammatory markers involved in the NFκB complex and pathway: p-p65 (NFκB complex subunit) and pIKKα/β (protein necessary for NFκB complex phosphorylation[53]) (example of tissue staining can be found in Supplementary Fig. 2), were quantified. Phosphorylated IKKα/β levels were increased in the *Eng*$^{+/-}$ wound sections (Fig. 8A). Sitagliptin treatment decreased pIKKα/β levels in *Eng*$^{+/-}$ wounds to comparable levels as WT wounds (Fig. 8A). Although a trend towards increased pIKKα/β is visible in the WT wounds treated with Sitagliptin, no significant effect on the pIKKα/β levels were observed (which could indicate a reverse response of IKK to DPP4 inhibition). This could indicate an anti-inflammatory effect of Sitagliptin in the *Eng*$^{+/-}$ wounds, the slight increase in pIKKα/β in WT animals signifies increased inflammation and could therefore explain the delayed wound healing observed in these animals.

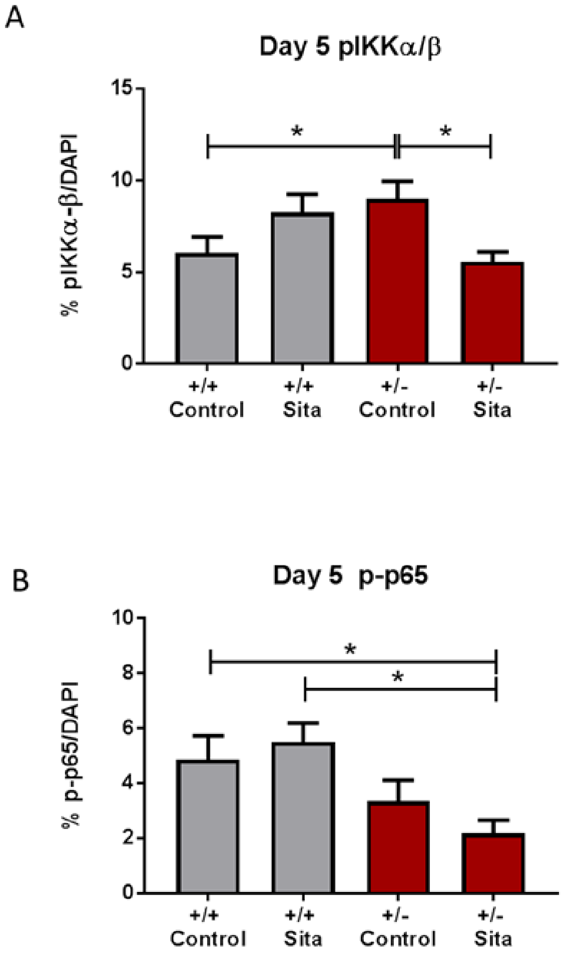

Figure 8. Sitagliptin treatment decreases the inflammatory cytokine response in Eng+/- wounds. A) Quantification of pIKKα/β levels in the wound area, 5 days post-wounding. B) Quantification of p-p65 levels in the wound area, 5 days post-wounding. Single or duplet measurements were made per individual mouse, SEM, n=4 mice per group,*=p<0.05

Phosphorylated p65 was not significantly different between WT and *Eng*$^{+/-}$ wounds (Fig. 8B). Interestingly, while no effect was observed on the p-p65 levels in the WT wounds treated with Sitagliptin, Sitagliptin treatment decreased the levels of phosphorylated p65 in the *Eng*$^{+/-}$ wounds compared to WT p-p65 levels (Fig. 8B). In summary, DPP4 inhibition decreases NFκB-mediated inflammatory response in the wound area of *Eng*$^{+/-}$ mice.

Discussion

Eng$^{+/-}$ mice are affected in their immune response[25-28], characterized by a skewed M1/M2 balance towards the pro-inflammatory M1 macrophages[34] and a prolonged and delayed wound healing[30,34]. Previously we showed that DPP4 inhibition could direct *Eng*$^{+/-}$ macrophage homing and/or differentiation towards the more reparative M2 macrophages. We aimed to restore dermal wound repair by using topical DPP4 inhibition.

The present study demonstrates that topical treatment with DPP4 inhibitor Sitagliptin results in an improved dermal wound repair in *Eng*$^{+/-}$ mice. Furthermore, we now show that in the *Eng*$^{+/-}$ macrophages, Sitagliptin is able to exert anti-inflammatory effects, reversing the *Eng*$^{+/-}$ macrophages to a less inflammatory phenotype. At the wounding site, *Eng*$^{+/-}$ mice had increased levels of myofibroblasts present. Whereas we observed only a slight decrease in wild type mice, treatment with Sitagliptin significantly decreased the myofibroblast content in the wounds of *Eng*$^{+/-}$ animals. These results imply an anti-fibrotic effect of DPP4 inhibition, consistent with findings in other disease studies like kidney or liver fibrosis[38-41]. Conversely, in diabetic Ob/Ob mice, myofibroblasts were found increased when treated with DPP4 inhibitor Linagliptin[54], of course the diabetic Ob/Ob–specific model/setting could be the reason of the pro-fibrotic outcome of DPP4 inhibition. However, this study also demonstrated that DPP4 inhibition did prove to have an anti-inflammatory effect, via the lowering of pro-inflammatory markers like cyclooxygenase-2 and MIP-2 (macrophage inflammatory protein-2)[54]. In our current study, we provide a mechanism for the anti-inflammatory effects in the *Eng*$^{+/-}$ mice, We show that in the *Eng*$^{+/-}$ mice Sitagliptin treatment decreased p-p65, pIKKα/β *ex vivo* and MCP-1 *in vitro*. Furthermore DPP4 inhibition decreased phosphorylation of other stress-related signaling like ERK1/2 and AKT in cultured macrophages, possibly accounting for the accelerated wound healing observed in these mice.

Because macrophages have major immune-regulatory functions in tissue repair[55], we focused only on this cell type. Determining the local effects on macrophage population, we showed that Sitagliptin increased the number of M2 macrophages present at the skin wounding site. However, the increase in M2 in the WT mice did not result in increased tissue repair, indicating that M2 macrophages are not sufficient or always beneficial in tissue repair[56,57].

Investigating bone marrow-derived macrophage responses to TGFβ and LPS stimulation, the intrinsic differences in stress signaling varied between wild type and *Eng*$^{+/-}$ macrophages. Already at baseline conditions, pERK1/2 was increased in *Eng*$^{+/-}$ macrophages. Ras-ERK1/2 pathway activation is associated with being pro-cell survival[44], moreover, with pro-inflammatory effects[58], suggesting this could be the reason of prolonged inflammation in the *Eng*$^{+/-}$ mice.

Activation of the SMAD/AKT pathway is associated with polarization towards M2 macrophages[59,60]. However, in our macrophage culture addition of Sitagliptin in both non- and inflammatory conditions reduced total AKT and p-AKT expression dramatically, in both the WT and *Eng*$^{+/-}$ cells. Therefore the M2 polarization in our skin model is most likely AKT-independent. The PI3K-AKT pathway has also been reported to be involved in proliferation and importantly, inducing macrophage activation[61]. This provides a correlation of macrophage activation with DPP4 inhibition; decreasing AKT signaling which leads to a decrease in macrophage activation. AKT therefore may in part be responsible for the anti-inflammatory responses we observed *in vivo* and *in vitro*.

Besides a disturbed inflammatory response, we also report that *Eng*$^{+/-}$ mice displayed increased fibroblast presence, and also co-localized with increased AKT phosphorylation (as reported by Pericacho et al.[31]). DPP4 inhibition decreased pAKT, thereby increasing wound repair via fibroblast activity; thus possibly providing the mechanism of accelerated wound healing in our study. Overall, we conclude that the inflammatory response of macrophages is increased in endoglin heterozygous conditions, and the intracellular macrophage signaling response to DPP4 inhibition seems to be increased in *Eng*$^{+/-}$ macrophages. DPP4 inhibition is able to decrease inflammatory markers in vivo. We conclude that DPP4 inhibitor treatment is most likely only beneficial for dermal wound healing in *Eng*$^{+/-}$ conditions.

The inflammation and stress-related signaling aberrations found in *Eng*$^{+/-}$ macrophages highlight the complexity of the immunological defects present in HHT1. Whereas in this study we focused on macrophages, the effects of DPP4 inhibition on other immune cells and tissue cells is still largely unknown. For example, DPP4 inhibition was shown to increase re-epithelization in a diabetic model using Ob/Ob mice[54]. Therefore in future research it is important to keep in mind the varying effects between DPP4 inhibitors[62] and also the complexity of the signaling pathways and reactions. Furthermore the other cell types affected by endoglin heterozygosity or DPP4 inhibition, and involved in tissue repair are also to be considered, such as endothelial[63] and epidermal progenitor cells[64], keratinocytes and fibroblasts[30,38,65].

In conclusion, the results presented in this paper suggest an inhibitory effect of DPP4 inhibition on inflammation and a decrease of local cell stress/proliferation responses in endoglin haploinsufficiency context. These findings suggest that the mechanisms by which DPP4 inhibition is able to positively direct wound healing in *Eng*$^{+/-}$ mice is by decreasing the pro-inflammatory signaling in the macrophages and injured tissue. Further research should focus on finding a direct correlation between canonical/non-canonical TGFβ signaling and DPP4 inhibition, and could lead to revealing new mechanisms in the pathogenesis of HHT1.

Acknowledgements

This work was financially supported by the Netherlands Institute for Regenerative Medicine (NIRM, FES0908), the Dutch Heart Foundation (NHS2009B063), and by the Netherlands Cardiovascular Research Initiative: the Dutch Heart Foundation, Dutch Federation of University Medical Centres, the Netherlands Organization for Health Research and Development, and the Royal Netherlands Academy of Sciences (CVON-PHAEDRA consortium).

Conflict of interest

On behalf of all authors, the corresponding author states that there is no conflict of interest.

Author Contributions

M.G, I.E.H, W.B and C.D conceptualized the study set up and design. C.D, K.L, and K.K performed experiments. C.D wrote the manuscript. All authors reviewed the manuscript.

References

1. Portou, M.J., Baker, D., Abraham, D. & Tsui, J. The innate immune system, toll-like receptors and dermal wound healing: A review. *Vascular Pharmacology* **71**, 31-36 (2015).

2. Gurtner, G.C., Werner, S., Barrandon, Y. & Longaker, M.T. Wound repair and regeneration. *Nature* **453**, 314-321 (2008).

3. Grose, R. & Werner, S. Wound-healing studies in transgenic and knockout mice. *Mol Biotechnol* **28**, 147-166 (2004).

4. Nahrendorf, M., *et al.* The healing myocardium sequentially mobilizes two monocyte subsets with divergent and complementary functions. *The Journal of experimental medicine* **204**, 3037-3047 (2007).

5. Park, J.E. & Barbul, A. Understanding the role of immune regulation in wound healing. *American Journal of Surgery* **187**, 2-7 (2004).

6. Torsney, E., Charlton, R., Parums, D., Collis, M. & Arthur, H.M. Inducible expression of human endoglin during inflammation and wound healing in vivo. *Inflammation research : official journal of the European Histamine Research Society ... [et al.]* **51**, 464-470 (2002).

7. Neuzillet, C., *et al.* Targeting the TGFbeta pathway for cancer therapy. *Pharmacol Ther* **147**, 22-31 (2015).

8. Goumans, M.J., Zwijsen, A., Ten Dijke, P. & Bailly, S. Bone Morphogenetic Proteins in Vascular Homeostasis and Disease. *Cold Spring Harb Perspect Biol* (2017).

9. Goumans, M.J. & Ten Dijke, P. TGF-beta Signaling in Control of Cardiovascular Function. *Cold Spring Harb Perspect Biol* (2017).

10. Lebrin, F., *et al.* Endoglin promotes endothelial cell proliferation and TGF-beta/ALK1 signal transduction. *EMBO J* **23**, 4018-4028 (2004).

11. Lebrin, F., Deckers, M., Bertolino, P. & Ten Dijke, P. TGF-beta receptor function in the endothelium. *Cardiovascular research* **65**, 599-608 (2005).

12. Liu, Z., *et al.* ENDOGLIN Is Dispensable for Vasculogenesis, but Required for Vascular Endothelial Growth Factor-Induced Angiogenesis. *PLOS ONE* **9**(2014).

13. Goumans, M.-j., Liu, Z. & ten Dijke, P. TGF-β signaling in vascular biology and dysfunction. *Cell Research* **19**, 116-127 (2009).

14. Sanz-rodriguez, F., Blanco, F.J. & Botella, L.M. Hereditary Hemorrhagic Telangiectasia, a Vascular Dysplasia Affecting the TGF-. **4**, 66-78 (2006).

15. Torsney, E., *et al.* Mouse model for hereditary hemorrhagic telangiectasia has a generalized vascular abnormality. *Circulation* **107**, 1653-1657 (2003).

16. Jerkic, M., *et al.* Reduced angiogenic responses in adult Endoglin heterozygous mice. *Cardiovascular research* **69**, 845-854 (2006).

17. Rossi, E., *et al.* Endoglin regulates mural cell adhesion in the circulatory system. *Cellular and Molecular Life Sciences* **73**, 1715-1739 (2016).

18. van Laake, L.W., *et al.* Endoglin Has a Crucial Role in Blood Cell-Mediated Vascular Repair.

Circulation **114**, 2288-2297 (2006).

19. Post, S., *et al.* Impaired recruitment of HHT-1 mononuclear cells to the ischaemic heart is due to an altered CXCR4/CD26 balance. *Cardiovascular Research* **85**, 494-502 (2010).

20. Horuk, R. Chemokine receptors. *Cytokine Growth Factor Rev* **12**, 313-335 (2001).

21. Askari, A.T., *et al.* Effect of stromal-cell-derived factor 1 on stem-cell homing and tissue regeneration in ischaemic cardiomyopathy. *Lancet* **362**, 697-703 (2003).

22. Ceradini, D.J., *et al.* Progenitor cell trafficking is regulated by hypoxic gradients through HIF-1 induction of SDF-1. *Nature medicine* **10**, 858-864 (2004).

23. Lambeir, A.-M., Durinx, C., Scharpé, S. & De Meester, I. Dipeptidyl-peptidase IV from bench to bedside: an update on structural properties, functions, and clinical aspects of the enzyme DPP IV. *Critical reviews in clinical laboratory sciences* **40**, 209-294 (2003).

24. Röhrborn, D., Wronkowitz, N. & Eckel, J. DPP4 in diabetes. *Frontiers in Immunology* **6**, 1-20 (2015).

25. Sanz-Rodriguez, F., *et al.* Mutation analysis in Spanish patients with hereditary hemorrhagic telangiectasia: deficient endoglin up-regulation in activated monocytes. *Clinical chemistry* **50**, 2003-2011 (2004).

26. Guilhem, A., Malcus, C., Clarivet, B. & Plauchu, H. Immunological abnormalities associated with hereditary haemorrhagic telangiectasia. 351-362 (2013).

27. Peter, M.R., *et al.* Impaired Resolution of Inflammation in the Endoglin Heterozygous Mouse Model of Chronic Colitis. *Mediators of Inflammation* **2014**, 1-13 (2014).

28. Ojeda-Fernández, L., *et al.* Mice Lacking Endoglin in Macrophages Show an Impaired Immune Response. *PLOS Genetics* **12**, e1005935 (2016).

29. ten Dijke, P., Goumans, M.-J. & Pardali, E. Endoglin in angiogenesis and vascular diseases. *Angiogenesis* **11**, 79-89 (2008).

30. Pérez-Gómez, E., *et al.* Impaired wound repair in adult endoglin heterozygous mice associated with lower NO bioavailability. *The Journal of investigative dermatology* **134**, 247-255 (2014).

31. Pericacho, M., *et al.* Endoglin Haploinsufficiency Promotes Fibroblast Accumulation during Wound Healing through Akt Activation. *PLoS ONE* **8**, e54687 (2013).

32. Dutta, P. & Nahrendorf, M. Monocytes in Myocardial Infarction. *Arteriosclerosis, Thrombosis, and Vascular Biology* **35**, 1066-1070 (2015).

33. Yanez, D.A., Lacher, R.K., Vidyarthi, A. & Colegio, O.R. The role of macrophages in skin homeostasis. *Pflugers Arch* **469**, 455-463 (2017).

34. Dingenouts, C.K.E., *et al.* Inhibiting DPP4 in a mouse model of HHT1 results in a shift towards regenerative macrophages and reduces fibrosis after myocardial infarction. *PLoS One* **12**, e0189805 (2017).

35. Wang, X., Ge, J., Tredget, E.E. & Wu, Y. The mouse excisional wound splinting model, including applications for stem cell transplantation. *Nature protocols* **8**, 302-309 (2013).

36. Kurakula, K., Hamers, A.A., van Loenen, P. & de Vries, C.J. 6-Mercaptopurine reduces

cytokine and Muc5ac expression involving inhibition of NFkappaB activation in airway epithelial cells. *Respir Res* **16**, 73 (2015).

37. Bainbridge, P. Wound healing and the role of fibroblasts. *J Wound Care* **22**, 407-408, 410-412 (2013).

38. Thielitz, A.*, et al.* Inhibitors of dipeptidyl peptidase IV-like activity mediate antifibrotic effects in normal and keloid-derived skin fibroblasts. *J Invest Dermatol* **128**, 855-866 (2008).

39. Shi, S., Koya, D. & Kanasaki, K. Dipeptidyl peptidase-4 and kidney fibrosis in diabetes. *Fibrogenesis & tissue repair* **9**, 1 (2016).

40. Gangadharan Komala, M., Gross, S., Zaky, A., Pollock, C. & Panchapakesan, U. Saxagliptin reduces renal tubulointerstitial inflammation, hypertrophy and fibrosis in diabetes. *Nephrology*, n/a-n/a (2015).

41. Kaji, K.*, et al.* Dipeptidyl peptidase-4 inhibitor attenuates hepatic fibrosis via suppression of activated hepatic stellate cell in rats. *Journal of Gastroenterology* **49**, 481-491 (2014).

42. Letarte, M.*, et al.* Reduced endothelial secretion and plasma levels of transforming growth factor-beta1 in patients with hereditary hemorrhagic telangiectasia type 1. *Cardiovascular research* **68**, 155-164 (2005).

43. Ervinna, N.*, et al.* Anagliptin, a DPP-4 Inhibitor, Suppresses Proliferation of Vascular Smooth Muscles and Monocyte Inflammatory Reaction and Attenuates Atherosclerosis in Male apo E-Deficient Mice. *Endocrinology* **154**, 1260-1270 (2013).

44. Monick, M.M.*, et al.* Constitutive ERK MAPK activity regulates macrophage ATP production and mitochondrial integrity. *Journal of immunology (Baltimore, Md. : 1950)* **180**, 7485-7496 (2008).

45. Inoue, M.*, et al.* SCRG1 suppresses LPS-induced CCL22 production through ERK1/2 activation in mouse macrophage Raw264.7 cells. *Mol Med Rep* **15**, 4069-4076 (2017).

46. Rao, K.M. MAP kinase activation in macrophages. *J Leukoc Biol* **69**, 3-10 (2001).

47. Deshmane, S.L., Kremlev, S., Amini, S. & Sawaya, B.E. Monocyte chemoattractant protein-1 (MCP-1): an overview. *J Interferon Cytokine Res* **29**, 313-326 (2009).

48. Hernandez-Quintero, M., Kuri-Harcuch, W., Gonzalez Robles, A. & Castro-Munozledo, F. Interleukin-6 promotes human epidermal keratinocyte proliferation and keratin cytoskeleton reorganization in culture. *Cell Tissue Res* **325**, 77-90 (2006).

49. Ghazizadeh, M. Essential role of IL-6 signaling pathway in keloid pathogenesis. *J Nippon Med Sch* **74**, 11-22 (2007).

50. Fernando, M.R., Reyes, J.L., Iannuzzi, J., Leung, G. & McKay, D.M. The pro-inflammatory cytokine, interleukin-6, enhances the polarization of alternatively activated macrophages. *PLoS One* **9**, e94188 (2014).

51. Sanmarco, L.M.*, et al.* IL-6 promotes M2 macrophage polarization by modulating purinergic signaling and regulates the lethal release of nitric oxide during Trypanosoma cruzi infection. *Biochim Biophys Acta* **1863**, 857-869 (2017).

52. Scharpfenecker, M., Floot, B., Russell, N.S. & Stewart, F.A. The TGF-beta co-receptor endoglin regulates macrophage infiltration and cytokine production in the irradiated mouse kidney. *Radiother Oncol* **105**, 313-320 (2012).

53. Adli, M., Merkhofer, E., Cogswell, P. & Baldwin, A.S. IKKalpha and IKKbeta each function to regulate NF-kappaB activation in the TNF-induced/canonical pathway. *PLoS One* **5**, e9428 (2010).

54. Schürmann, C., *et al.* The dipeptidyl peptidase-4 inhibitor linagliptin attenuates inflammation and accelerates epithelialization in wounds of diabetic ob/ob mice. *The Journal of pharmacology and experimental therapeutics* **342**, 71-80 (2012).

55. Snyder, R.J., *et al.* Macrophages: A review of their role in wound healing and their therapeutic use. *Wound Repair and Regeneration* **24**, 613-629 (2016).

56. van den Bosch, T.P., *et al.* CD16+ Monocytes and Skewed Macrophage Polarization toward M2 Type Hallmark Heart Transplant Acute Cellular Rejection. *Front Immunol* **8**, 346 (2017).

57. Jetten, N., *et al.* Wound administration of M2-polarized macrophages does not improve murine cutaneous healing responses. *PLoS ONE* **9**, 1-9 (2014).

58. Jung, Y.C., *et al.* Anti-inflammatory effects of galangin on lipopolysaccharide-activated macrophages via ERK and NF-kappaB pathway regulation. *Immunopharmacol Immunotoxicol* **36**, 426-432 (2014).

59. Tian, Y., Piras, B.A., Kron, I.L., French, B.A. & Yang, Z. Adenosine 2B Receptor Activation Reduces Myocardial Reperfusion Injury by Promoting Anti-Inflammatory Macrophages Differentiation via PI3K/Akt Pathway. *Oxid Med Cell Longev* **2015**, 585297 (2015).

60. Barrett, J.P., Minogue, A.M., Falvey, A. & Lynch, M.A. Involvement of IGF-1 and Akt in M1/M2 activation state in bone marrow-derived macrophages. *Exp Cell Res* **335**, 258-268 (2015).

61. Covarrubias, A.J., Aksoylar, H.I. & Horng, T. Control of macrophage metabolism and activation by mTOR and Akt signaling. **27**, 286-296 (2015).

62. Shi, S., Kanasaki, K. & Koya, D. Linagliptin but not Sitagliptin inhibited transforming growth factor-β2-induced endothelial DPP-4 activity and the endothelial-mesenchymal transition. *Biochemical and Biophysical Research Communications* **471**, 184-190 (2016).

63. Um, J., *et al.* Substance P enhances EPC mobilization for accelerated wound healing. *Wound Repair Regen* **24**, 402-410 (2016).

64. Guo, R., *et al.* Stromal cell-derived factor 1 (SDF-1) accelerated skin wound healing by promoting the migration and proliferation of epidermal stem cells. *In vitro cellular & developmental biology. Animal* **1**(2015).

65. Rinkevich, Y., *et al.* Skin fibrosis. Identification and isolation of a dermal lineage with intrinsic fibrogenic potential. *Science* **348**, aaa2151 (2015).

Supplementary figures

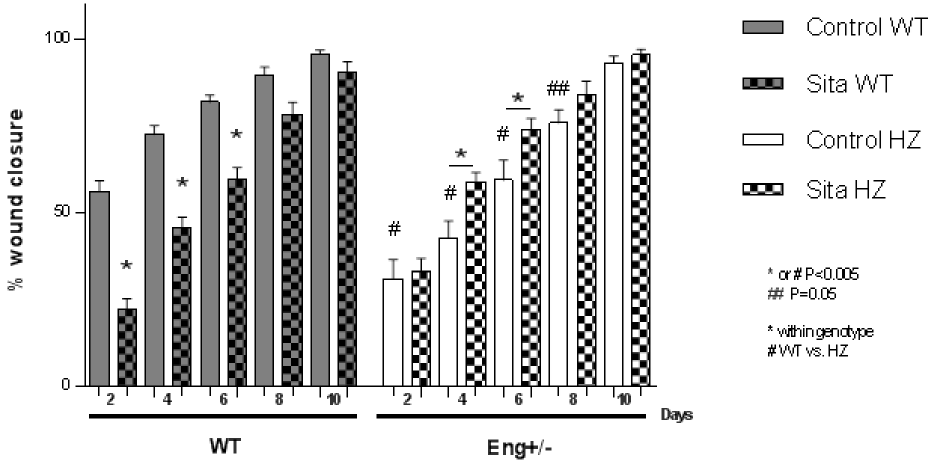

Supplementary Figure 1. Sitagliptin enhances tissue repair in Eng+/- mice. A) Quantification of wound closure over time. Sitagliptin delays tissue repair in wild type mice. Sitagliptin enhances tissue repair in Eng+/- mice. WT = wild type mice, HZ = Endoglin heterozygous mice.

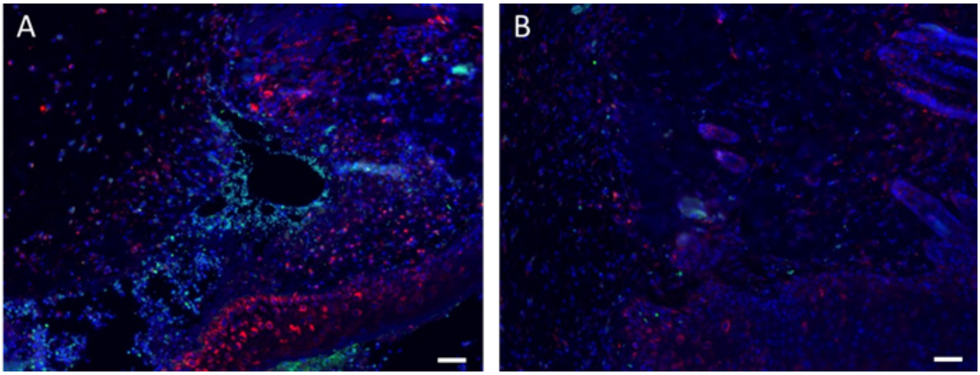

Supplementary Figure 2. Example of p-p65 (NFκB complex subunit) and pIKKα/β (regulators of NFκB activation) staining.
A. Day 5 post-wounding, Eng+/- skin sample control treated. P-p65 in green, pIKKα/β in red, DAPI in blue. Scale bar = 50µm. B. Day 5 post-wounding , Eng+/- skin sample Sitagliptin treated. P-p65 in green, pIKKα/β in red, DAPI in blue. Scale bar = 50µm.

6

Endoglin deficiency alters the epicardial response following myocardial infarction

Calinda K.E. Dingenouts[1*&], Asja T. Moerkamp[1*], Kirsten Lodder[1], Tessa van Herwaarden[1], Anna M. D. Végh[1], Esther Dronkers[1], Boudewijn P.T. Kruithof[1], Karien C. Wiesmeijer[1], Janita A. Maring[1], Helen M. Arthur[2], Marie-José Goumans[1#†], Anke M. Smits[1#†]

1. Department of Cell and Chemical Biology, Leiden University Medical Center, Leiden, the Netherlands.
2. Institute of Genetic Medicine, Newcastle University, International Centre for Life, Newcastle upon Tyne, United Kingdom.

*/# Both authors contributed equally

&Current address: Department of Infectious Diseases, Leiden University Medical Center, Leiden, the Netherlands.

Manuscript in submission

Introduction

The epicardium is a dynamic epithelial layer covering the surface of the heart. It plays a critical role in heart formation by differentiating into cardiovascular cell types and providing paracrine factors to the developing myocardium [9]. In the adult heart, upon myocardial infarction (MI) the dormant epicardial layer is reactivated and supports the underlying myocardium during repair [24, 34, 40]. The epicardial response to injury includes upregulation of a developmental gene program, such as re-expression of Wilms' tumour 1 (WT1), proliferation, thickening of the epicardial layer and covering of the damaged myocardium [15, 43, 44]. Furthermore, the epicardial cells undergo epithelial to mesenchymal transition (EMT), thereby forming epicardial-derived cells (EPDCs) that contribute to endogenous repair [34, 40]. Decreased expansion of the epicardial layer and minimal collagen deposition in the (sub)epicardial region, suggesting deficient EMT, result in ventricular dilatation and impaired cardiac function [13]. As such, epicardial EMT is important for a 'healthy' epicardial post-injury response.

The transforming growth factor beta (TGFβ) signaling pathway plays a key role in epicardial EMT. *In vitro*, stimulation of EPDCs with TGFβ results in loss of their epithelial character and induces transition into a mesenchymal phenotype [5, 35]. TGFβ exerts its effect via phosphorylation of the transcription factors small mothers against decapentaplegic 2/3 (SMAD2/3) or SMAD1/5 [18]. These downstream mediators of the TGFβ pathway are upregulated in the epicardial region upon MI [44]. The TGFβ co-receptor endoglin plays an important role in defining the balance between these two TGFβ-responsive pathways resulting in different behavioral outcomes [11, 19]. Mice heterozygous for the TGFβ co-receptor endoglin (*Eng+/-*) display a reduced cardiac function post-MI suggesting that endoglin is important in the cardiac response to injury [26]. Endoglin is well known for its expression in activated endothelial cells and its essential role during angiogenesis [11]. Endoglin knockout embryos die around embryonic day 10.5 due to vascular abnormalities [3, 7, 30]. However, it is becoming clear that the role of endoglin goes beyond maintenance of vascular homeostasis and, for example, also affects the immune response to injury [12]. We previously reported that endoglin is expressed by EPDCs [35]. Furthermore, Bollini *et al.* (2014) showed an increased number of WT1+/endoglin+ EPDCs upon induction of MI [6]. This suggests that upregulation of endoglin in the active epicardium is part of the cardiac injury response.

Due to the important role of EPDCs following cardiac injury [34, 40], the epicardium is a tantalizing therapeutic target for cardiac regeneration. Therefore, a thorough understanding of epicardial behavior is paramount to appreciate its potential in cardiac repair. Given the deteriorated heart function following MI in *Eng+/-* mice and the pivotal role of TGFβ signaling in epicardial EMT, we investigated if endoglin contributes to the epicardial response to injury.

In this study, we analyzed the composition and the behavior of the epicardial layer at different time-points post-MI. Our data suggest that the epicardial injury response of thickening and coverage of the (diseased) myocardium with a WT1+ layer is aberrant upon endoglin heterozygosity. In the first days after MI, thickening of the epicardium in *Eng+/-* mice is less pronounced compared to wild type (wt) hearts. In contrast, at 14 days post-MI, a significantly thicker epicardial layer is observed in *Eng+/-* animals which coincides with a thinner ventricular wall. We show that these observations are not due to a difference in the epicardium at baseline and occur independently of extra-cardiac contributions from the circulation. Moreover, we found that the epicardial response can be influenced by systemic delivery of Diprotin A, an inhibitor of CD26/dipeptidyl peptidase 4 (DPP4). Altogether, we show that endoglin is important for the post-injury response, and suggest an important role of this TGFβ co-receptor in relation to epicardial behavior.

Methods

Animals

Experiments and analyses were conducted on male and female endoglin wild type (wt) and endoglin heterozygous (*Eng*+/-) mice [3] which were maintained on a C57BL/6Jlco background (Charles River). All mouse experiments were approved by the regulatory authorities of Leiden University (The Netherlands) and were in compliance with the guidelines from Directive 2010/63/EU of the European Parliament on the protection of animals used for scientific purposes.

Induction of myocardial infarction in mice and Diprotin A treatment

Myocardial infarction (MI) was experimentally induced in male mice as described before [41]. Briefly, mice were anesthetized with isoflurane (1.5-2.5%), orally intubated and ventilated, after which the left anterior descending (LAD) coronary artery was permanently ligated by a suture. During the first 5 days post-MI, the mice were randomized and treated daily with either 100 µl distilled water (MQ) or 100 µl Diprotin A (50 µM, DipA, Bachem) via intraperitoneal injection. Mice were euthanized at 4 or 14 days after MI using carbon-dioxide.

Immunofluorescent staining

Hearts were fixed overnight at 4°C in 4% paraformaldehyde, washed with phosphate-buffered saline (PBS) followed by dehydration to xylene and embedded in paraffin. Six µm thick sections were mounted onto coated glass slides (VWR SuperFrost Plus microscope slides; Klinipath), deparaffinized and rehydrated to PBS. Antigen retrieval was performed as previously described [29]. Primary antibodies, incubated overnight at 4°C, included: anti-pSMAD1/5/9 (rabbit; dilution 1:1000 using Tyramide Signal Amplification [15]; Cell Signaling), anti-pSMAD2 (rabbit; dilution 1:200; Cell Signaling), anti-WT1 (rabbit, dilution 1:100, Abcam), anti-MAC3 (rat, dilution 1:200, BD Biosciences), anti-αSMA (rabbit, dilution 1:500, Abcam), anti-cTnI (goat, dilution 1:1000, HyTest), anti-PECAM1 (mouse, dilution 1:800, Santa Cruz) and anti-Ki67 (rabbit, dilution 1:100, Millipore). Fluorescently-labelled secondary antibodies (Invitrogen) were incubated for 1.5 hour at a 1:250 dilution. The slides were mounted with Prolong Gold-DAPI Antifade (Invitrogen) reagent.

Staining of fibrotic tissue was performed using a Picrosirius Red (PSR) collagen staining which includes deparaffinization, 1 h incubation with PSR solution, washing in acidified water and mounting with Entellan (Merck) reagent. All stainings were scanned at 40x magnification with the Pannoramic slide scanner and analyzed using CaseViewer 2.0 (3D Histech).

Morphometry

Heart sections were taken at approximately 300 µm intervals along the transverse axis of the heart. All measurements are given as average of at least three levels along the infarct area (unless otherwise stated). Infarct size was determined in PSR stained sections by calculating the percentage of infarct area of the total left ventricular area. Thickness of the ventricular wall was measured in the PSR stained sections. Measurements were taken at two separate levels along the infarct area, and given as the average of eight measurements per level.

The epicardial border zone was defined as the epicardial layer lining the 'healthy' myocardium bordering the infarct area at both sides (see also Figure 1D-E). This region was determined to be around 600 µm in length (based on [32]). The epicardial border zone included the outer epicardium (single-cell layer that surrounds the heart) and subepicardial layer (cell layer(s) between myocardium and outer epicardium), while the pericardium was excluded from analysis. Analyses of the epicardial border zone are presented as the average of both border zones.

Epicardial thickness was calculated as the average of at least four measurements per epicardial border zone (600 µm in length) or remote epicardial layer. The total cell content of the epicardial border zone was counted using DAPI staining as the total of nuclei per µm cardiac outline. Positive cells (WT1, MAC3 and Ki67) within the epicardial border zone are depicted as the percentage of total number of nuclei. Finally, pSMAD levels were quantified as the area fluorescent signal corrected for the number of nuclei within that region.

Coverage of the (injured) myocardium with a WT1+ epicardial layer was measured using the WT1 stained sections, and was quantified as the percentage WT1+ outline of the total cardiac circumference.

Culturing mouse hearts

Wt and *Eng+/-* female mouse hearts were cultured in the miniature tissue culture system [31] as previously described [25] with the following modifications. The inflow needle of the perfusion chamber was inserted in the aorta of the isolated intact heart and ligated with suture. The outflow needle was replaced with a 14 Gauge Blunt Tip Needle which allowed the medium to exit the perfusion chamber. Using a speed of 1100 µl/min, flow was introduced through the aorta directing the medium into the coronary circulation. The medium exited the heart via the right atrium and recirculated to the reservoir. After 7 days of culture the hearts were isolated and fixed overnight in 4% PFA at 4°C.

Isolation, culture and migration of human EPDCs

Adult human atrial samples (auricles) were collected as surgical waste during cardiac surgery and under general informed consent. Handling of human heart tissues was carried out according to the official guidelines of the Leiden University Medical Center and approved by the local Medical Ethics Committee. This research conforms to the Declaration of Helsinki.

EPDCs were isolated, cultured and a scratch assay was performed as previously described [35]. In short, the adult epicardium was separated from the underlying myocardium. Epicardial tissue was cut into pieces and treated with Trypsin/EDTA (Serva and USH products) at 37^{0}C. A single cell suspension was obtained by passing the samples through a series of syringes. EPDCs were plated on 0.1% gelatin (Sigma) coated culture dishes in a 1:1 mixture of Dulbecco's modified Eagle's medium (DMEM-glucose low; Invitrogen) and Medium 199 (M199; Invitrogen) supplemented with 10% heat-inactivated fetal calf serum (Hi-FCS; Gibco), 100 U/ml penicillin/streptomycin (Gibco) and 10 µM SB431542 (SB; Tocris Bioscience). Scratch assays were performed with mesenchymal (spindle) EPDCs which were obtained by stimulating EPDCs with 1 ng/ml TGFβ3. Spindle EPDCs were split and grown to confluency upon which the scratch was placed. The cells were monitored for 12 hours and the percentage gap closure was measured using Matlab (version 2016a).

Statistics

Graphs are represented as mean ± SD. Samples were compared using an unpaired Student's t-test or one-way ANOVA testing for difference between multiple groups. Significance was assumed when $p<0.05$. GraphPad Prism (Version 6) was used for statistical analysis.

Results

Aberrant TGFβ signaling in *Eng+/-* epicardial layer

Since endoglin heterozygosity impairs cardiac recovery after MI and endoglin is expressed by EPDCs [35], we questioned the role of endoglin in the epicardial response post-MI. A schematic outline of the experiment together with an overview of the factors measured is presented in Figure 1A.

Given that endoglin defines the balance between the TGFβ-responsive pathways (pSMAD2/3 and pSMAD1/5) [18, 20], we performed immunofluorescence staining for pSMAD1/5/9 and pSMAD2. Both pathways are active in the epicardial layer post-MI (Figure 1B). However, we observed an increase in pSMAD1/5/9 levels in *Eng+/-* versus wt mice, while no differences were observed in pSMAD2 (Figure 1C). This indicates that endoglin heterozygosity results in altered signaling within the epicardial layer.

Epicardial thickening and activation is altered in *Eng+/-* mice at 4 days post-MI

Given the disturbed TGFβ signaling upon endoglin heterozygosity, we questioned whether this results in a difference in epicardial phenotype. First, we analyzed the epicardium and myocardium of adult non-MI mice in transverse heart sections and observed no aberrations in *Eng+/-* compared to wt animals (data not shown). Epicardial thickening upon cardiac injury has been described to occur in the entire epicardium, but is most pronounced near the infarct area [43, 44]. Therefore, we focused our analysis on the epicardium and subepicardium that lines the myocardium directly bordering the ischemic area. This region is represented as the epicardial border zone (schematically pictured in Figure 1D-E).

Four days post-injury, wt and *Eng+/-* mice showed no difference in infarct characteristics, including infarct size and infarct outline (Supplementary Figure 1A-C). However, when investigating the epicardial layer in more detail, we observed that the epicardial border zone was significantly thinner in *Eng+/-* mice (Figure 1F; wt: 22.24±3.01 *Eng+/-*: 18.77±3.47). This phenomenon was not observed at the remote area lining the right ventricle, although wt

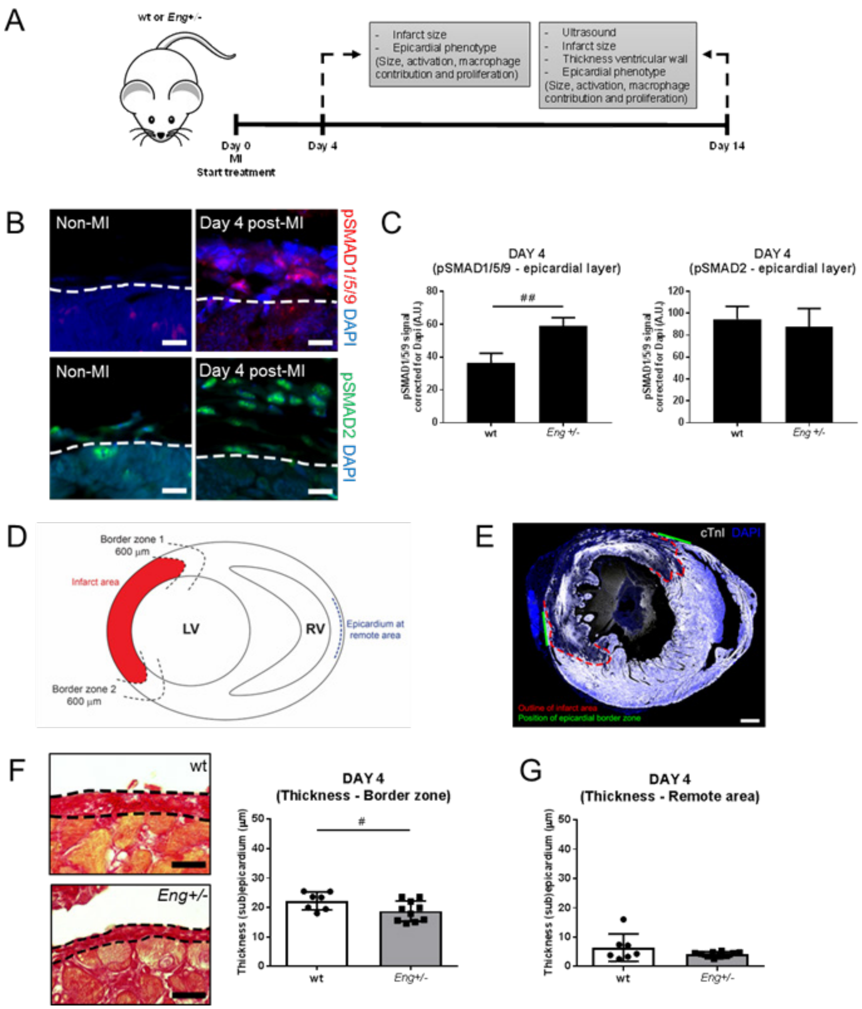

Figure 1. Aberrant TGFβ signaling and epicardial thickening in Eng+/- at 4 days post-MI. A. Overview of experiment and measured entities. Wt or Eng+/- mice were sacrificed at 4 and 14 days after the induction of MI. B. pSMAD1/5/9 and pSMAD2 are upregulated in the epicardial layer upon MI. The dashed line represents the border between myocardium and epicardium. Scale bars: 10 µm. C. Quantification of immunofluorescent stainings suggest a higher staining intensity for pSMAD1/5/9 in the epicardial layer (outlined) of Eng+/- compared to wt mice. (n = 3-4 mice for each group). Scale bars: 20 µm. D. Schematic representation of transverse section of the heart. Depicted is the infarct area (red) with at both sides a border zone. The border zone has an estimated width of 600 µm and represents 'healthy' myocardium lining the infarct area. The remote area is at the right ventricle, opposite to the infarct. E. Example of transverse section of the infarcted heart. The red line represents the border between infarcted and 'healthy' myocardium. The green lines show the position of the investigated epicardial layer at both border zones with a length of 600 µm. Scale bar: 500 µm. F. In PSR stainings, the outer collagen layer at the border zone (outlined; scale bars: 20 µm) is thinner in Eng+/- mice (n = 7-10 mice for each group). G. The thickness of the epicardial layer at a remote area is equal between Eng+/- and wt hearts (n = 7-10 mice for each group). Data information: #: $p<0.05$ and # #: $p<0.01$

mice displayed a larger variation in thickness (Figure 1G).

The thinner epicardial border zone after induction of MI can be explained by the presence of fewer cells within this region in *Eng*+/- compared to wt mice (Figure 2A-B). Interestingly, not only the border zone, but the entire epicardial layer contains less cells in *Eng*+/- hearts (Figure 2C). A difference in cell number within the epicardial region could be the result of a defect in cell proliferation. Therefore, we determined the number of cycling cells by performing a Ki67 staining (Figure 2D). However, no difference in the percentage of Ki67+ cells within the epicardial border zone in *Eng*+/- compared to wt mice was observed (Figure 2E).

The expression of WT1 in the epicardium is considered to be one of the first steps in epicardial activation post-injury [14]. Although the *Eng*+/- epicardial border zone contains a reduced number of total cells, we observed a higher percentage of WT1+ cells within this region compared to the wt border zone (Figure 2F-G). Since epicardial activation occurs organ-wide, including the remote area, we quantified the presence of WT1+ cells within the entire epicardial layer. Consistent with the border zone, the percentage of WT1+ cells throughout the epicardial layer was significantly higher in *Eng*+/- mice compared to wt animals (Figure 2H). This difference in WT1 is not related to the infarct size, indicating that it does not result from a difference in cardiac damage (data not shown). In addition, we observed no difference in the expression of the epicardial activation markers WT1 and Transcription factor 21 (TCF21; [1, 8]) in non-infarcted wt and *Eng*+/- hearts (data not shown). This suggests that the increased percentage of WT1+ cells in *Eng*+/- mice at 4 days post-MI is not caused by a difference in epicardial activity at baseline.

In summary, the thinner epicardial layer in *Eng*+/- mice at 4 days post-MI is the result of a lower number of cells within the (sub)epicardial space. Our data suggest no difference in proliferation (at 4 days post-MI) and endoglin heterozygosity does not lead to an aberrant epicardial and myocardial phenotype at baseline. This suggests that the difference in the epicardium between wt and *Eng*+/- mice is directly caused by the induced injury and its related processes. Furthermore, a higher percentage of WT1+ cells indicates a difference in composition and activation of the *Eng*+/- epicardial layer.

Epicardial phenotype in *Eng*+/- mice is independent of extra-cardiac cell contributions

We further investigated the contribution of circulating cells to the phenotype of the (sub) epicardium in *Eng*+/- and wt mice. The subepicardial space is known to harbor immune cells [16, 21]. Zhou *et al.* reported infiltration of monocytes into the epicardial layer following MI [44]. We previously observed that *Eng*+/- mononuclear cells have a reduced ability to migrate towards the infarct area [26, 38]. Therefore, the presence of immune-reactive cells, as an extra-cardiac derived cell source, could contribute to a difference in total epicardial cell count. Macrophages are the major cell type invading the heart upon MI [27]. We analyzed the number of macrophages in the epicardial border zone by staining for MAC3 (LAMP2/CD107b). There is no overlap between WT1 and MAC3 expression, indicating that the WT1+ cells are not macrophages (Figure 3A). In addition, at 4 days post-MI we observed no difference in the percentage of macrophages within the epicardial border zone (Figure 3B) suggesting that the presence of macrophages is not the cause of a decreased presence of (sub) epicardial cells within the *Eng*+/- epicardial border zone compared to wt.

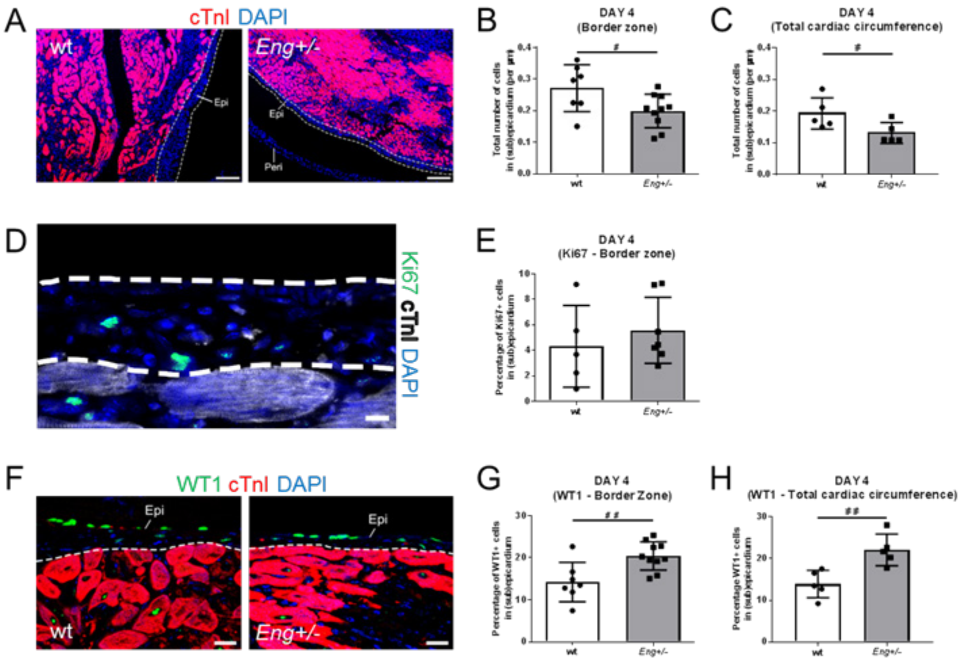

Figure 2. Altered composition of the Eng+/- epicardial layer. A. Cardiac troponin I (cTnI)/DAPI immunofluorescence stainings show the wt and Eng+/- epicardial border zone which are located in between the dashed lines. Epi: (sub)epicardium, Peri: pericardium. Scale bar: 100 µm. B,C. The number of cells was quantified for the epicardial layer lining B. the border zone (n = 7-10 mice for each group) and C. total cardiac circumference (n = 5 mice for each group). D,E The percentage of Ki67+ cells within the epicardial border zone is equal between Eng+/- and wt mice (n = 5-7 mice for each group). Scale bar: 10 µm. F-H. WT1 immunofluorescence staining of the wt and Eng+/- epicardial border zone. In F. the dashed line represents the border between myocardium and (sub)epicardium. Scale bar: 20 µm. Epi: (sub)epicardium, Peri: pericardium. In Eng+/- mice, a higher percentage of epicardial cells is positive for WT1 compared to wt animals in both G. the epicardial border zone (n = 7-10 mice for each group) and H. the entire epicardial layer (n = 5 mice for each group). Data information: #: p<0.05 and # #: p<0.01

To investigate the extra-cardiac cell contribution in more detail, we analyzed thickening of the epicardium in the absence of circulating cells. We cultured wt and *Eng+/-* hearts *ex vivo* in a continuous flow of culture medium using a novel miniature tissue culture system [25, 31]. As a result of the *ex vivo* culture conditions, the epicardial layer is activated and responds by becoming thicker. Interestingly, in *Eng+/-* hearts the thickening of the epicardial layer was significantly less pronounced as compared to wt (Figure 3C-D). This indicates that a thinner epicardial layer in *Eng+/-* mice occurs independently of extra-cardiac cell contributions from the circulation.

Coverage of the infarcted heart with a WT1+ epicardial layer is altered in *Eng+/-* mice at 4 days post-MI

The organ-wide re-expression of WT1 in the epicardial layer is a spatio-temporal dynamic process, peaking between day 1 and 5 post-MI [43, 44]. Interestingly, at day 4 post-MI, a

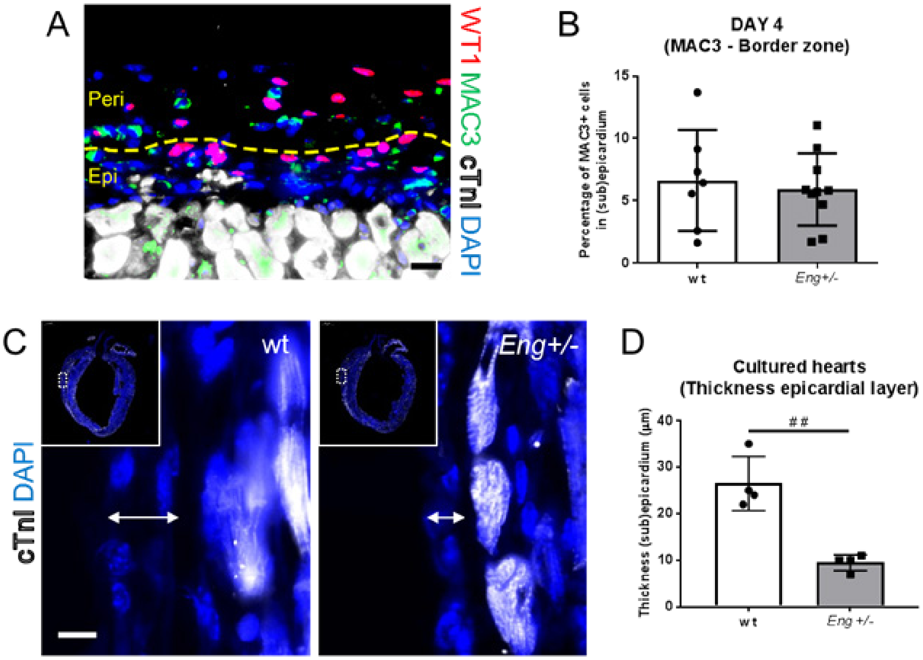

Figure 3. Epicardial phenotype in Eng+/- mice is independent of extra-cardiac cell contributions. A. Immunofluorescence staining shows that there is no overlap between WT1+ and MAC3+ cells in the epicardial border zone. The dashed line represents the border between (sub)epicardium and pericardium, Epi: (sub)epicardium, Peri: pericardium. Scale bar: 10 µm. B. Quantification of MAC3+ cells in the (sub)epicardium. No difference was observed in the percentage of MAC3+ cells within the epicardial border zone between wt or Eng+/- hearts (n = 7-10 mice for each group). C. Longitudinal section of a wt and Eng+/- cultured heart highlighting the epicardial layer (white arrows). cTnI=white, DAPI=blue. Scale bar: 10 µm. D. The thickness of the epicardial layer as measured in sections of cultured hearts of wt and Eng+/- mice (n = 4 mice for each group). Data information: # #: p<0.01

larger part of the cardiac circumference was covered by a WT1+ epicardial layer in *Eng+/-* compared to wt mice (Figure 4A-B). This difference in WT1 coverage is not related to the infarct size (data not shown). We questioned whether this altered coverage could result from a difference in migration rate. Therefore we modulated endoglin expression in EPDCs and performed an *in vitro* scratch assay. Strikingly, upon endoglin knockdown, epicardial cells migrate significantly faster (Figure 4C). Overall, these data suggest altered epicardial behavior upon endoglin heterozygosity, including increased migration and coverage of the infarcted heart with a WT1+ epicardial layer.

Thicker epicardial layer in *Eng+/-* mice at day 14 post-MI

In contrast to day 4, at 14 days post-MI we observed a significantly thicker epicardial layer at both the border zone (Figure 5A) and the remote area (Figure 5B) in *Eng+/-* compared to wt mice. In addition, the *Eng+/-* epicardial border zone contained more cells (Figure 5C). Interestingly, wt animals displayed a decrease in the size of the epicardial border zone from day 4 to day 14 post-MI (from ±23 µm to ±17 µm). In contrast, in *Eng+/-* mice the thickness

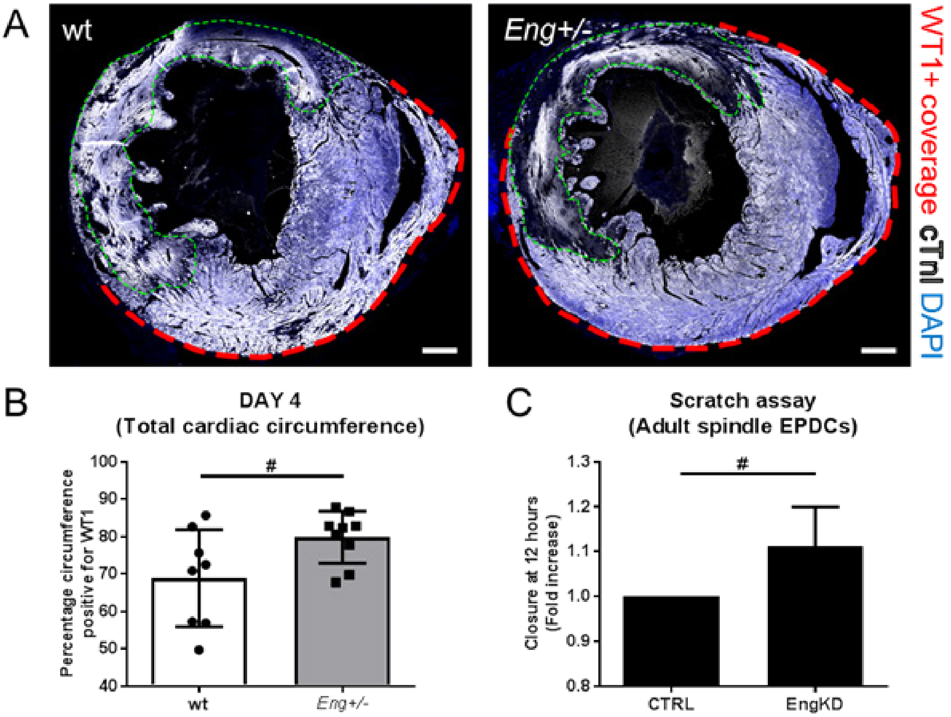

Figure 4. Coverage of the infarcted heart with a WT1+ epicardial layer is altered in Eng+/- mice at 4 days post-MI. A. The pattern of activation of the epicardial layer at day 4 is represented by the percentage of cardiac circumference covered by a WT1+ epicardial layer. The infarct is outlined in green and the epicardial layer positive for WT1 is marked by a red dotted line. Scale bars: 500 µm. B. In Eng+/- mice, a higher percentage of the circumference is positive for WT1 (n = 8-9 mice for each group). C. Upon endoglin knockdown (KD) human adult EPDCs migrate faster in a scratch assay (n = 5 measurements). Data information: #: p<0.05

of the epicardial layer continues to increase over time (from ±19 µm to ±26 µm) suggesting a delay in epicardial thickening upon MI.

As a potential underlying cause of a thicker epicardial layer in *Eng+/-* mice, differences in the degree of activation (WT1 expression) and proliferation were studied. At day 14 post-MI, the entire cardiac circumference was covered with a WT1+ epicardial layer with no difference between *Eng+/-* and wt mice (data not shown). Moreover, we observed no difference in the presence of WT1+ (Figure 5D) or Ki67+ (Figure 5E) cells within the epicardial border zone. This suggests that epicardial activation and cell proliferation are not aberrant at 14 days post-MI upon endoglin heterozygosity.

It was previously shown that the clearance of inflammatory cells is impaired in *Eng+/-* mice [37]. Therefore we analyzed the presence of MAC3+ cells within the epicardial region. Compared to day 4, the total number of MAC3+ cells in the epicardial border zone in both groups is low (from ±6 percent at day 4 to ±2 percent at day 14). Furthermore, the percentage of MAC3+ cells within the epicardial border zone was equal between wt and *Eng+/-* animals (Figure 5F), showing that there was no defect in clearance of macrophages from the epicardial border zone.

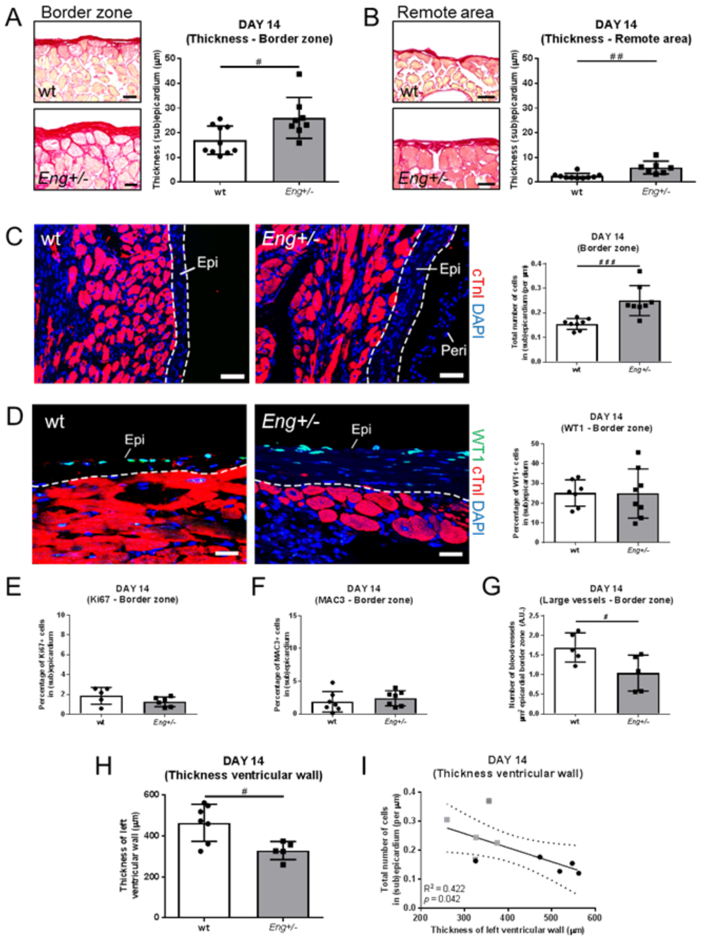

Figure 5. Delayed epicardial thickening in Eng+/- mice at day 14 post-MI is related to thinner ventricular wall. A-C. The collagen layer (representing the epicardial layer) is thicker in Eng+/- animals (Scale bar: 20µm) both at A. the border zone and B. a remote region. C. The epicardial border zone of Eng+/- mice contains more cells. The dashed lines outline the epicardial layer (n = 7-10 mice for each group). Scale bar: 50µm. D. The percentage of WT1 positive cells within the epicardial border zone is equal between wt and Eng+/- mice. The dashed lines indicate the boundary between myocardium and (sub)epicardium (n = 7-8 mice for each group). Scale bar: 20µm. E,F. The percentage of E. Ki67+ (n = 5-6 mice for each group) and F. MAC3+ cells is equal between wt and Eng+/- mice in the epicardial border zone (n = 7 mice for each group). G. Number of blood vessels per µm2 epicardial border zone (A.U.) at day 14 post-MI. Eng+/- mice have a lower density of large blood vessels compared to wt (n = 5 mice for each group). H. Ventricular wall thickness (µm). At day 14 post-MI, the left ventricular wall is thinner in Eng+/- compared to wt animals (n = 5-7 mice for each group). I. Correlation of the total number of cells in (sub) epicardium (per µm) to the thickness of the left ventricular wall (µm). A negative correlation was observed between the total number of cells within the epicardial border zone and the thickness of the left ventricular wall. Eng+/- mice are depicted in grey/square data points (n = 5 mice for each group). Data information: Epi: (sub)epicardium, Peri: pericardium and #: p<0.05, # #: p<0.01 and # # #: p<0.005

Since the epicardium develops in close relation to the coronary vasculature [28] and endoglin plays an important role during angiogenesis, we quantified the blood vessel content (large blood vessels and capillaries) of the epicardial border zone (Supplementary Figure 2). We observed a lower density of large (non-capillary) blood vessels in *Eng*+/- mice (Figure 5G), suggesting that the thicker epicardial border zone is not due to a difference in the number of vessels. Therefore, it appears that the thicker *Eng*+/- epicardial border zone at 14 days post-MI is caused by an increase in (sub)epicardial cells. In *Eng*+/- mice, myocardial infarction results in greater deterioration of heart function compared to wt animals [26]. At 14 days post-infarct we detected a significant thinner left ventricular wall in *Eng*+/- mice (Figure 5H). Therefore, we investigated whether a greater cardiac damage is associated with a thicker epicardial border zone at 14 days post-MI. We observed no correlation between the number of cells within the epicardial border zone and the infarct size of wt and *Eng*+/- mice (Supplementary Figure 3). Furthermore, the size of the epicardial border zone was not correlated to the percentage of ejection fraction (data not shown). Interestingly, however, the total number of cells within the epicardial border zone is negatively correlated with the thickness of the left ventricular wall (Figure 5I).

Our data strongly suggest that thickening of the (sub)epicardial layer is dysregulated in *Eng*+/- mice and the size of this layer correlates to the thickness of the left ventricular wall.

DipA treatment significantly alters the epicardial post-MI response

We questioned whether we can reduce the epicardial size (thickness and number of cells) of *Eng*+/- hearts at day 14 post-MI to wt levels, given its correlation with a thinner left ventricular wall. The highly conserved SDF1/C-X-C motif chemokine receptor 4 (CXCR4) signaling axis plays an essential role in the epicardial/myocardial crosstalk during cardiac healing [22]. In addition, EPDCs express CXCR4 (data not shown) and TGFβ signaling influences the SDF1/CXCR4 axis [2, 36, 38].

Wt and *Eng*+/- mice were treated with DipA or MQ for the first 5 days following induction of MI (Figure 6A). DipA is a selective inhibitor of CD26/DPP4 and thereby a positive modulator of SDF1-CXCR4 interaction. DipA treatment has been shown to increase migration and homing of cells [10]. Indeed, at 4 days post-MI, DipA treatment significantly increased the number of MAC3+ cells localized to the epicardial border zone of *Eng*+/- animals (Supplementary Figure 4A). This suggests that DipA treatment was effective, as it resulted in increased homing of immune-reactive cells towards the site of injury.

We next investigated the long-term (14 days post-MI) effect of DipA administration. Strikingly, after DipA treatment the thickness of the epicardial border zone in *Eng*+/- mice is reduced to wt levels (Figure 6B). The reduction in epicardial size could be explained by a decrease in the total number of cells and was related to a significantly thicker ventricular wall in DipA treated *Eng*+/- animals (grey bars in Figure 6C-E). In contrast, in wt mice we observed a significant increase in the number of cells within the epicardial border zone and a trend towards a decrease in left ventricular wall thickness upon treatment (white bars in Figure 6C-E). This change in epicardial size was not due to a difference in macrophage percentage, since we observed no significant changes in the presence of MAC3+ cells within the epicardial border zone (Supplementary Figure 4B). Altogether our data demonstrate that systemic administration of DipA influences the epicardial phenotype. More importantly, they suggest that, for *Eng*+/- animals, DipA treatment during the first week following MI results in restoration of epicardial thickness to wt levels and limited left ventricular wall thinning.

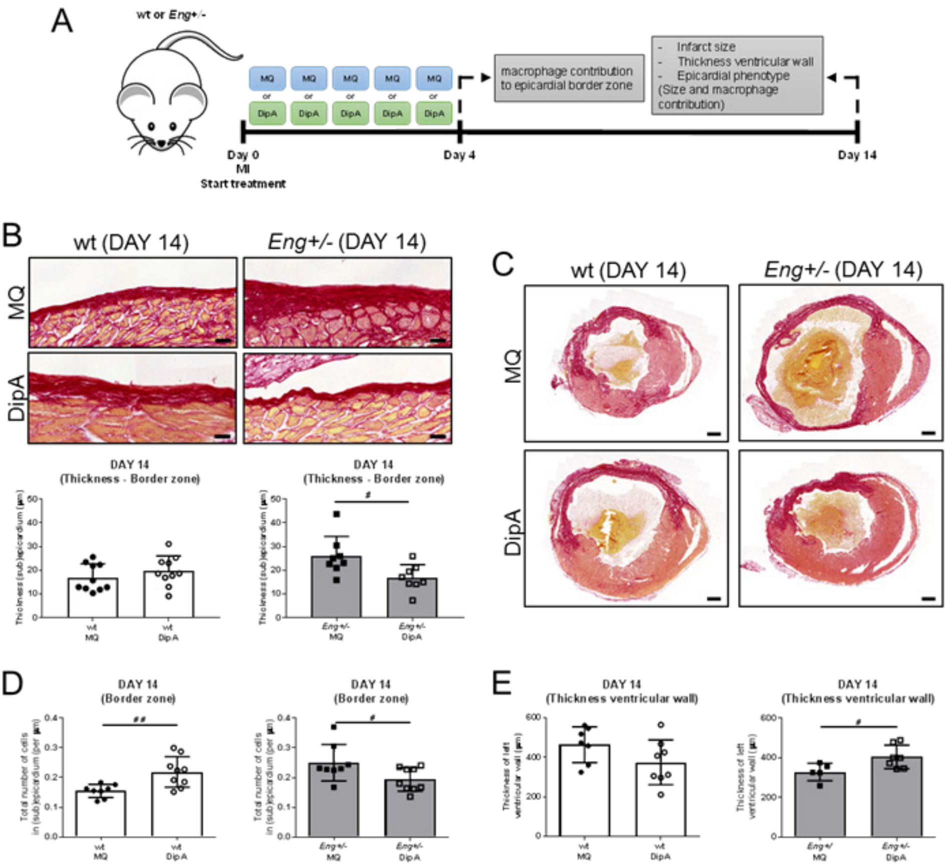

Figure 6. DipA treatment significantly alters the epicardial post-MI response at 14 days post-MI. A. Overview of experiment and measured entities. Wt or Eng+/- mice were given Diprotin A (DipA) or control (MQ) treatment and sacrificed at day 4 and day 14 after the induction of MI. B. PSR stainings of the wt and Eng+/- epicardial border zone (Scale bars: 20 µm). DipA administration significantly decreases the thickness of the epicardium in Eng+/- mice while no change was observed in wt animals (n = 8-10 mice for each group). C. PSR stainings of wt and Eng+/- transverse heart sections, MQ or DipA treated, showing the thickness of the left ventricular wall (Scale bar: 500 µm). D. DipA treatment significantly increases and decreases the total number of epicardial cells at border zone for wt and Eng+/- animals, respectively (n = 8-9 mice for each group). E. DipA treatment significantly increases the thickness of the left ventricular wall in Eng+/- animals (n = 5-8 mice for each group). Data information: #: $p<0.05$ ##: $p<0.01$

Discussion

The mechanisms underlying the behavior of the epicardial layer following MI are not fully understood which makes it difficult to use this layer as a source for repair of cardiac injury. Using *Eng*+/- mice, our data indicate an important role for endoglin in the epicardial MI-response. Higher pSMAD1 levels in the *Eng*+/- epicardial layer suggest a misbalance within the TGFβ signaling pathway. We observed aberrant epicardial thickening in *Eng*+/- hearts which appears to occur independently of extra-cardiac cell contributions from the circulation. At day 4 post-MI, the *Eng*+/- epicardial layer harbors a higher percentage of WT1+ cells suggesting increased activation of this layer. In addition, the correlation between the thickness of the epicardial layer and ventricular wall strengthens the importance of studying the epicardium as a myocardial support mechanism. Moreover, in *Eng*+/- mice the thickness of the epicardial border zone and ventricular wall were reversed to wt levels upon systemic administration of DipA.

Besides angiogenesis, endoglin appears to be important for a fully functional immune system [12] and a change in the immune response may be the underlying cause of a difference in epicardial phenotype. *Eng*+/- mononuclear cells are impaired in their homing capacity to the infarcted heart [26, 38] and persistent inflammation was observed in *Eng*+/- mice following injury [37]. As a consequence, a thinner epicardial layer in *Eng*+/- animals at day 4 could have been the result of a potential delayed immune response, while a thicker layer at day 14 may be due to persistent inflammation. Therefore, we cultured wt and *Eng*+/- hearts *ex vivo*, without the presence of circulating immune cells. Interestingly, also in culture we observed a thinner epicardial layer in *Eng*+/- compared to wt suggesting an intrinsic defect occurring independently of extra-cardiac cell contributions. However, we cannot exclude the contribution of resident immune cells. From another point of view, Huang and colleagues showed that inhibition of epicardial activation results in reduced number of immune cells in the infarcted area [21]. This observation suggests that the defects in MI-induced inflammation in *Eng*+/- mice may also be caused by aberrant epicardial behavior. However, future studies will be required to dissect a potential cross-talk between the epicardium and immune-system in more detail.

After MI, the epicardium lining the infarct area is lost. Cells from the epicardial border zones proliferate and gradually close the (epicardial) gap, ultimately covering the infarct surface with a WT1+ epicardial layer [43]. At 4 days following MI, *Eng*+/- hearts had a higher percentage of their cardiac circumference covered with a WT1+ layer which may be related to an increased migration rate of EPDCs upon partial loss of endoglin. Increased migration of EPDCs may result a faster closure of the epicardial gap in *Eng*+/- mice and as a consequence a higher coverage of the infarcted heart with a WT1+ epicardial layer.

A higher percentage of WT1+ cells results in an altered composition of the *Eng*+/- epicardial layer compared to wt animals which may cause paracrine changes in the cardiac environment. The transcription factor WT1 is, besides a marker for epicardial activation, an important regulator of epicardial EMT [5, 14, 17, 33, 42]. Upon activation, epicardial cells undergo EMT and form the subepicardium. When EPDCs go through EMT, they lose their nuclear expression of WT1 [5]. A higher percentage of WT1+ cells within the epicardial layer may indicate increased activation or affected transition through EMT causing *Eng*+/- EPDCs to remain in a WT1+ stadium for an extended period of time. Alternatively, potential increased migration of WT1-EPDCs into the underlying myocardium may result in a thinner epicardial layer and as a consequence a higher proportion of WT1+ cells within this layer. Which of these mechanisms underlie the altered size and composition of the *Eng*+/- epicardial layer shortly after MI is an important aspect of future research.

Partial loss of endoglin can have both a detrimental and beneficial effect on heart function which appears to be dependent on the underlying cause of the disease [23, 26]. In a mouse model of pressure-overload induced heart failure, endoglin deficiency has been shown to preserve left ventricular function resulting in increased survival [23]. Our data suggest that there is a correlation between the number of cells within the (sub)epicardial layer and thickness of the left ventricular wall. A defect in the epicardial response following MI has been reported to result in ventricular dilatation and reduced cardiac performance [13]. Therefore, an increase in epicardial size may be the underlying cause of a thinner ventricular wall. However, a thicker epicardial layer may also be a protective mechanism contributing to reducing heart failure and cardiac rupture. Whether the observed changes in epicardial behavior upon partial loss of endoglin are beneficial for cardiac repair remains subject to future studies.

The epicardium plays an important role as a myocardial support mechanism. The correlation between the size of the epicardial layer and left ventricular wall may indeed suggest a dialog with the underlying myocardium. The SDF1/CXCR4 axis has been proposed to be an important endogenous pathway involved in epicardial-myocardial crosstalk [22]. Upon MI, SDF1 is upregulated in the myocardium [4] and EPDCs are able to migrate towards the SDF1 chemokine [39]. Our data suggest that enhancing this pathway, via DipA treatment, results in fewer epicardial cells within the epicardial region. This might point towards, besides a potential alteration in the extra-cardiac cell contribution, an increased homing of EPDCs towards the underlying diseased myocardium. DipA treatment could increase the migration ability of EPDCs in the direction of myocardial SDF1 via the inhibition of its catalytic enzyme, DPP4. In this context, it is interesting to note that human *Eng+/-* mononuclear cells have a misbalanced SDF1/CXCR4 axis resulting in reduced homing towards a SDF1 gradient. In addition, DipA pre-treatment of these human *Eng+/-* mononuclear cells enhanced their homing capacity towards to injured myocardium upon injection into the tail vein [38].

The epicardium plays an important role following cardiac injury. This layer has been proposed to serve as an endogenous source of cardiovascular cell types and/or support the myocardium via paracrine signaling, both during the early phase following injury as during scar modulation [40]. In conclusion, our data give an insight in epicardial behavior following injury and suggest that endoglin is an important player in this context. These new insights may help in exploiting the epicardium as a therapeutic target for cardiac repair and regeneration.

Acknowledgements

We thank the remaining members of our group for valuable discussions and W.C.R. Sloos, J.C.A.G. Wiegant and A.M.A van der Laan for technical assistance. We thank Prof. Dr. P. ten Dijke (Department of Molecular Cell Biology, LUMC, Leiden, the Netherlands), and J.C. Peterson and Prof. Dr. M.C. de Ruiter (Department of Anatomy and Embryology, LUMC, Leiden, the Netherlands) for providing antibodies. We are grateful to the department of Cardiothoracic Surgery (LUMC, Leiden, the Netherlands) for collecting and providing human adult heart tissue.

Conflict of interest

The authors declare that they have no conflict of interest.

Funding

This work was supported by the Netherlands Institute for Regenerative Medicine (NIRM1.7), the Dutch Heart Foundation (30710), the ZonMw-TAS program (116002016), the Netherlands Organization for Scientific Research (NWO) VENI (016.146.079) (AM Smits) and a LUMC Research fellowship (AM Smits).

References

1. Acharya A, Baek ST, Huang G, Eskiocak B, Goetsch S, Sung CY, Banfi S, Sauer MF, Olsen GS, Duffield JS, Olson EN, Tallquist MD (2012) The bHLH transcription factor Tcf21 is required for lineage-specific EMT of cardiac fibroblast progenitors. Development 139:2139–2149. doi: 10.1242/dev.079970

2. Ao M, Franco OE, Park D, Raman D, Williams K, Hayward SW (2007) Cross-talk between paracrine-acting cytokine and chemokine pathways promotes malignancy in benign human prostatic epithelium. Cancer Res 67:4244–4253. doi: 10.1158/0008-5472.CAN-06-3946

3. Arthur HM, Ure J, Smith a J, Renforth G, Wilson DI, Torsney E, Charlton R, Parums D V, Jowett T, Marchuk D a, Burn J, Diamond a G (2000) Endoglin, an ancillary TGFbeta receptor, is required for extraembryonic angiogenesis and plays a key role in heart development. Dev Biol 217:42–53. doi: 10.1006/dbio.1999.9534

4. Askari AT, Unzek S, Popovic ZB, Goldman CK, Forudi F, Kiedrowski M, Rovner A, Ellis SG, Thomas JD, DiCorleto PE, Topol EJ, Penn MS (2003) Effect of stromal-cell-derived factor 1 on stem-cell homing and tissue regeneration in ischaemic cardiomyopathy. Lancet 362:697–703. doi: 10.1016/S0140-6736(03)14232-8

5. Bax NAM, Van Oorschot AAM, Maas S, Braun J, Van Tuyn J, De Vries AAF, Gittenberger-De Groot AC, Goumans MJ (2011) In vitro epithelial-to-mesenchymal transformation in human adult epicardial cells is regulated by TGFβ-signaling and WT1. Basic Res Cardiol 106:829–847. doi: 10.1007/s00395-011-0181-0

6. Bollini S, Vieira JMN, Howard S, Dubè KN, Balmer GM, Smart N, Riley PR (2014) Re-activated adult epicardial progenitor cells are a heterogeneous population molecularly distinct from their embryonic counterparts. Stem Cells Dev 23:1719–30. doi: 10.1089/scd.2014.0019

7. Bourdeau A, Dumont DJ, Letarte M (1999) A murine model of hereditary hemorrhagic telangiectasia. J Clin Invest 104:1343–51. doi: 10.1172/JCI8088

8. Braitsch CM, Combs MD, Quaggin SE, Yutzey KE (2012) Pod1/Tcf21 is regulated by retinoic acid signaling and inhibits differentiation of epicardium-derived cells into smooth muscle in the developing heart. Dev Biol 368:345–357. doi: 10.1016/j.ydbio.2012.06.002

9. Carmona R, Guadix JA, Cano E, Ruiz-Villalba A, Portillo-Sánchez V, Pérez-Pomares JM, Muñoz-Chápuli R (2010) The embryonic epicardium: An essential element of cardiac development. J Cell Mol Med 14:2066–2072. doi: 10.1111/j.1582-4934.2010.01088.x

10. Christopherson KW, Hangoc G, Mantel CR, Broxmeyer HE (2004) Modulation of hematopoietic stem cell homing and engraftment by CD26. Science (80-) 305:1000–1003. doi: 10.1126/science.1097071

11. ten Dijke P, Goumans M-J, Pardali E (2008) Endoglin in angiogenesis and vascular diseases. Angiogenesis 11:79–89. doi: 10.1007/s10456-008-9101-9

12. Dingenouts CKE, Goumans MJ, Bakker W (2015) Mononuclear cells and vascular repair in HHT. Front Genet. doi: 10.3389/fgene.2015.00114

13. Duan J, Gherghe C, Liu D, Hamlett E, Srikantha L, Rodgers L, Regan JN, Rojas M, Willis M, Leask A, Majesky M, Deb A (2012) Wnt1/βcatenin injury response activates the epicardium and cardiac fibroblasts to promote cardiac repair. EMBO J 31:429–42. doi: 10.1038/emboj.2011.418

14. Duim SN, Goumans M-J, Kruithof BPT (2016) WT1 in Cardiac Development and Disease. Wilms Tumor. doi: 10.15586/codon.wt.2016.ch13

15. Duim SN, Kurakula K, Goumans MJ, Kruithof BPT (2015) Cardiac endothelial cells express Wilms' tumor-1. Wt1 expression in the developing, adult and infarcted heart. J Mol Cell Cardiol 81:127–135. doi: 10.1016/j.yjmcc.2015.02.007

16. Gherghiceanu M, Popescu LM (2009) Human epicardium: Ultrastructural ancestry of mesothelium and mesenchymal cells. J Cell Mol Med 13:2949–2951. doi: 10.1111/j.1582-4934.2009.00869.x

17. von Gise A, Zhou B, Honor LB, Ma Q, Petryk A, Pu WT (2011) WT1 regulates epicardial epithelial to mesenchymal transition through beta-catenin and retinoic acid signaling pathways. Dev Biol 356:421–431. doi: S0012-1606(11)00983-3 [pii]10.1016/j.ydbio.2011.05.668

18. Goumans M-J, Dijke P ten (2017) TGF-β Signaling in Control of Cardiovascular Function. Cold Spring Harb Perspect Biol. doi: 10.1101/cshperspect.a022210

19. Goumans M-J, Liu Z, ten Dijke P (2009) TGF-beta signaling in vascular biology and dysfunction. Cell Res 19:116–27. doi: 10.1038/cr.2008.326

20. Goumans M-J, Zwijsen A, Dijke P ten, Bailly S (2017) Bone Morphogenetic Proteins in Vascular Homeostasis and Disease. Cold Spring Harb Perspect Biol. doi: 10.1101/cshperspect.a031989

21. Huang GN, Thatcher JE, McAnally J, Kong Y, Qi X, Tan W, DiMaio JM, Amatruda JF, Gerard RD, Hill JA, Bassel-Duby R, Olson EN (2012) C/EBP Transcription Factors Mediate Epicardial Activation During Heart Development and Injury. Science 338:1599–1603. doi: 10.1126/science.1229765

22. Itou J, Oishi I, Kawakami H, Glass TJ, Richter J, Johnson A, Lund TC, Kawakami Y (2012) Migration of cardiomyocytes is essential for heart regeneration in zebrafish. Development 139:4133–42. doi: 10.1242/dev.079756

23. Kapur NK, Wilson S, Yunis AA, Qiao X, MacKey E, Paruchuri V, Baker C, Aronovitz MJ, Karumanchi SA, Letarte M, Kass DA, Mendelsohn ME, Karas RH (2012) Reduced endoglin activity limits cardiac fibrosis and improves survival in heart failure. Circulation 125:2728–2738. doi: 10.1161/CIRCULATIONAHA.111.080002

24. Kennedy-Lydon T, Rosenthal N (2015) Cardiac regeneration: epicardial mediated repair. Proc R Soc B Biol Sci 282:20152147. doi: 10.1098/rspb.2015.2147

25. Kruithof B, Lieber S, Kruithof-de Julio M, Gaussin V, Goumans M (2015) Culturing Mouse

Cardiac Valves in the Miniature Tissue Culture System. J Vis Exp. doi: 10.3791/52750

26. Van Laake LW, Van Den Driesche S, Post S, Feijen A, Jansen MA, Driessens MH, Mager JJ, Snijder RJ, Westermann CJJ, Doevendans PA, Van Echteld CJA, Ten Dijke P, Arthur HM, Goumans MJ, Lebrin F, Mummery CL (2006) Endoglin has a crucial role in blood cell-mediated vascular repair. Circulation 114:2288–2297. doi: 10.1161/CIRCULATIONAHA.106.639161

27. Lambert JM, Lopez EF, Lindsey ML (2008) Macrophage roles following myocardial infarction. Int J Cardiol 130:147–158. doi: 10.1016/j.ijcard.2008.04.059

28. Lavine KJ, Ornitz DM (2008) Fibroblast growth factors and Hedgehogs: at the heart of the epicardial signaling center. Trends Genet 24:33–40. doi: 10.1016/j.tig.2007.10.007

29. Leung HW, Moerkamp AT, Padmanabhan J, Ng S-W, Goumans M-J, Choo A (2015) mAb C19 targets a novel surface marker for the isolation of human cardiac progenitor cells from human heart tissue and differentiated hESCs. J Mol Cell Cardiol 82:228–37. doi: 10.1016/j.yjmcc.2015.02.016

30. Li DY, Sorensen LK, Brooke BS, Urness LD, Davis EC, Taylor DG, Boak BB, Wendel DP (1999) Defective angiogenesis in mice lacking endoglin. Science 284:1534–1537. doi: 10.1126/science.284.5419.1534

31. Lieber SC, Kruithof BPT, Aubry N, Vatner SF, Gaussin V (2010) Design of a miniature tissue culture system to culture mouse heart valves. Ann Biomed Eng 38:674–82. doi: 10.1007/s10439-010-9922-8

32. Loennechen JP, Støylen A, Beisvag V, Wisløff U, Ellingsen O (2001) Regional expression of endothelin-1, ANP, IGF-1, and LV wall stress in the infarcted rat heart. Am J Physiol Heart Circ Physiol 280:H2902-10. doi: 0363-6135/01

33. Martínez-Estrada OM, Lettice LA, Essafi A, Guadix JA, Slight J, Velecela V, Hall E, Reichmann J, Devenney PS, Hohenstein P, Hosen N, Hill RE, Muñoz-Chapuli R, Hastie ND (2010) Wt1 is required for cardiovascular progenitor cell formation through transcriptional control of Snail and E-cadherin. Nat Genet 42:89–93. doi: 10.1038/ng.494

34. Masters M, Riley PR (2014) The epicardium signals the way towards heart regeneration. Stem Cell Res 13:683–692. doi: 10.1016/j.scr.2014.04.007

35. Moerkamp AT, Lodder K, Herwaarden T van, Dronkers E, Dingenouts CKE, Tengström FC, Brakel TJ van, Goumans M-J, Smits AM (2016) Human fetal and adult epicardial-derived cells: a novel model to study their activation. Stem Cell Res Ther. doi: 10.1186/s13287-016-0434-9

36. Nakamura T, Shinriki S, Jono H, Guo J, Ueda M, Hayashi M, Yamashita S, Zijlstra A, Nakayama H, Hiraki A, Shinohara M, Ando Y (2015) Intrinsic TGF-β2-triggered SDF-1-CXCR4 signaling axis is crucial for drug resistance and a slow-cycling state in bone marrow-disseminated tumor cells. Oncotarget 6:1008–1019. doi: 10.18632/oncotarget.2826

37. Peter MR, Jerkic M, Sotov V, Douda DN, Ardelean DS, Ghamami N, Lakschevitz F, Khan MA, Robertson SJ, Glogauer M, Philpott DJ, Palaniyar N, Letarte M (2014) Impaired resolution of inflammation in the Endoglin heterozygous mouse model of chronic colitis. Mediators Inflamm. doi: 10.1155/2014/767185

38. Post S, Smits AM, Van Den Broek AJ, Sluijter JPG, Hoefer IE, Janssen BJ, Snijder RJ, Mager JJ, Pasterkamp G, Mummery CL, Doevendans PA, Goumans MJ (2010) Impaired recruitment of HHT-1 mononuclear cells to the ischaemic heart is due to an altered CXCR4/CD26 balance. Cardiovasc Res 85:494–502. doi: 10.1093/cvr/cvp313

39. Ruiz-Villalba A, Simón AM, Pogontke C, Castillo MI, Abizanda G, Pelacho B, Sánchez-Domínguez R, Segovia JC, Prósper F, Pérez-Pomares JM (2015) Interacting resident epicardium-derived fibroblasts and recruited bone marrow cells form myocardial infarction scar. J Am Coll Cardiol 65:2057–2066. doi: 10.1016/j.jacc.2015.03.520

40. Smits A, Riley P (2014) Epicardium-Derived Heart Repair. J Dev Biol 2:84–100. doi: 10.3390/jdb2020084

41. Smits AM, Van Laake LW, Den Ouden K, Schreurs C, Szuhai K, Van Echteld CJ, Mummery CL, Doevendans PA, Goumans MJ (2009) Human cardiomyocyte progenitor cell transplantation preserves long-term function of the infarcted mouse myocardium. Cardiovasc Res 83:527–535. doi: 10.1093/cvr/cvp146

42. Takeichi M, Nimura K, Mori M, Nakagami H, Kaneda Y (2013) The Transcription Factors Tbx18 and Wt1 Control the Epicardial Epithelial-Mesenchymal Transition through Bi-Directional Regulation of Slug in Murine Primary Epicardial Cells. PLoS One. doi: 10.1371/journal.pone.0057829

43. van Wijk B, Gunst QD, Moorman AFM, van den Hoff MJB (2012) Cardiac Regeneration from Activated Epicardium. PLoS One. doi: 10.1371/journal.pone.0044692

44. Zhou B, Honor LB, He H, Qing M, Oh JH, Butterfield C, Lin RZ, Melero-Martin JM, Dolmatova E, Duffy HS, Von Gise A, Zhou P, Hu YW, Wang G, Zhang B, Wang L, Hall JL, Moses MA, McGowan FX, Pu WT (2011) Adult mouse epicardium modulates myocardial injury by secreting paracrine factors. J Clin Invest 121:1894–1904. doi: 10.1172/JCI45529

Supplementary figures

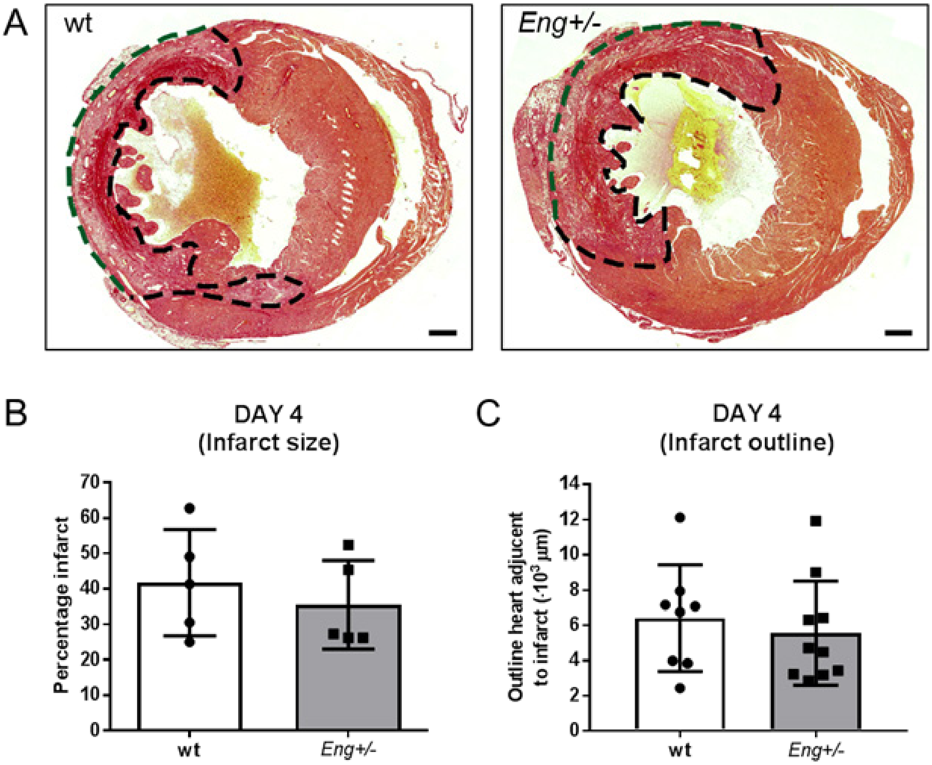

Supplementary Figure 1: Infarct size is equal between wt and Eng+/- hearts. A. In PSR stainings, the infarct area is outlined by a dashed line and the periphery of the infarct is indicated by a green dashed line. Scale bars: 500 µm. B,C. At 4 days post-MI, B. Wt and Eng+/- mice have an equal infarct size (n = 5 mice for each group). and C. no difference in the infarct periphery (n = 8-10 mice for each group)

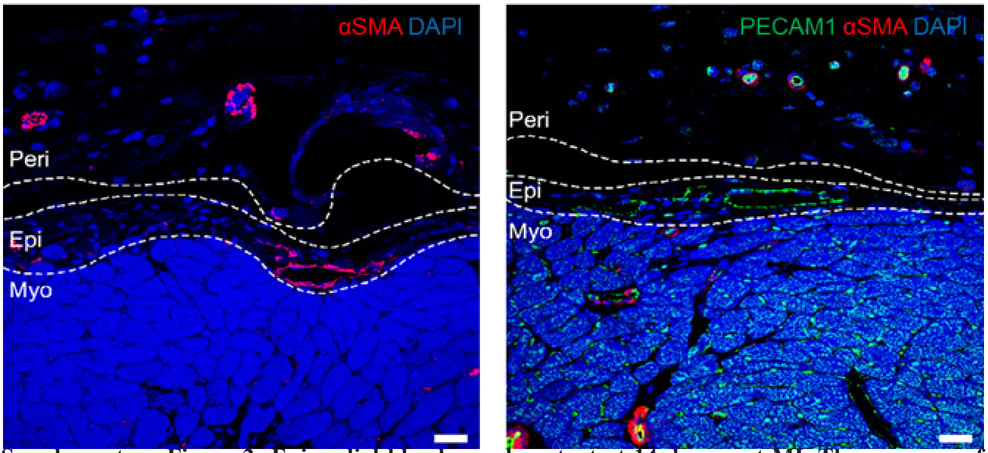

Supplementary Figure 2: Epicardial blood vessel content at 14 days post-MI. The presence of blood vessels within the epicardial border zone was quantified in alpha smooth muscle actin (αSMA) and platelet and endothelial cell adhesion molecule 1 (PECAM1) co-stainings. The dashed lines indicate the border between myocardium, (sub)epicardium and pericardium. Scale bars: 20 µm. Epi: (sub)epicardium, Myo: myocardium and Peri: pericardium

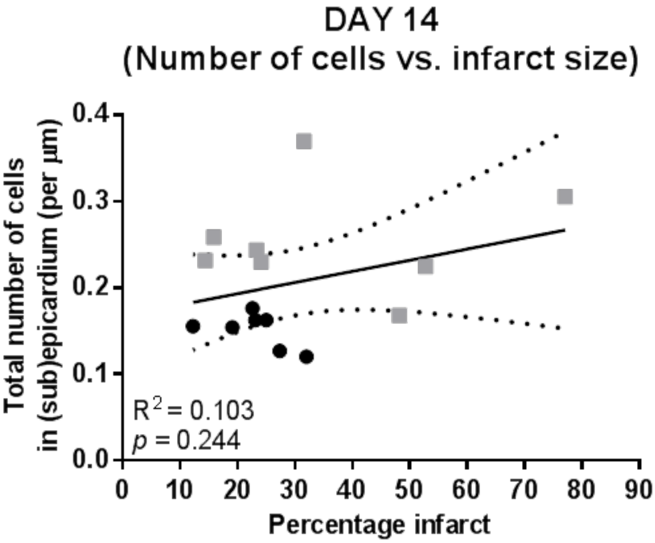

Supplementary Figure 3: Size of the epicardial border zone is not correlated with infarct size. Plotting the infarct size of wt and Eng+/- mice at day 14 post-MI against the number of cells within the epicardial border zone shows that there is no correlation. Eng+/- mice are depicted in grey/square data points (n = 7-8 mice for each group)

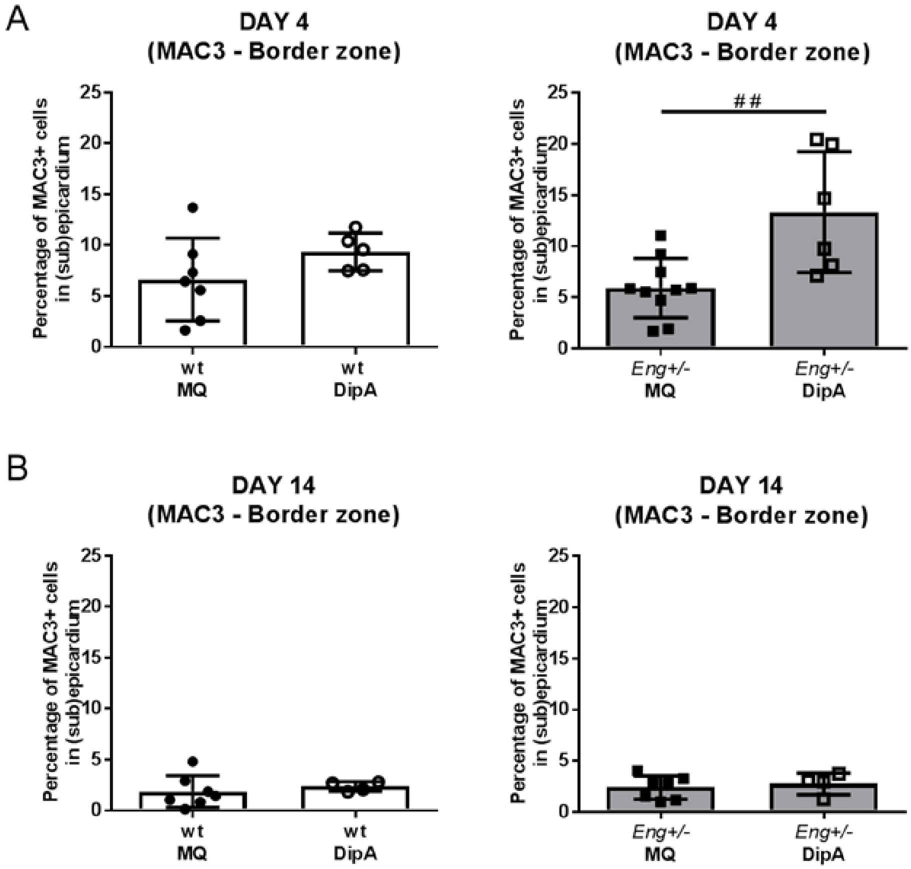

Supplementary Figure 4: Percentage of MAC3+ cells within the epicardial border zone upon DipA administration. A. MAC3+ cells in the (sub)epicardial border zone, 4 days post-MI. DipA treatment only significantly increases the percentage of MAC3+ cells within the Eng+/- epicardial border zone (n = 6-10 mice for each group). B. MAC3+ cells in the (sub)epicardial border zone, 14 days post-MI. At 14 days, no difference was observed in the percentage of MAC3+ cells within the epicardial border zone upon treatment for both wt and Eng+/- mice (n = 4-7 mice for each group). Data information: # #: $p<0.01$

7

General Discussion

HHT1 is caused by mutations in endoglin, the TGFβ co-receptor. Its main symptoms include severe epistaxis and hemorrhages, and as a result HHT1 was long considered a disorder affecting angiogenesis only. As it became clear that endoglin heterozygosity disturbs the function of many more cell types and processes, such as wound repair, the aim of my thesis was to understand the role of immune cells on tissue repair in the context of endoglin heterozygosity. We therefore investigated the impact of increased TGFβ signaling and the systemic application of DPP4 inhibition in endoglin heterozygous mouse models.

DPP4 regulation is essential for the controlled manner in which MNCs to home towards damaged tissue and contribute to repair. MNC homing in endoglin heterozygous mice is impaired, therefore we studied the effect of DPP4 inhibition in order to increase homing and thus enhance tissue repair. Furthermore, endoglin heterozygosity causes the TGFβ and BMP signaling balance to be disturbed. To investigate the effect of skewing the BMP/TGFβ signaling pathways towards increased TGFβ signaling, we inhibited BMP signaling using BMPRI inhibitor LDN. We investigated the effects of LDN and DPP4 inhibitor treatments in various ischemic and wounding models: MI, HLI and wound healing of the dermis, for WT and *Eng*$^{+/-}$ mice, both at functional and molecular level. Below the findings and their implications are discussed in more detail.

Inhibition of DPP4 increases MNC homing and drives differentiation of macrophages

Cardiovascular disease is a major health issue in the western world. Understanding and improving tissue repair in HHT1 setting could help improve treatment for other patients with tissue damage as well. For tissue repair, the initial immune response to damage is similar to that of inflammation caused by pathogens. A normal inflammatory response clears away cell debris and initiates fibrosis and angiogenesis. HHT1 is hallmarked by impaired angiogenesis and subsequent decreased maturation of the vasculature formed. In addition, an elevated immune response adds to the impaired tissue repair. As we discuss in Chapter 3, we were able to restore MNC homing and short term improvement of cardiac function after MI in a murine model of HHT1. However, cardiac function did not show any major long term improvement. So although fibrotic scarring was significantly reduced and angiogenesis increased, it became apparent that this is not sufficient for tissue repair. In the DPP4 treated *Eng*$^{+/-}$ mice, we also found that arteriogenesis was reduced, indicating maturation of vessels is still not optimal. Furthermore, an effect on macrophage differentiation was observed. Both HHT1 patients and *Eng*$^{+/-}$ mice have elevated numbers of M1 inflammatory macrophages, and after treating with a DPP4 inhibitor, the number of M1 in the infarct border zone significantly increased. Looking at the inflammation (14 days post-MI) in normal, healthy animals the inflammation was resolved, and only a few macrophages were still present in the infarct border zone, however in *Eng*$^{+/-}$ animals, these numbers were highly increased. This long term increased macrophage presence points out the imbalance in the HHT1 immune response, underlining the defect in inflammation and an intrinsic problem regarding macrophage function.

Interestingly, DPP4 inhibitor treatment increased the number of reparative macrophages (M2) in the infarct border zones of the *Eng*$^{+/-}$ mice. DPP4 inhibition seems therefore able to either recruit more M2-like macrophages, or induce their differentiation. The increase of M2 macrophages was not observed in wild type (WT) mice, therefore I hypothesize that either the defect in TGFβ signaling affects macrophage differentiation and/or function, and another possibility is that the differentiation in 'healthy' mice is already optimal, so therefore we do not detect any differences when treating WT mice with DPP4 inhibitor. The variation in stimuli-response between WT and *Eng*$^{+/-}$ mice was also apparent when we treated macrophages *in*

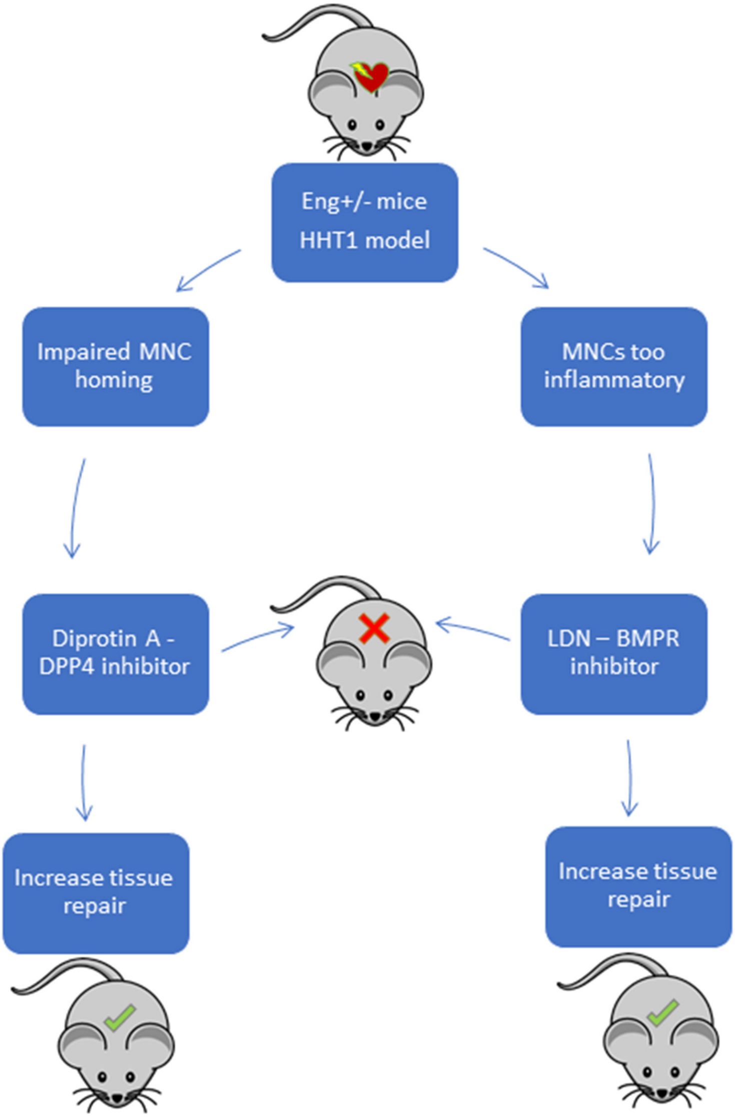
Eng+/- mice
HHT1 model
Impaired MNC homing
MNCs too inflammatory
Diprotin A - DPP4 inhibitor
LDN – BMPR inhibitor
Increase tissue repair
Increase tissue repair

Fig. 1 Influencing the homing and differentiation of MNCs in HHT1. Depicted is a schematic representation of the thesis subjects. Endoglin heterozygous mice were used to model HHT1. In various experimental methods inducing ischemic and/or tissue damage, we improved tissue repair in the mice via two approaches. First, using DPP4 inhibition, via increase of the SDF1-CXCR4 homing mechanism, we restored the impaired homing capacity of HHT1-MNCs, and also increased reparative M2 macrophage numbers post-MI. The second treatment approach focused on stimulating TGFβ signaling and M2 differentiation via use of the BMPR inhibitor LDN. In vitro studies showed LDN increased M2 differentiation. In vivo, we observed increased tissue repair in several experimental models, however we did not find an effect on macrophage differentiation. Combining the DPP4 inhibitor and LDN treatment together did not result in a positive outcome on repair after induction of MI. Thus, the stand-alone treatments improved tissue repair in Eng+/- mice, but the combined treatments did not.

vitro with TGFβ in Chapter 4. In this chapter we applied TGFβ to macrophage cultures, and we observed that M2 macrophages were induced in wild type cells, which did not happen in the *Eng*$^{+/-}$ cells. Only upon combining TGFβ with ALK1/2/3 inhibition using LDN did these macrophages differentiate towards M2. Furthermore, LDN treatment reduced fibrosis after MI, increased heart function, and increased blood flow recovery after HLI – however in the heart LDN treatment did not have any effect on macrophage M1/M2 differentiation or numbers present (Fig. 2), suggesting perhaps other effects of LDN that cause the increased tissue repair. Indeed we found that non-SMAD signaling in *Eng*$^{+/-}$ macrophages was severely blunted, and although LDN treatment did not affect these non-SMAD responses, SMAD2 phosphorylation was significantly increased in *Eng*$^{+/-}$ macrophages compared to WT upon treatment with LDN. Furthermore, the effects on signaling described were performed on cultured macrophages, of course as LDN is given systemically to the mice *in vivo*, we cannot exclude effects on other cell types, such as fibroblasts or endothelial cells.

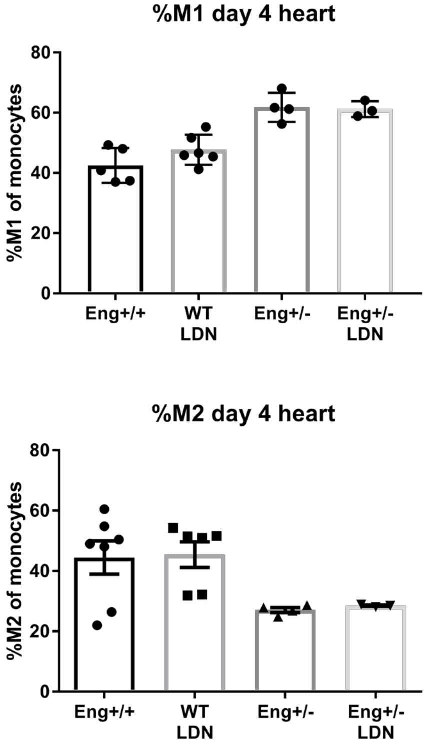

Fig. 2 LDN treatment had no effect on in vivo macrophage differentiation in the heart. Flow cytometric analysis of MNCs isolated from the left cardiac ventricle. Measurement 4 days post-MI. Ly6Chigh =M1 Ly6Clow =M2.

The separate beneficial results by DPP4 inhibition and BMPR inhibition on tissue repair in *Eng*$^{+/-}$ mice made us question if combined therapy with the two compounds would have a synergistic effect on cardiac repair post-MI. In Chapter 3, we obtained improved MNC homing and M1/M2 balance via DPP4 inhibition using Diprotin A, and in Chapter 4, ischemic damage was restored back to WT levels by BMP inhibition, using LDN. Furthermore, the reduction of infarct size and increased angio- and arteriogenesis by both individual treatments implied that a combination of treatments could be promising. We therefore induced MI in WT and *Eng*$^{+/-}$ mice, and treated the mice with both the DPP4 inhibitor Diprotin A (DipA) and the BMPR inhibitor LDN, and monitored their cardiac function over time using ultrasound. Usually, about 10-20% of the mice perish because of cardiac rupture during the first week after MI. Unexpectedly, in the first week after myocardial infarction, 60% of the WT animals treated with the DipA/LDN combination therapy died of acute cardiac rupture, while only 20% of *Eng*$^{+/-}$ mice died when receiving the same treatment (Fig. 3).

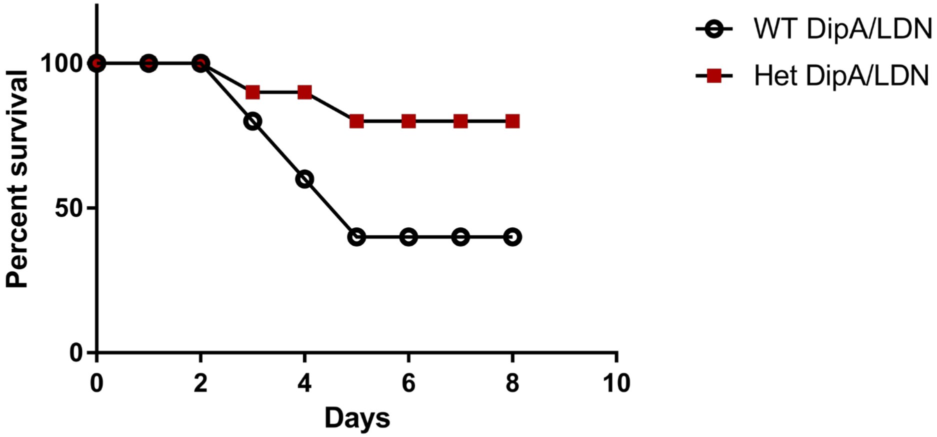

Fig. 3 DipA/LDN co-treatment causes acute cardiac rupture in WT mice. Survival graph: black = WT, red= Eng+/- animals. All animals were treated with the DipA/LDN combination therapy. N=10 mice per group.

Mice that died of acute rupture were assessed for infarct size, and measurements showed that the relative infarct size was larger compared to the surviving mice (Fig. 4). This suggests animals with large infarct sizes, and in particular WT animals, are negatively affected by treatment with DipA/LDN, causing cardiac ruptures. We hypothesize that because all ruptures were in the first week post-MI; this coincides with the acute phase of tissue repair, where MNCs infiltrate the damaged tissue. In WT mice post-MI, this process is optimal, and treatment with DipA/LDN could actually be interfering with this process. I hypothesize that where DipA stimulates homing and influences differentiation, and LDN reduces the level of fibrosis; the cardiac tissue is not able to handle the influx of cells and consequently ruptures.

Of the surviving mice, DipA/LDN treatment did not show a short or long term beneficial effect (Fig. 5), confirming the combined treatment has no positive effect on cardiac recovery, even with smaller infarct sizes.

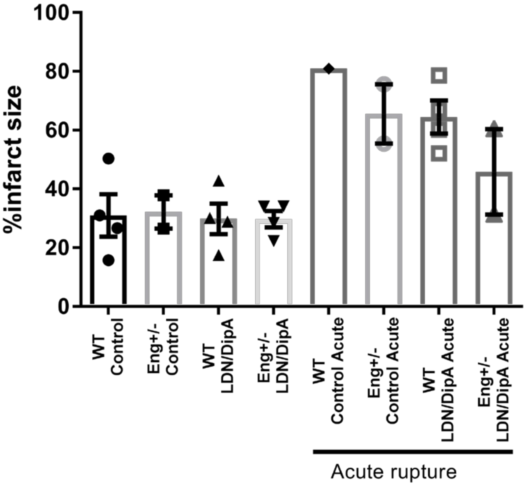

Fig. 4 Infarct size. On the left side of the graphs: animals that survived up to 3 months post-MI, right side of the graph; animals that died of acute cardiac ruptures (minus 2 mice where the heart was not isolated). DipA/LDN co-treatment. N=1-4 per group. Hematoxylin and Eosin staining of cardiac tissue, percentage infarct size area of the left ventricle.

Endoglin heterozygosity blunts intracellular TGFβ signaling in macrophages

Further investigating macrophage function and signaling in *Eng*$^{+/-}$ mice, we found that while the SMAD response was not severely affected, the non-canonical pathways were highly unresponsive to any TGFβ stimulation or inhibition.

In Chapter 5 the baseline levels of several non-canonical signaling proteins were compared. The *Eng*$^{+/-}$ levels for pERK1/2 and p-p38 were significantly higher than the wild types. ERK and p38 are involved in inflammation, cell survival and apoptosis[1-4], moreover p38 is also involved in M2 differentiation and activation[5,6]. The varying levels of these signaling pathways indicate that the macrophage responses to stress are affected. Therefore we hypothesized that there could be a direct link between endoglin/TGFβ signaling and DPP4. DPP4 is a transmembrane protein, found on multiple cell types and as discussed previously, regulates MNC homing. It was reported that DPP4 has stimulatory functions regarding T cell activation[7-9], indicating there are possibly more unknown functions of DPP4 involving the immune system. We found that DPP4 inhibition decreases phosphorylation of several non-canonical TGFβ signaling molecules involved in the pro-inflammatory response: ERK1/2 and AKT (Chapter 5). Other studies showed that TGFβ downregulates DPP4 expression[10] and in another study DPP4 inhibition was reported to increase TGFβ secretion in MNCs[11]. The decrease in ERK1/2 and AKT activation, together with the direct link between TGFβ decreasing DPP4 expression suggests that DPP4 can have either direct and/or indirect effects on TGFβ signaling. At the least for inflammatory conditions, my study in Chapter 5 and other studies show that DPP4 inhibition has immunosuppressive actions[12]; phosphorylation of pro-inflammatory NFκB-related proteins such as p65, IκBα and JNK were found to be decreased when macrophages were stimulated with LPS and treated with a DPP4 inhibitor.

In Chapter 6 we observed that DPP4 inhibition increased the percentage of macrophages present in the epicardium of *Eng*$^{+/-}$ mice after MI. We conclude here that endoglin is important for a fully functional immune system and a change in the immune response may be the cause the decreased epicardial repair in *Eng*$^{+/-}$ mice after MI. We demonstrated that

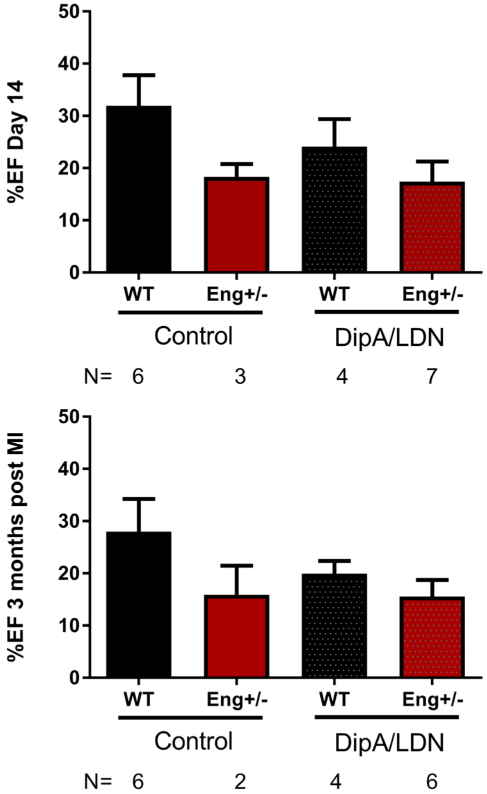

Fig. 5 Long term cardiac function does not improve with DipA/LDN combination treatment. A. Percent ejection fraction 14 days post-MI. Control versus DipA/LDN co-treatment in mice. Measurements taken via cardiac ultrasound of the left ventricle. B. Percent ejection fraction 14 days post-MI. Control versus DipA/LDN co-treatment in mice. Measurements taken via cardiac ultrasound of the left ventricle.

where *Eng*$^{+/-}$ mice after MI typically show increased epicardial thickening, short term DPP4 inhibitor treatment normalizes epicardial thinning to WT levels.

In conclusion, DPP4 inhibitors can affect macrophage polarization, as is also reported in a murine model of obesity where DPP4 inhibition resulted in M2 polarization in the liver and adipose tissues, reducing the obesity-induced inflammation response and resistance to insulin[13]. This M2 shift we too observed in the myocardial infarct border zone and in dermal tissue treated with a DPP4 inhibitor (Chapter 3 and 5 respectively), suggesting DPP4 inhibitors are anti-inflammatory and can modulate macrophage differentiation toward the reparative M2 macrophages.

Modulation of DPP4-mediated processes

An interesting point of discussion is that DPP4 can be either membrane-bound or shedded/cleaved to a soluble form. It is therefore interesting to take into account what the differences in signaling and mechanistic effects of these two types of the protein are. Solubilization of DPP4 is a process not yet completely understood, but in hypoxic conditions is mediated by several MMPs, resulting in the shedding of DPP4[14]. An important source for soluble

DPP4 are the kidneys, although recent research also points towards the leukocytes and macrophages[15]. The intracellular and transmembrane parts of DPP4 are absent in the soluble form, but its enzymatic function remains intact[16,17]. Soluble DPP4 was shown to induce endothelial constriction, possibly contributing to exacerbation of cardiovascular disease[18]. In disease setting, soluble DPP4 can either have good or bad prognostic values when measured as a biomarker in the serum; high plasma levels DPP4 activity were found associated with increased occurrence of coronary artery disease[19], the progression of atherosclerosis in mice[20] and was indicative of colorectal metastases in patients[21].
Another point of discussion is that when DPP4 cleaves SDF1, GLP1 or any of its other ligands, we can question whether or not these cleaved products are completely inactive[22]. DPP4 inhibition may therefore modulate ligand activity in subtle or unexpected ways, and this can vary for every type of DPP4 inhibitor molecule available[23]. For example, Linagliptin is known to block EndoMT, whereas Sitagliptin does not[23,24]. Further research into these inhibitors is therefore necessary, especially in HHT1 context, where endoglin heterozygosity influences more functions and processes in the immune system and macrophages that we currently know of. For example, endoglin was shown to have direct cross-talk with the Hippo pathway (regulating cell proliferation and apoptosis), resulting in altered monocyte chemotactic protein-1 (MCP1/CCL2) expression[25]. The interactions of DPP4 and endoglin thus remain interesting targets for immune modulation.

Clinical applications of DPP4 inhibitors and future perspectives

Many DPP4 inhibitors have been developed and are currently used in the clinic. The different DPP4 inhibitors have various mechanisms of action[23]; for example because of permanent or reversible binding to their targets. Therefore the differences between the various DPP4 inhibitors need to be extensively researched and documented, as the disease type, organ and cell type can severely affect results[23,26,27]. The protein DPP4 itself is able to interact, degrade or bind to many other proteins, such as SDF1, GLP1, NPY, ADA, fibronectin and collagen[28]. Therefore, DPP4 inhibition could be used in several clinical applications other than improving the MNC homing in HHT1 or decreasing the fibrotic response in tissue repair. DPP4 inhibitors are known to regulate microRNA levels, possibly useful in decreasing kidney disease progression in chronic renal disease and diabetes mellitus type 2 (DMT2)[27,29]. Also in atherosclerosis, DPP4 inhibition led to decreased vascular smooth muscle cell proliferation, decreased macrophage inflammation status and reduced foam cell induction[30,31]. In accordance with our findings for DPP4, inhibiting DPP8 and 9 (which are highly expressed in AS plaques) *in vitro* reduced inflammation status of murine macrophages[32], confirming the immunomodulatory role of DPP4 and its related proteins.
DPP4 inhibitors have possible applications in many fields of medicine. In anti-tumor therapy, DPP4 inhibition was able to improve T cell migration *in vivo*, and resulted in improved reactions to immunotherapy[33,34]. DPP4 has even been linked to stress and depression disorders; soluble DPP4 was found decreased in patients suffering from depression and could be reversed by anti-depressive treatment[35]. Contrastingly, in another patient cohort plasma DPP4 activity was found increased[36], confirming more research is necessary, and already suggesting possible population and disorder/treatment differences exist for DPP4 plasma activity.
DPP4 is highly expressed on lymphocytes[28] and high membrane DPP4 was shown to decrease recovery of cardiac function in CVD patients[37]. Inhibition of DPP4 could therefore possibly be a suitable treatment in cardiovascular disease patients. DPP4 inhibition in clinical trials is well tolerated and despite some reports about adverse effects[38-41], its

overall use seems to be either beneficial[42-45] or results show treatment had no effect on cardiovascular outcome or risk[46-48]. In future research, DPP4 inhibition is best used in concert with other drugs or therapies that stimulate cardiac repair, like anti-coagulants or cell therapy.
More research is needed to understand the beneficial impact of DPP4 inhibition on the HHT1 immune system and tissue repair, and the research presented in this thesis aimed to improve insight on the mechanisms involved in endoglin heterozygosity, in order to improve treatment in not only HHT1 patients, but also patients with ischemic injury.

References

1. Jung, Y.C., *et al.* Anti-inflammatory effects of galangin on lipopolysaccharide-activated macrophages via ERK and NF-kappaB pathway regulation. *Immunopharmacol Immunotoxicol* **36**, 426-432 (2014).

2. Wang, C., *et al.* Microgravity activates p38 MAPK-C/EBPbeta pathway to regulate the expression of arginase and inflammatory cytokines in macrophages. *Inflamm Res* **64**, 303-311 (2015).

3. Monick, M.M., *et al.* Constitutive ERK MAPK activity regulates macrophage ATP production and mitochondrial integrity. *Journal of immunology (Baltimore, Md. : 1950)* **180**, 7485-7496 (2008).

4. Shao, Q., Han, F., Peng, S. & He, B. Nur77 inhibits oxLDL induced apoptosis of macrophages via the p38 MAPK signaling pathway. *Biochem Biophys Res Commun* **471**, 633-638 (2016).

5. Jimenez-Garcia, L., Herranz, S., Luque, A. & Hortelano, S. Critical role of p38 MAPK in IL-4-induced alternative activation of peritoneal macrophages. *Eur J Immunol* **45**, 273-286 (2015).

6. Zhang, O. & Zhang, J. Atorvastatin promotes human monocyte differentiation toward alternative M2 macrophages through p38 mitogen-activated protein kinase-dependent peroxisome proliferator-activated receptor gamma activation. *Int Immunopharmacol* **26**, 58-64 (2015).

7. Thompson, C. Fiery entrance for the HIV co-receptor. *Lancet* **343**, 49 (1994).

8. Gorrell, M.D., Gysbers, V. & McCaughan, G.W. CD26: a multifunctional integral membrane and secreted protein of activated lymphocytes. *Scandinavian journal of immunology* **54**, 249-264 (2001).

9. Hildebrandt, M., *et al.* Apheresis-related enrichment of CD26++ T lymphocytes: phenotypic characterization and correlation with unfavorable outcome in autologous hematopoietic progenitor cell transplantation. *Transplantation and cellula therapy* **52**, 765-776 (2012).

10. Uematsu, T., Tanaka, H., Yamaoka, M. & Furasawa, K. Effects of Oral Squamous Cell Carcinoma-derived TGF-β1 on CD26/DPPIV Expression in T Cells. *Anticancer research* **24**, 619-624 (2004).

11. Reinhold, D., *et al.* Inhibitors of dipeptidyl peptidase IV induce secretion of transforming growth factor beta 1 in PWM-stimulated PBMC and T cells. *Immunology* **91**, 354-360 (1997).

12. Shinjo, T., *et al.* DPP-IV inhibitor anagliptin exerts anti-inflammatory effects on macrophages, adipocytes, and mouse livers by suppressing NF-kappaB activation. *Am J Physiol Endocrinol Metab* **309**, E214-223 (2015).

13. Zhuge, F., *et al.* DPP-4 Inhibition by Linagliptin Attenuates Obesity-Related Inflammation and Insulin Resistance by Regulating M1/M2 Macrophage Polarization. *Diabetes* **65**, 2966-2979

(2016).

14. Röhrborn, D., Wronkowitz, N. & Eckel, J. DPP4 in diabetes. *Frontiers in Immunology* **6**, 1-20 (2015).

15. Wang, Z*., et al.* Soluble DPP4 originates in part from bone marrow cells and not from the kidney. *Peptides* **57**, 109-117 (2014).

16. Lambeir, A.-M., Durinx, C., Scharpé, S. & De Meester, I. Dipeptidyl-peptidase IV from bench to bedside: an update on structural properties, functions, and clinical aspects of the enzyme DPP IV. *Critical reviews in clinical laboratory sciences* **40**, 209-294 (2003).

17. Waumans, Y*., et al.* The dipeptidyl peptidase family , prolyl oligopeptidase , and prolyl carboxypeptidase in the immune system and inflammatory disease , including atherosclerosis Reviewed by :. **6**, 1-18 (2015).

18. Romacho, T*., et al.* Soluble dipeptidyl peptidase-4 induces microvascular endothelial dysfunction through proteinase-activated receptor-2 and thromboxane A2 release. *J Hypertens* **34**, 869-876 (2016).

19. Yang, G*., et al.* Increased Plasma Dipeptidyl Peptidase-4 Activities in Patients with Coronary Artery Disease. *PLoS One* **11**, e0163027 (2016).

20. Ervinna, N*., et al.* Anagliptin, a DPP-4 Inhibitor, Suppresses Proliferation of Vascular Smooth Muscles and Monocyte Inflammatory Reaction and Attenuates Atherosclerosis in Male apo E-Deficient Mice. *Endocrinology* **154**, 1260-1270 (2013).

21. De Chiara, L*., et al.* Postoperative serum levels of sCD26 for surveillance in colorectal cancer patients. *PLoS One* **9**, e107470 (2014).

22. Cantini, G., Di Franco, A., Mannucci, E. & Luconi, M. Is cleaved glucagon-like peptide 1 really inactive? Effects of GLP-1(9-36) on human adipose stem cells. *Mol Cell Endocrinol* **439**, 10-15 (2017).

23. Shi, S., Kanasaki, K. & Koya, D. Linagliptin but not Sitagliptin inhibited transforming growth factor-β2-induced endothelial DPP-4 activity and the endothelial-mesenchymal transition. *Biochemical and Biophysical Research Communications* **471**, 184-190 (2016).

24. Kaji, K*., et al.* Dipeptidyl peptidase-4 inhibitor attenuates hepatic fibrosis via suppression of activated hepatic stellate cell in rats. *Journal of Gastroenterology* **49**, 481-491 (2014).

25. Young, K*., et al.* BMP9 Crosstalk with the Hippo Pathway Regulates Endothelial Cell Matricellular and Chemokine Responses. *PloS one* **10**, e0122892 (2015).

26. Dushenko, S*., et al.* Gate-Tunable Spin-Charge Conversion and the Role of Spin-Orbit Interaction in Graphene. *Phys Rev Lett* **116**, 166102 (2016).

27. Shi, S., Koya, D. & Kanasaki, K. Dipeptidyl peptidase-4 and kidney fibrosis in diabetes. *Fibrogenesis & tissue repair* **9**, 1 (2016).

28. Klemann, C., Wagner, L., Stephan, M. & von Horsten, S. Cut to the chase: a review of CD26/dipeptidyl peptidase-4's (DPP4) entanglement in the immune system. *Clin Exp Immunol* **185**, 1-21 (2016).

29. Kanasaki, K*., et al.* Linagliptin-Mediated DPP-4 Inhibition Ameliorates Kidney Fibrosis in Streptozotocin-Induced Diabetic Mice by Inhibiting Endothelial-to-Mesenchymal Transition in a

Therapeutic Regimen. *Diabetes* **63**, 2120-2131 (2014).

30. Brenner, C*., et al.* DPP-4 inhibition ameliorates atherosclerosis by priming monocytes into M2 macrophages. *International Journal of Cardiology* **199**, 163-169 (2015).

31. Yang, C.-J., Fan, Z.-X., Yang, J. & Yang, J. DPP-4 inhibitors: A potential promising therapeutic target in prevention of atherosclerosis. *International Journal of Cardiology* **202**, 797-798 (2016).

32. Waumans, Y*., et al.* The Dipeptidyl Peptidases 4, 8, and 9 in Mouse Monocytes and Macrophages: DPP8/9 Inhibition Attenuates M1 Macrophage Activation in Mice. *Inflammation* **39**, 413-424 (2016).

33. Barreira da Silva, R*., et al.* Dipeptidylpeptidase 4 inhibition enhances lymphocyte trafficking, improving both naturally occurring tumor immunity and immunotherapy. *Nat Immunol* **16**, 850-858 (2015).

34. Ohnuma, K., Hatano, R. & Morimoto, C. DPP4 in anti-tumor immunity: going beyond the enzyme. *Nature immunology* **16**, 791-792 (2015).

35. Wagner, L*., et al.* Identifying neuropeptide Y (NPY) as the main stress-related substrate of dipeptidyl peptidase 4 (DPP4) in blood circulation. *Neuropeptides* **57**, 21-34 (2016).

36. Zheng, T*., et al.* Increased Dipeptidyl Peptidase-4 Activity Is Associated With High Prevalence of Depression in Middle-Aged and Older Adults: A Cross-Sectional Study. *J Clin Psychiatry* **77**, e1248-e1255 (2016).

37. Post, S*., et al.* Reduced CD26 expression is associated with improved cardiac function after acute myocardial infarction. *Journal of Molecular and Cellular Cardiology* **53**, 899-905 (2012).

38. Monami, M., Dicembrini, I. & Mannucci, E. Dipeptidyl peptidase-4 inhibitors and heart failure: A meta-analysis of randomized clinical trials. *Nutrition, Metabolism and Cardiovascular Diseases* **24**, 689-697 (2014).

39. Savarese, G*., et al.* Cardiovascular effects of dipeptidyl peptidase-4 inhibitors in diabetic patients: A meta-analysis. *International Journal of Cardiology* **181**, 239-244 (2015).

40. Kannan, S*., et al.* Risk of overall mortality and cardiovascular events in patients with type 2 diabetes on dual drug therapy including metformin: A large database study from the Cleveland Clinic. *J Diabetes* **8**, 279-285 (2016).

41. Tagaya, Y., Okada, S., Hisada, T., Niijima, Y. & Yamada, M. Interstitial pneumonia during administration of dipeptidyl peptidase-4 inhibitors. *J Diabetes* **8**, 442 (2016).

42. Zhou, J.B., Bai, L., Wang, Y. & Yang, J.K. The benefits and risks of DPP4-inhibitors vs. sulfonylureas for patients with type 2 diabetes: accumulated evidence from randomised controlled trial. *Int J Clin Pract* **70**, 132-141 (2016).

43. Foroutan, N., Muratov, S. & Levine, M. Safety and efficacy of dipeptidyl peptidase-4 inhibitors vs sulfonylurea in metformin-based combination therapy for type 2 diabetes mellitus: Systematic review and meta-analysis. *Clin Invest Med* **39**, E48-62 (2016).

44. Monami, M., Ahrén, B., Dicembrini, I. & Mannucci, E. Dipeptidyl peptidase-4 inhibitors and cardiovascular risk: a meta-analysis of randomized clinical trials. *Diabetes, Obesity and Metabolism* **15**, 112-120 (2013).

45. Ou, S.M*., et al.* Dipeptidyl peptidase-4 inhibitors and cardiovascular risks in patients with

pre-existing heart failure. *Heart* **103**, 414-420 (2017).

46. Koska, J., Sands, M., Burciu, C. & Reaven, P. Cardiovascular effects of dipeptidyl peptidase-4 inhibitors in patients with type 2 diabetes. *Diab Vasc Dis Res* **12**, 154-163 (2015).

47. Theiss, H.D., *et al.* Safety and efficacy of SITAgliptin plus GRanulocyte-colony-stimulating factor in patients suffering from Acute Myocardial Infarction (SITAGRAMI-Trial)—Rationale, design and first interim analysis. *International journal of cardiology* **145**, 282-284 (2010).

48. Zhong, J., Maiseyeu, A., Davis, S.N. & Rajagopalan, S. DPP4 in Cardiometabolic Disease: Recent Insights From the Laboratory and Clinical Trials of DPP4 Inhibition. *Circulation Research* **116**, 1491-1504 (2015).

Summary

Nederlandse Samenvatting

Acknowledgements

Curriculum Vitae

List of Publications

Summary

Hereditary hemorrhagic telangiectasia (HHT) or Rendu-Osler-Weber disease, is a rare genetic disorder, known for its endothelial dysplasia causing vessel malformations, severe nose bleeds and internal bleedings. In the majority of patients mutations are found in genes belonging to the TGFβ superfamily, causing a disbalance in the TGFβ signaling pathway by haploinsufficiency of the remaining functional protein. HHT type 1 (HHT1) is the most prevalent HHT variant, and its mutation lies in the endoglin gene, encoding a protein which functions as co-receptor of TGFβ, and is crucial to neo-angiogenesis and vascular repair.

The TGFβ signaling pathway is tightly controlled and involves many activators and inhibitors. Although endothelial cells and pericytes have been the main research focus for HHT, it is now known that mononuclear cells (MNCs) also play an important role in vascular homeostasis, integrity and repair. The process by which MNCs are attracted to ischemic, damaged or inflamed tissue is tightly regulated via the stromal cell derived factor-1 (SDF1) – CXCR4 axis. SDF1 is produced in tissues shortly after an ischemic event, and mobilizes MNCs from the bone marrow to the circulation. Subsequent homing of CXCR4$^+$ cells from the blood to the site of injury is mediated by the SDF1 gradient and its receptor CXCR4. The enzyme DPP4 enzymatically inactivates SDF1, therefore playing a critical role in limiting MNC recruitment, limiting the inflammatory response.

There is a delicate balance between SDF1 and CXCR4, and skewing of either one of the proteins or regulators involved in their activation or inhibition will result in impaired homing, a defective inflammatory response and hamper wound healing and tissue repair.

HHT1 was long considered a disorder affecting angiogenesis only. In recent years it has become clear that endoglin heterozygosity disturbs the function of many more cell types and processes. In **Chapter 2**, we discussed HHT genetics, etiology and signaling, in particular focusing on the role of circulating mononuclear cells, both their impaired homing and contribution to tissue repair in HHT context.

We then showed that inhibiting DPP4 *in vivo* by treating *Eng*$^{+/-}$ mice after experimentally induced myocardial infarction (MI), restored homing of MNCs and benefits short term cardiac recovery by reducing fibrosis in **Chapter 3**. Here, the number of reparative M2 macrophages increased, suggesting that DPP4 inhibition reduced the pro-inflammatory immune response after MI.

By inhibiting BMP signaling using LDN, we aimed to stimulate TGFβ signaling in the *Eng*$^{+/-}$ animals in **Chapter 4**. *In vitro* analysis of macrophage differentiation revealed that LDN treatment increased the number of reparative macrophages. Treatment of *Eng*$^{+/-}$ mice with LDN restored cardiac function and reduced fibrosis after MI. In a second ischemia model, experimentally induced hind limb ischemia, and we showed that LDN improved blood flow recovery of *Eng*$^{+/-}$ mice. We found that macrophage signaling via canonical and non-canonical pathways is severely impaired by endoglin heterozygosity.

As macrophage differentiation and tissue repair is impaired in HHT1, in **Chapter 5** we studied the effect of DPP4 inhibition in a dermal wounding model in *Eng*$^{+/-}$ animals, assessing the healing of the lesion. Compared to untreated animals, dermal application of a DPP4 inhibitor increased wound closure speed and increased M2 macrophage numbers in the lesion area. Levels of fibrosis were decreased, signifying a reduction in scarring of the wound site. Furthermore, investigation of intracellular signaling in macrophages showed that in cultured

Eng$^{+/-}$ macrophages, non-canonical signaling was severely deregulated.

In **Chapter 6,** we described the abnormal epicardial response after myocardial damage in HHT1 mice. In this study, we analyzed the composition and the behavior of the epicardial layer at different timepoints post-MI and found that epicardial thickening is delayed. Furthermore, the epicardium was hyperactive in its response to cardiac ischemic injury. Treatment of *Eng*$^{+/-}$ mice with a DPP4 inhibitor reduced epicardial thickening and increased the percentage of macrophages present in the epicardial infarct border zone.

In conclusion, in this thesis we studied different aims and approaches to influence HHT1-MNC homing and differentiation to restore their contribution to tissue repair. In various experimental methods inducing ischemic and/or direct tissue damage, we aimed to improve tissue repair in the *Eng*$^{+/-}$ mice. Using DPP4 inhibition, we increased the SDF1-CXCR4 homing mechanism, to restore the impaired homing capacity of the HHT1-MNCs. Furthermore, we focused on correcting the M1/M2 differentiation in *Eng*$^{+/-}$ mice. Via use of the BMP receptor inhibitor LDN we aimed to restore the skewed BMP/TGFβ signaling; stimulating the TGFβ pathway signaling to induce M2 differentiation. We concluded that DPP4 inhibition can be used to improve the HHT1 immune system and tissue repair, and is best used in concert with other drugs or therapies that stimulate cardiac or tissue repair, like anti-coagulants or cell therapy.

Nederlandse samenvatting

Hereditaire hemorragische teleangiëctasieën (HHT) of de ziekte van Rendu-Osler-Weber, is een zeldzame genetische ziekte, gekenmerkt door endotheel dysplasie dat misvormde vaten, bloedneuzen en interne bloedingen veroorzaakt. In het merendeel van de patiënten worden mutaties gevonden die zich in de genen van de TGFβ superfamilie bevinden. Hierdoor ontstaat een onbalans in de TGFβ signaal route doordat er niet genoeg functioneel eiwit aanwezig is. HHT type 1 (HHT1) is de meest voorkomende vorm van HHT, met de mutatie in het endoglin gen, dat codeert voor een eiwit dat functioneert als co-receptor voor TGFβ, cruciaal voor neo-angiogenese en vaat-herstel.

De TGFβ signaal route is een zeer gecontroleerd proces en bestaat uit veel activators en inhibitoren. Hoewel endotheel cellen en pericyten de voornaamste onderzoeksfocus waren voor HHT, is het nu bekend dat mononucleaire cellen (MNCs) ook een belangrijke rol spelen in vaat-homeostase, integriteit en herstel. Het proces waardoor MNCs worden aangetrokken naar ischemische, beschadigd of ontstoken weefsel is gereguleerd via de stromaal cel-afkomstige factor-1 (SDF1) – CXCR4 as. SDF1 wordt geproduceerd in weefsels kort na een ischemische gebeurtenis, en mobiliseert MNCs van het beenmerg naar de bloed circulatie. Vervolgens migreren CXCR4+ cellen van het bloed naar de plek van schade, gemedieerd door het volgen van de SDF1 gradiënt met zijn receptor CXCR4. Het enzym DPP4 kan SDF1 enzymatisch inactiveren, en speelt daardoor een essentiële rol in het beperken van MNC migratie, en daarmee het beperken van de ontstekingsreactie.

Er is een delicate balans tussen SDF1 en CXCR4, en verandering van een van de eiwitten of regulatoren betrokken bij hun activatie of inhibitie zal zorgen voor verminderde migratie, een defecte immuunrespons en bemoeilijkt wondheling en weefselherstel.

HHT1 werd lang gezien als een ziekte die voornamelijk de bloedvaten aantast. De laatste jaren is duidelijk geworden dat endoglin deficiëntie de functie verstoord van veel meer cel types en processen. In **Hoofdstuk 2** worden HHT genetica, etiologie en signaleringsroutes besproken, met de focus op de rol van circulerende MNCs, en zowel hun verminderde migratie en aandeel in weefselherstel in HHT perspectief.

We laten verder zien dat het inhiberen van DPP4 *in vivo* door het behandelen van *Eng*$^{+/-}$ muizen na experimenteel geïnduceerd myocard infarct (MI) het migreren van de MNCs herstelde en het herstel van het hart op korte termijn verbeterde door vermindering van fibrose vorming in **Hoofdstuk 3**. Verder verhoogde het aantal reparatieve M2 macrofagen, wat suggereert dat DPP4 inhibitie de pro-ontstekingsrespons na een MI kon verminderen.

Door het inhiberen van BMP signalering met gebruik van LDN hadden we als doel om TGFβ signalering in de *Eng*$^{+/-}$ muizen te stimuleren in **Hoofdstuk 4**. Na *in vitro* analyse van macrofaag differentiatie bleek dat LDN behandeling het aantal reparatieve macrofagen verhoogde. Behandeling van de *Eng*$^{+/-}$ muizen met LDN herstelde de hartfunctie en verminderde fibrose na MI. In een tweede model voor ischemie, lieten we zien dat LDN het bloedstroom herstel verbeterde in de *Eng*$^{+/-}$ muizen. We vonden verder dat macrofaag signalering via de hoofd- en ongebruikelijke routes sterk verminderd is door endoglin deficiëntie.

Omdat macrofaag differentiatie en weefsel herstel verminderd zijn in HHT1, bestudeerden we in **Hoofdstuk 5** het effect van DPP4 inhibitie in een huidwond-model in de *Eng*$^{+/-}$ muizen, waarbij we het herstel van de huidwond bekeken. Vergeleken met de onbehandelde dieren, toediening van een DPP4 inhibitor op het huidoppervlak zorgde ervoor dat het wondherstel sneller verliep, en de aanwezigheid van M2 macrofagen werd verhoogd. Het fibrose niveau werd verlaagd, wat duidt op een vermindering van litteken vorming van de wonden. Verder onderzoek van intracellulaire signalering in macrofagen liet zien dat de ongebruikelijke signaleringsroute sterk was aangetast in gekweekte *Eng*$^{+/-}$ macrofagen.

In **Hoofdstuk 6** beschrijven we de abnormale epicardiale reactie na myocard schade in de HHT1 muizen. In deze studie analyseerden we de compositie en het gedrag van de epicardiale laag op verschillende tijdspunten na MI, en vonden dat het verdikken van de epicardiale laag is vertraagd. Verder bleek het epicard hyperactief in de reactie op ischemische schade van het hart. Behandeling van de *Eng*$^{+/-}$ muizen met een DPP4 inhibitor verminderde het verdikken van het epicardium en verhoogde het percentage macrofagen aanwezig in het grenszone van het myocard infarct.

In conclusie, in dit proefschrift zijn verschillende doelen en aanpakken bestudeerd om de HHT1-MNC migratie en differentiatie te beïnvloeden, om de bijdrage aan weefselherstel te verbeteren. In verschillende experimentele methoden die ischemische of direct weefselschade veroorzaken, probeerden we weefsel herstel te verhogen in de *Eng*$^{+/-}$ muizen. Door middel van DPP4 inhibitie konden we de SDF1-CXCR4 signaal verhogen, en daarmee de migratie capaciteit van de HHT1-MNCs herstellen. Verder focusten we op het herstellen van de verstoorden balans van de M1/M2 macrofaag differentiatie in de *Eng*$^{+/-}$ muizen. Gebruikmakend van de BMP receptor inhibitor LDN hadden wij als doel de verstoorde BMP/TGFβ signalering te herstellen; door het stimuleren van de TGFβ signaal route konden wij de differentiatie van M2 macrofagen induceren. We concluderen dat DPP4 inhibitie kan worden gebruikt om het HHT1 immuunsysteem te herstellen en weefselherstel te verbeteren, maar DPP4 inhibitie kan het beste worden ingezet in combinatie met andere medicatie of therapieën die hart of ander weefselherstel stimuleren, zoals antistollingsmiddelen of celtherapie.

Acknowledgements

In this final section of my thesis I would like to express my thanks and gratitude to all who have helped and supported me during my PhD project.

Dear Prof. Goumans, Marie-José, thank you for taking me on as a PhD student, and training me to become versatile researcher. You have inspired me and I have learned a lot with you as a role model.

Wineke, thank you for your mentorship and guidance, which you continued even after you left the LUMC. I always felt encouraged by your words and supported by having you as a co-promotor.

What made my Phd extra special, is that with me, the 6 months before that, Asja, Sjoerd, and José had also started their PhDs. We quickly bonded, and as we formed our PhD-kindred spirits group, Kirsten (or Kirstie -as I have named you), you naturally became our group core center and parental supervisor, and the movie-nights, tea-times, dinners, movie outings, city trips and many more we had during my PhD were invaluable. You are a great technician and colleague. I'm happy we kept our bond and may we continue this way forward.

Dear Sjoerd, you were my office-buddy for most of the 5 years I spent as a PhD. Your enthusiasm, humor and energy were amazing and you never made being at the lab or office boring. From playing (and singing to-) 'foute muziek', pulling pranks with dry ice, and discussing science and the meaning of life, I will never forget working with you. Thank you for everything, I'm sure I'll never have a colleague quite like you again.

Dear Asja, or as we named you, 'Buuf', we had an amazing time as colleagues, and continue as friends. Even though you now live in Switzerland, we keep in touch though our group-chat every day, and I'm so happy for it. You are a great scientist, and your kindness, down-to-earth view on things and your dry-wit humor is amazing. We went through some tough times, and I value your support and friendship so much. Thank you for everything.

Dear José, 'Goseetje', my dear travel-buddy and fellow-bunny owner, we have an amazing friendship which is hard to translate onto paper. Thank you so much for your friendship, support, creating a 'foute vrijdag' and all the fun times, during and after our PhD. You are a great scientist as well, and I'm so proud of your hard work. I love our tea-times, travels, and Starbucks trips. We have several travel ideas for the coming years, I already look forward to them.

Of course I would like to thank all other colleagues from the MCB-STAR group; Anke, Babu, Boudewijn, Laurens, Vera, Annemarie, Tessa, Karien and my student Joyce. Thank you for your friendship, collaborations, expertise, advise and insights.

Furthermore I'd like to thank:

My collegues of CCB, especially Willem, Gerard, Joop, Annelies, Julia and Steve. Prof. Hans Tanke, Prof. Peter ten Dijke and the people in his group, especially: Midory, Maarten, Gonzalo and Amaya.

My colleagues of INZI, and especially my K5 colleagues Krista, Cassandra, Paula, Anne, Matthias, Frank, Roel, Mariateresa, Maria, Arthur, Susan, Suus, Kimberley, Louis, Edwin and Anouk, thank you for your friendship, lifting my spirits and supporting me during the final phases of my PhD. Of course my extended thanks to Tom and Simone, thank you so much for allowing me to finish up my PhD while working in your research team. It has been amazing and I have learned so much in this time as a postdoc.

My dear friends Mirjam, Emma and Inge, and from ‘Leiden’ my friends Edith and Lotte, from Sydney Steff, thank you for you friendship and support all these years!

Claire, you and your family, Quinte, Tymo and Yoënne are as close to me as my own family. We call each other ‘Zus’ and that is what our friendship represents. I care about you so much, and thank you for always being there for me.

Lieve pa en ma, natuurlijk mogen jullie niet ontbreken in dit dankwoord; bedankt voor jullie onvoorwaardelijke steun en liefde, jullie trots maakt deze reis het allemaal waard!

Curriculum vitae

Calinda Dingenouts was born on October 21st, 1986 in the city of Vlaardingen, the Netherlands. She graduated from the Schravenlant Lyceum (Schiedam) in 2005. In 2008, she obtained her Bachelor's diploma in Biomedical Sciences at Leiden University, Leiden, the Netherlands. As part of her study she did an internship at the department of Immunology, Erasmus Medical Centre, Rotterdam, the Netherlands. Here, she focused on the optimization of gene therapy for patients with RAG 1 and 2 Severe Combined Immunodeficiency, working with Dr. Karin Pike-Overzet and Mark Rodijk in Prof. Dr. Frank Staal's group.

In 2009, she followed the master Biomedical Sciences at Leiden University and obtained her Master's diploma in 2011. During her first Junior Research Project she joined the group of Dr. Niels De Wind, and under supervision of Dr. Giel Hendriks she studied the mechanisms involved in transcription-associated mutagenesis in mammalian stem cells, at the department of Toxicogenetics, Leiden University Medical Centre, Leiden, the Netherlands.

For her second Junior Research Project she joined the group of Prof. Dr. Antony Cooper, under additional guidance of Stephanie Kong and Kathryn Hill. She investigated the role of LRRK2 and alpha-synuclein in Parkinson's disease at the department of Diabetes and Obesity, the Garvan Institute of Medical Research, Sydney, Australia. This project was supported with individual grants by the Princess Beatrice Fund, the Leiden University Fund and the Leiden University 'Outbound Study' grant.

In 2012 she started her PhD studies in the group of Prof. Dr. Marie-José Goumans at the department of Molecular Cell Biology (now Cell and Chemical Biology) at the Leiden University Medical Center under the supervision of Dr. Wineke Bakker. The results of this work are presented in this thesis.

In 2017 she was appointed as a Post-doctoral scientist at the department of Infectious Diseases at the Leiden University Medical Center. Joining the group of Prof. Dr. Tom Ottenhoff and under supervision of Associate Prof. Dr. Simone Joosten, she is working on vaccine development for tuberculosis by characterizing specific T-cell subsets in patients with latent tuberculosis infection.

List of publications

1. Dingenouts C.K.E., Goumans M.J. and Bakker W. Mononuclear *cells and vascular repair in HHT.* Frontiers in Genetics. 2015 Mar 23;6:114. doi: 10.3389/fgene.2015.00114. eCollection 2015.

2. Dingenouts C.K.E., Bakker W., Lodder K., Wiesmeijer K.C., Moerkamp A.T., Maring J.A., Arthur H.M., Smits A.M., Goumans M.J. Inhibiting DPP4 in a mouse model of HHT1 results in a shift towards regenerative macrophages and reduces fibrosis after myocardial infarction. PLoS One. 2017 Dec 18;12(12):e0189805. doi: 10.1371/journal.pone.0189805. eCollection 2017.

3. Moerkamp A.T., Lodder K., van Herwaarden T., Dronkers E., Dingenouts C.K.E., Tengström F.C., van Brakel T.J., Goumans M.J., Smits A.M. *Human fetal and adult epicardial-derived cells: a novel model to study their activation.* Stem Cell Res Ther. 2016 Nov 29;7(1):174.

4. Moerkamp A.T., Leung H.W., Bax N.A.M., Holst S., Lodder K., Berends T., Dingenouts C.K.E., Choo A.B.H., Smits A.M., Goumans M.J. *Glycosylated cell surface markers for the isolation of human cardiac progenitors.* Stem Cells and Development. 2017 Sep 11. do: 10.1089/scd.2017.0048.

5. Maring J.A., Lodder K., Mol E., Verhage V., Dingenouts C.K.E., Moerkamp A.T., Wiesmeijer C.C., Deddens J.C., Vader P., Smits A.M., Sluijter J.P.G., Goumans M.J. Cardiac Progenitor Cell-Derived Extracellular Vesicles Reduce Infarct Size and Associate with Increased Cardiovascular Cell Proliferation. J Cardiovasc Transl Res. 2018 Nov 19. doi: 10.1007/s12265-018-9842-9.

Manuscripts submitted or in preparation

6. Dingenouts C.K.E.*, Moerkamp A.T.*, Lodder K., van Herwaarden T., Végh A.M.D., Dronkers E., Kruithof B.P.T., Wiesmeijer K.C., Maring J.A., Kruithof B.P.T., Arthur H.M., Goumans M.J., Smits A.M. *Endoglin deficiency alters the epicardial response following myocardial infarction.*

7. Dingenouts C.K.E.*, Bakker W.*, Lodder K., Wiesmeijer K.C., Moerkamp A.T., Mager H.J., Snijder R., Westerman C.C.J., de Vries M. R., Quax P.H.A., Goumans M.J. *BMP receptor inhibition enhances tissue repair in endoglin heterozygous mice.*

8. Dingenouts C.K.E., Lodder K., Moerkamp A.T., Kurakula K.B., Bakker W., Hoefer I.E., Arthur H.M., Goumans M.J. DPP4 inhibition enhances wound healing in endoglin heterozygous mice through modulation of macrophage signaling and differentiation.

*Both authors contributed equally